Dissertation zur Erlangung des Doktorgrades
der Fakultät für Chemie und Pharmazie
der Ludwig-Maximilians-Universität München

NOVEL CHEMICAL TOOLS FOR THE

MODULATION OF TWO PORE CHANNEL 2

Susanne Daniela Gerndt

aus

Schweinfurt

2020

Table of contents

1   Introduction

"The most fruitful basis of the discovery of a new drug is to start with an old drug."

Sir James Black

With these words the pharmacologist and Nobel laureate Sir James Black established a basis for drug repurposing. The fact that an already known drug is used for a new indication that differs from the original indication is called drug repurposing. Thereby new targets can be identified for the old drugs. Another approach, beside these new targets, is that the scaffolds of the old drugs or natural compounds can also serve as an inspiration for the synthesis of novel small-molecules[1].

This thesis deals with two pore channel 2 (TPC2) as the target and tetrandrine (**1**, **Figure 1**) as the natural compound with the need to be developed. In 2015, Sakurai et al. linked the entry of Ebola virus into host cells to two pore channels (TPCs). The inhibition of TPCs with tetrandrine (**1**) halted virus trafficking and prevented infection[2], creating the fundament for this work.
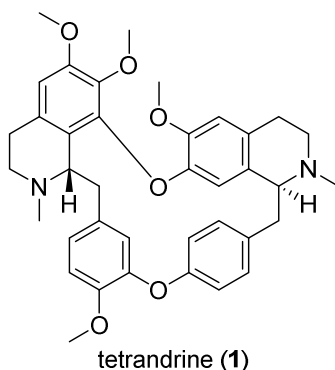
tetrandrine (**1**)

Figure 1: Chemical structure of the alkaloid tetrandrine (**1**), identified as a TPC2 inhibitor.

1.1 Two pore channels

Two pore channels are part of the family of voltage-gated ion channels and are localized in the endo-lysosomal system. They share parts of the sequential identity with voltage-gated calcium (Ca_v) and sodium (Na_v) channels[3]. Two isoforms of two pore channels (TPC1 and TPC2) can be found in primates. TPC1 is preferentially found in early endosomal compartments and TPC2 in late endosomal and lysosomal compartments[4-6]. In 2016, Kintzler and Stroud presented the crystal structure of the NAADP antagonist *trans*-Ned-19 (**2**) bound to TPC1 from *Arabidopsis*

thaliana[7]. The cryo-EM structure of human TPC2 has recently been resolved by She et al.[8] and verifies the dimeric nature and the duplicated domains of two pore channels. Two times six transmembrane helices form one domain and two domains form the ion channel. TPCs are non-selective cation channels, permeable to calcium and sodium and they are involved in endo-lysosomal trafficking, autophagy, mTOR and TFEB signaling[9]. Whether TPC2 is sodium or calcium permeable was subject of controversial debates in the last decade. While TPC2 was first described as non-selective, calcium permeable cation channel activated by NAADP (**3**)[10-14], other research groups claimed that TPC2 was a sodium-selective channel activated by the endo-lysosomal phosphoinositide $PI(3,5)P_2$ (**4**)[15, 16]. Both views independently received support in the past couple of years[5, 17-21] and the controversy has just recently been resolved[22] in the course of this project, as described in chapter 3.4.5.

Two pore channels have been a hot topic in recent literature, not only because of their controversially discussed ion permeability but also because of their involvement in various diseases like viral and bacterial infections and cancer cell migration. This makes two pore channels a promising target for drug research.

1.2 Two pore channels and disease

As mentioned before, in recent years TPCs have emerged as highly exciting potential drug targets for a number of diseases associated with the endo-lysosomal system[23]. Dysfunction of TPCs has been found to interfere with cholesterol trafficking resulting in fatty liver disease[5], the *β*-adrenergic stimulation of glucagon secretion in diabetes[24] and *β*-adrenoceptor signaling in the heart in cardiovascular diseases[25]. Melanin production and pigmentation are also influenced by TPC activity[26-28]. Furthermore, Parkinson's disease caused by LRRK2 mutations has been linked to TPC functions[29]. In addition, several bacterial toxins such as diphtheria toxin, anthrax toxin, cholera toxin, or *Pasteurella multocida* toxin have been shown to require functional TPCs[4, 6]. Beside its role in bacterial infections, TPCs have been demonstrated to play a role in various infectious diseases such as Ebola filovirus, Middle East respiratory syndrome coronavirus (MERS-CoV), severe acute respiratory syndrome coronavirus 2 (SARS-CoV-2), or HIV-1 retrovirus infections [2, 30-33]. Furthermore there is a growing amount of evidence that TPCs are necessary for sustaining cancer hallmarks like cell migration and neoangiogenesis[9, 34-36].

1.2.1 Two pore channels and cancer

The role of TPCs in cancer research is complex, because TPCs are involved in different processes during carcinogenesis. The fact that prostate cancer patients with high levels of TPC2 gene expression showed poor survival probabilities was a strong evidence for the correlation between TPCs and cancer hallmarks[37]. Nguyen et al. confirmed these results and showed that silencing of TPC2 reduced migration and adhesion of invasive lung tumor cells[36]. The endo-lysosomal system promotes trafficking of integrins. During cell migration integrins pass the endocytic cycle. They are released from their substrate and taken back by endocytosis. If this recycling process is disturbed, cancer cell migration *in vitro* and metastasis *in vivo* are impaired[36]. Vascular endothelial growth factors (VEGF) play an important role during neoangiogenesis, including vascularization of solid tumors. Inhibition of VEGF reduces vessel formation, a fundamental step for the vascularization of solid tumors. Hence VEGF inhibitors are already used to treat cancer[38]. The role of TPC2-mediated calcium release in neoangiogenesis was demonstrated in TPC knockout mice. In TPC2, but not in TPC1, knockout mice the VEGF pathway was inhibited and vessel formation was reduced[35]. Whether TPCs and especially TPC2 are involved in other cancer hallmarks, such as proliferation and dysregulation of the cellular energy metabolism[38], remained largely unknown and was investigated in the studies presented in chapter 3.6.3.

1.2.2 Two pore channels and viral infections

Especially in the year 2020, viral infections are a hot topic. The corona pandemic has hospitals reaching their bed capacities, causing many deaths. The WHO is currently promoting a study for drug repurposing, including drugs that have already been in use for HIV and malaria therapy[39]. The connection between viral infections and two pore channel activity has already been shown for Ebola virus, MERS-CoV, HIV-1 and lately for the new SARS-CoV-2[2, 30-33]. Ou et al. described that SARS-CoV-2 enters the cell *via* endocytosis and that PIKfyve and TPC2 were required for entering the cells[33]. The enzyme PIKfyve is responsible for phosphorylation of phosphatidylinositol 3-phosphate in C-5 position to $PI(3,5)P_2$ (**4**), an endogenous compound that is activating TPCs and is regulating endo-lysosomal vesicle trafficking. Inhibition of the mucolipin TRPML1 (see chapter 1.3) using an unfortunately not further specified TRPML1 inhibitor was ineffective, while inhibition of TPC2 with tetrandrine (**1**) halted the SARS-CoV-2 entry[33]. Tetrandrine (**1**) has already been shown to successfully prevent Ebola virus infection by blocking TPC1 and TPC2 activity[2]. A link to the transporter protein Niemann-Pick C1 has been demonstrated for SARS-CoV[40], similar to Ebola virus[2]. For Ebola virus both isoforms of TPC, TPC1 and TPC2, are required for virus trafficking and infectivity while for SARS-CoV-2 this correlation is not confirmed. Many facts are still unknown with respect to these correlations

and further investigation is of high interest. Having tailored tool compounds would surely boost studies to assess the correlation of TPCs and SARS-CoV-2 in more detail and would benefit the combat against viral infections.

1.3 Modulators of two pore channels

As part of the controversial debate about the ion permeability of TPCs, two different hydrophilic **activators** have been used in the past decade. The phosphoinositide phosphatidylinositol 3,5-bisphosphate (PI(3,5)P$_2$ (**4**)), a major constituent of endo-lysosomal membranes, has first been described by Dong et al.[41] as an activator of transient receptor potential mucolipin (TRPML) channels. TPCs and TRPMLs share PI(3,5)P$_2$ (**4**) as activator but are only distantly related to each other in terms of sequence similarities[15, 16]. Both channel families share a number of functional features. They are non-selective cation channels located in endo-lysosomes and permeable to sodium and calcium. Both are involved in endo-lysosomal trafficking, autophagy, TFEB and mTOR signaling[9]. Thus, TPCs are, in addition to PI(3,5)P$_2$ (**4**), activated by nicotinic acid adenine dinucleotide phosphate (NAADP (**3**))[10-14]. Both activators are highly hydrophilic and are not plasma membrane permeable. A plasma membrane permeable variant of NAADP (**3**), NAADP/AM (**5**) is commercially available[42, 43]. This lipophilic acetoxymethyl (AM) ester prodrug (**5**) is, however, due to its instability very limited in use (**Figure 2**).
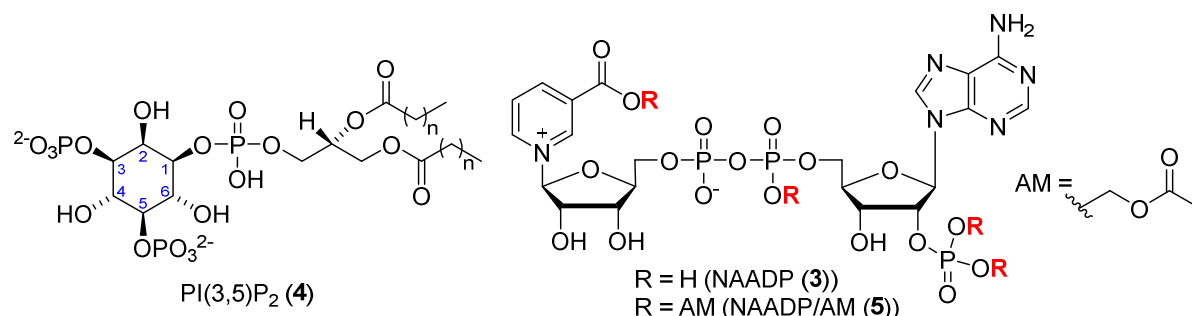
Figure 2: Phosphatidylinositol 3,5-bisphosphate (PI(3,5)P$_2$ (**4**)) and NAADP (**3**) and its membrane permeable variant NAADP/AM (**5**). Inositol **4** carries phosphate glycerol esters and various fatty acids in C-1 position (e.g. n = 16 or 18).

The same applies to the membrane permeable PI(3,5)P$_2$ variant. Dinkel et al. published a synthesis for the PI(3,5)P$_2$ variant with increased lipophilicity and membrane permeability. AM-esters were introduced to protect phosphate residues, as it was already known from NAADP/AM (**5**), and the secondary alcohol groups were protected as butyrates[44]. Unfortunately, these derivatives are only available *via* an extensive, multi-step synthesis.

As there is an urgent need for lipophilic, plasma membrane permeable small-molecule activators of TPCs, a high-throughput screening for the identification of novel, small-molecule

TPC2 activators was arranged. The screening of an 80.000 compound strong library obtained from Roche (Basel, CH) was performed within this project.

For the identification of TPC **inhibitors**, different approaches were pursued. Penny et al. performed a virtual screening of Ebola virus entry inhibitors in order to identify possible TPC blockers[31]. The hits were confirmed as TPC2 inhibitors by blocking NAADP-evoked calcium release in a sea urchin egg homogenate model and *via* patch clamp experiments. This group identified different dopamine receptor-affine drugs and selective estrogen receptor modulators (SERMs) as additional TPC blockers: the anti-psychotics trifluoperazine, prochlorperazine, thioridazine and fluphenazine (**6**) as well as the SERMs clomiphene, tamoxifen, toremifene, bazedoxifene and raloxifene (**7**).
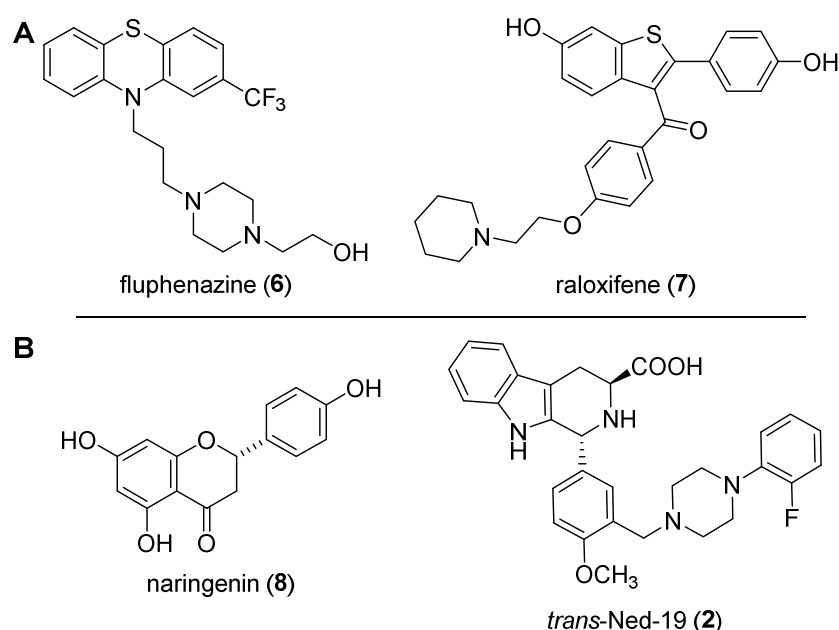
Figure 3: Structures of TPC2 inhibitors. (**A**) Most promising TPC2 inhibitors identified by Penny et al.[31]: raloxifene (**7**) and fluphenazine (**6**). (**B**) The flavonoid naringenin (**8**) and *trans*-Ned-19 (**2**).

The most promising TPC2 inhibitors identified by Penny et al., raloxifene (**7**) and fluphenazine (**6**), are approved drugs (**Figure 3 A**). Both exhibited low IC_{50} values in endo-lysosomal patch clamp experiments (0.63 µM and 8.2 µM) after stimulation with $PI(3,5)P_2$ (**4**)[31]. The SERM raloxifene (**7**) is known to reduce breast cancer risk[45] and is used for treatment and prevention of osteoporosis. Moreover, it is limited in its approval to postmenopausal women regarding the influence upon hormone levels. It has also been reported that raloxifene (**7**) blocks L-type and T-type voltage-sensitive calcium channels[46, 47] as well as Kv4.3 channels[48]. Fluphenazine (**6**) is an anti-psychotic drug used to treat psychotic disorders such as schizophrenia with severe adverse effects, in particular extrapyramidal effects including acute dystonia, akathisia, tardive dyskinesia and Parkinsonism[49]. Fluphenazine (**6**) blocks postsynaptic mesolimbic

dopaminergic D1 and D2 receptors in the brain, neuronal voltage-gated sodium channels[50] and the ATP-sensitive potassium (KATP) channel[51].

Besides its known broad spectrum of targets in mammalian organisms, the flavonoid naringenin (**8**, **Figure 3 B**) was also identified as a TPC2 blocker by Pafumi et al.[52]. Furthermore, it was investigated on its inhibitory effect in cell migration[53]. Naringenin (**8**) can also block several other ion channels: the melastatin channel TRPM3 (calcium channel)[54], voltage-gated sodium channels (Na$_v$s)[55] and cardiac HERG channels (potassium channel)[56]. Additionally it enhances the activity of large-conductance Ca^{2+}-activated potassium (BK) channels[57]. However, naringenin (**8**) is most prominent for the inhibitory effect on cytochrome P450 enzymes like CYP1A2[58] or CYP3A4[59] – a property which bears the risk of undesired drug-drug interactions.

The NAADP antagonist and therefore indirect TPC2 blocker *trans*-Ned-19 (**2**, **Figure 3 B**) has been known for many years[60] and the crystal structure solved by Kintzler and Stroud confirmed the interaction with TPCs[7], albeit discussed controversially.

Examining these compounds, it is of interest that many of them are discussed in their relationship to cancer. Aforementioned, raloxifene (**7**) is known to reduce breast cancer risk[45]. Naringenin (**8**) was investigated on its inhibitory effect in cell migration[53] and to affect VEGF-evoked tube formation[52] but requires very high concentrations (≥ 500 μM), as well as *trans*-Ned-19 (**2**). The latter, *trans*-Ned-19 (**2**), was able to reduce NAADP-induced Ca^{2+} release and prevented the activation of the VEGF signaling pathway[35] as well as cancer cell migration[36] in high micromolar doses (≥ 100 μM). All these compounds are not applicable for *in vivo* experiments due to the side effects or required high doses. Though, there is an emerging need for the development of efficacious TPC2 inhibitors with drug-like properties and antitumor activity to study the involvement of TPC2 in cancer.

Tetrandrine (**1**, **Figure 3 A**) is the most prominent TPC inhibitor in current literature and was first described as such by Sakurai et al. in 2015[2]. It is known to also block voltage-gated Ca^{2+} channels, large-conductance Ca^{2+}-activated K$^+$ (BK) channels and intracellular Ca^{2+} pumps[61]. Additionally, tetrandrine (**1**) was recently identified to effectively inhibit cancer cell migration[36] and infections with Ebola[2], MERS-CoV[30] and SARS-CoV-2[33] viruses. These effects were most likely induced *via* directly acting on TPCs. Tetrandrine (**1**) is used in different studies as exemplary TPC inhibitor and therefore represents a promising lead structure for the development of TPC2 blockers.

1.4 Tetrandrine (1) – opportunities and limitations

The bisbenzylisoquinoline alkaloid tetrandrine (**1**) is isolated from the Asian plant *Stephania tetrandra* and is used in traditional Chinese medicine for treating asthma, tuberculosis, malaria or hyperglycemia[62]. Apart from its traditional applications, tetrandrine (**1**) is under pharmacological investigation. Its activity spectrum extends inflammations, antidiabetic effects, antimicrobial and anticancer activities, the use as antioxidant, P-gp and calcium channel inhibition[62], as depicted in **Figure 4**. Plenty of these pharmacological activities can also be related to TPCs, as tetrandrine (**1**) is a known TPC1 and 2 inhibitor[2]. Studies about viral infections (Ebola[2], MERS-CoV[30] and SARS-CoV-2[33]) and the influence of TPC2 were carried out using tetrandrine (**1**) but it is also under investigation for bacterial infections (e.g. *Staphylococcus aureus*)[63] or fungus (e.g. *Candida albicans*)[64]. Also for investigations in cancer research connected with TPCs, tetrandrine (**1**) is state-of-the-art[36]. Tetrandrine (**1**) was also highlighted in a study to prevent diabetes[65], which now can be related to its inhibitory effect on TPCs[24].
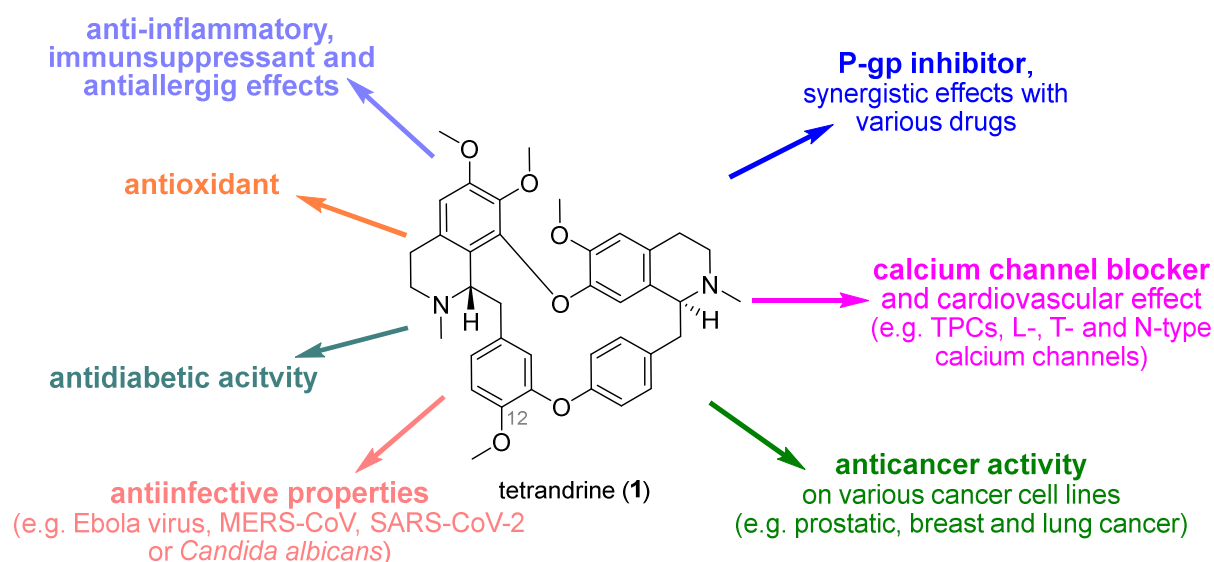
Figure 4: Overview of the activity spectrum of tetrandrine (**1**).

P-glycoprotein (P-gp) however, appears as novel target for tetrandrine (**1**), which was identified as a highly potent P-gp inhibitor[66, 67]. P-gp is an efflux pump with a broad substrate spectrum. These transporters pump foreign substances out of cells and are therefore responsible for multidrug resistance of tumors. Correlations to TPCs have not been investigated yet.

Despite all these positive features tetrandrine (**1**) also has a few drawbacks. One example is the poor solubility. In some studies the sample preparation was not commented[68, 69] and others reported that they needed to acidify the injection solution for dissolution before *in vivo* application[2, 70]. These circumstances make tetrandrine (**1**) poorly applicable for *in vivo* studies.

Furthermore, a high toxicity is described in animal models. There are hints that the toxicity of tetrandrine (**1**) is based on oxidative metabolism by cytochromes P450s 3A4 and 3A5. The authors claimed that the methoxy group at C-12 (**Figure 4**) is metabolized to a free phenol and further oxidized to give a reactive *para*-quinone methide intermediate that can directly be trapped by bio-nucleophiles like glutathione[70, 71]. This toxicity is based on the reaction with other bio-nucleophiles like cysteine residues in proteins that would then be destroyed, while glutathione would detox the *para*-quinone methide intermediate. The broad activity spectrum of tetrandrine (**1**) is maybe related to its ability to inhibit TPC1 and 2, but other side effects are certain to occur and need to be reduced as well.

The alkaloid is mainly obtained by extraction of the roots of *Stephania tetrandra* or by complex, multi-step chemical synthesis. The synthesis of enantiomerically pure tetrandrine (**1**) involves more than 20 steps[72]. A recently published synthesis from our research group shortened the sequence to 12 steps after which the racemic mixture of tetrandrine (**1**) is obtained[73].

The opportunities and limitations of tetrandrine (**1**) generate a suitable basis for the development of this long known bioactive compound. The outlined drawbacks were aimed to be overcome in this project by simplification of the structure, substitutions and derivatizations.

2 Objectives

TPCs are of rising importance. Involved in many diseases but mechanistically poorly understood, there is an emerging need for further investigations. Despite its drawbacks, tetrandrine (**1**) was the most promising candidate for developing new TPC inhibitors.

New anti-cancer agents with the potential to block TPCs were e.g. easily accessible derivatives of tetrandrine (**1**) with modifications in C-5[74, 75] and C-14[76, 77] position, other related natural compounds like fangchinoline (**9**, also originated from *Stephania tetrandra*)[78], analogs of berbamine (**10**, from *Berberis amurensis*)[79], or *seco*-derivatives as dauricine (**11**, from *Menispermum dauricum DC*)[80] and neferine (**12**, from *Nelumbo nucifera*)[81], as depicted in **Figure 5**.
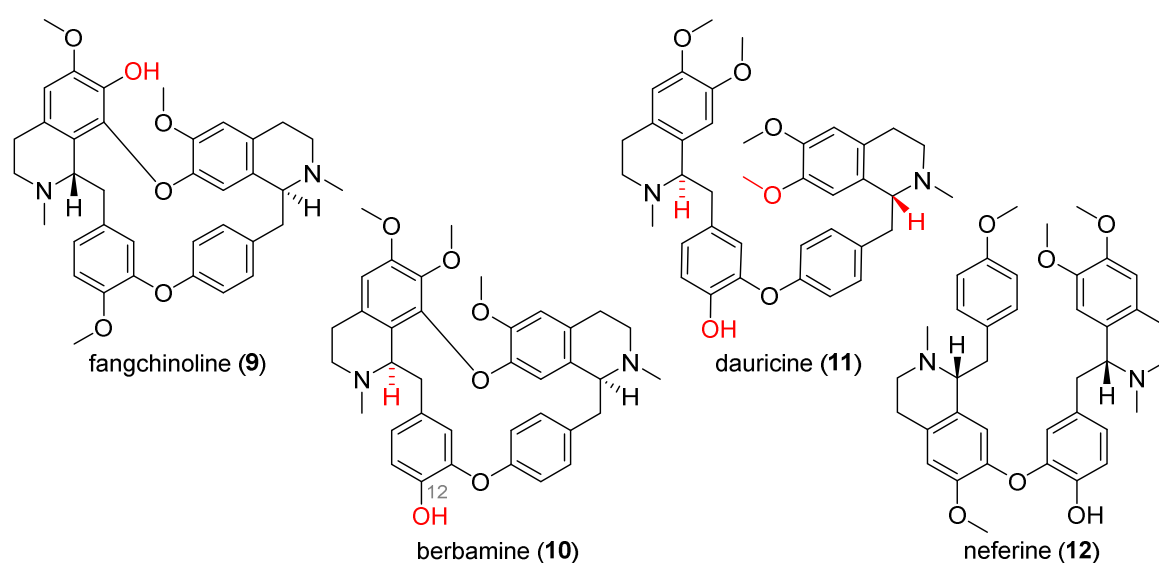
Figure 5: Structures of the alkaloids fangchinoline (**9**), berbamine (**10**), dauricine (**11**) and neferine (**12**). Berbamine analogs are glycosides in C-12 position of berbamine (**10**). Differences to tetrandrine (**1**) are marked in red.

All these molecules, however, lacked variability because they were obtained from natural extracts and their derivatization was restricted to certain functional groups. If isolation from plants was not possible or a diversified substitution pattern was encouraged, complex multi-step syntheses need to be performed. Iturriaga-Vásquez et al. designed simplified and more accessible congeners of tetrandrine (**1**), only representing one benzylisoquinoline half of the molecule and carrying extensions like *O*-benzyl groups (**Figure 6**). These derivatives had similar potential to block L-type calcium channels (Ca$_v$s) like tetrandrine (**1**)[82]. The fact that TPCs were a family intermediate of channels related to voltage-gated calcium (Ca$_v$) and sodium channels (Na$_v$)[83] suggested that these simplified structures could have high potential to block TPCs and further have high anticancer or antiviral activity. In addition, these truncated variants could overcome the lack of bioavailability, increase efficacy, be less toxic, more

specific, have a good solubility and are easily accessible and variable *via* a short, fast and efficient synthesis.

tetrandrine (**1**)   truncated variant
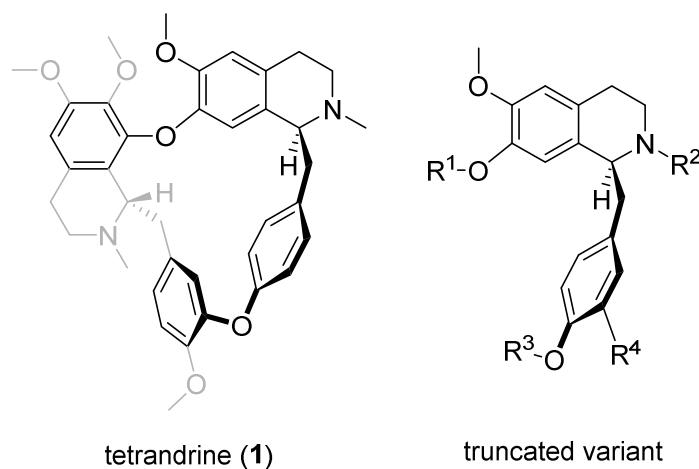
Figure 6: Truncation of tetrandrine (**1**) should give monomers, resembling one half of tetrandrine (**1**)[82].

To analyze TPC inhibitors in cellular systems the unique lysosomal patch clamp technique is required. Channel inhibition can be observed by this technique right after activation with the endogenous TPC2 activators $PI(3,5)P_2$ (**4**) or NAADP (**3**). Though this is a complex technique and only a few people in the world are able to perform these complex experiments. In order to analyze large compound libraries of potential TPC2 blockers, an easily accessible experimental setup was crucial. Ca^{2+} imaging experiments, using different Ca^{2+} indicating dyes like Fura-2 (**13**) or Fluo-4 (**14**) are well known but require intact cells and cell-permeable activators.

Therefore, novel small-molecule activators of TPC2 need to be identified first, synthesized and further analyzed to investigate their biological and pharmacological properties. These activators would then be used in a second step as chemical tools for the identification and analysis of TPC2 blockers, but in addition may play an independent role as lead structures for potential therapeutics in lysosomal storage diseases (LSDs).

3   Results and discussion

The results of this thesis are presented in this section and are divided into two main parts, agonists and antagonists of TPC2.

Starting with the performance of a high-throughput screening, the first part represents the identification of novel TPC2 activators. These hits were confirmed by synthesis, characterization and subsequent pharmacological experiments. Furthermore, analogs of these hits were synthesized to analyze structure-activity relationships (SAR). This was achieved by single cell Ca^{2+} imaging experiments. Concentration-effect relationships were analyzed and further results from cooperation partners are briefly described to present of the whole outcome of this interdisciplinary project.

The second main part of this chapter describes the synthesis and characterization of truncated tetrandrine analogs as novel TPC2 inhibitors. A Ca^{2+} imaging protocol to analyze TPC2 inhibitors, using our novel TPC2 activators, was developed. Biological activity of the inhibitors is of high interest and the effects on cancer were evaluated by cooperation partners. Furthermore, the enantiomers of the most promising substances were separated to distinguish between eutomer and distomer.

Additionally, results of some side projects are presented and briefly described.

3.1 Identification of novel TPC2 activators

Lysosomal storage diseases (LSDs) are a very hot topic not only in academic research, but also in industrial research. A cooperative project with F. Hoffmann-La Roche (Basel, CH) provided the opportunity to use two of their compound libraries (Xplore X30 and X50) to perform a high-throughput screening (HTS). The aim of this screening was to identify novel activators of Battenin (CLN3) and TPC2.

CLN3 is a putative lysosomal transporter or channel of unknown function but with a high relevance in inherited neurodegenerative disorder (Batten disease). Mutations in CLN3 lead to the loss of CLN3 function, causing Batten disease, also known as juvenile neuronal ceroid lipofuscinosis (JNCL) disease[84, 85]. Batten disease is the most common NCL with an onset of symptoms in childhood, characterized by progressive loss of vision, seizures, psychomotor disturbances and eventually premature death[86, 87]. As CLN3 and TPC2 are both lysosomal transmembrane proteins both proteins were screened in parallel serving as controls for each other.

In cooperation with Dr. Phuong Nguyen from Prof. Dr. Angelika Vollmar's group (LMU, Munich) and Prof. Dr. Michael Schaefer's group (Rudolf Boehm Institute, Leipzig) the high-throughput

screening was performed in Leipzig, using a custom-made fluorescence imaging plate reader (FLIPR) built into a robotic liquid handling station (for 96 tips), as previously described[88]. HEK293 cells stably expressing the plasma membrane variant of hTPC2, TPC2[L11A/L12A]-RFP and another cell line stably expressing the plasma membrane variant of hCLN3, CLN3[L253A/I254A] -RFP were used[22]. For the screening around 80.000 compounds on 221 384-well plates from two different libraries (X50 and X30) were provided by Roche (Basel, CH). All compounds were tested on both cell lines and double positive hits were excluded to ensure the accuracy of the hits in a first instance.

The membrane permeable, single-wavelength fluorescent dye Fluo-4/AM (**15**) was selected as Ca^{2+}-indicator. With this indicator experiments in cell suspension were possible, which was ideal for high-throughput screenings (**Figure 7 A**). Fluo-4/AM (**15**) entered the cells as lipophilic ester and was hydrolyzed inside the cells by esterases. Resulting Fluo-4 (**14**) is barely fluorescent, but fluorescence increases at least 100 times on Ca^{2+} binding when excited at 488 nm (**Figure 7 B**). An increase in fluorescence reflects rise in cytoplasmic Ca^{2+} levels caused by activation of the ion channels[89, 90].
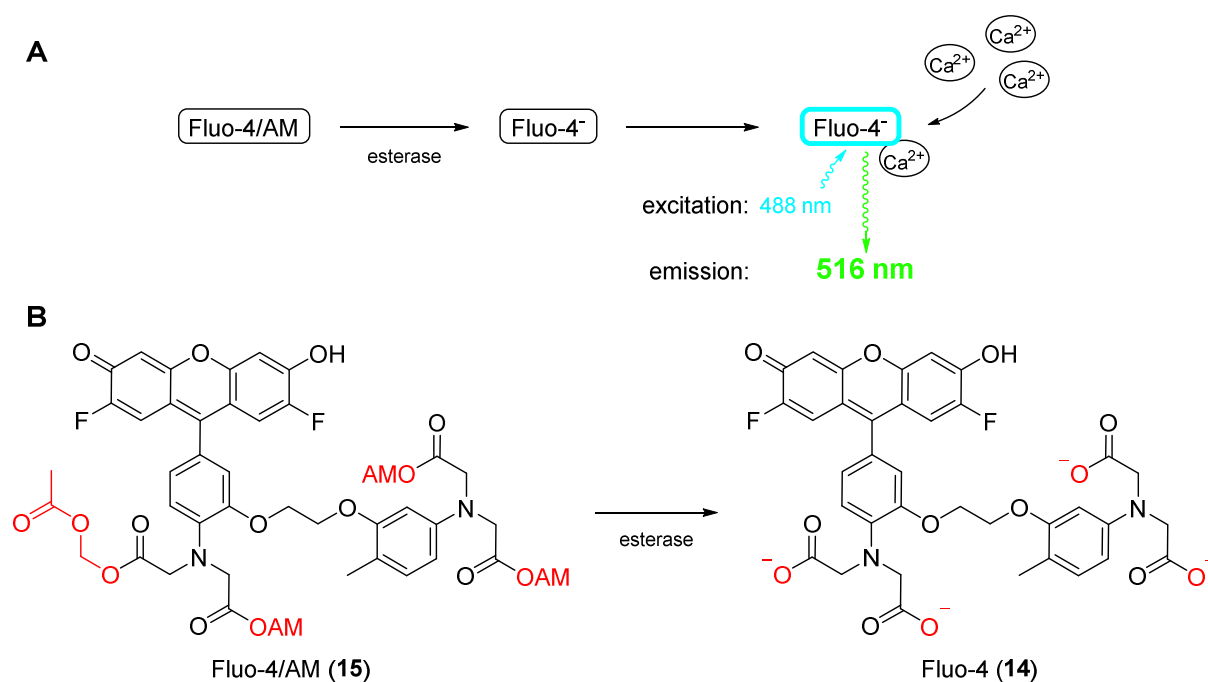
Figure 7: The principle of Fluo-4 based Ca^{2+}-imaging. (**A**) Short schematic overview of Fluo-4 based Ca^{2+}-imaging. Fluo-4/AM (**15**) can enter the cell as a membrane permeable molecule. Esterases cleave the AM esters and the free dye **14** remains. Fluo-4 (**14**) can complex Ca^{2+} ions which results in increased fluorescence at 516 nm. (**B**) Structures of Fluo-4/AM (**15**) and the free Fluo-4 (**14**) anion.

Compounds were screened on both cell lines. Hitlists of single hits were generated giving a total amount of 118 CLN3 primary hits and 133 TPC2 primary hits (**Figure 8 A**). Since

availability of the compounds as well as the quantity was limited, only the strongest hits (highest fluorescence increase) for each cell line were selected and further investigated by concentration-effect experiments. Thus, only 25 CLN3 primary hits and 12 TPC2 primary hits were further considered. Concentration-effect experiments in the range of 50 µM to 24 nM resulted in two secondary CLN3 hits (A09 and C15) and four secondary TPC2 hits (N19, N10, H07 and L13). These secondary hits were all evaluated in Fura-2 based Ca^{2+}-imaging experiments (see chapter 3.4 for the method). None of the analyzed CLN3 hits showed a specific activation. One TPC2 hit had no effect and another one showed unspecific or toxic effects. Hence only two final hits for TPC2 (N19, named TPC2-A1-N (**16**) and H07, named TPC2-A1-P (**17**)) remained that were able to activate the TPC2 ion channel (**Figure 8 B**). The activity of these two compounds was further confirmed by the electrophysiological endo-lysosomal patch clamp technique.
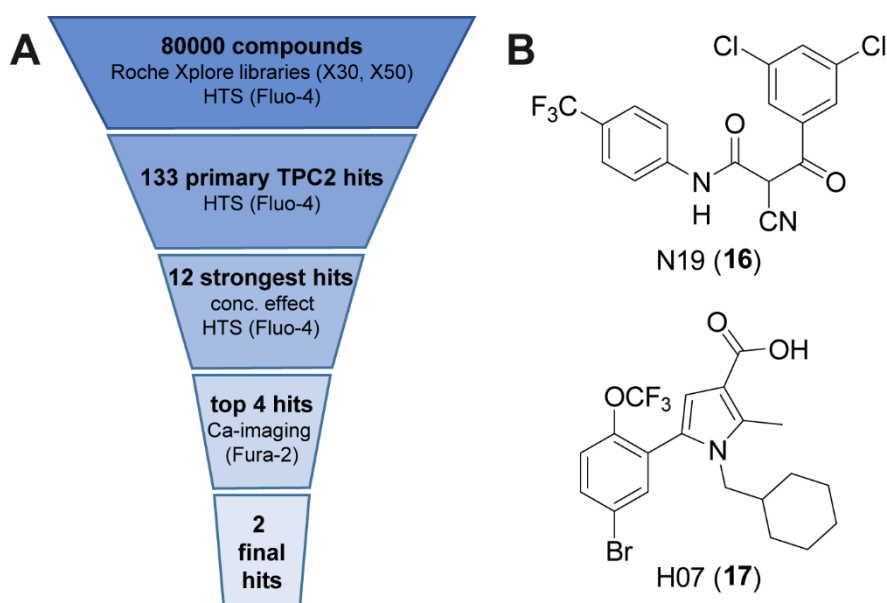
Figure 8: Summary of the high-throughput screening. (**A**) Simplified overview for the stepwise identification of the two TPC2 screening hits. (**B**) Structure of the two screening hits N19 (new name: TPC2-A1-N (**16**)) and H07 (new name: TPC2-A1-P (**17**)), as presented to us by Roche (Basel, CH).

To verify the postulated structure and assess SAR, generally applicable syntheses for both hits had to be developed and the resulting compounds had to be re-evaluated *via* Fura-2 calcium imaging

3.2 Synthesis of TPC2-A1-N (16) and analogs

Starting with TPC2-A1-N (**16**), first a synthesis to confirm the structure of the hit had to be developed. A fast, efficient and versatile synthesis was desired. Thus, a compound library can be generated to examine SAR. Variations of both aromatic rings, the necessity of a secondary amide, as well as the extension of the middle part were investigated. Sjogren et al. published a two-step synthesis for related *α*-cyano-*β*-hydroxypropenamides, which resulted in exactly the desired scaffold of TPC2-A1-N (**I**, **Scheme 1**)[91].
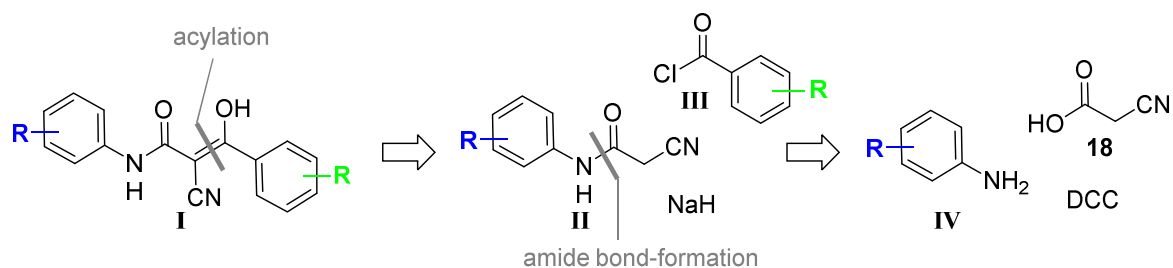
Scheme 1: Retrosynthetic overview showing the synthesis of *α*-cyano-*β*-hydroxypropenamides (**I**) in two steps. By using different aniline (**IV**) and benzoic acid (**III**) building blocks, a large variability of combinations is possible.

Following these procedures an C-acylation using different activated benzoic acid building blocks (**III**, **Scheme 1**) and NaH as strong base should easily yield desired hydroxypropeneamides (**I**, **Scheme 1**). Therefore the required *α*-cyano amide (**II**, **Scheme 1**) could be synthesized using different aniline building blocks (**IV**, **Scheme 1**), 2-cyanoacetic acid (**18**) and a standard coupling reagent as DCC. This synthesis resulted in the desired *α*-cyano-*β*-hydroxypropenamides (**I**, **Scheme 1**) in only two steps and without need for purification by column chromatography, which gave the opportunity to establish a broad compound library.
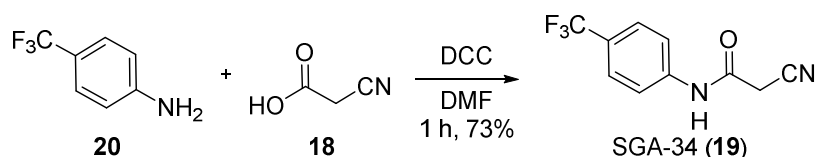
Scheme 2: Synthesis of 2-cyano-*N*-(4-(trifluoromethyl)phenyl)acetamide (SGA-34, **19**), according to Sjogren et al.[91].

Starting with the structure confirmation of the hit TPC2-A1-N (**16**) commercially available 4-(trifluoromethyl)aniline (**20**), 2-cyanoacetic acid (**18**) and DCC were used in DMF. After one hour the reaction was completed. Purification by filtration and recrystallization yielded the pure 2-cyano-*N*-(4-(trifluoromethyl)phenyl)acetamide (SGA-34, **19**) in high yield (73%, **Scheme 2**).

Only a few modifications in equivalents were made compared to the original literature in order to achieve the best results. For the synthesis of variably substituted *α*-cyano amides this method was applied (**II**, **Table 1**). This resulted in mainly *p*-substituted *α*-cyano amides (entry 1-14, **Table 1**), as well as unsymmetrically (entry 15-19, **Table 1**) and symmetrically substituted aryls (entry 20, 21, **Table 1**). Electron-withdrawing groups like halide, nitro, nitrile or carbonyl substituents represented the majority. The methyl group (entry 2, **Table 1**) was introduced as the electron-donating bioisostere to the screening hit's trifluoromethyl group (entry 1, **Table 1**). A variant with a tertiary amide (entry 22, **Table 1**) and another one being derived from a benzylamine (entry 23, **Table 1**) completed the *α*-cyano amides. Yields were all moderate to high, very poor only for *N*-benzyl-acetamide (entry 23, **Table 1**).

Table 1: Overview of the results for the synthesis of *α*-cyano amides (**II**). Different aniline building blocks (**IV** and a homologous benzylamine in entry 23) and 2-cyanoacetic acid (**18**) were used as starting materials.
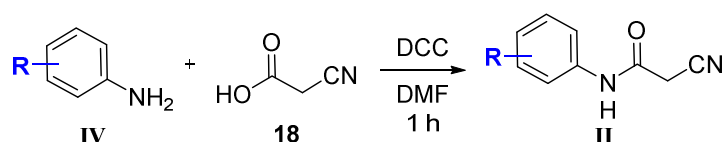
entry	starting material (**IV**)	product (**II**)	yield
1	R = 4-CF$_3$ (**20**)	2-cyano-*N*-(4-(trifluoromethyl)phenyl)acetamide (SGA-34, **19**)	73%
2	R = 4-CH$_3$	2-cyano-*N*-(*p*-tolyl)acetamide (**21**)	71%
3	R = H	2-cyano-*N*-phenylacetamide (**22**)	76%
4	R = 4-OCH$_3$	2-cyano-*N*-(4-methoxyphenyl)acetamide (**23**)	41%
5	R = 4-Cl	*N*-(4-chlorophenyl)-2-cyanoacetamide (**24**)	77%
6	R = 4-Br	*N*-(4-bromophenyl)-2-cyanoacetamide (**25**)	40%
7	R = 4-F	2-cyano-*N*-(4-fluorophenyl)acetamide (**26**)	75%
8	R = 4-I	2-cyano-*N*-(4-iodophenyl)acetamide (**27**)	77%
9	R = 4-NO$_2$	2-cyano-*N*-(4-nitrophenyl)acetamide (**28**)	62%
10	R = 4-CN	2-cyano-*N*-(4-cyanophenyl)acetamide (**29**)	78%
11	R = 4-Ac	*N*-(4-acetylphenyl)-2-cyanoacetamide (**30**)	54%
12	R = 4-OPr	2-cyano-*N*-(4-propoxyphenyl)acetamide (**31**)	62%
13	R = 4-OCF$_3$	2-cyano-*N*-(4-(trifluoromethoxy)phenyl)acetamide (**32**)	72%
14	R = 4-COOCH$_3$	methyl 4-(2-cyanoacetamido)benzoate (**33**)	65%
15	R = 2-Br, 4-Cl	*N*-(2-bromo-4-chlorophenyl)-2-cyanoacetamide (**34**)	69%
16	R = 2-I	2-cyano-*N*-(2-iodophenyl)acetamide (**35**)	70%
17	R = 2,4-F$_2$, 3-Cl	*N*-(3-chloro-2,4-difluorophenyl)-2-cyanoacetamide (**36**)	68%
18	R = 3,4-(OCH$_3$)$_2$	2-cyano-*N*-(3,4-dimethoxyphenyl)acetamide (**37**)	76%
19	R = 2,3-Cl$_2$	2-cyano-*N*-(2,3-dichlorophenyl)acetamide (**38**)	29%
20	R = 2,6-Br$_2$	2-cyano-*N*-(2,6-dibromophenyl)acetamide (**39**)	40%
21	R = 3,5-(CF$_3$)$_2$	*N*-(3,5-bis(trifluoromethyl)phenyl)-2-cyanoacetamide (**40**)	81%

| 22 | *N*-methyl-4-(trifluoromethyl)aniline | 2-cyano-*N*-methyl-*N*-(4-(trifluoromethyl)phenyl)acetamide (**41**) | 74% |
| 23 | 4-(trifluoromethyl)benzylamine | 2-cyano-*N*-(4-(trifluoromethyl)benzyl)acetamide (**42**) | 7% |

For the synthesis of TPC2-A1-N (**16**) acylation of the appropriate *α*-cyano acetamide (SGA-34, **19**) was performed using 3,5-dichlorobenzoyl chloride (**43**) and NaH in THF[91]. After one hour the reaction was completed and purification by filtration and recrystallization yielded pure 2-cyano-3-(3,5-dichlorophenyl)-3-hydroxy-*N*-(4-(trifluoromethyl)phenyl)acrylamide (TPC2-A1-N, **16**) in high yield (69%, **Scheme 3**). NMR analysis of TPC2-A1-N (**16**) showed that the enol-form is favored compared with the keto-form, as described below.
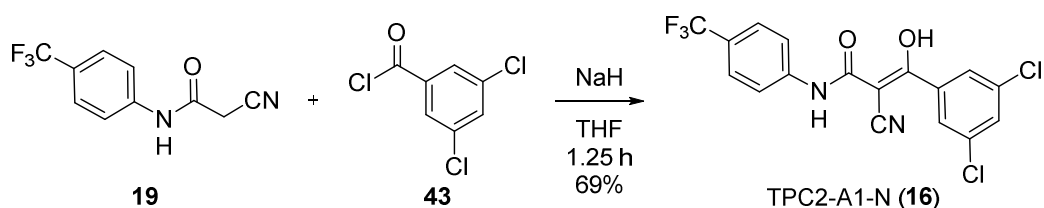
Scheme 3: Synthesis of 2-cyano-3-(3,5-dichlorophenyl)-3-hydroxy-*N*-(4-(trifluoromethyl)phenyl)-acrylamide (TPC2-A1-N, **16**), following a procedure published by Sjogren et al.[91].

This procedure was beneficial in many ways. It was fast and the easy work up gave highly pure crystalline products. These products did not need purification by FCC, which saved time and material. Furthermore FCC would also cause problems, as it is reported that 1,3-diketones form chelate complexes with metal ions, e.g. Fe^{3+}[91-93]. The commonly used silica in chemical laboratories contains slight impurities of Fe^{3+}, which would result in colorful contaminated products. Different *α*-cyano amides (**II**, **Table 2**) were already prepared and plenty benzoic acid building blocks (**III**) were commercially available. Depending on biological results a variety of compounds could be synthesized by different combinations of these building blocks. Hence, a set of *α*-cyano-*β*-hydroxypropenamides (**I**, **Table 2**) was synthesized using this method. This resulted in a compound library of 44 TPC2-A1-N analogs. The newly synthesized *α*-cyano amides (blue, **II**, **Table 2**) were used for different moieties on the anilide side (blue, entry 1-7, 10, 11, 14, 15, 18-20, 27-32, 43, **Table 2**) of the molecule. Widely varying benzoic acid building blocks (green, **III**, **Table 2**) were commercially available, which gave the opportunity to introduce 17 different aryl groups (green, entry 1, 8, 9, 12, 13, 17, 21-23, 34, 36-39, 41, 42, 44, **Table 2**). Combinations of different amide (**II**, **Table 2**) and benzoic acid (**III**, **Table 2**) building blocks resulted in 6 more compounds (entry 16, 24-26, 33, 35, **Table 2**). One variant with a tertiary amide (entry 40, **Table 2**) and another one replacing the anilide moiety with a benzyl amide (entry 45, **Table 2**), completed the compound list. Nearly all yields are
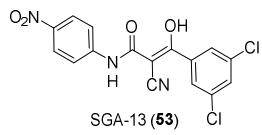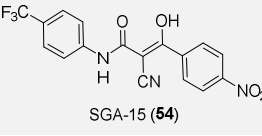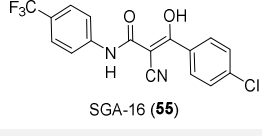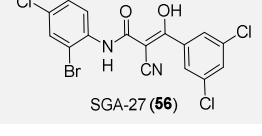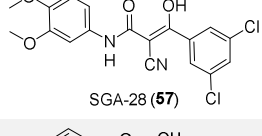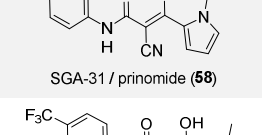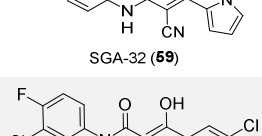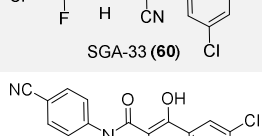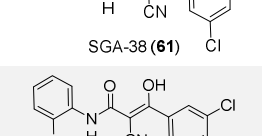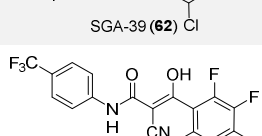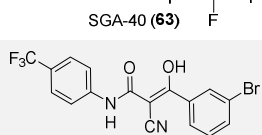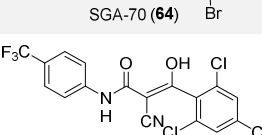
moderate to high, which indicates that this protocol is extendable to a wide variety of α-cyano amides (**II**, **Table 2**) and benzoic acid building blocks (**III**, **Table 2**).

Table 2: Overview of the results for the synthesis of α-cyano-β-hydroxypropenamides (**I**). Different benzoic acid building blocks (**III**) are combined with the α-cyano amides (**II**). *If the appropriate acid chloride was not commercially available, the benzoic acid was converted into the acid chloride using thionyl chloride.
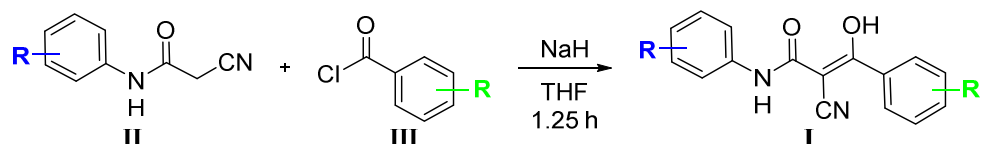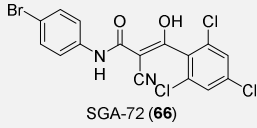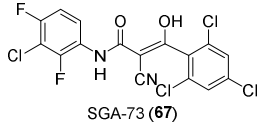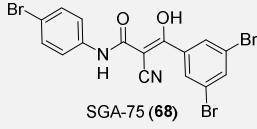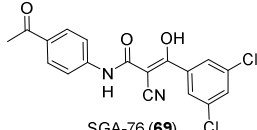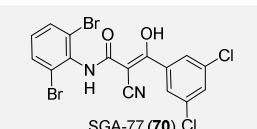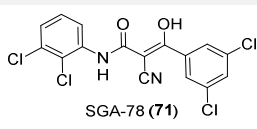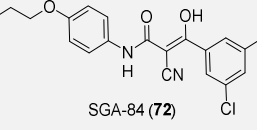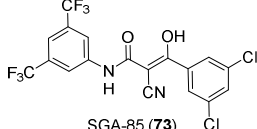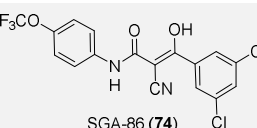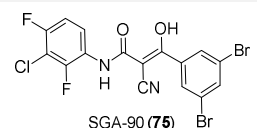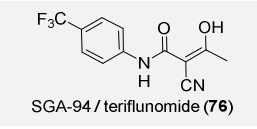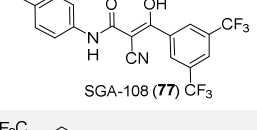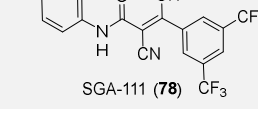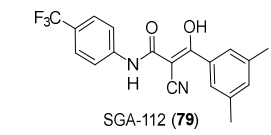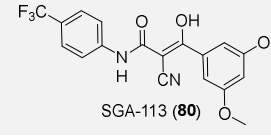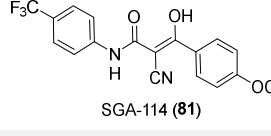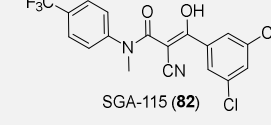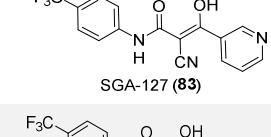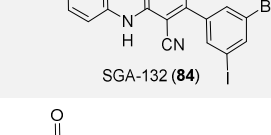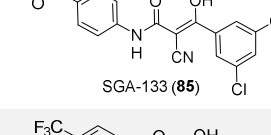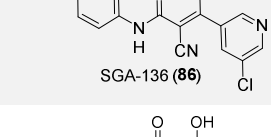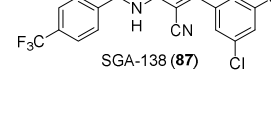
entry	amide (II)	benzoic acid chloride* (III)	product (I)	yield
1	R = 4-CF₃ (SGA-34, **19**)	R = 3,5-Cl₂ (**43**)	TPC2-A1-N (**16**)	69%
2	R = H (**22**)	R = 3,5-Cl₂ (**43**)	SGA-1 (**44**)	68%
3	R = 4-Cl (**24**)	R = 3,5-Cl₂ (**43**)	SGA-2 (**45**)	70%
4	R = 4-Br (**25**)	R = 3,5-Cl₂ (**43**)	SGA-3 (**46**)	70%
5	R = 4-CH₃ (**21**)	R = 3,5-Cl₂ (**43**)	SGA-4 (**47**)	53%
6	R = 4-F (**26**)	R = 3,5-Cl₂ (**43**)	SGA-8 (**48**)	63%
7	R = 4-I (**27**)	R = 3,5-Cl₂ (**43**)	SGA-9 (**49**)	61%
8	R = 4-CF₃ (SGA-34, **19**)	R = H	SGA-10 (**50**)	56%
9	R = 4-CF₃ (SGA-34, **19**)	R = 3,5-(NO₂)₂	SGA-11 (**51**)	29%
10	R = 4-OCH₃ (**23**)	R = 3,5-Cl₂ (**43**)	SGA-12 (**52**)	61%

11	R = 4-NO$_2$ (**28**)	R = 3,5-Cl$_2$ (**43**)	SGA-13 (**53**)	55%
12	R = 4-CF$_3$ (SGA-34, **19**)	R = 4-NO$_2$	SGA-15 (**54**)	69%
13	R = 4-CF$_3$ (SGA-34, **19**)	R = 4-Cl	SGA-16 (**55**)	61%
14	R = 2-Br, 4-Cl (**34**)	R = 3,5-Cl$_2$ (**43**)	SGA-27 (**56**)	74%
15	R = 3,4-(OCH$_3$)$_2$ (**37**)	R = 3,5-Cl$_2$ (**43**)	SGA-28 (**57**)	51%
16	R = H (**22**)	1-methylpyrrole-2-carbonyl chloride	SGA-31 / prinomide (**58**)	75%
17	R = 4-CF$_3$ (SGA-34, **19**)	1-methylpyrrole-2-carbonyl chloride	SGA-32 (**59**)	66%
18	R = 2,4-F$_2$, 3-Cl (**36**)	R = 3,5-Cl$_2$ (**43**)	SGA-33 (**60**)	72%
19	R = 4-CN (**29**)	R = 3,5-Cl$_2$ (**43**)	SGA-38 (**61**)	38%
20	R = 2-I (**35**)	R = 3,5-Cl$_2$ (**43**)	SGA-39 (**62**)	52%
21	R = 4-CF$_3$ (SGA-34, **19**)	R = 2,3,4,5,6-F$_5$	SGA-40 (**63**)	56%
22	R = 4-CF$_3$ (SGA-34, **19**)	R* = 3,5-Br$_2$	SGA-70 (**64**)	42%
23	R = 4-CF$_3$ (SGA-34, **19**)	R = 2,4,6-Cl$_3$	SGA-71 (**65**)	36%

24	R = 4-Br (**25**)	R = 2,4,6-Cl$_3$	SGA-72 (**66**)	51%
25	R = 2,4-F$_2$, 3-Cl (**36**)	R = 2,4,6-Cl$_3$	SGA-73 (**67**)	50%
26	R = 4-Br (**25**)	R* = 3,5-Br$_2$	SGA-75 (**68**)	44%
27	R = 4-Ac (**30**)	R = 3,5-Cl$_2$ (**43**)	SGA-76 (**69**)	79%
28	R = 2,6-Br$_2$ (**39**)	R = 3,5-Cl$_2$ (**43**)	SGA-77 (**70**)	13%
29	R = 2,3-Cl$_2$ (**38**)	R = 3,5-Cl$_2$ (**43**)	SGA-78 (**71**)	86%
30	R = 4-OPr (**31**)	R = 3,5-Cl$_2$ (**43**)	SGA-84 (**72**)	63%
31	R = 3,5-(CF$_3$)$_2$ (**40**)	R = 3,5-Cl$_2$ (**43**)	SGA-85 (**73**)	68%
32	R = 4-OCF$_3$ (**32**)	R = 3,5-Cl$_2$ (**43**)	SGA-86 (**74**)	83%
33	R = 2,4-F$_2$, 3-Cl (**36**)	R* = 3,5-Br$_2$	SGA-90 (**75**)	76%
34	R = 4-CF$_3$ (SGA-34, **19**)	acetyl chloride	SGA-94 / teriflunomide (**76**)	76%
35	R = 4-CH$_3$ (**21**)	R = 3,5-(CF$_3$)$_2$	SGA-108 (**77**)	50%
36	R = 4-CF$_3$ (SGA-34, **19**)	R = 3,5-(CF$_3$)$_2$	SGA-111 (**78**)	76%

37	R = 4-CF$_3$ (SGA-34, **19**)	R = 3,5-(CH$_3$)$_2$	SGA-112 (**79**)	49%
38	R = 4-CF$_3$ (SGA-34, **19**)	R = 3,5-(OCH$_3$)$_2$	SGA-113 (**80**)	79%
39	R = 4-CF$_3$ (SGA-34, **19**)	R = 4-OCF$_3$	SGA-114 (**81**)	48%
40	*N*-methyl-acetamide (**41**)	R = 3,5-Cl$_2$ (**43**)	SGA-115 (**82**)	48%
41	R = 4-CF$_3$ (SGA-34, **19**)	nicotinoyl chloride	SGA-127 (**83**)	51%
42	R = 4-CF$_3$ (SGA-34, **19**)	R* = 3-Br, 5-I	SGA-132 (**84**)	62%
43	R = 4-COOCH$_3$ (**33**)	R = 3,5-Cl$_2$ (**43**)	SGA-133 (**85**)	85%
44	R = 4-CF$_3$ (SGA-34, **19**)	5-chloronicotinic acid*	SGA-136 (**86**)	61%
45	benzyl-acetamide (**42**)	R = 3,5-Cl$_2$ (**43**)	SGA-138 (**87**)	55%

The methyl ester group of SGA-133 (**85**, entry 43, **Table 2**) could easily be converted into the free carboxylic acid using alkaline hydrolysis. With an excess of LiOH, the ester was cleaved within 3 h at room temperature. Precipitation gave the free acid SGA-137 (**88**) in high yield (**Scheme 4**).
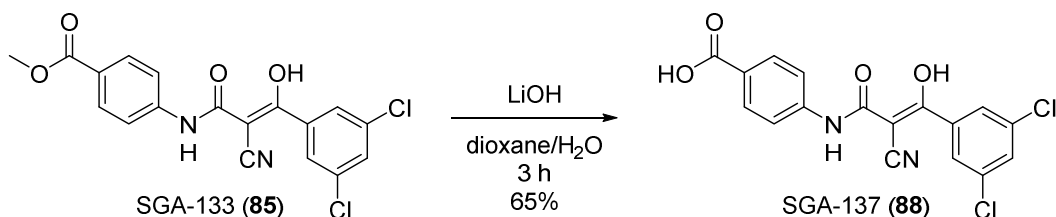
Scheme 4: Deprotection of ester SGA-133 (**85**) using alkaline conditions gave the free acid SGA-137 (**88**).

20

Sjogren et al. applied a second method to generate *α*-cyano-*β*-hydroxypropenamides (**I**, **Table 2**). This procedure was using benzoic acid building blocks (**III**, **Table 2**) and acetonitrile to give 3-oxopropanenitriles and condensed these with isocyanates or isothiocyanates[91]. More precisely the thioamide analog of TPC2-A1-N (**16**) was synthesized this way within an Erasmus project, as depicted in **Scheme 5**. Benzoyl chloride **43** together with the lithium salt of acetonitrile gave the 3-oxopropanenitrile **89**. Subsequent condensation with arylisothiocyanate **90** in the presence of NaH yielded SGA-167 (**91**) in moderate yields, which was in accordance with literature[91]. Due to a complex work-up of the intermediate **89**, yields were not as high as on the first route.
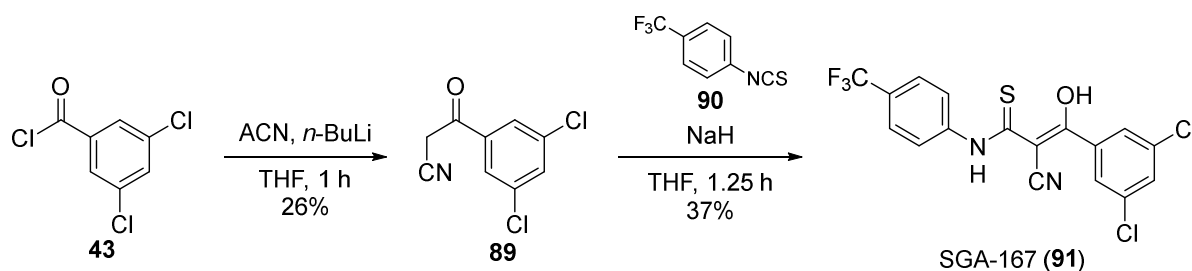
Scheme 5: Synthesis of SGA-167 (**91**) according to Sjogren et al.[91].

Structural analysis of TPC2-A1-N (**16**) and analogs was a more difficult process as expected. ^{1}H-NMR analysis showed mainly aromatic signals and ^{13}C NMR spectra of the numerous fluorinated products showed plenty carbon fluorine splits. The carbon fluorine coupling resulted in ^{1}J coupling constants of around 270 Hz, ^{2}J coupling constants of around 30 Hz, ^{3}J coupling constants of around 3.5 Hz and a multiplicity of n + 1. The ^{1}J coupling constant was observed in every ^{13}C spectrum of a fluorine containing substance, the more distant ones were only observed in the absence of heteroatoms. As known from related 1,3-dicarbonyl compounds such as acetylacetone, two tautomeric structures are possible, the keto- and the enol-form, which could also be observed by ^{1}H-NMR. It is reported, that the enol-form of acetylacetone is more stable than the keto-form, due to the formation of a hydrogen bond between one carbonyl and the enol-hydroxy group[94]. For *β*-ketoamides a hydrogen bond between the *β*-ketone group and the amide NH is also possible ("keto-amide" form; **Scheme 6**). Both forms were found by Laurella et al. in studies of tautomeric equilibria of *β*-ketoamides. Furthermore these authors discovered that electron-withdrawing groups at the benzoyl ring stabilize the enol-amide tautomer, electron donors stabilize the keto-amide form and bulky groups in C-2 position favor the enol-form as well[95]. Transferred to the scaffold of TPC2-A1-N (**16**), the enol-tautomer was more likely to be the fitting style, as the nitrile residue is highly electronegative. This was further confirmed by NMR analysis. In most ^{1}H-NMR spectra no standard or shifted hydroxyl group was observed, but nevertheless no proton in C-2 position was found. In addition, this carbon was always indicated as quaternary in ^{13}C/HSQC analysis.
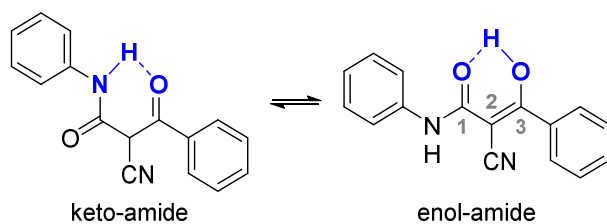
Scheme 6: Keto-enol tautomerism of the blank TPC2-A1-N scaffold. The two most likely tautomers to occur are displayed, the keto-amide (left) and the enol-amide (right). Both structures are able to form a hydrogen bond to stabilize the conformation.

Collectively, 47 compounds were synthesized in moderate to high yields, including the hit TPC2-A1-N (**16**), the amide SGA-34 (**19**) as half of the molecule, two drugs (prinomide (**58**) and teriflunomide (**76**)) and a large variety of analogs. All of them were fully characterized by NMR, TLC, HRMS, IR and melting points and the purities were confirmed by analytical HPLC.

3.3 Synthesis of TPC2-A1-P (17) and analogs

The same procedure as for TPC2-A1-N (**16**) needed to be applied for TPC2-A1-P (**17**). In more detail, the hit TPC2-A1-P (**17**) needed to be confirmed, a synthesis to generate TPC2-A1-P (**17**) and analogs had to be developed and a variety of analogs had to be synthesized and characterized for structure-activity analysis.

Examining the structure of TPC2-A1-P (**17**) the highly substituted pyrrole moiety stands out. Pyrrole syntheses have been known for decades and syntheses of highly substituted pyrroles were thoroughly examined by many groups. Nevertheless, construction of the appropriately substituted pyrrole ring was the key step. The free carboxylic acid (**I**, **Scheme 7**) could be generated by alkaline deprotection of an ester intermediate (**II**, **Scheme 7**), which is generated by suitable pyrrole synthesis. The easily available and variable α-halogenated acetophenone (**IV**, **Scheme 7**), β-ketoester (**V**, **Scheme 7**) and primary amine (**III**, **Scheme 7**) building blocks are the basis for pyrrole formation (**Scheme 7**).
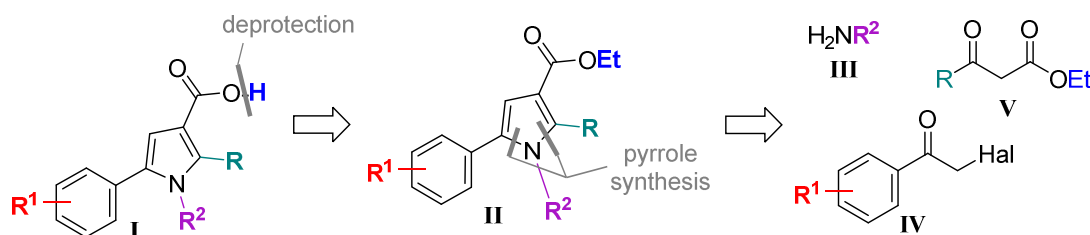
Scheme 7: Retrosynthetic overview for the synthesis of TPC2-A1-P (**17**) and analogs (**I**) derived from different α-halogenated acetophenone (**IV**), β-ketoester (**V**) and primary amine (**III**) building blocks.

The Hantzsch pyrrole synthesis is one famous reaction to generate pyrroles[96]. Condensation of primary amine (**III**, **Scheme 8**) and *β*-ketoester (**V**, **Scheme 8**) building blocks gives an enamino ester intermediate (**VI**, **Scheme 8**). C-Alkylation by the *α*-halogenated acetophenone (**IV**, **Scheme 8**) gives a 2-substituted enamino ester (**VII**, **Scheme 8**) which undergoes intramolecular cyclocondensation to give the desired 2,3,5-trisubstituted pyrrole (**II**, **Scheme 8**)[96-98].
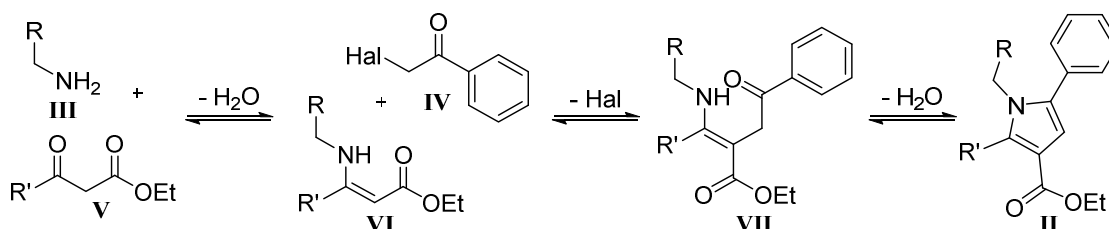
Scheme 8: Commonly accepted mechanism for the Hantzsch pyrrole synthesis, yielding a multi-substituted pyrrole (**II**).

Zhao et al. published a microwave-assisted one-pot method for the synthesis of *N*-substituted 2-methyl-1*H*-pyrrole-3-carboxylate derivatives[99]. This method is notable because of the absence of solvents and catalysts as well as the fast and easy implementation. The appropriate *α*-halogenated acetophenone to yield TPC2-A1-P (**17**) is not commercially available. Therefore, two commercially available *α*-bromo acetophenones (**92** and **93**) were used for model reactions. Hereby, building block **93** would provide a product very similar to TPC2-A1-P (**17**), with only the trifluoromethoxy group being replaced by a methoxy group. Together with *β*-ketoester (**94**) and cyclohexanemethanamine (**95**) they were added into one microwave reactor each. After irradiation at 8 bar and 240 °C for 1 h, no residues of bromoacetophenones **92** and **93** were detected. Pyrrole **96** was isolated in low yield, though no product formation could be observed for the pyrrole **97** closely related to TPC2-A1-P (**17**) (**Scheme 9**). Hence this method was not further pursued.

R = H (**92**)
R = 2-OCH$_3$, 5-Br (**93**)

94

95

R = H (**96**) 10%
R = 2-OCH$_3$, 5-Br (**97**) 0%
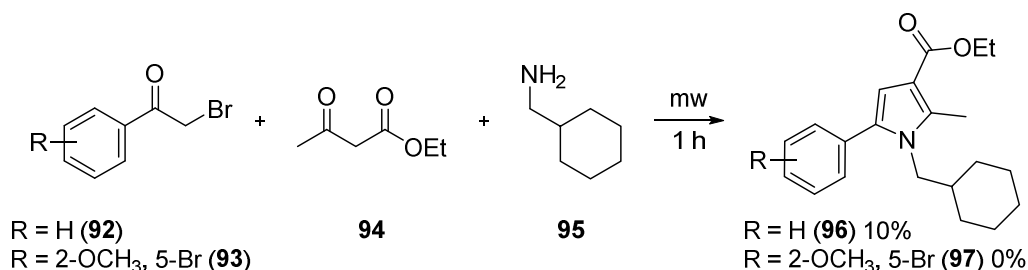
Scheme 9: Synthetic approach for the Hantzsch pyrrole synthesis to yield the methoxy analog of TPC2-A1-P **97** and ester **96**.

Another method, related to the Hantzsch synthesis, is the Paal-Knorr pyrrole synthesis[100, 101]. Condensation of 1,4-diketone building blocks (**VIII**, **Scheme 10**) with a primary amine building block (**III**, **Scheme 10**) under protic or Lewis acidic conditions yields multi-substituted pyrroles (**II**, **Scheme 10**)[102]. The drawback of this method is, that the 1,4-diketone building blocks (**VIII**, **Scheme 10**) have to be synthesized in an additional step. A procedure, published by Kang et al.[103], exactly describes this route. With α-halogenated acetophenone (**IV**, **Scheme 10**) and β-ketoester (**V**, **Scheme 10**) building blocks 1,4-diketones (**VIII**, **Scheme 10**) are synthesized using NaH as base. The authors used ammonium acetate in acetic acid to yield N-unsubstituted pyrroles, or primary amine building blocks (**III**, **Scheme 10**) with p-toluenesulfonic acid in ethanol to receive N-alkyl pyrroles[103]. Most primary amine building blocks (**III**, **Scheme 10**) that will be used are liquids, therefore they don't need organic solvents to be dissolved and acetic acid is chosen as preferred acid.
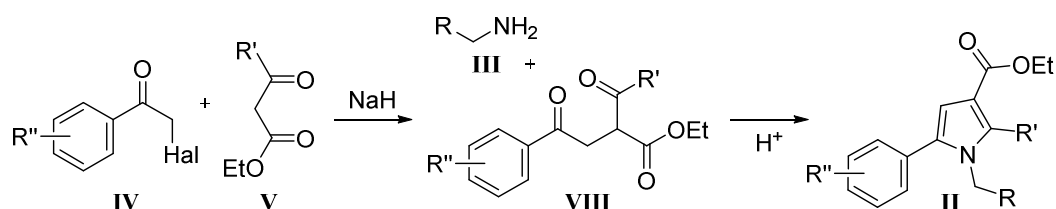
Scheme 10: General reaction equation for the formation of 1,4-diketone building blocks (**VIII**)[103] and subsequent Paal-Knorr pyrrole synthesis yielding a highly substituted pyrrole derivative (**II**)[102].

In model reactions α-bromoacetophenones **92** and **93** together with β-ketoester **94**, KI and NaH gave the 1,4-diketones **98** and **99**. After standard work-up these diketones (**98** and **99**) were pure enough for further proceedings and following Paal-Knorr reaction using cyclohexanemethanamine (**95**) yielded pyrroles SGA-43 (**96**) and SGA-54 (**97**) in high yields over two steps. KI was added for an *in situ* Finkelstein reaction to boost the conversion of the first step. For the sake of time and material savings the 1,4-diketone building blocks (**VIII**, **Scheme 10**) were used right away after preparation, without further purification or analysis.
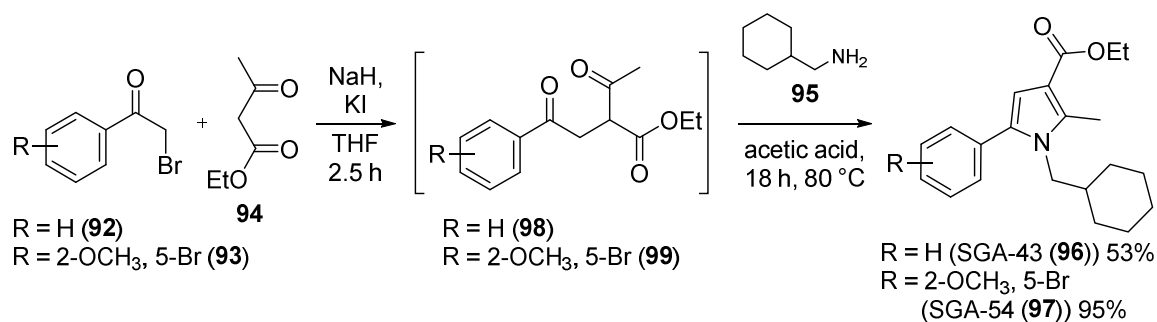
Scheme 11: Model reactions for the synthesis of 2,3,5-trisubstituted pyrroles, yielding SGA-43 (**96**) and SGA-54 (**97**).

The final step in the synthesis of the desired carboxylic acids was the deprotection of the esters. Esters can be cleaved by hydrolysis in acidic or alkaline conditions. Kang et al. described a method using NaOH[103], which is the reason why alkaline conditions were chosen. For screening of deprotection conditions ester SGA-43 (**96**) was chosen. Using NaOH in dioxane/H_2O at room temperature only gave starting material after 15 h (entry 1, **Table 3**). Changing to LiOH, THF/H_2O[104] and reflux gave the same result (entry 2, **Table 3**), as well as refluxing with NaOH in dioxane/H_2O[105] (entry 3, **Table 3**). A pressure tube was used to increase the power of the reaction, but still no deprotection was observed (entry 4, **Table 3**). To generate maximum power, a microwave reaction was applied. With dioxane/H_2O rough conditions could be achieved and after 2 h total conversion of the ester **96** was observed (entry 5, **Table 3**). For better handling LiOH was examined, also giving the carboxylic acid **100** in high yield (entry 6, **Table 3**).

Table 3: Screening of conditions for the ester saponification using SGA-43 (**96**).

SGA-43 (**96**)   SGA-50 (**100**)
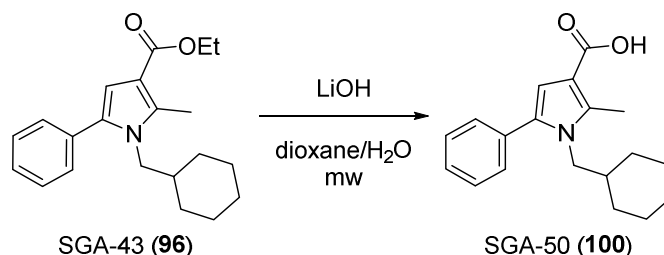
entry	base	solvent	temperature / conditions	time	product
1	NaOH	dioxane/H_2O (5:1)	rt	15 h	only s.m.
2	LiOH	THF/H_2O (4:1)	60 °C / reflux condenser	12 h	only s.m.
3	NaOH	dioxane/H_2O (5:1)	100 °C / reflux condenser	15 h	only s.m.
4	NaOH	dioxane/H_2O (5:1)	100 °C / pressure tube	18 h	only s.m.
5	NaOH	dioxane/H_2O (5:1)	microwave reactor (p_{max} = 8 bar, P_{max} = 80 W, T_{max} = 160 °C)	2 h	93%
6	LiOH	dioxane/H_2O (5:1)	microwave reactor (p_{max} = 8 bar, P_{max} = 200 W, T_{max} = 180 °C)	2 h	89%

With this newly developed method for the synthesis of carboxylic acid (**I**, **Scheme 10**), only the access to the starting materials needed to be examined. Most starting materials are commercially available and just two *α*-halogenated acetophenones (**IV**, **Scheme 10**) had to be synthesized to give all designed analogs for complete structure-activity relationships: 2-Bromo-1-(2-(trifluoro-methoxy)phenyl)ethan-1-one (**101**) and 1-(5-bromo-2-(trifluoromethoxy)-phenyl)-2-chloroethan-1-one (**102**).

Inspired by a poorly detailed patented procedure[106] mono-bromination of 2'-(trifluoromethoxy)-acetophenone (**103**) was carried out under acidic conditions. Only one equivalent of *N*-

bromosuccinimide (NBS) and a catalytic amount of *p*-toluenesulfonic acid were used to yield the desired bromoketone **101** in moderate yield (**Scheme 12**).
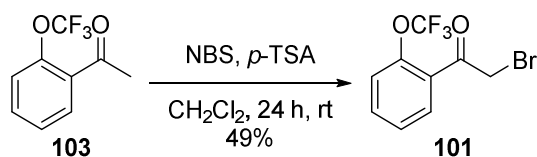
Scheme 12: Mono-bromination of acetophenone **103** in acidic conditions to give bromoketone **101**.

For the synthesis of the hit TPC2-A1-P (**17**), chloroketone **102** needed to be synthesized. Schlosser et al. published a procedure for lithiation of 1-bromo-4-(trifluoromethoxy)benzene (**104**) with LDA at C-3 (directed metalation), followed by carboxylation at -100 °C with dry ice[107]. The authors claimed that these conditions reduce the competing *ortho*- or *meta*-lithiation (positions to the OCF_3 group) in a ratio of 99:1 to receive a regioselective *ortho*-product. As the desired *ortho*-lithiation is favored, the reaction was carried out at -78 °C using the Weinreb amide 2-chloro-*N*-methoxy-*N*-methylacetamide (**105**) instead of dry ice. Though the desired *α*-chloroketone **102** did not occur and only decomposition of the starting material was observed (a, **Scheme 13**). Same applied to the use of freshly prepared LDA, according to Schlosser et al. (b, **Scheme 13**)[107]. Furthermore a Friedel-Crafts acylation was performed, using $AlCl_3$ and chloroacetyl chloride in 1,2-dichloroethane (EDC), but no product formation was observed (c, **Scheme 13**).
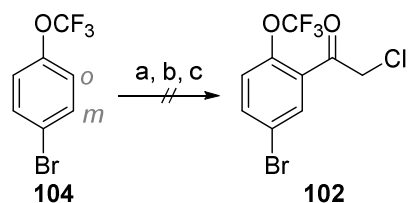
Scheme 13: Attempted chloroacetylation of **104**. Different reaction conditions were screened. a) **104**, LDA, THF, -78 °C, 4 h; then 2-chloro-*N*-methoxy-*N*-methylacetamide (**105**) in THF, -78 °C, 5 min. b) **104**, LDA, generated out of DIPA and *n*-BuLi, -78 °C, 2 h; then 2-chloro-*N*-methoxy-*N*-methylacetamide (**105**) in THF, -78 °C, 5 min. c) **104**, $AlCl_3$, chloroacetyl chloride, EDC, 0 °C – 50 °C, 5 h.

Lui et al. developed a method for the oxidative trifluoromethylation of phenols[108]. Among their examples there were *ortho*- and *para*-halogenated phenols, which seemed promising. The reaction was performed with commercially available phenol **106** in a custom made glove box, but again no product could be isolated (**Scheme 14**).
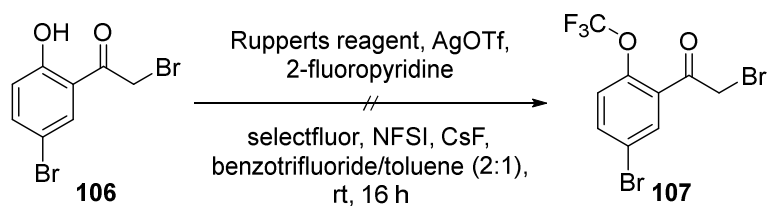
Scheme 14: Reaction conditions for the attempted trifluoromethylation of phenol **106**.

Another attempt to synthesize chloroketone **102** involved an iodine-lithium exchange, which should be favored over the bromo-lithium exchange[109]. Weinreb amide **105** was used to give the ketone **102** in order to avoid side reactions and over-additions. According to Nahm and Weinreb, a stable chelate complex is formed as intermediate, which avoids further additions to the ketone. Aqueous acidic work up then could yield the desired ketone (**Scheme 15 A**)[110]. The reaction was performed using commercially available iodine **108** and *n*-BuLi at -78 °C. After 20 minutes, Weinreb amide **105** was added and the reaction was monitored by TLC and NMR. The NMR sample was taken from the reaction mixture and after mini work-up dried under nitrogen flow. ¹H-NMR analysis clearly showed total conversion of the starting material and formation of a new substance with all NMR signals required for the desired ketone **102** after 1 h. After standard work-up of the whole reaction and NMR analysis of the material, no product could be observed anymore. Therefore, it was assumed that the desired ketone **102** was highly volatile and not even stable under reduced pressure, as a rotary evaporator generates (40 °C, 1 mbar). The newly developed work-up avoided rotary evaporation. The product was dried overnight under a nitrogen flow and gave ketone **102** in moderate yield (**Scheme 15 B**).
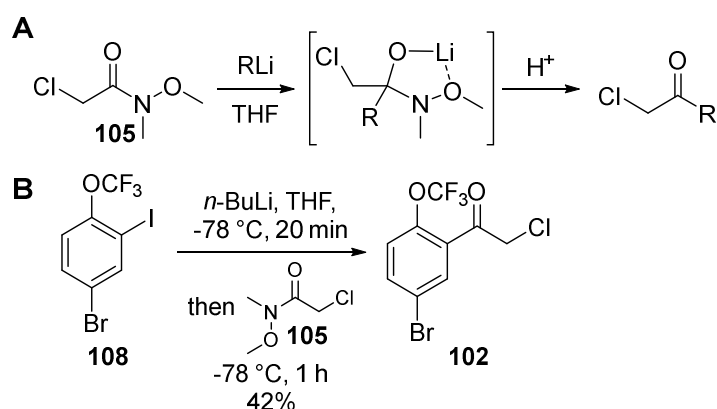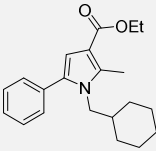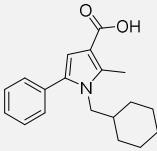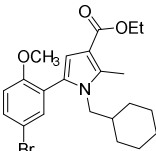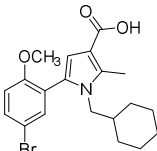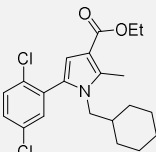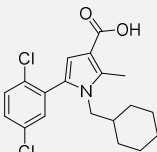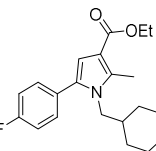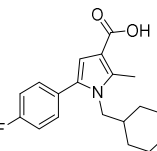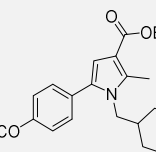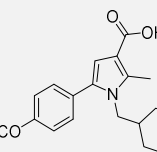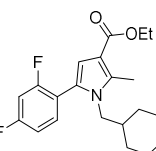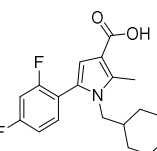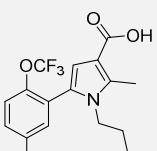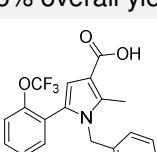
Scheme 15: Synthesis of *α*-chloroketone **102** using *in situ* generated organolithium reagents and Weinreb amide **105**. (**A**) Reaction mechanism according to M. Weinreb[110]. (**B**) Successful reaction conditions for the synthesis of *α*-chloroketone **102**.
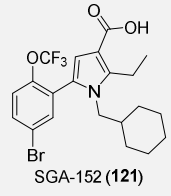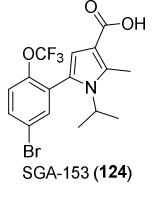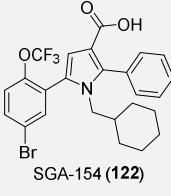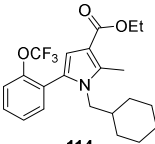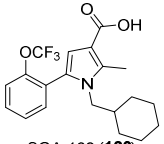
With all building blocks at hand and a well-established route, the synthesis of TPC2-A1-P (**17**) and analogs could be applied. Finally ester SGA-140 (**109**, entry 1, **Table 4**) could be synthesized in moderate yield using *α*-chloroketone **102**, ethyl acetoacetate (**94**) and cyclohexanemethanamine (**95**). Deprotection of ester **109** gave the hit compound TPC2-A1-P (**17**) in good yield. Varying the *α*-halogenated ketone building block (**IV**, **Table 4**) allowed the synthesis of seven more esters that were all isolated in moderate to high yields (entry 2-7, 13, **Table 4**). The bioisosteric ester SGA-54 (**97**) was lacking the trifluoromethoxy group at C-2 position of the aromatic ring and was instead bearing a methoxy group (entry 3, **Table 4**). The 2,5-dichloro variant SGA-48 (**110**) also shared the substitution pattern of the hit compound (entry 4, **Table 4**). Esters SGA-59 (**111**) and SGA-61 (**112**) both had *para*-substituents (entry 5, 6, **Table 4**) and SGA-62 (**113**) was the 2,4-difluoro analog (entry 7, **Table 4**). Ester **114** was lacking the bromine in C-5 position of the aromatic ring (entry 13, **Table 4**). All of these esters were further deprotected to yield the carboxylic acids SGA-50 (**100**), SGA-55 (**115**), SGA-52 (**116**), SGA-66 (**117**), SGA-67 (**118**), SGA-68 (**119**) and SGA-162 (**120**) in moderate to high yields (entry 2-7, 13, **Table 4**). These compounds had in common that their *α*-halogenated ketone building blocks (**IV**, **Table 4**) were stable, which is the reason why they could be easily purified. Simple FCC yielded the pure esters. Purification attempts of esters synthesized with the volatile *α*-chloroketone **102** were very complicated and time consuming. A first set of biological experiments revealed that the ester SGA-140 (**109**) does in comparison to the carboxylic acid TPC2-A1-P (**17**) not show any effect in Ca^{2+} imaging experiments (**Figure 15**). Therefore there was no need to purify and isolate the pure esters anymore and FCC was just performed as a pre-cleaning process. This was of great importance, because the precipitating of the carboxylic acids was otherwise not successful and additional extractions had to be included. The absence of colorful impurities was critical as this would disturb experiments using fluorescent dyes.

Table 4: Products synthesized according to the newly elaborated method for the synthesis of highly substituted pyrrolecarboxylic acids (**I**). *cy = cyclohexyl

entry	R¹	R	R²	ester (II)	acid (I)
1	R = 2-OCF₃, 5-Br	R = CH₃	R = CH₂cy*	SGA-140 (**109**) 46%	TPC2-A1-P (**17**) 54%

2	-	R = CH$_3$	R = CH$_2$cy*	SGA-43 (**96**) 53%	SGA-50 (**100**) 89%
3	R = 2-OCH$_3$, 5-Br	R = CH$_3$	R = CH$_2$cy*	SGA-54 (**97**) 95%	SGA-55 (**115**) 63%
4	R = 2,5-Cl$_2$	R = CH$_3$	R = CH$_2$cy*	SGA-48 (**110**) 46%	SGA-52 (**116**) 81%
5	R = 4-F	R = CH$_3$	R = CH$_2$cy*	SGA-59 (**111**) 97%	SGA-66 (**117**) 88%
6	R = 4-OCH$_3$	R = CH$_3$	R = CH$_2$cy*	SGA-61 (**112**) 51%	SGA-67 (**118**) 90%
7	R = 2,4-F$_2$	R = CH$_3$	R = CH$_2$cy*	SGA-62 (**113**) 78%	SGA-68 (**119**) 88%
8	R = 2-OCF$_3$, 5-Br	R = CH$_3$	R = pentyl	not isolated	SGA-149 (**123**) 15% overall yield
9	R = 2-OCF$_3$, 5-Br	R = CH$_3$	R = benzyl	not isolated	SGA-150 (**125**) 10% overall yield

10	R = 2-OCF₃, 5-Br	R = CH₂CH₃	R = CH₂cy*	not isolated	SGA-152 (**121**) 9% overall yield
11	R = 2-OCF₃, 5-Br	R = CH₃	R = *i*Pr	not isolated	SGA-153 (**124**) 12% overall yield
12	R = 2-OCF₃, 5-Br	R = phenyl	R = CH₂cy*	not isolated	SGA-154 (**122**) 28% overall yield
13	R = 2-OCF₃	R = CH₃	R = CH₂cy*	**114** 95%	SGA-162 (**120**) 93%

Different *β*-ketoester building blocks (**V**, **Table 4**) were used to generate SGA-152 (**121**) and SGA-154 (**122**), both with larger residues in C-2 position of the pyrrole (entry 10, 12, **Table 4**). Modifications in 1-position of the pyrrole were achieved with altering primary amine building blocks (**III**, **Table 4**) to give carboxylic acids SGA-149 (**123**) with a long and SGA-153 (**124**) with a branched side chain as well as SGA-150 (**125**) with a benzyl moiety (entry 8, 9, 11, **Table 4**). All yields are low to moderate but over two steps acceptable.

Collectively, a synthesis for TPC2-A1-P (**17**) was developed that was also suitable for synthesizing analogs. In total 13 esters were synthesized and 8 of them isolated, including the ester SGA-140 (**109**). Alkaline deprotection under microwave irradiation yielded the hit **17** itself and 12 analogs varying all substituents of the pyrrole moiety. These 21 substances were fully characterized by NMR, TLC, HRMS, IR and melting points and the purity was confirmed by analytical HPLC.

3.4 Pharmacological investigation of TPC2 agonists

The agonistic effects of the synthesized screening hits TPC2-A1-N (**16**) and TPC2-A1-P (**17**) and their analogs were confirmed by Fura-2 single cell calcium imaging and SAR were analyzed. Concentration-effect relationships using Fluo-4 calcium imaging were analyzed and further results from cooperation partners are briefly described for presentation of the whole outcome of this interdisciplinary project. Finally our novel TPC2 agonists were compared to activators, recently published by Zhang et al.[111]. All studies were performed in close cooperation with Prof. Dr. Michael Schaefer's group (HTS, performed by myself, Fluo-4 based experiments, performed by Nicole Urban), Prof. Dr. Dr. Christian Grimm's as well as Prof. Dr. Martin Biel's groups (Fura-2 based calcium imaging, performed by myself and patch clamp experiments, performed by Dr. Yu-Kai Chao and Dr. Cheng-Chang Chen).

3.4.1   Confirmation of TPC2-A1-N (16) and TPC2-A1-P (17) as TPC2 agonists

Single cell Ca^{2+} imaging experiments had confirmed the two HTS hits, using HEK293 cells transiently expressing the plasma membrane variant of human TPC2 (hTPC2[L11A/L12A])[22]. The membrane permeable, ratiometric dye Fura-2/AM (**126**) was selected as Ca^{2+} indicator for these experiments. Ca^{2+} imaging using Fura-2 (**13**) enables the detection of changes in calcium levels in adherent cells[112].
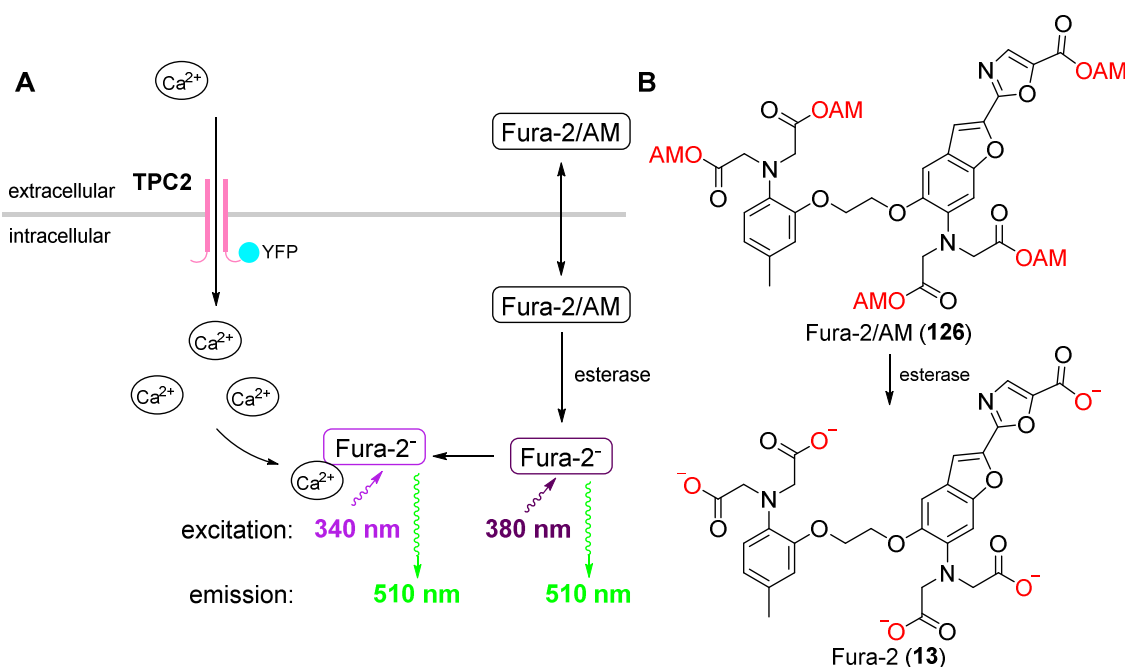
Figure 9: The principle of Fura-2 based Ca^{2+}-imaging. (**A**) Schematic overview of Fura-2/AM based Ca^{2+}-imaging. Fura-2/AM (**126**) can enter the cell as membrane permeable AM ester. Esterases cleave the AM esters and the free dye **13** remains. Excitation wavelength for Fura-2 (**13**) changes upon complexation from 380 nm (no Ca^{2+}) to 340 nm (with Ca^{2+}). Emission can be detected at 510 nm. (**B**) Structures of Fura-2/AM (**126**) and the free Fura-2 (**13**) anion.

Fura-2/AM (**126**) can enter cells as a lipophilic AM ester and is hydrolyzed inside the cells by esterases. The Fura-2 (**13**) anion can complex Ca^{2+} ions and shifts its absorption maximum from 380 nm to 340 nm, both emitting at 510 nm (**Figure 9 A** and **B**). While Ca^{2+} concentrations rise, an increase of fluorescence for excitation at 340 nm can be observed. The level of transfection, as well as the loading of the cell with Fura-2 (**13**) have an impact on the fluorescence intensity. To avoid measurement inaccuracies, the ratio of chelated Fura-2 (340 nm) divided by free Fura-2 (**13**, 380 nm) is determined.
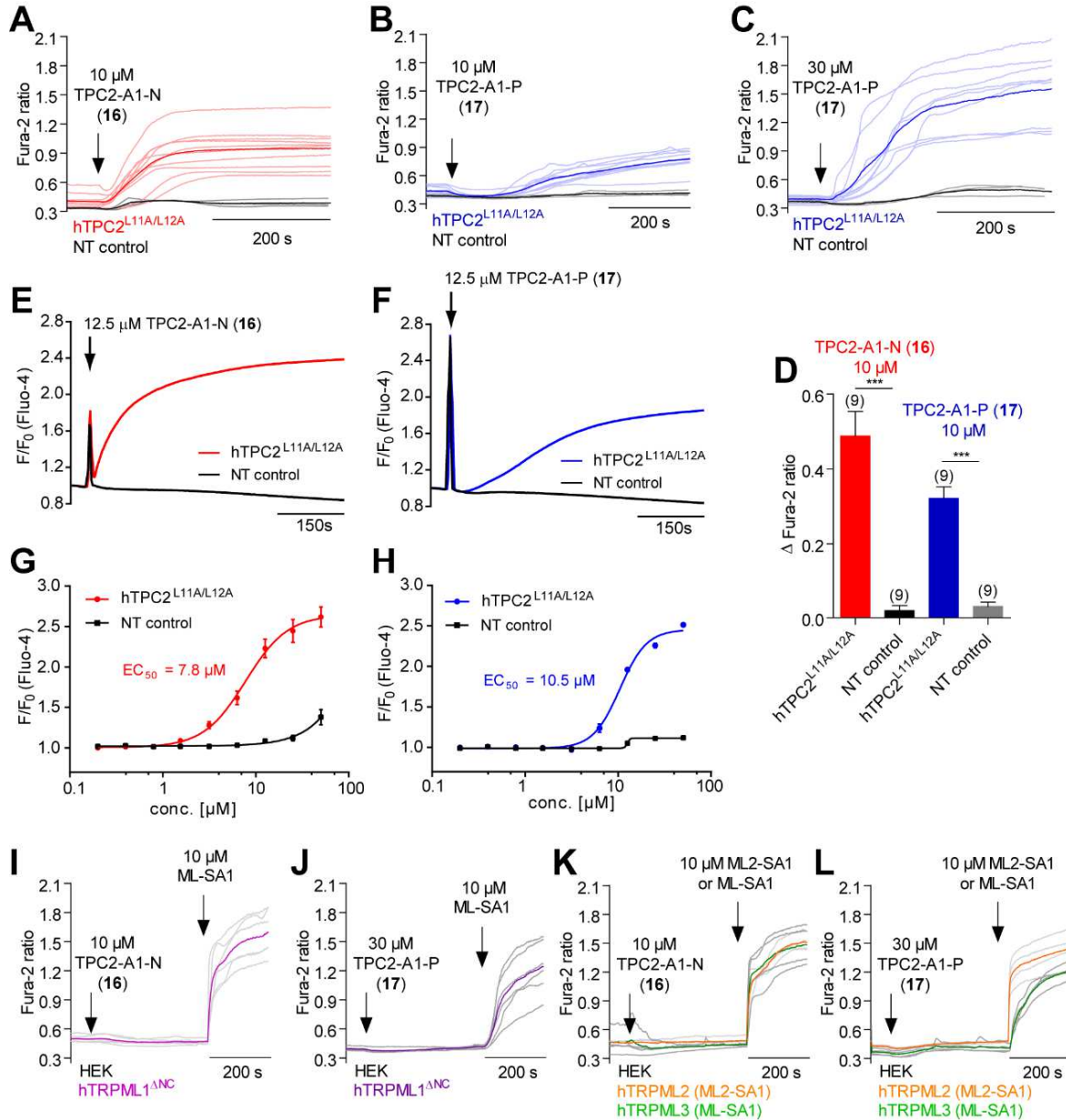
Figure 10: Confirmation of TPC2-A1-N (**16**) and TPC2-A1-P (**17**) as TPC2 agonists. (**A**) Representative Ca^{2+} signals recorded from HEK293 cells loaded with the ratiometric Ca^{2+} indicator, Fura-2 (**13**) and stimulated with TPC2-A1-N (**16**, 10 µM) and monitored for 400 s. Cells were transiently transfected with plasma membrane targeted human TPC2 (hTPC2$^{L11A/L12A}$). Highlighted lines represent the mean response from a population of cells. Shaded traces represent responses of single cells (n = 10 cells for hTPC2; n = 3 cells for NT cells). (**B**) Similar to A except that cells were stimulated with TPC2-A1-P (**17**, 10 µM) and monitored for 600 s. Shaded traces represent single cells responses (n = 10 cells for hTPC2; n = 3 cells for NT cells). (**C**) Similar to A except that cells were stimulated with TPC2-A1-P (**17**, 30 µM). Shaded traces represent single cells responses (n = 9 cells for hTPC2; n = 3 cells for NT cells). (**D**)

Statistical analysis of the maximal change in Fura-2 (**13**) ratio (mean ± SEM) with the number of independent transfections in parentheses. Experiments were performed over the period of 9 months and on the same days, each. ***p < 0.001, using one-way ANOVA followed by Tukey's post hoc test. (**E-F**) Representative FLIPR-generated Ca^{2+} signals (Fluo-4 (**14**)) in TPC2$^{L11A/L12A}$–expressing cells (red and blue line) or non-transfected (NT) control cells (black) after addition of TPC2-A1-N (**16**, E) or TPC2-A1-P (**17**, F). Experiments were performed by Nicole Urban. (**G-H**) Concentration-effect relationships for Ca^{2+} increases (Fluo-4 (**14**)) in response to different concentrations of TPC2-A1-N (**16**, G) and TPC2-A1-P (**17**, H). Experiments were performed by Nicole Urban. (**I-J**) Representative Ca^{2+} signals recorded from HEK293 cells loaded with the ratiometric Ca^{2+} indicator, Fura-2 (**13**) and sequentially stimulated with TPC2-A1-N (**16**, 10 µM, I, n = 6 cells) or TPC2-A1-P (**17**, 30 µM, J, n = 6 cells) and the TRPML agonist ML-SA1 (10 µM). Cells were transiently transfected with human TRPML1$^{\Delta NC}$. Means are highlighted and single cell responses are shaded. (**K-L**) Experiment as in I-J, but HEK293 cells transiently transfected with human TRPML2, or TRPML3. Cells were sequentially stimulated with TPC2-A1-N (**16**, 10 µM, K, n = 4 cells) or TPC2-A1-P (**17**, 30 µM, L, n = 4 cells) and the TRPML agonist ML-SA1 (10 µM) or the TRPML2 selective agonist ML2-SA1 (10 µM). Means are highlighted and single cell responses are shaded. Fura-2 based calcium imaging experiments were performed on a Polychrome IV mono-chromator (TILL photonics).

Both screening hits, investigated as the independently synthesized substances, reproducibly evoked Ca^{2+} signals. Thereby the correct structures of the HTS hits were confirmed. The signals evoked by the compounds showed different kinetics whereby the TPC2-A1-N (**16**) response reached its plateau faster than TPC2-A1-P response (**17**, **Figure 10 A-B** and **E-F**). The slower activation could be reduced by stimulation with higher concentrations of TPC2-A1-P (**17**), while control cells still remained unaffected (**Figure 10 C**). Hence, recommended experimental concentration for TPC2-A1-P (**17**) is 30 µM. Long term statistical analysis of TPC2-A1-N (**16**) and TPC2-A1-P (**17**) showed robust and significant activation of TPC2 (**Figure 10 D**). Concentration-effect relationships indicated EC_{50} values of 7.8 µM and 10.5 µM, for TPC2-A1-N (**16**) and TPC2-A1-P (**17**), respectively (**Figure 10 G** and **H**). Both agonists failed to evoke Ca^{2+} signals in cells expressing human TRPML1 re-routed to the plasma membrane (TRPML1$^{\Delta NC}$)[113, 114] at the recommended working concentrations (**Figure 10 I** and **J**). Similar negative results were obtained with the TRPML agonists ML-SA1 and ML2-SA1[115] as positive controls in cells expressing TRPML2 or TRPML3 (**Figure 10 K** and **L**). These results indicate that both hits are selective TPC2 agonists with different modes of activation.

3.4.2 Structure-activity relationships for TPC2-A1-N (16) and analogs

Fura-2 based calcium imaging experiments were performed with transiently transfected HEK293 cells, which allowed selection of transfected cells and non-transfected (NT) control cells in one experiment. False positive analogs could straight away be eliminated and unspecific effects on intact cells could be determined. If a compound showed no effect in Ca^{2+} imaging experiments, a control had to be added. At the beginning of the screening, TPC2-A1-N (**16**) was not fully established as TPC2 activator and therefore ionomycin (4 µM) was used as a control for a well-functioning experiment. Ionomycin is a membrane permeable Ca^{2+}

ionophore and causes an intracellular calcium rise by transporting Ca^{2+} across biological membranes[116, 117]. This is not selective for TPC2, thus ionomycin is a control for the accuracy of the experiment. Stimulation of the cells with a selective activator determines whether a compound is inactive or an inhibitor.
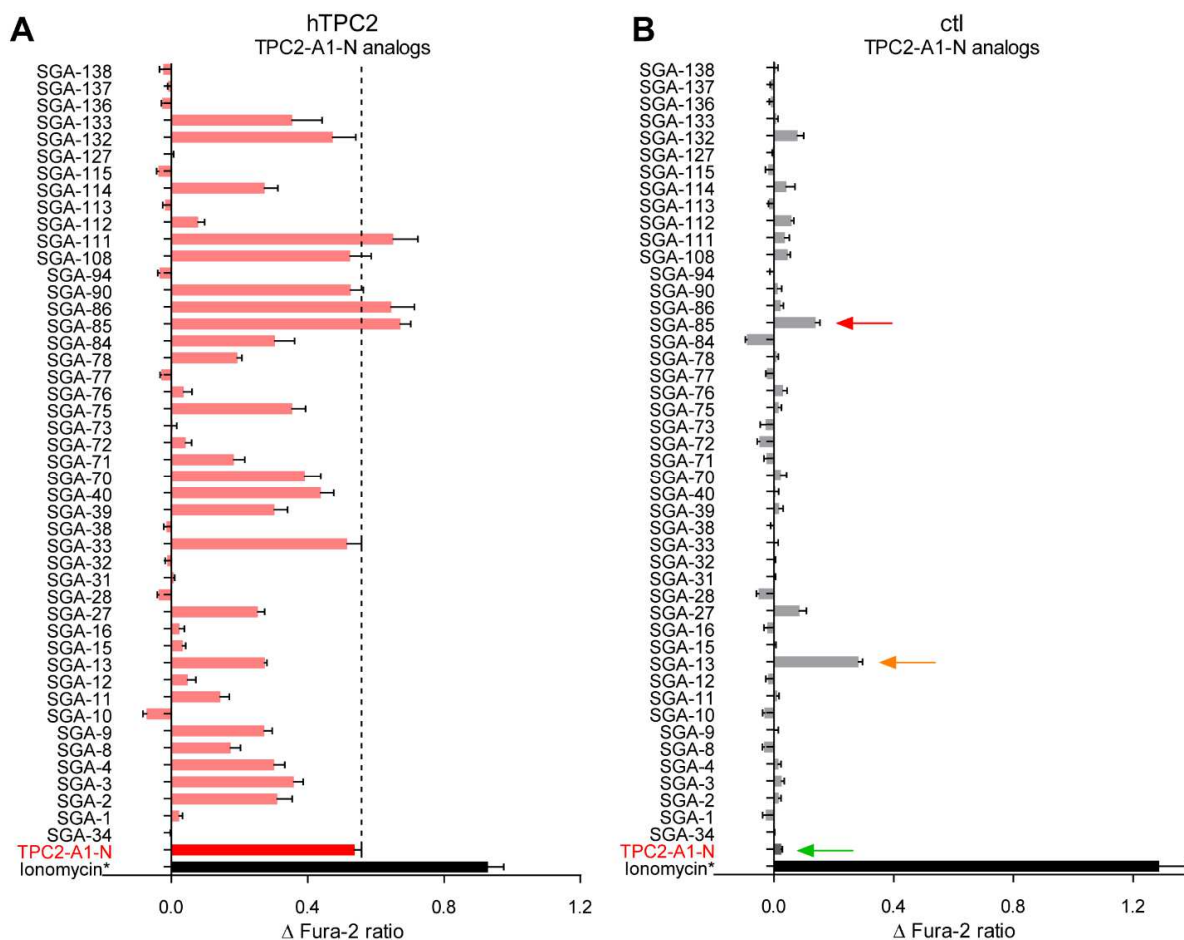
Figure 11: Fura-2 based Ca^{2+} imaging results for all TPC2-A1-N (**16**) analogs. (**A-B**) Fura-2 based Ca^{2+} imaging results showing the effect of TPC2-A1-N (**16**) and its analogs (10 µM, each) on HEK293 cells transiently transfected with hTPC2$^{L11A/L12A}$-YFP (A, red) and control cells (B, grey). The red arrow indicates unspecific effect on control cells, the orange arrow indicates auto fluorescence and the green arrow indicates no effect. Mean values normalized to basal (400 s after compound application) ± SEM of at least three independent experiments with 3–10 cells each are shown. All experiments were performed on a Polychrome IV mono-chromator (TILL photonics).

All synthesized analogs of TPC2-A1-N (**16**) were tested on their ability to activate TPC2. Out of 46 analogs, 23 substances have shown significant agonistic effects (**Figure 11 A**) and 6 more barely any activation (SGA-1 (**44**), SGA-12 (**52**), SGA-16 (**55**), SGA-38 (**61**), SGA-72 (**66**), SGA-112 (**79**), **Figure 11 A**). Ionomycin or TPC2-A1-N (**16**) were added for the purpose of verifying the accuracy of the experiments. In all experiments with inactive compounds TPC2-A1-N (**16**) was added at least once. Thus there were not enough data for statistical analysis to verify that the inactive compounds do not inhibit the activation of TPC2. SGA-13 (**53**) showed increased levels of activation on control cells that could be identified as auto fluorescence

(**Figure 11 B**). Three substances (SGA-27 (**56**), SGA-85 (**73**), SGA-132 (**84**)) also had slight unspecific effects on control cells, that were not related to auto fluorescence. Seven substances (SGA-33 (**60**), SGA-85 (**73**), SGA-86 (**74**), SGA-90 (**75**), SGA-108 (**77**), SGA-111 (**78**), SGA-132 (**84**)) had comparable efficacy to TPC2-A1-N (**16**), while all others were less effective.

Analyzing the structures of the 8 most potent TPC2 activators within this series showed that TPC2-A1-N analogs have *meta*-disubstitution patterns with electron-withdrawing groups located on the benzoyl ring system (**Figure 12**). In contrast, substitution pattern at the phenyl ring on the anilide side of the molecule was more variable. Electron-withdrawing and -releasing groups (TPC2-A1-N (**16**), SGA-86 (**74**) vs. SGA-108 (**77**)) did not cause significant changes in activity. Substitution patterns could also differ from *para* to *meta* (TPC2-A1-N (**16**), SGA-85 (**73**)) or even more strongly (SGA-33 (**60**), SGA-90 (**75**)).
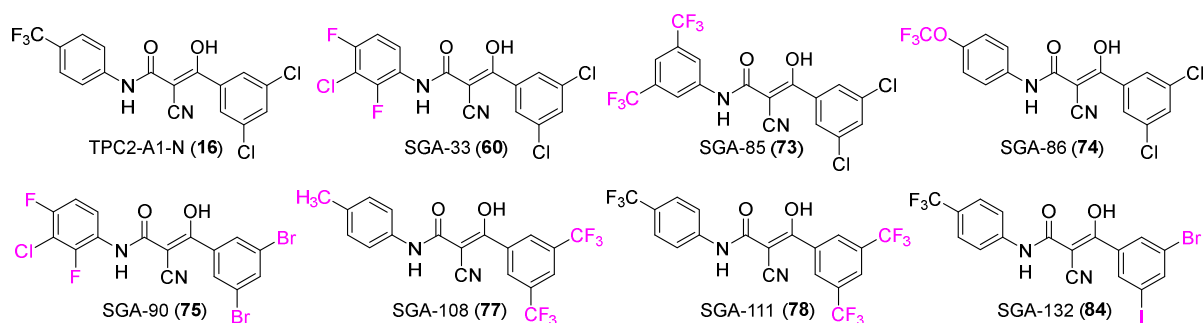
Figure 12: Structures of the 8 most potent TPC2 activators within the TPC2-A1-N (**16**) series. Structural differences are marked in magenta.

Harsh changes on the benzoyl moiety (replacement by methyl or pyrrole residues), as demonstrated for the approved drugs teriflunomide (SGA-94, **76**) and prinomide (SGA-31, **58**) as well as the 4-trifluoromethyl variant of prinomide (SGA-32, **59**) led to a complete loss of activity (**Figure 13**). Teriflunomide (**76**) and SGA-32 (**59**) did not show inhibitory effects after activation with TPC2-A1-N (**16**, **Figure 13 B** and **D**). Stimulation with ionomycin (**Figure 13 C**) indicates the accuracy of the experiment by strong, unspecific calcium influx as described above. Teriflunomide (**76**) is an approved drug for the treatment of multiple sclerosis and prinomide (**58**) for rheumatoid arthritis[118, 119]. Dysregulation of calcium homeostasis can be associated with several neurodegenerative disorders like multiple sclerosis (MS)[120], but there is no direct link between MS and TPC2 up to now.
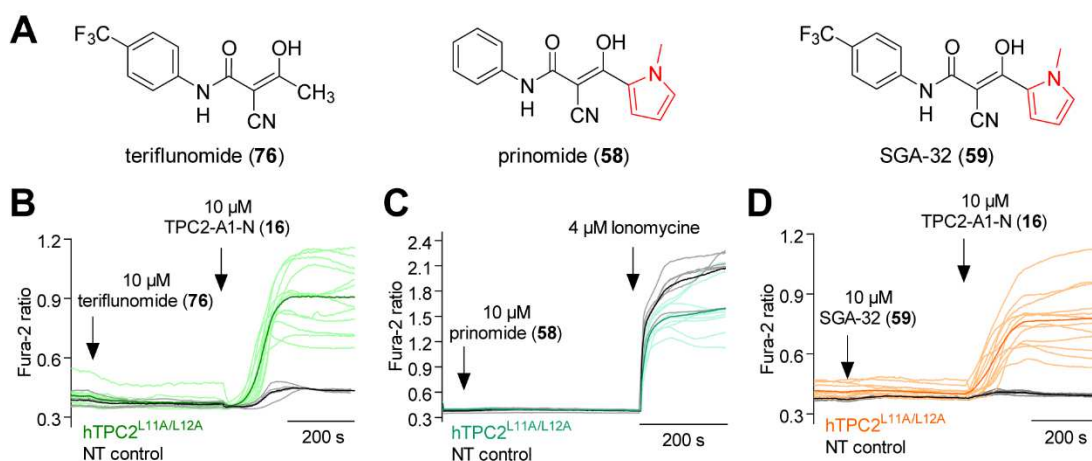
Figure 13: Approved drugs structurally related to TPC2-A1-N (**16**) show no effect on TPC2. (**A**) Structures of the approved drugs teriflunomide (SGA-94, **76**) and prinomide (SGA-31, **58**) and analog SGA-32 (**59**). (**B-D**) Representative calcium signals from HEK293 cells transiently transfected with hTPC2$^{L11A/L12A}$-YFP. Cells were stimulated with teriflunomide (**76**, 10 µM, A, n = 12 cells for hTPC2; n = 7 cells for NT cells), prinomide (**58**, 10 µM, B, n = 10 cells for hTPC2; n = 6 cells for NT cells) or SGA-32 (**59**, 10 µM, C, n = 12 cells for hTPC2; n = 4 cells for NT cells) for 400 s each, followed by activation with TPC2-A1-N (**16**, 10 µM, B and D, 400 s) or ionomycin (C, 4 µM, 200 s). Highligted lines represent the mean response from a population of cells. Shaded traces represent responses of single cells. Fura-2 based calcium imaging experiments were performed on a Polychrome IV mono-chromator (TILL photonics).

Thio-analog SGA-167 (**91**) was synthesized as last compound within an Erasmus project (**Figure 14 A**). At that time, a new Ca^{2+}-imaging setup was put into operation. Direct comparison from experiments using the old setup (Polychrome IV mono-chromator, TILL photonics) with the new setup (Leica DMi8 live cell microscope) is not possible. Intensities can vary due to the power of the light sources and analysis of the experiments using the manufacturers' software (TILLvisION or LAS X) could also cause differences in intensities. Therefore, TPC2-A1-N (**16**) was re-evaluated and used as an established activator to analyze differences in agonistic effects compared to SGA-167 (**91**). The thio-analog **91** activates TPC2 significantly less than TPC2-A1-N (**16**, **Figure 14 B**), clearly indicating very special SAR in this chemotype.
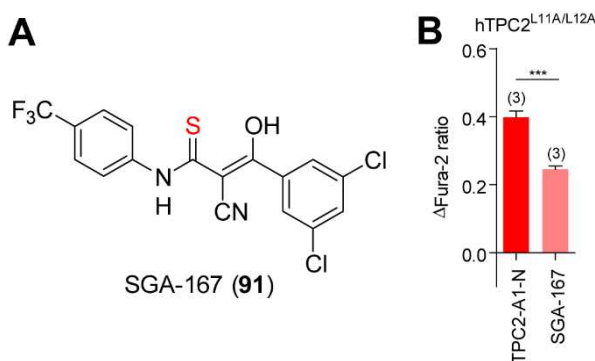
Figure 14: Thio-analog SGA-167 (**91**) activates TPC2 less than the hit. (**A**) Structure of SGA-167 (**91**). Differences to TPC2-A1-N (**16**) are marked in red. (**B**) Fura-2 based Ca^{2+} imaging results showing the

effect of TPC2-A1-N (**16**, 10 µM) and its analog SGA-167 (**91**, 10 µM) on HEK293 cells stably expressing hTPC2[L11A/L12A]-RFP. Mean values normalized to basal (400 s after compound application) ± SEM of at least three independent experiments with 3–10 cells each are shown. ***$p < 0.001$ using unpaired student's t-test. Fura-2 based calcium imaging experiments were performed on a Leica DMi8 live cell microscope.

All findings were affirmed by full analysis of concentration-effect relationships, performed by our cooperation partner Nicole Urban, Rudolf-Boehm-Institute, Leipzig. The Fluo-4 based calcium imaging experiments were chosen because a large number of compounds at different concentrations can be analyzed in a high-throughput manner. The barely activating compounds show either high EC_{50} values (entry 3, 11, 13, 19, **Table 5**) or were not calculable because activation started at concentrations above 50 µM. With EC_{50} values above 100 µM substances were not suitable anymore because such high concentrations can cause unwanted side effects and solubility problems. Substances that were inactive in Fura-2 calcium imaging, did not show agonistic effects in Fluo-4 imaging as well. This confirmed all results from the Fura-2 imaging experiments. Nearly all EC_{50} values of the 8 most potent substances are in the same range, thus SGA-33 (**60**, 23 µM) is higher to some extent (**Table 5**). SGA-85 (**73**) and SGA-132 (**84**) have a slightly lower EC_{50} (3.3 µM and 5.3 µM) than TPC2-A1-N (**16**, 7.8 µM), which is relativized by the fact that control cells showed increased levels of activation in Fura-2 imaging for SGA-85 (**73**) and SGA-132 (**84**, **Figure 11 B**).

Further analysis of structural motifs shows that replacing the *para*-trifluoromethyl group on the anilide side of the molecule (R[1]; blue) gives more opportunities than changes on the benzoyl residue. Electron-withdrawing groups in *para*-position on the anilide side causes no significant changes (e.g. entry 2, 3, 5, 6, **Table 5**). Even the introduction of electron-releasing groups in *para*-position is tolerated to some extent (SGA-4 (**47**), SGA-84 (**72**), SGA-108 (**77**)). For the substitution pattern of the benzoyl ring system (R[2], green), *meta*-disubstitution patterns with electron-withdrawing groups are most beneficial.

Table 5: Structure variations and EC_{50} values of TPC2-A1-N (**16**) and the active analogs. No significantly increased efficacies or potencies were observed for the analogs. EC_{50} (Fluo-4 (**14**)) values are received via Fluo-4 based Ca^{2+} imaging experiments, performed by Nicole Urban as previously described[22]. IC_{50} values (MTT) are received from in-house MTT experiments, performed by Martina Stadler. *experiment was performed at a later time. n.a. = not applicable.
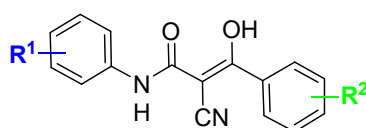
entry	name	R[1] =	R[2] =	EC_{50} =	IC_{50} (MTT) =
1	TPC2-A1-N (**16**)	4-CF_3	3,5-Cl_2	**7.8 µM**	> 50 µM
2	SGA-34 (**19**)	4-CF_3	-	n.a.	> 50 µM
3	SGA-1 (**44**)	H	3,5-Cl_2	35 µM	> 50 µM

4	SGA-2 (**45**)	4-Cl	3,5-Cl$_2$	24 µM	> 50 µM
5	SGA-3 (**46**)	4-Br	3,5-Cl$_2$	20 µM	> 50 µM
6	SGA-4 (**47**)	4-CH$_3$	3,5-Cl$_2$	15 µM	> 50 µM
7	SGA-8 (**48**)	4-F	3,5-Cl$_2$	22 µM	> 50 µM
8	SGA-9 (**49**)	4-I	3,5-Cl$_2$	34 µM	48 µM
9	SGA-10 (**50**)	4-CF$_3$	H	n.a.	> 50 µM
10	SGA-11 (**51**)	4-CF$_3$	3,5-(NO$_2$)$_2$	38 µM	> 50 µM
11	SGA-12 (**52**)	4-OCH$_3$	3,5-Cl$_2$	33 µM	> 50 µM
12	SGA-15 (**54**)	4-CF$_3$	4-NO$_2$	> 100 µM	> 50 µM
13	SGA-16 (**55**)	4-CF$_3$	4-Cl	47 µM	> 50 µM
14	SGA-27 (**56**)	2-Br, 4-Cl	3,5-Cl$_2$	10 µM	> 50 µM
15	SGA-28 (**57**)	3,4-(OCH$_3$)$_2$	3,5-Cl$_2$	n.a.	> 50 µM
16	SGA-31 (**58**)	prinomide		n.a.	> 50 µM
17	SGA-32 (**59**)	2-cyano-3-(1-methyl-1H-pyrrol-2-yl)-3-hydroxy-N-(4-(trifluoromethyl)phenyl)acrylamide		n.a.	> 50 µM
18	SGA-33 (**60**)	2,4-F$_2$, 3-Cl	3,5-Cl$_2$	**23 µM**	> 50 µM
19	SGA-38 (**61**)	4-CN	3,5-Cl$_2$	51 µM	> 50 µM
20	SGA-39 (**62**)	2-I	3,5-Cl$_2$	> 100 µM	> 50 µM
21	SGA-40 (**63**)	4-CF$_3$	2,3,4,5,6-F$_5$	41 µM	> 50 µM
22	SGA-70 (**64**)	4-CF$_3$	3,5-Br$_2$	13 µM	> 50 µM
23	SGA-71 (**65**)	4-CF$_3$	2,4,6-Cl$_3$	40 µM	> 50 µM
24	SGA-72 (**66**)	4-Br	2,4,6-Cl$_3$	> 100 µM	> 50 µM
25	SGA-73 (**67**)	2,4-F$_2$, 3-Cl	2,4,6-Cl$_3$	n.a.	> 50 µM
26	SGA-75 (**68**)	4-Br	3,5-Br$_2$	22 µM	> 50 µM
27	SGA-76 (**69**)	4-Ac	3,5-Cl$_2$	> 100 µM	> 50 µM
28	SGA-77 (**70**)	2,6-Br$_2$	3,5-Cl$_2$	n.a.	> 50 µM
29	SGA-78 (**71**)	2,3-Cl$_2$	3,5-Cl$_2$	n.a.	> 50 µM
30	SGA-84 (**72**)	4-OC$_3$H$_7$	3,5-Cl$_2$	14 µM	> 50 µM
31	SGA-85 (**73**)	3,5-(CF$_3$)$_2$	3,5-Cl$_2$	**3.0 µM**	29 µM
32	SGA-86 (**74**)	4-OCF$_3$	3,5-Cl$_2$	**9.5 µM**	49 µM
33	SGA-90 (**75**)	2,4-F$_2$, 3-Cl	3,5-Br$_2$	**12 µM**	> 50 µM
34	SGA-94 (**76**)	teriflunomide		n.a.	> 50 µM
35	SGA-108 (**77**)	4-CH$_3$	3,5-(CF$_3$)$_2$	**7.1 µM**	> 50 µM
36	SGA-111 (**78**)	4-CF$_3$	3,5-(CF$_3$)$_2$	**6.2 µM**	> 50 µM
37	SGA-112 (**79**)	4-CF$_3$	3,5-(CH$_3$)$_2$	> 100 µM	> 50 µM
38	SGA-113 (**80**)	4-CF$_3$	3,5-(OCH$_3$)$_2$	n.a.	> 50 µM
39	SGA-114 (**81**)	4-CF$_3$	4-OCF$_3$	> 100 µM	> 50 µM
40	SGA-115 (**82**)	2-cyano-3-(3,5-dichlorophenyl)-3-hydroxy-N-methyl-N-(4-(trifluoromethyl)phenyl)-acrylamide		> 100 µM	35 µM
41	SGA-127 (**83**)	2-cyano-3-hydroxy-3-(pyridin-3-yl)-N-(4-(trifluoromethyl)phenyl)acrylamide		n.a.	> 50 µM
42	SGA-132 (**84**)	4-CF$_3$	3-Br, 5-I	**5.3 µM**	32 µM

43	SGA-133 (**85**)	4-COOCH₃	3,5-Cl₂	21 µM	> 50 µM
44	SGA-136 (**86**)	3-(5-chloropyridin-3-yl)-2-cyano-3-hydroxy-*N*-(4-(trifluoromethyl)phenyl)acrylamide		n.a.	> 50 µM
45	SGA-137 (**88**)	4-COOH	3,5-Cl₂	n.a.	> 50 µM
46	SGA-138 (**87**)	2-cyano-3-(3,5-dichlorophenyl)-3-hydroxy-*N*-(4-(trifluoromethyl)benzyl)acrylamide		> 100 µM	48 µM
47*	SGA-167 (**91**)	2-cyano-3-(3,5-dichlorophenyl)-3-hydroxy-*N*-(4-(trifluoromethyl)phenyl)prop-2-enethioamide		31 µM	> 50 µM

The toxicity of all substances was examined by in-house MTT assays using HL-60 cells and was performed by Martina Stadler. The MTT assay indicates the metabolic cell activity and reflects cell viability[121]. IC_{50} represents the concentration that is required for half maximal inhibition and compounds with values smaller than 50 µM are acknowledged as cytotoxic. Nearly all analogs and the hit itself did not show toxicity and only 6 substances had slight cytotoxic effects (entry 8, 31, 32, 40, 42, 46, **Table 5**). Out of the 8 most potent substances, only three substances showed slight toxicity (SGA-85 (**73**), SGA-86 (**74**), SGA-132 (**84**), entry 31-32, 42, **Table 5**) while the hit compound TPC2-A1-N (**16**) itself showed no toxicity (entry 1, **Table 5**).

The HTS hit TPC2-A1-N (**16**) itself and some of its analogs bearing residues in *para*-position at the benzoyl residue are known as anthelmintic agents[91]. The authors performed mechanism of action studies using *Ascaris mitochondria* and have shown that these compounds are uncouplers of oxidative phosphorylation, comparable to salicylanilide anthelmintic agents[122]. There are no indications in current literature that this effect is related to TPC2.

In summary, none of the 46 modified versions of TPC2-A1-N (**16**, auto-fluorescent SGA-13 (**53**) already excluded) showed significantly increased efficacies or potencies on TPC2 (**Figure 11**, **Table 5**) and the TPC2-A1-N chemotype showed a very flat structure-activity relationship on TPC2. TPC2-A1-N (**16**) thus remained a promising chemical tool for studies of TPC2.

3.4.3 Structure-activity relationships for TPC2-A1-P (17) and analogs

Fura-2 based calcium imaging experiments were performed as described above for TPC2-A1-N (**16**) and analogs (**Figure 15 A**). Experiments with inactive substances were subsequently activated with TPC2-A1-N (**16**) or stimulated with ionomycin (**Figure 15**, **E** and **F**). Also, for TPC2-A1-P (**17**) and analogs full concentration-effect experiments were performed by Nicole Urban (Leipzig), using the Fluo-4 based high-throughput setup as described before (**Table 6**).

Similar to the results obtained for TPC2-A1-N (**16**), modified versions of TPC2-A1-P (**17**) showed no improvement of potency or efficacy. Virtually all 19 analogs were inactive, only compound SGA-150 (**125**), in which the *N*-cyclohexylmethyl residue is replaced by an *N*-benzyl group (of identical size) showed noteworthy, but reduced activity (**Figure 15 A**, **Table 6**). Analysis of SAR revealed that the free carboxylic acid is essential for the activating effect, as the ester SGA-140 (**109**) was not active (entry 2, **Table 6**). It may serve as a prodrug of TPC2-A1-P (**17**) in living systems, but this has not been investigated further. Both, the trifluoromethoxy and the bromine substituent at the phenyl ring were essential for activating TPC2, as exemplified by the inactive methoxy (SGA-55, **115**, entry 8, **Table 6**) and des-bromo (SGA-162, **120**, entry 20, **Table 6**) analogs. Even moderate expansions of the size of the substituent at C-2 position of the pyrrole (methyl in TPC2-A1-P (**17**) vs. ethyl in SGA-152 (**121**) and phenyl analog SGA-154 (**122**), entry 1 vs. 17, 19, **Table 6**), had the same detrimental effect.
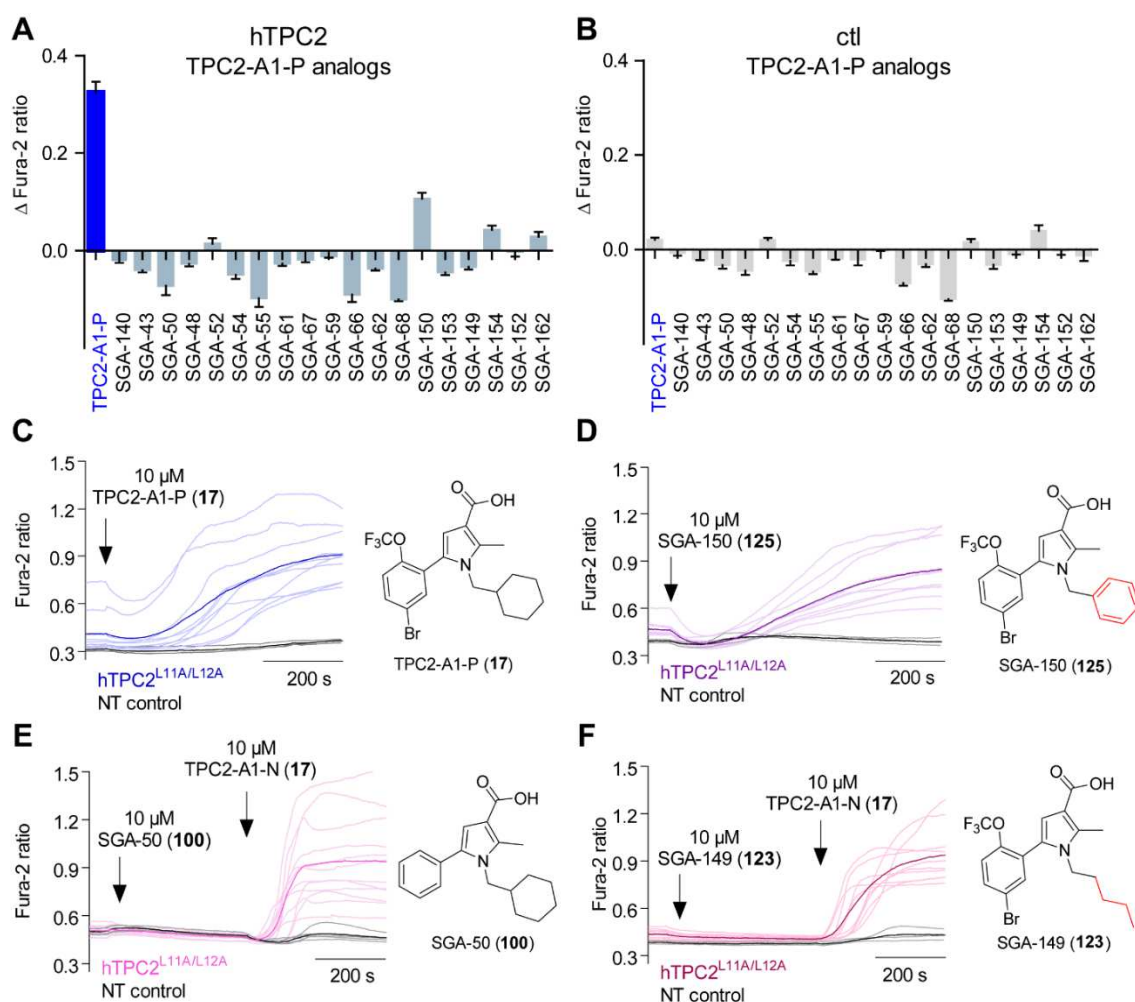
Figure 15. Fura-2 based Ca^{2+} imaging results for all TPC2-A1-P (**17**) analogs. (**A-B**) Fura-2 based Ca^{2+} imaging results showing the effect of TPC2-A1-P (**17**) and its analogs (10 µM; each) on HEK293 cells transiently transfected with hTPC2$^{L11A/L12A}$-YFP (A, blue) and control cells (B, grey). Mean values normalized to basal (400 s after compound application) ± SEM of at least three independent experiments with 3–10 cells each are shown. TPC2-A1-P (**17**) is highlighted and the analogs are shaded. (**C-D**) Representative calcium signals from HEK293 cells transiently transfected with hTPC2$^{L11A/L12A}$-YFP.

Cells were stimulated with TPC2-A1-P (**17**, C, 10 µM, 600 s, n = 10 cells for hTPC2; n = 3 cells for NT cells) or SGA-150 (**125**, D, 10 µM, 800 s, n = 10 cells for hTPC2; n = 3 cells for NT cells). Highligted lines represent the mean response from a population of cells. Shaded traces represent responses of single cells. Each structure is depicted on the right of the graph and structural differences to TPC2-A1-P (**17**) are marked in red. (**E-F**) Experiment as in C-D, but cells were sequentially stimulated with SGA-50 (**100**, E, 10 µM) or SGA-149 (**123**, F, 10 µM) and the TPC2 activator TPC2-A1-N (**16**, 10 µM) for 400 s each. All experiments were performed on a Polychrome IV mono-chromator (TILL photonics).

Aforementioned, the only fairly tolerable structure modification was the replacement of the cyclohexylmethyl moiety in 1-positon of the pyrrole ring by a benzyl residue (SGA-150, **125**, entry 16, **Table 6**). The efficacy of TPC2-A1-P (**17**) was significantly higher than of SGA-150 (**125**) (**Figure 15 A**) while for both compounds control cells remained unaffected (**Figure 15 B**). Linear or branched alkyl chains (SGA-149 (**123**), SGA-153 (**124**), entry 15, 18, **Table 6**), however, induced loss of activity.

Fura-2 based single cell calcium imaging traces for the activation of TPC2 were shown in **Figure 15 C-F**. These experiments showed the slow and weak activation of TPC2 with SGA-150 (**125**). This activation was even slower than the abovementioned activation using TPC2-A1-P at 10 µM (**17**, **Figure 15 C** and **D**). This indicated a lower affinity of SGA-150 (**125**) on TPC2 compared to TPC2-A1-P (**17**). Exemplary Fura-2 traces for the inactive compounds SGA-50 (**100**) and SGA-149 (**123**) were shown in **Figure 15 E** and **F**. Both substances had no effect on TPC2 and following activation using TPC2-A1-N (**16**) was successful, indicating that SGA-50 (**100**) and SGA-149 (**123**) were neither activators, nor inhibitors.

Table 6: Structure variations and EC_{50}/IC_{50} values of TPC2-A1-P (**17**), its ester SGA-140 (**109**) and all other analogs. EC_{50} values were received via Fluo-4 based Ca^{2+} imaging experiments, performed by Nicole Urban (Leipzig) as previously described[22]. IC_{50} values (MTT) were received from in-house MTT experiments, performed by Martina Stadler. n.a. = not applicable.
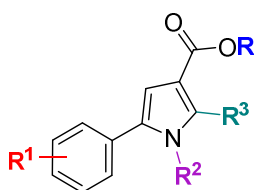
entry	compound	R =	R¹ =	R² =	R³ =	EC_{50} =	IC_{50} (MTT) =
1	TPC2-A1-P (**17**)	H	2-OCF₃, 5-Br	CH₂cy*	CH₃	10.5 µM	27 µM
2	SGA-140 (**109**)	CH₂CH₃	2-OCF₃, 5-Br	CH₂cy*	CH₃	n.a.	24 µM
3	SGA-43 (**96**)	CH₂CH₃	-	CH₂cy*	CH₃	n.a.	48 µM
4	SGA-50 (**100**)	H	-	CH₂cy*	CH₃	n.a.	32 µM
5	SGA-48 (**110**)	CH₂CH₃	2,5-Cl₂	CH₂cy*	CH₃	n.a.	> 50 µM
6	SGA-52 (**116**)	H	2,5-Cl₂	CH₂cy*	CH₃	n.a.	15 µM
7	SGA-54 (**97**)	CH₂CH₃	2-OCH₃, 5-Br	CH₂cy*	CH₃	n.a.	> 50 µM
8	SGA-55 (**115**)	H	2-OCH₃, 5-Br	CH₂cy*	CH₃	n.a.	> 50 µM
9	SGA-59 (**111**)	CH₂CH₃	4-F	CH₂cy*	CH₃	n.a.	40 µM
10	SGA-66 (**117**)	H	4-F	CH₂cy*	CH₃	n.a.	> 50 µM

11	SGA-61 (**112**)	CH_2CH_3	4-OCH_3	CH_2cy*	CH_3	n.a.	42 µM
12	SGA-67 (**118**)	H	4-OCH_3	CH_2cy*	CH_3	n.a.	> 50 µM
13	SGA-62 (**113**)	CH_2CH_3	2,4-F_2	CH_2cy*	CH_3	n.a.	> 50 µM
14	SGA-68 (**119**)	H	2,4-F_2	CH_2cy*	CH_3	n.a.	> 50 µM
15	SGA-149 (**123**)	H	2-OCF_3, 5-Br	pentyl	CH_3	n.a.	14 µM
16	SGA-150 (**125**)	H	2-OCF_3, 5-Br	benzyl	CH_3	34 µM	36 µM
17	SGA-152 (**121**)	H	2-OCF_3, 5-Br	CH_2cy*	CH_2CH_3	n.a.	21 µM
18	SGA-153 (**124**)	H	2-OCF_3, 5-Br	iPr	CH_3	n.a.	31 µM
19	SGA-154 (**122**)	H	2-OCF_3, 5-Br	CH_2cy*	phenyl	n.a.	14 µM
20	SGA-162 (**120**)	H	2-OCF_3	CH_2cy	CH_3	n.a.	> 50 µM

The toxicity of all substances was examined by in-house MTT assays as described above for TPC2-A1-N (**16**). Most substances could be classified as non-toxic (SGA-48 (**110**), SGA-54 (**97**), SGA-55 (**115**), SGA-66 (**117**), SGA-67 (**118**), SGA-62 (**113**), SGA-68 (**119**), SGA-162 (**120**), entry 5, 7, 8, 10, 12-14, 20, **Table 6**). Some IC_{50} values are in a moderate range between 25 and 50 µM (entry 1, 3, 4, 9, 11, 16, 18), and 5 compounds have lower IC_{50} values (SGA-140 (**109**), SGA-52 (**116**), SGA-149 (**123**), SGA-152 (**121**) SGA-154 (**122**), entry 2, 6, 15, 17, 19, **Table 6**). TPC2-A1-P (**17**) itself has an IC_{50} of 27 µM on HL-60 cells. Recommended working concentration is 30 µM and control experiments are highly relevant to exclude false results.

Only little information was found in the literature about biological activities of TPC2-A1-P-like substances. TPC2-A1-P (**17**) itself was namely mentioned as a precursor in the synthesis of cannabinoid-1 receptor (CB1R) inverse agonists, whereas the final active compounds contained a carboxamide group instead of the free carboxylic acid function[105]. Phenylpyrrolecarboxamides derived from SGA-50 (**100**) binding to 5-HT_{2A}, 5-HT_{2C} receptors and the 5-HT transporter were evaluated as antidepressant compounds[103]. This applies only to the carboxamides and there were no data published for the carboxylic acids.

TPC2-A1-P (**17**) and its 19 analogs were fully analyzed in Fura-2 and Fluo-4 imaging experiments. Only one analog (SGA-150 (**125**)) was able to activate TPC2 besides the hit **17**. No pharmacological targets were published for TPC2-A1-P (**17**). With its steep structure-activity relationship TPC2-A1-P (**17**) developed from hit to a promising chemical tool.

Comparing the results of both activator classes identified by HTS of the Roche library, a considerable number of TPC2-A1-N analogs caused noteworthy TPC2 activation, but none of them showed significantly increased efficacies or potencies compared to the HTS hit TPC2-A1-N (**16**). In contrast, the second hit TPC2-A1-P (**17**) showed an unusually steep structure-activity relationship, and except for one modestly active analog (SGA-150, **125**) none of the analogs showed any activity. Thus, the two high-throughput screening hits TPC2-A1-N (**16**) and TPC2-A1-P (**17**) can be regarded as strong chemical tools that need further pharmacokinetic and pharmacological characterization.

3.4.4 Further results of the novel TPC2 agonists

Within our cooperation with Prof. Dr. Schaefer's group, Leipzig, we had the opportunity to perform a selectivity screening of the best TPC2 activators identified in our investigations. The selected activators were tested on a broad panel of ion channels of the TRP superfamily. The screening was performed by Nicole Urban in the Schaefer lab (Leipzig).
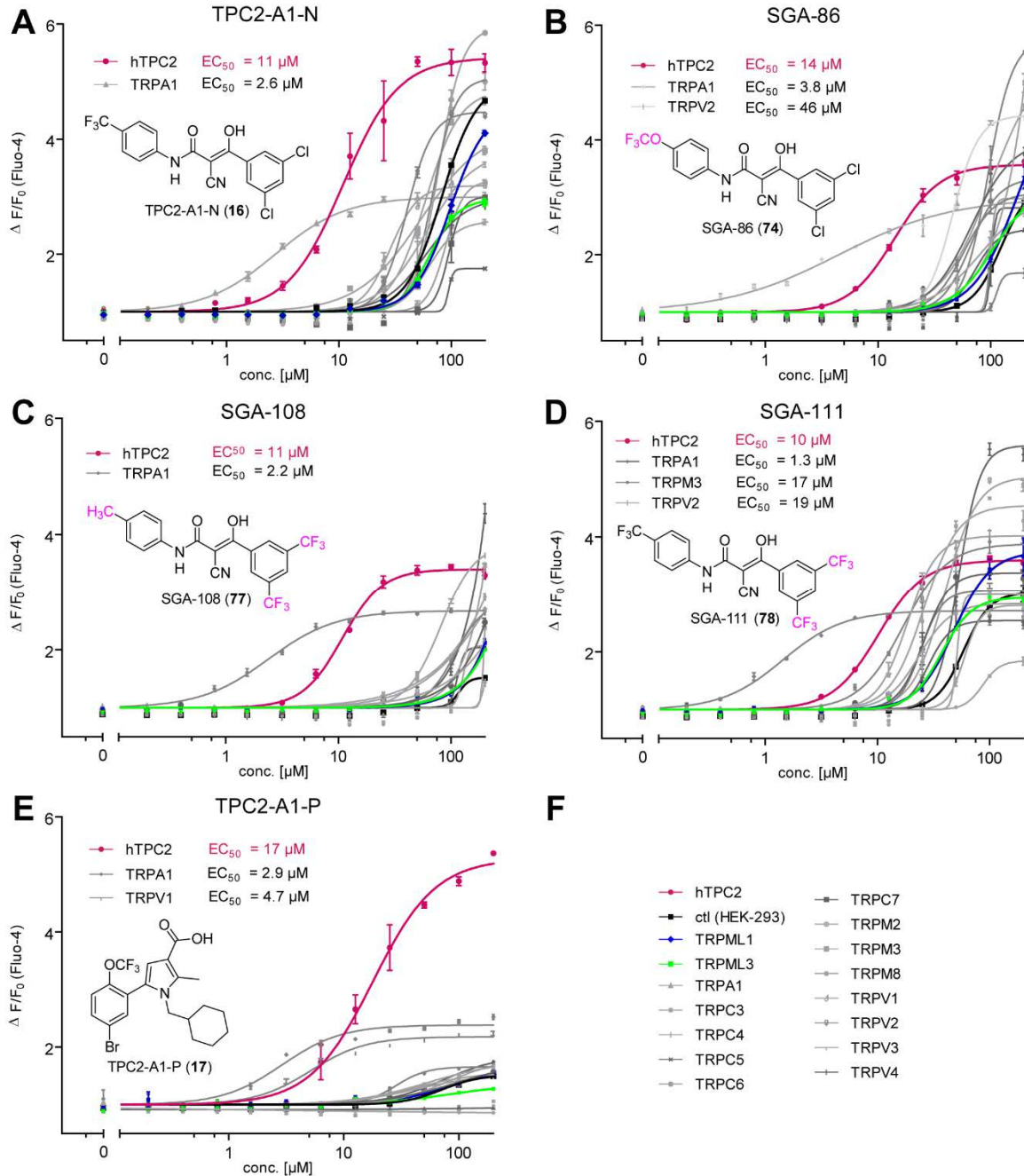
Figure 16: Selectivity screening of TPC2-A1-N (**16**), SGA-86 (**74**), SGA-108 (**77**), SGA-111 (**78**) and TPC2-A1-P (**17**). (**A-E**) Concentration-effect relationships for Ca^{2+} increases (Fluo-4 (**14**)) in response to different concentrations of TPC2-A1-N (**16**, A), SGA-86 (**74**, B), SGA-108 (**77**, C), SGA-111 (**78**, D) and TPC2-A1-P (**17**, E). Different stably expressing cell lines were used and activated with the activator indicated. hTPC2, control cells (HEK293), TRPML1 and TRPML3 are highlighted. (**F**) Legend of the different cell lines used. All experiments were performed by Nicole Urban.

44

At the beginning of the selectivity screening the custom-made fluorescence imaging plate reader was modified and cleaned, which resulted in higher intensities and slightly higher EC_{50} values (for TPC2-A1-N (**16**) from 7.8 µM to 11 µM; for TPC2-A1-P (**17**) from 10.5 µM to 17 µM, **Figure 16 A** and **E**). TPC2-A1-P (**17**), TPC2-A1-N (**16**) and some of the most potent analogs were analyzed. Earlier experiments already indicated that SGA-85 (**73**) and SGA-132 (**84**) had nonspecific activation on control cells (**Figure 11 B**). The highly substituted analogs SGA-33 (**60**) and SGA-90 (**75**) had low solubility which is problematic for experiments using high concentrations. Therefore, these four compounds were excluded. The selected compounds were tested on TPC2, non-transfected HEK-293 cells, the mucolipins TRPML1 and 3, TRPA1, TRPC3-7, TRPM2, 3, 8 and TRPV1-4 (**Figure 16 F**). Experiments were performed with test concentrations up to 200 µM for analysis of possible side effects.

Comparing the maximum activation, TPC2-A1-P (**17**) and TPC2-A1-N (**16**) had the highest efficacy (**Figure 16 A** and **E**) and EC_{50} values within the TPC2-A1-N analogs were all in the same range (9.7 µM to 14 µM, **Figure 16 A-D**). All tested pre-selected compounds were able to activate TRPA1 at low micromolar concentrations. The activation of TRPA1 was to be expected because TRPA1 is a chemosensory cation channel, which reacts *inter alia* to chemical substances and generates biological signals[123, 124]. SGA-86 (**74**) and SGA-111 (**78**) were able to activate TRPV2 with an EC_{50} of 46 µM and 19 µM, respectively (**Figure 16 B** and **D**). TPC2-A1-P (**17**) activated TRPV1 at low micromolar concentrations with a very low efficacy (**Figure 16 E**). The transient receptor potential cation channel subfamily V ("vanilloid") is related to thermal sensation and responsible for regulating body temperature[125, 126]. SGA-111 (**78**) was also able to activate TRPM3 with an EC_{50} of 17 µM (**Figure 16 D**). Comparing the TPC2-A1-N series, all substances showed effects on other TRP channels in high concentrations (≥ 100 µM). SGA-108 (**77**) showed the highest selectivity and TPC2-A1-N (**16**) the highest efficacy. SGA-111 (**78**) was less specific than all other probes and had a significantly lower efficacy. As mentioned before, all of these compounds have electron-withdrawing groups on the benzoyl moiety and are *para*-substituted on the anilide side (**Figure 12**). SGA-108 (**77**) was the only one with an electron-releasing group on the anilide side, which was generating selectivity for TPC2 at the expense of efficacy. TPC2-A1-P (**17**) showed high selectivity for TPC2 with high efficacy. The screening further confirmed that potencies were not increased compared to the hits TPC2-A1-N (**16**) and TPC2-A1-P (**17**) and despite large efforts in chemical synthesis, these hit structures could not be improved concerning TPC2 activation.

In house agar diffusion test was used to analyze antimicrobial effects of the new compounds on bacteria (*Escherichia coli*, *Pseudomonas marginalis*, *Staphylococcus equorum*, *Streptococcus entericus*), yeasts (*Yarrowia lipolytica*, *Saccharomyces cerevisiae*) and dermatophytes (*Hyphopichia burtonii*). The compounds did not show any inhibition zones for

the investigated bacteria and yeasts, while some analogs of TPC2-A1-N and the hit compound itself (**16**) showed small (but irrelevant) inhibition zones for the dermatophyte *Hyphopichia burtonii* (**Table 7**).

Table 7: Inhibition zones for the dermatophyte *Hyphopichia burtonii*. Agar diffusion experiments were performed by Martina Stadler.

entry	compound	inhibition zone (*Hyphopichia burtonii*)
1	TPC2-A1-N (**16**)	16 mm
2	SGA-1 (**44**)	12 mm
3	SGA-2 (**45**)	8 mm
4	SGA-3 (**46**)	8 mm
5	SGA-4 (**47**)	8 mm
6	SGA-9 (**49**)	12 mm
7	SGA-12 (**52**)	8 mm
8	SGA-16 (**55**)	10 mm
9	SGA-27 (**56**)	12 mm
10	SGA-39 (**62**)	12 mm
11	SGA-70 (**64**)	12 mm
12	SGA-71 (**65**)	12 mm
13	SGA-72 (**66**)	10 mm

3.4.5 Malleable cation selectivity of TPC2

TPC2-A1-N (**16**) and TPC2-A1-P (**17**) were further investigated together with different cooperation partners and the results are presented in a recent publication[22]. Both compounds did not activate TPC1 in patch clamp experiments which is stressing the selectivity of these compounds. Cell permeability was proven by GCamp6 experiments, which clearly demonstrated that both activators are able to activate TPC2. The calcium indicator GCamp6, located on the lysosomal membrane, is able to detect calcium efflux from the lysosome, thus proving the membrane permeability of the compounds.

Furthermore, by means of the two novel small-molecules we were able to resolve the conflict of TPC2 being an NAADP-activated Ca^{2+} release channel[5, 12, 14, 127, 128] or a $PI(3,5)P_2$ gated Na^+ channel[15, 20, 129]. TPC2-A1-N (**16**) rendered the channel more calcium permeable, similar to NAADP-activated TPC2, whereas TPC2-A1-P (**17**) increased sodium permeability, similar to the $PI(3,5)P_2$-activated channel. Consequently, ion permeation through TPC2 is ligand-dependent, indicating that TPC2 is a non-selective cation channel with malleable cation selectivity. Appropriately, the $PI(3,5)P_2$ (**4**) binding site in TPC2[8] has been identified to broadly overlapping with the one for TPC2-A1-P (**17**). It has been demonstrated that TPC2-A1-N (**16**) induces an alkalinization of single vesicles in cells expressing wild-type TPC2, as previously reported for NAADP (**3**)[130, 131]. These findings confirmed that TPC2 activation is coupled to

lysosomal pH and vesicle motility in an agonist-dependent manner. The effect of both activators on lysosomal exocytosis was further evaluated. TPC2-A1-P (**17**), but not TPC2-A1-N (**16**) promoted lysosomal exocytosis. Manipulation of lysosomal exocytosis may provide a therapeutic approach for LSDs[132-134].

These findings would not have been achievable without the availability of the lipophilic small-molecule activators TPC2-A1-N (**16**) and TPC2-A1-P (**17**) identified in this project. These tools have the potential to elevate studies regarding TPC2 to the next level, which will result in a better understanding of the various ion channel functions.

3.4.6 The race to identify new TPC activators

Small-molecule modulators of two pore channels have been a hot topic in recent literature. In 2019, Zhang et al. identified tricyclic and phenothiazine antidepressants as TPC1 and 2 activators by screening Sigma's LOPAC library, containing 1280 compounds[111]. With calcium imaging experiments, followed by confirmation using whole-cell recordings in TPC2[LL/AA]-expressing HEK293 cells, the authors identified 8 compounds as TPC2 activators. The dibenzazepine-type tricyclic antidepressants (TCAs) clomipramine (**127**), desipramine (**128**), imipramine (**129**), amitriptyline (**130**) and nortriptyline (**131**), as well as the phenothiazine-based antidepressants chlorpromazine (**132**) and triflupromazine (**133**) were found to activate TPC2 (**Figure 17 A** and **B**). The EC_{50} values were between 43 and 112 µM and therefore these activators are presumably less potent than TPC2-A1-N (**16**, **Figure 10 G**) and TPC2-A1-P (**17**, **Figure 10 H**) from our project. The authors described that currents elicited with TCAs were strongly voltage-dependent while riluzole (**134**, **Figure 17 C**) activation was voltage-independent. Some TCAs, clomipramine (**127**) and desipramine (**128**), also activated TPC1 in a voltage-dependent manner, while chlorpromazine (**132**) and riluzole (**134**) inhibited TPC1. It was barely possible to analyze structure-activity relationships with only seven identified structures. Nevertheless, the dibenzazepine carbamazepine (**135**) and native phenothiazine (**136**, **Figure 17 D**) did not activate TPC2, which highlighted the necessity of the aminoalkyl side chain at the central ring of the tricyclic core[135].
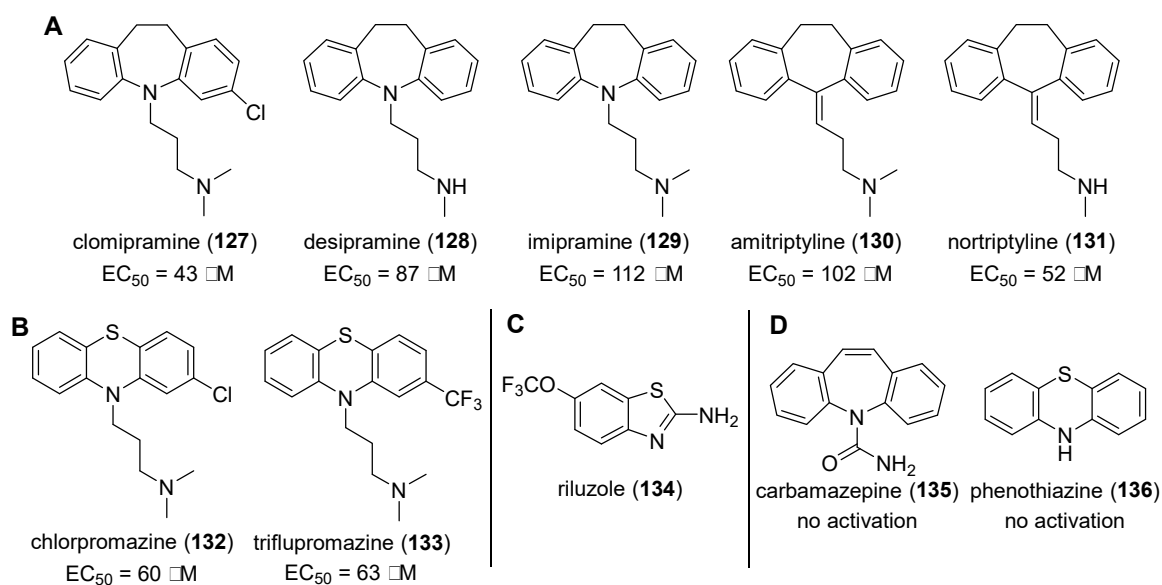
Figure 17: Structures and EC_{50} values, published by Zhang et al.[111]. (**A-B**) Structures and EC_{50} values of TCAs (A) and related phenothiazines (B) as TPC2 activators. EC_{50} values were obtained from whole-cell recordings at -140 mV. (**C**) Structure of riluzole (**134**). (**D**) Structures of the inactive carbamazepine (**135**) and phenothiazine (**136**).

Evaluating the current literature it was noticeable that the phenothiazines triflupromazine (**133**) and fluphenazine (**6**), recently published by Penny et al.[31], share the same skeleton but have huge differences in their pharmacological activity (**Figure 18**). While fluphenazine (**6**) was inhibiting TPC2 signals evoked by NAADP (**3**) with an IC_{50} of 42 μM[31], triflupromazine (**133**) was identified as TPC2 activator. An inhibitor of TPC2 was most likely converted into an activator of TPC2 by introducing only slight changes in the side chain[135]. This example demonstrates how close activators and inhibitors of an ion channel can resemble each other and how important the analysis of structure-activity relationships is.

triflupromazine (**133**)   fluphenazine (**6**)
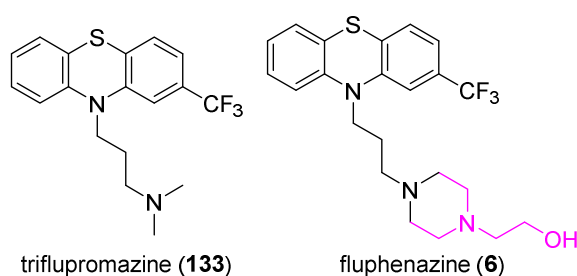
Figure 18: Structures of the TPC2 activator triflupromazine (**133**) and the TPC2 inhibitor fluphenazine (**6**)[31, 111]. Differences are marked in magenta.

The two independently performed HTSs by Zhang et al. and within this project created a panel of small-molecule TPC activators, compared in our recently published review[135]. Zhang et al. focused on drug repurposing and thereby identified TCAs, phenothiazines and the benzothiazole riluzole (**134**) that activate TPC2. Originally, TCAs are used to treat e.g. depression, bipolar disorder, panic disorder, chronic pain, and insomnia and inhibit *inter alia* monoamine (serotonin, norepinephrine, dopamine) reuptake. TCAs have a wide range of adverse effects and are therefore replaced as antidepressants by the selective serotonin reuptake inhibitors (SSRI)[136]. In addition, amitriptyline (**130**), imipramine (**129**), and clomipramine (**127**) are also potent CYP450 inhibitors, significantly inhibiting CYP450 2C19 and 1A2[137]. Aforementioned, this bears the risk of undesired drug-drug interactions. Riluzole (**134**) blocks TTX-sensitive sodium channels, kainite receptors and NMDA receptors, has neuroprotective effects and it is currently approved for the treatment of amyotrophic lateral sclerosis (ALS)[138-142]. The activators identified in this thesis, TPC2-A1-N (**16**) and TPC2-A1-P (**17**), are no listed drugs. Comparing the results of both screenings, there is comprehensive knowledge on the pharmacological profiles of the repurposed TCA/phenothiazine-type TPC2 activators due to their long term application in therapy, but as well a large list of undesired effects. Our newly identified activators still need full pharmacokinetic and pharmacological characterization, though have the potential to address TPCs as their main target with a high affinity and thus have less side effects.

Lately performed docking studies with the TPC2 agonists on the apo-state hTPC2 structure confirmed that TPC2-A1-P (**17**) and PI(3,5)P$_2$ (**4**), as well as TPC2-A1-N (**16**) and riluzole (**134**) share one binding pocket, each[135]. This suggests that TPC2-A1-N (**16**) and riluzole (**134**) both mimic NAADP (**3**) actions. Furthermore the binding free energies were calculated and suggest that TPC2-A1-N (**16**) and TPC2-A1-P (**17**) are more efficacious than clomipramine (**127**) and chlorpromazine (**132**). This corresponds with the higher EC$_{50}$ values for the repurposed activators (42 – 112 µM) compared to TPC2-A1-N (**16**, 7.8 µM) and TPC2-A1-P (**17**, 10.5 µM).

Now there is the opportunity to choose from an impressive and highly diverse collection of new lipophilic small-molecule activators for either selectively activating TPC2 or activation of both TPC1 and TPC2 with the warning that some of the compounds are also blocking TPC1. Physiology and pathophysiology of TPCs can be studied in more detail with the cell permeable small-molecule activators. Most importantly, the novel compounds allow studies in intact cells and can be used as chemical tool for analyzing TPC2 inhibitors. They may also be applicable for *in vivo* studies and perhaps even for therapy[135].

3.5 A new generation of TPC2 inhibitors

A high-throughput analysis of TPC2 inhibitors can be accomplished using the newly developed membrane permeable and small-molecule TPC2 activators. Therefore, a library of TPC2 inhibitors was created to gain first insights into SAR for truncated variants of tetrandrine (**1**). Aforementioned, our concept was to develop TPC2 inhibitors derived from the lead structure tetrandrine (**1**). One major intention was to develop less complex analogs of this bisbenzylisoquinoline alkaloid. Hence, we considered both, natural products of this chemotype from different sources as well as monomeric benzylisoquinolines and newly synthesized analogs of tetrandrine (**1**).

3.5.1   Collection of alkaloids and 1-benzylisoquinolines

Consequently, this library included benzylisoquinoline-type intermediates of the morphine biosynthesis like *O*,*O*-dibenzyl coclaurine (Z3, **137**), available from the substance collection of Prof. Dr. Meinhart Zenk (passed away in 2011), tetrandrine (**1**) and derivatives such as fangchinoline (**9**), kindly provided by Prof. Dr. Peter Pachaly (passed away in 2019), and commercially available benzylisoquinoline alkaloids like dauricine (**11**) and oxyacanthine (**138**, **Figure 19**).
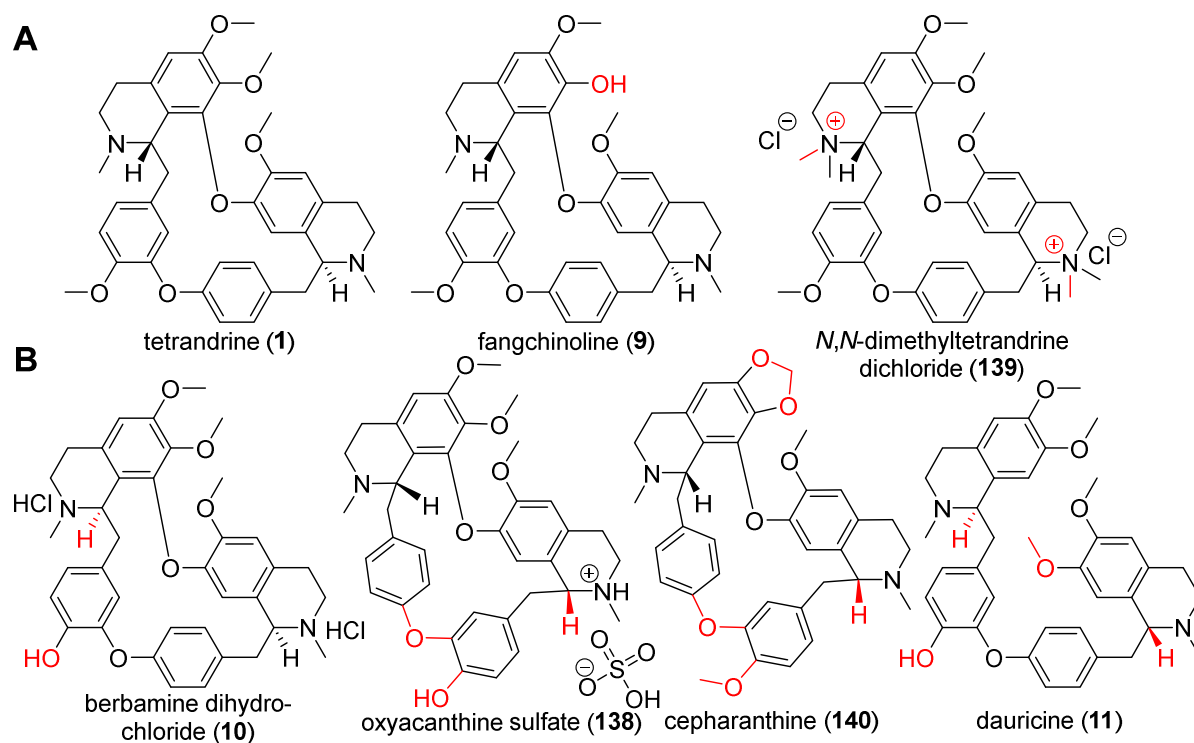
Figure 19: Strutures of investigated bisbenzylisoquinoline alkaloids. (**A**) Structures of the alkaloids tetrandrine (**1**), fanglchinoline (**9**) and *N*,*N*-dimethyltetrandrine dichloride (**139**), kindly provided by Prof. Dr. Peter Pachaly[†]. (**B**) Structures of the commercially available alkaloids berbamine dihydrochloride (**10**), oxyacanthine sulfate (**138**), cepharanthine (**140**) and dauricine (**11**). Structural differences compared to tetrandrine (**1**) are marked red.

The bisbenzylisoquinoline alkaloids, provided from Prof. Dr. Peter Pachaly[†] were analyzed by NMR, HRMS, specific rotation and purity was confirmed by analytical HPLC. Only tetrandrine (**1**) from natural source had to be purified by column chromatography and recrystallized from EtOH/water before it was subjected to biological experiments. All analytical data were in accordance with literature[143-145]. All substances from the collection of Prof. Dr. Meinhart Zenk[†] (**Figure 20**) were analyzed by NMR, HRMS and specific rotation in order to distinguish (if not clearly indicated) racemic from enantiomerically pure substances. Purity was confirmed by analytical HPLC. If a compound was not pure enough (HPLC purity < 96%), purification was accomplished by FCC. Analytical data for all substances were in accordance to literature or are stated in the experimental part of this thesis.
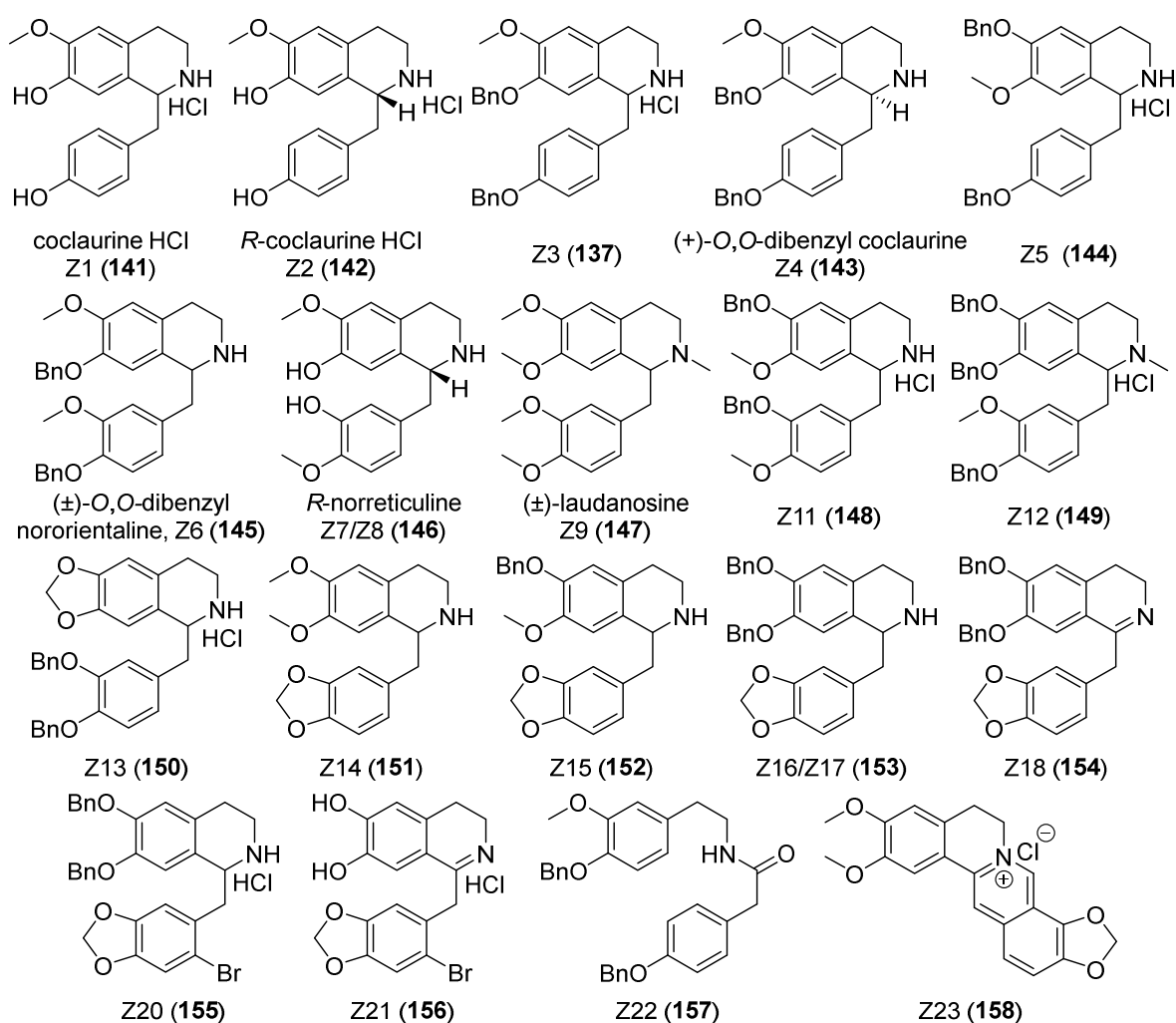
Figure 20: Structures of substances, kindly received from Prof. Dr. Meinhart Zenk[†].

3.5.2 Synthesis plan

A new generation of truncated analogs of tetrandrine (**1**) should be synthesized to receive molecules that resemble tetrandrine (**1**, **Figure 21**). A short and efficient synthesis was developed therefore. These molecules should mimic one of the two benzyltetrahydroisoquinoline moieties of tetrandrine (**1**), therefore the racemic natural product *N*-methyl coclaurine (SG-132, **159**) was chosen as basic structure. Further decoration not only in form of *O*-benzyl derivatives, but also as diaryl ethers are supposed to closely imitate tetrandrine (**1**) in shape and size. Bisbenzylisoquinolines with anti-cancer activity have already been described aforementioned. They have different stereochemistry at their two stereocenters, e.g. cepharanthine (*S*,*R*, **140**)[146] or the *seco*-variant dauricine (*R*,*R*, **11**)[80], compared to tetrandrine (*S*,*S*, **1**), as shown in **Figure 19 A** and **B**. Within a first series of endolysosomal patch clamp experiments, performed by Dr. Yu-Kai Chao, antagonistic effects of cepharanthine (**140**), dauricine (**11**) and (±)-*O*,*O*-dibenzyl coclaurine (Z3 (**137**), **Figure 20**) on TPC2 were confirmed (**Figure 22**). Aforementioned stereochemistry was not limited to one isomer, a racemic synthesis for the truncated analogs of tetrandrine (**1**) would be most appropriate. Compared to the rigid, macrocyclic bisbenzylisoquinoline tetrandrine (**1**), the new truncated analogs of tetrandrine bear only one benzylisoquinoline unit. However the *O*-benzyl or *O*-phenyl residues mimic the two benzenoid rings of the second benzylisoquinoline moiety of the parent compound making these compounds similar to tetrandrine (**1**) in size, but are much more flexible. This flexibility should enable the compounds to adapt perfectly to the binding site in the target proteins.
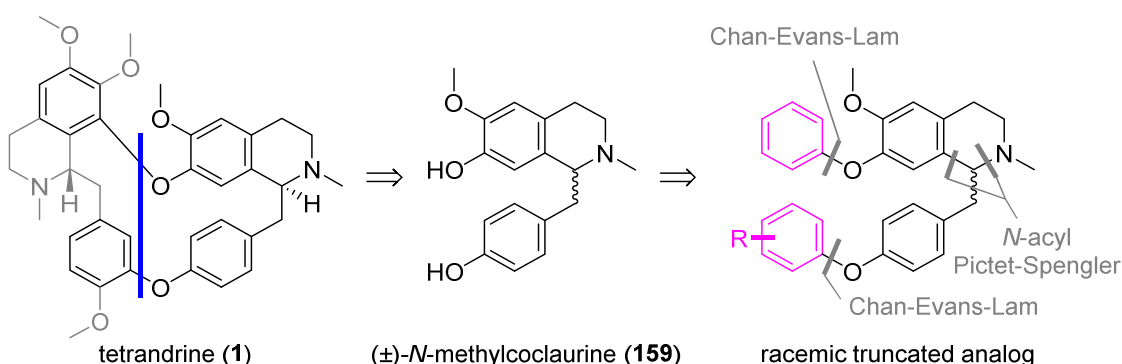
Figure 21: Truncation of tetrandrine (**1**). The racemic alkaloid (±)-*N*-methylcoclaurine (**159**) already represents one half of tetrandrine (**1**). Introduction of additional aromatic moieties (right, marked in magenta) enables the molecule to resemble the overall molecular geometry of tetrandrine (**1**).

Key steps for the synthesis of truncated tetrandrine analogs are the *N*-acyl Pictet-Spengler reaction to construct the 1-benzyltetrahydroisoquinoline and the Chan-Evans-Lam coupling for introduction of diaryl ethers (**Figure 21**, right). According to Comins et al.[147], the precursors for the *N*-acyl Pictet-Spengler reaction would be different carbamate building blocks of type **I**

and enol ether building blocks of type **II**. These building blocks would be easily accessible from commercially available aldehydes bearing different residues in *meta-* and *para*-position (**i**, **Scheme 16**). If desired, the phenol group of these aldehydes can be protected as benzyl ether or alkyl carbonate (**ii** and **v**, **Scheme 16**). The utilization of benzyl ethers as protecting groups is commonly known, while the introduction of alkyl carbonates is new. Following a procedure published by Pouysegu et al.[148], a Henry reaction using commercially available benzaldehydes and nitromethane would give nitrovinyl compounds (**iii**, **Scheme 16**) and reduction using lithium alanate would yield desired arylethylamine (**iv**, **Scheme 16**). This sequence only needs to be performed for the introduction of benzyl ethers, because many arylethylamines (**iv**, **Scheme 16**) are already commercially available (e.g. 3-methoxytyramine (**160**) and 3,4-dimethoxyphenyl-ethylamine **161**). Using ethyl chloroformate (**162**) and NEt$_3$ would give the carbamate group and further, in the case of a free phenol group, an ethyl carbonate (**I**, **Scheme 16**)[149]. Depending on the work-up conditions, the ethyl carbonate could remain unaffected using neutral conditions or cleaved using alkaline conditions[73, 149]. The resulting free phenol group of the alkaline work-up could then be used for the introduction of an aryl ether *via* Chan-Evans-Lam coupling. Wittig olefination of 4-substituted benzaldehydes (**i**, **Scheme 16**) would give enol ethers of type **II** (**Scheme 16**) as masked arylacetaldehyde.
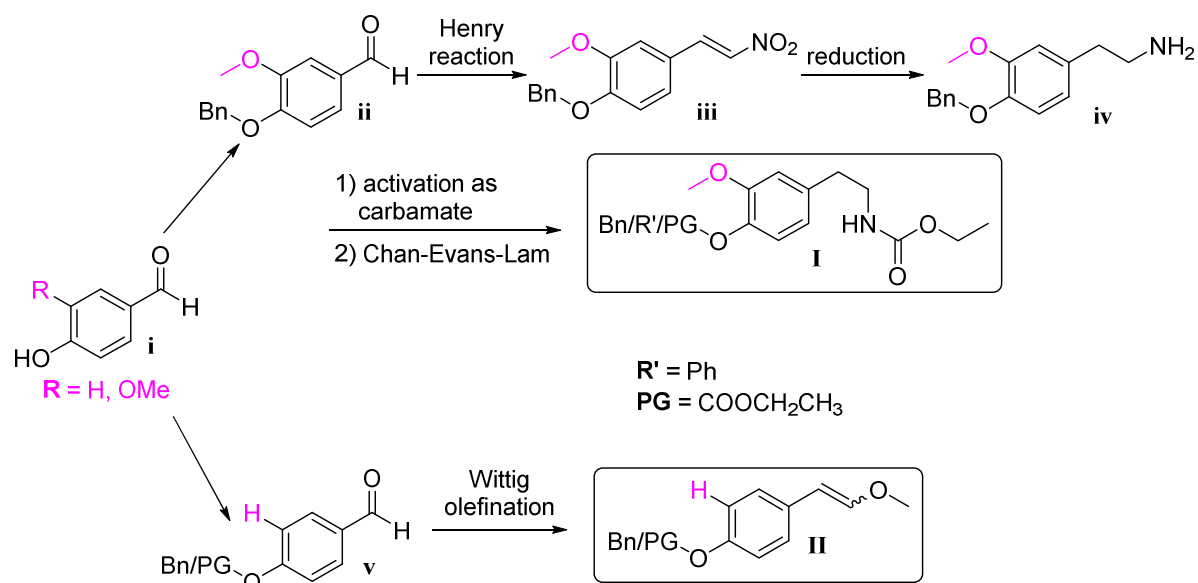
Scheme 16: Synthesis plan for the preparation of the precursors for the *N*-acyl Pictet-Spengler reaction. Carbamate building blocks of type **I** and enol ether building blocks of type **II** are easily accessible from commercially available aldehydes or arylethylamines.

The 1-benzyl-1,2,3,4-tetrahydroisoquinolines **III** were to be prepared by *N*-acyl Pictet-Spengler reactions using precursors **I** and **II** (**Scheme 17 A**). Comins et al. published a procedure for an TFA catalyzed *N*-acyl Pictet-Spengler reaction, which would be pursued[147]. Utilization of arylethylcarbamates for *N*-acyl Pictet-Spengler reactions is a common method in

the Bracher research group. While standard Pictet-Spengler tetrahydroisoquinoline synthesis requires harsh reaction conditions like heating to reflux with strong acids, *N*-acyl Pictet-Spengler reaction proceeds under mild conditions. This is caused by formation of an *N*-acyliminium ion **163** as intermediate, which is a much stronger electrophile in comparison to the less powerful electrophile iminium intermediate **164** which occurs in regular Pictet-Spengler reactions (**Scheme 17 B**). Even nucleophiles that are relatively unreactive as non-activated benzenoids, participate effectively in cyclizations with *N*-acyliminum species[150, 151].
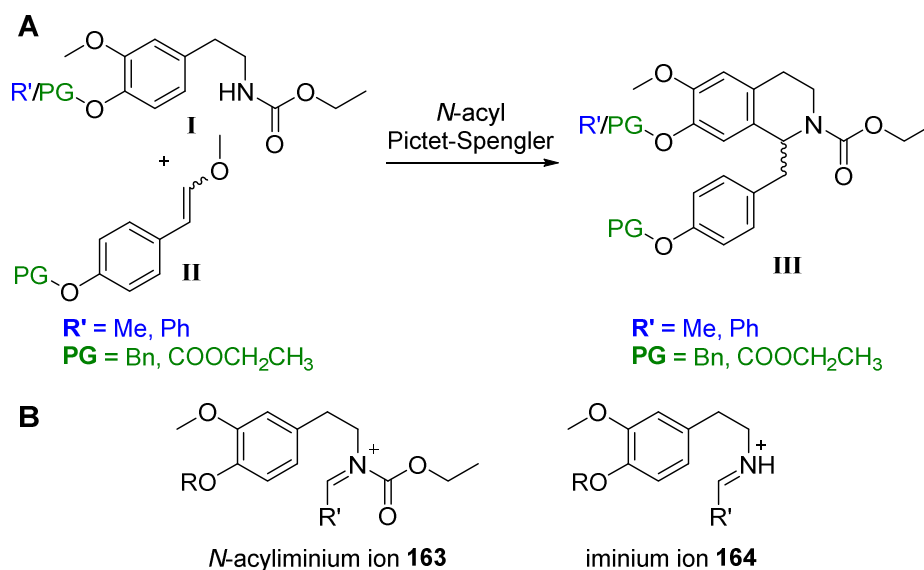
Scheme 17: The *N*-acyl Pictet-Spengler reaction. (**A**) Planed synthesis for the construction of the tetrahydroisoquinoline **III** via *N*-acyl Pictet-Spengler reaction. (**B**) *N*-Acyliminium ion **163** (left) and iminium ion **164** (right) as intermediates for Pictet-Spengler-type cyclizations.

Tertiary *N*-methyl amines **IV** are available *via* reduction of carbamates **III** using lithium alanate (**Scheme 18**)[152]. Furthermore all carbonate esters can be cleaved under these conditions, directly yielding the free phenols and tertiary *N*-methyl amines in one step, while the benzyl protecting groups of the phenols are not affected by these conditions (not depicted).
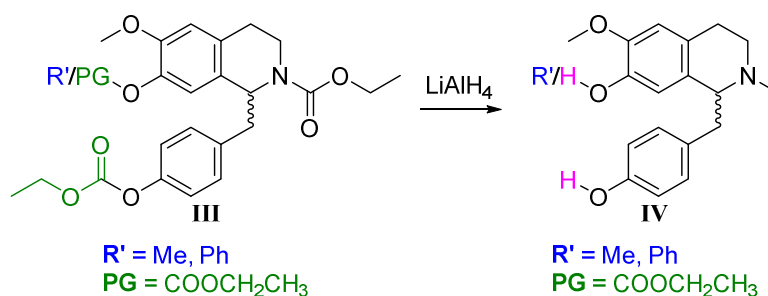
Scheme 18: Planned simultaneous deprotection of ethyl carbonates and reduction of carbamates to give *N*-methyl amines of type **IV**.

For the synthesis of truncated tetrandrine analogs, as depicted in **Figure 21**, diaryl ethers had to be introduced to the appropriate free phenols. Choosing an environmental-friendly catalyst led to copper-catalyzed coupling reactions. One famous example is the Ullmann coupling for diaryl ether synthesis[153]. Hereby, aryl halides and phenols are converted into diaryl ethers under copper-promotion. Requiring high temperatures and being limited on the substitution patterns of both coupling partners, the Ullmann coupling is not generally applicable, and a new version of this coupling reaction was selected. The Chan-Evans-Lam coupling was developed in 1998 and represents a modern copper-catalyzed oxidative coupling of boronic acids and heteroatom nucleophiles[154-156]. Advantages of the Chan-Evans-Lam coupling are milder reaction conditions (room temperature and the presence of oxygen), cheap copper catalysts, good to excellent yields, and a diverse substrate scope[157].
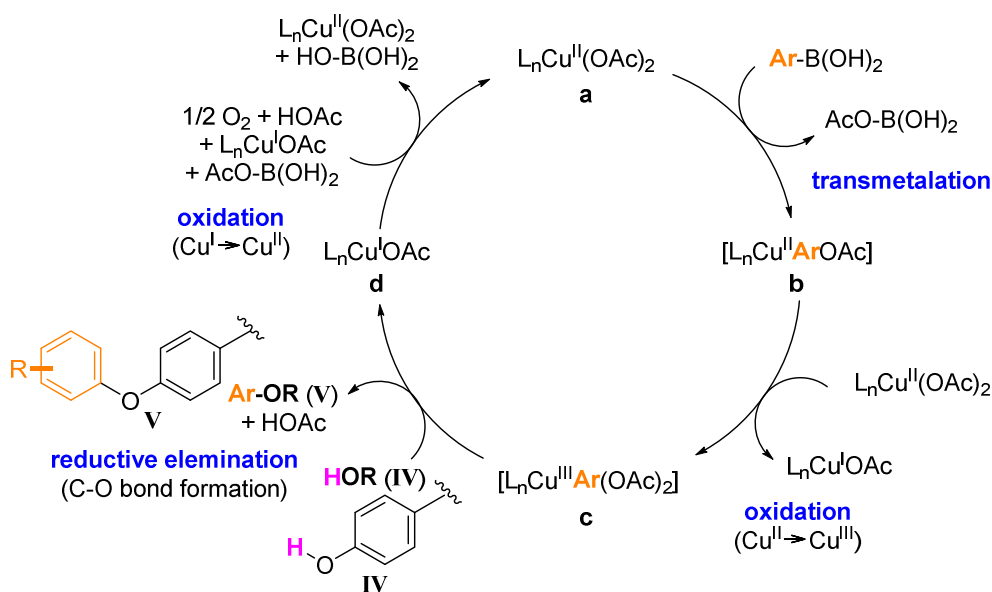
Scheme 19: Proposed mechanism for the Chan-Evans-Lam diaryl ether synthesis, based on the studies of Stahl and coworkers[158].

A boronic acid dimethyl ester in MeOH was used as example for the studies by Stahl and coworkers of the mechanism of this etherification process[158, 159]. This catalytic cycle starts with a Cu(II) species (**a**, **Scheme 19**), in this scheme Cu(OAc)$_2$ and e.g. pyridine as ligand (L$_n$). Transmetalation with an aryl boronic acid (marked in orange) gives aryl Cu(II) complex (**b**, **Scheme 19**). Oxidation of this complex (**b**, **Scheme 19**) to a Cu(III) complex (**c**, **Scheme 19**) occurs *via* disproportionation with another equivalent of the starting Cu(II) species (**a**, **Scheme 19**). The C-O bond formation takes place within the reductive elimination to give the desired diaryl ether (orange, **Scheme 19**) and a Cu(I) species (**d**, **Scheme 19**), which is re-oxidized by oxygen.
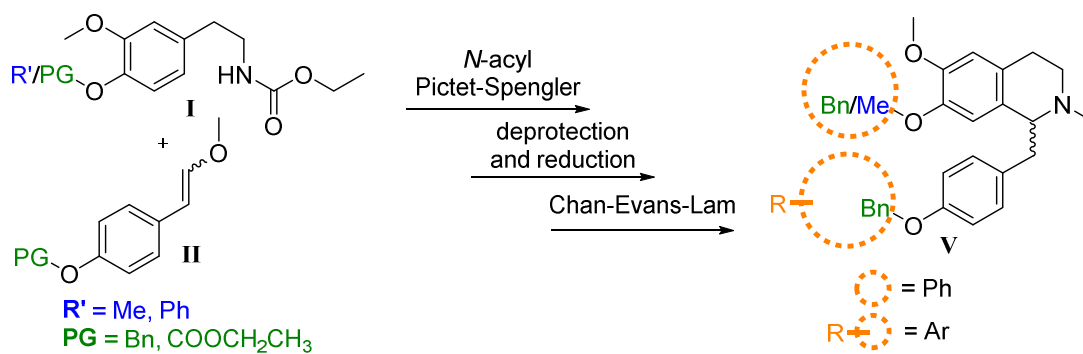
Scheme 20: Summary of the synthesis plan for truncated tetrandrine analogs. These analogs (**V**) can be achieved in three steps, starting from precursors **I** and **II**.

Following this sequence would give desired truncated tetrandrine analogs in only three steps, starting from building blocks **I** and **II** (**Scheme 20**). This short sequence was to be used to introduce a variety of different diaryl ethers for the generation of a set of truncated analogs to study SAR.

3.5.3 Synthesis of a new generation of TPC2 inhibitors

First, the building blocks for the *N*-acyl Pictet-Spengler reaction were synthesized. Using ethyl chloroformate (**162**) and NEt$_3$, amines can be converted into carbamates and phenols into ethyl carbonates. The commercially available 3-methoxytyramine hydrochloride (**160**) was protected under these conditions and depending on further proceedings yielded carbamate **165** (bearing an ethyl carbonate protecting group) or **166** (having a free phenol group) in high to moderate yields (**Scheme 21**)[73, 149]. While neutral extraction gave the protected phenol **165**, the addition of NaOH (1 M) in ethanol deprotected the aryl-alkyl carbonate and resulted in phenol **166**. If the reaction mixture was extracted using 2 M aq. NaOH, the deprotection of carbamate **165** was not complete, because of the two-phase mixture.
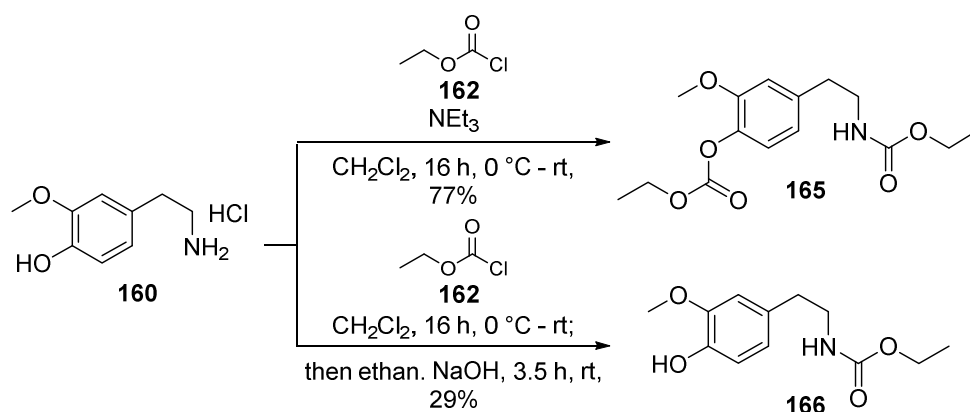
Scheme 21: Synthesis of carbamates **165** and **166** using ethyl chloroformate (**162**) under basic conditions. Depending on the work up, a protected phenol **165** or deprotected phenol **166** was obtained.

Diaryl ether **167** was synthesized using the mild coupling conditions of the Chan-Evans-Lam reaction. Copper catalyzed and under alkaline conditions carbamate **166** and phenylboronic acid (**168**) were used to give diary ether **167** in high yields (**Scheme 22**). Full characterization (TLC, NMR, HRMS, IR, m.p.) confirmed the structure and analytical HPLC the purity. Initial experiments for this reaction were performed within the Bachelor thesis of F. Talay.
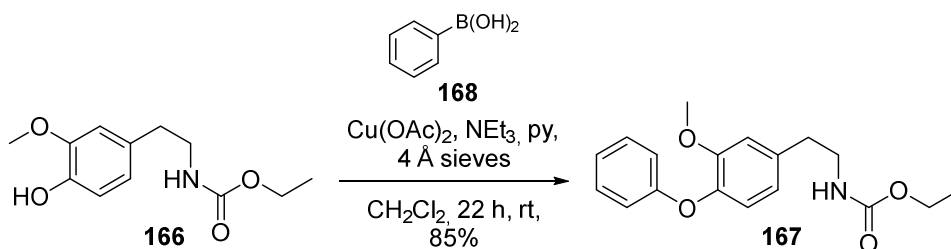
Scheme 22: Copper catalyzed Chan-Evans-Lam coupling of carbamate **166** to give diaryl ether **167**.

The aforementioned method to generate carbamates was applied for the synthesis of carbamate **169** as well, with commercially available 3,4-dimethoxyphenylethylamine **161** as starting material. The reaction time was reduced to 4 h by refluxing the mixture to give carbamate **169** in high yields (**Scheme 23**). Carbamate **169** was fully characterized (TLC, NMR, HRMS, IR, m.p.) and ^{1}H and ^{13}C NMR data were in accordance with literature[160].
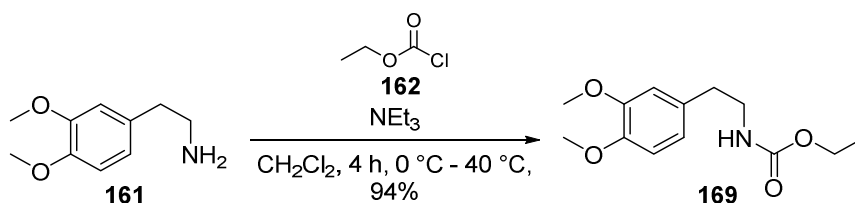
Scheme 23: Protection of amine **161** with accelerated reaction time.

To receive an *O*-benzylated carbamate (**170**, **Scheme 25**), the corresponding amine **171** had to be synthesized first. Following a procedure published by Pouysegu et al.[148], 4-benzyloxy-3-methoxybenzaldehyde **172** was used as starting material for a Henry reaction, giving nitrovinyl compound **173** in good yield. Reduction using lithium alanate yielded the desired arylethylamine **171** in high yield (**Scheme 24**). Both products were fully characterized and analytical data are in accordance with literature.
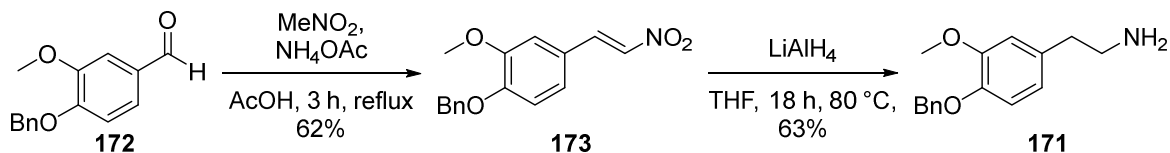
Scheme 24: Synthesis of benzyl-protected amine **171** in two steps, according to Pouysegu and colleagues[148].

Using ethyl chloroformate (**162**) and NEt$_3$, amine **171** was protected, giving carbamate **170** in moderate yield (**Scheme 25**). The compound was characterized by TLC, NMR, HRMS, IR and melting point and the analytical data were in accordance with literature[149].
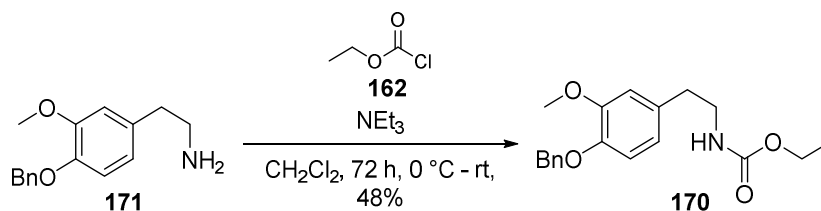
Scheme 25: Synthesis of carbamate **170** utilizing the above mentioned method.

Enol ethers were utilized as masked arylacetaldehyde equivalents, because the corresponding arylacetaldehydes are often instable due to their ability to easily polymerize[161]. The E/Z stereochemistry of the enol ethers is not relevant for the following *N*-acyl Pictet-Spengler reaction and a simple Wittig olefination of aromatic aldehydes was chosen for the synthesis. Enol ether **174** was to be formed starting with 4-hydroxybenzaldehyde (**175**), (methoxymethyl)-triphenyl-phosphonium chloride and a strong base (**Scheme 26**). First, the phosphonium salt is deprotonated to give a colorful ylide, which then forms an oxaphosphetane *via* a [2+2] cycloaddition with the aldehyde. Elimination of triphenylphosphine oxide yields the desired E/Z-alkene. The synthesis of enol ether **174** is known using *tert*-butoxide (conditions a)[162] or LHMDS (conditions b)[163]. Though, the first step, the ylide formation, did not show any conversion for potassium *tert*-butoxide and only slight conversion using the stronger base LHMDS. The even stronger base LDA (conditions c) was further tried and finally ylide formation was observed by formation of a deep red complex. Both known procedures described high yields for the Wittig olefination (81% and >95%), however, this was not reproducible. Formation of the enol ether **174** was observed *via* GC-MS but not completed even after 24 h, therefore another route was chosen.
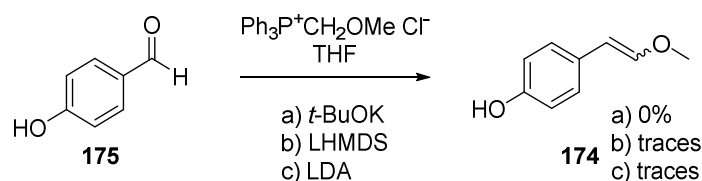
Scheme 26: Synthetic approach to yield enol ether **174**, using different conditions.

An ethyl carbonate protecting group for phenols was already used for some carbamate building blocks and was now introduced for protection of the free phenolic group of aldehyde **175**. Hence 4-hydroxybenzaldehyde (**175**) was protected using ethyl chloroformate (**162**) and NEt₃ to give aldehyde **176** in high yield (**Scheme 27**).
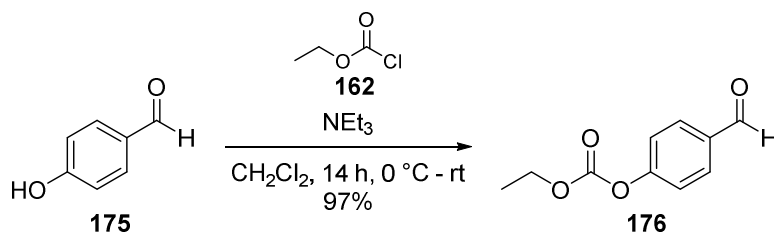
Scheme 27: Synthesis of protected aldehyde **176** using ethyl chloroformate (**162**) and NEt₃.

Aforementioned formation of the ylide for Wittig olefination was most successful using LDA. Hence LDA was used for olefination reaction of aldehyde **176**. With (methoxymethyl)-

triphenylphosphonium chloride and aldehyde **176**, enol ether **177** was obtained in good yield (**Scheme 28**). The reaction was monitored by TLC and staining with DNPH as both starting material and product had the same R_f value. DNPH indicated the end of the reaction by different colors of the formed hydrazones. While the aromatic, highly conjugated aldehyde **176** resulted in a deep orange color, the aliphatic enol ether **177** gave a lighter, yellow color. The generation of a side product, enol ether **174**, was observed and starting material **175** was found as well. The ethyl carbonate protecting group is labile under alkaline conditions and therefore only one equivalent LDA was used. Maybe the basicity of the formed ylide is strong enough to cleave the ethyl carbonate protecting group and yield enol ether **174** or aldehyde **175** (if the starting material was deprotected). Consequentially, the reaction cannot result in a full conversion of aldehyde **176** into enol ether **177**, as not enough ylide was present. Both side products were separated from the desired enol ether **177** by column chromatography. While being stored the enol ether **177** decomposes, as already described for enol ether **174**[162]. Therefore it was analyzed by TLC, NMR and HRMS as fast as possible and quickly used for the next step without full characterization.
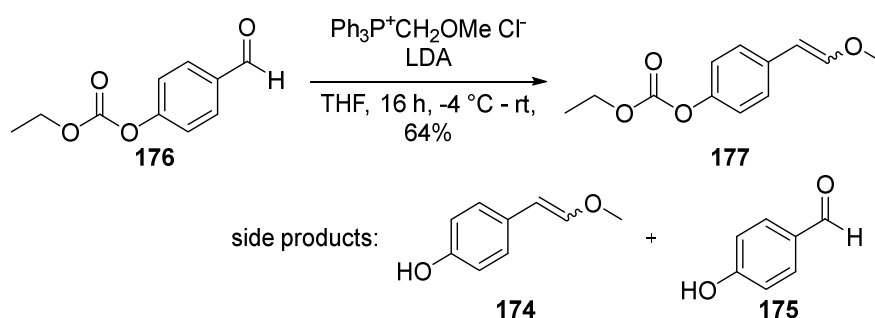
Scheme 28: Wittig olefination of aldehyde **176**. Besides the desired enol ether **177**, also two side products were identified.

This method was further applied for other *para*-substituted benzaldehydes. Besides *para*-carbonate protecting group in enol ether **177** (entry 1, **Table 8**), a diaryl ether enol ether **178** (entry 2, **Table 8**) and a benzyloxy enol ether **179** (entry 3, **Table 8**) were synthesized in moderate to high yields. Due to the instability of enol ether **177** and the reports in literature about it[162], all of them were analyzed by TLC, NMR and HRMS as fast as possible and used without full characterization for the next step.

Table 8: Wittig olefination of different aldehydes to give enol ethers using (methoxymethyl)-triphenyl-phosphonium chloride and LDA as base.
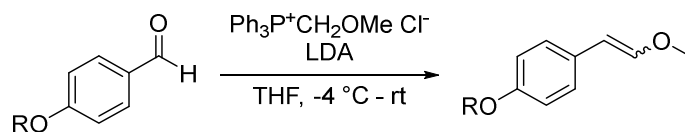
entry	starting material	reaction time	product	yield
1	R = COOEt (**176**)	16 h	**177**	63%
2	R = Ph	50 h	**178**	59%
3	R = Bn	16 h	**179**	85%

With the four different carbamates of type **I** and the three enol ethers of type **II** (**Scheme 20**) both building blocks for *N*-acyl Pictet-Spengler reactions were successfully synthesized and ready to be combined.

For performing the *N*-acyl Pictet-Spengler reaction TFA in dichloromethane was chosen as acidic catalyst, according to Comins et al.[147]. Molecular sieves (4 Å) were added to ensure an aqueous free environment and avoid side or decomposition reactions. These conditions gave racemic tetrahydroisoquinoline **180** in high yield (**Scheme 29**). NMR analysis was performed at 100 °C in tetrachloroethane. In NMR experiments performed at room temperature, different rotamers of the molecule were observed. This is the result of isomers arising from hindered single-bond rotation in a time frame that it is detectable by NMR. Heating up the NMR sample to 100 °C boosted the rotation to give a single set of resonances.
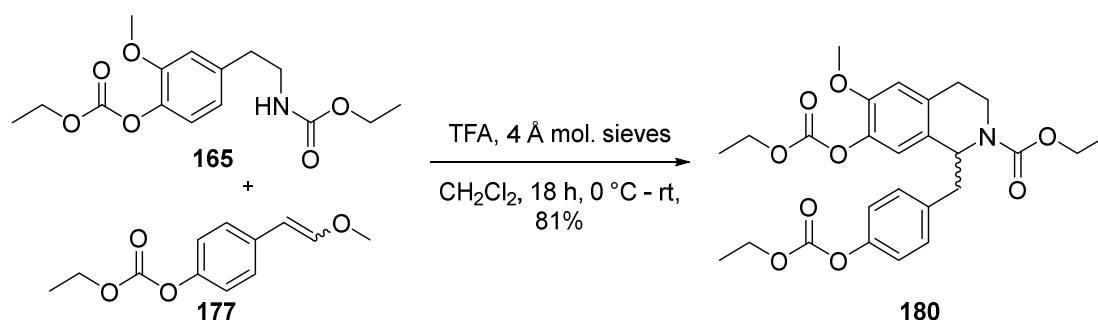
Scheme 29: *N*-Acyl Pictet-Spengler reaction to give racemic tetrahydroisoquinoline **180**. Carbamate **165** and enol ether **177** were used as starting materials.

These reaction conditions were further applied in the synthesis for racemic tetrahydroisoquinolines (**III**, **Table 9**) generated out of different combinations of the synthesized carbamates and enol ethers (**I** and **II**, **Table 9**). As precursor for the natural

product (±)-*N*-methylcoclaurine (**159**) served the ethyl carbonate protecting group (entry 1, **Table 9**). To analyze the influence of residues in C-7 position of the tetrahydroisoquinoline a methoxy group (entry 2 and 5, **Table 9**), a diaryl ether (entry 3, **Table 9**) and a benzyl ether (entry 4, **Table 9**) were introduced. The *O*-benzylated tetrahydroisoquinoline (entry 4, **Table 9**) was more complex to purify because FCC mainly gave impure fractions. Hence this yield is lower. All other *N*-acyl Pictet-Spengler reactions gave the racemic tetrahydroisoquinolines in high yield. NMR analysis at 100 °C (to avoid rotameric NMR resonances), TLC, HRMS and IR confirmed the identity and analytical HPLC the purity.

Table 9: Synthesis of various racemic 1-substituted tetrahydroisoquinolines (**III**) starting from different carbamate and enol ether building blocks (**I** and **II**) using *N*-acyl Pictet-Spengler reactions. *Initial experiments for this reaction were performed within the Bachelor thesis of F. Talay.
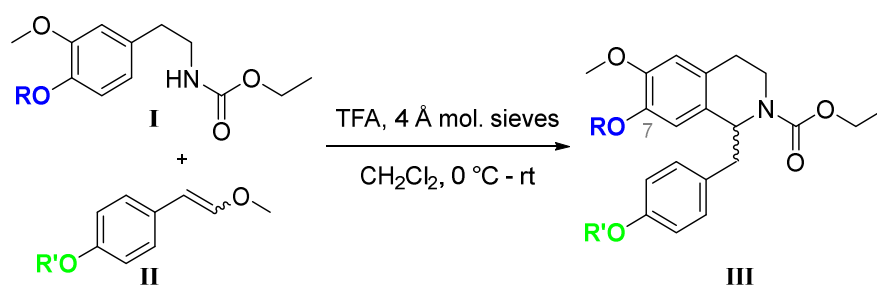
entry	carbamate I	enol ether II	reaction time	product III	yield
1	165	177	18 h	180	81%
2	169	177	20 h	SG-089 (181)	77%
3	167	177	90 h	182	90%*
4	170	179	18 h	SG-145 (183)	32%
5	169	178	20 h	184	92%

Reduction of the carbamate group of tetrahydroisoquinolines **III** (**Table 10**) using LiAlH$_4$[152] directly yielded the corresponding *N*-methyl compounds. Preparation of the corresponding secondary amines from the carbamate intermediates is feasible in general, but would need other reaction conditions, like carbamate hydrolysis using KOH and hydrazine hydrate at 120 °C for many days[164] or refluxing in aq. 10 M HCl solution overnight[165]. Though, tertiary amines were preferred, as they showed more resemblance to the structure of tetrandrine (**1**). Furthermore ethyl carbonate protecting groups were cleaved one-pot within the reduction of the carbamate using lithium alanate, resulting in a number of *N*-methyl compounds (**IV**, **Table 10**).

A procedure published by Cava et al. was applied for the synthesis of *N*-methyl amines of type **IV** (**Table 10**) by refluxing carbamates (**III**, **Table 10**) with an excess of LiAlH$_4$ under dry conditions in THF. For reaction work-up avoiding undesirable treatment with water under formation of aluminum hydroxide gels Glauber's salt was chosen, which is Na$_2$SO$_4$ x 10 H$_2$O. The crystal water of this salt causes a slow and moderate decomposition of the LiAlH$_4$ excess and prevents uncontrolled heating of the mixture. The reaction was finished when no gas evolution could be observed anymore. After filtration the product was purified by extraction using the phase swap technique in which the crude organic product phase was extracted with 2 M aq. HCl solution to transfer the protonated amine into the aqueous phase. Then, neutralization of the aqueous phase yielded the tertiary amine again and re-extraction with organic solvents resulted in the pure product. This technique avoids the more time-consuming FCC, especially for upscale reactions. By this means all synthesized carbamates (**III**) were reduced to the corresponding tertiary *N*-methyl amines (**IV**, **Table 10**) in moderate to high yields. Two natural products ((±)-*N*-methylcoclaurine (**159**) and (±)-armepavine (**185**)) were synthesized in their racemic form this way (entry 1, 2, **Table 10**), one derivative of a natural product (entry 4, **Table 10**) and two new synthetic tetrahydroisoquinolines (entry 3, 5, **Table 10**). Full characterization (TLC, NMR, HRMS, IR, m.p.) confirmed the structure and analytical HPLC the purity of the products.

Table 10: Reduction of the carbamate function and deprotection of carbonic acids of tetrahydroisoquinolines (**II**) using LiAlH₄ gave *N*-methyl amines of type **IV**. * Initial experiments for this reaction were performed within the Bachelor thesis of F. Talay.
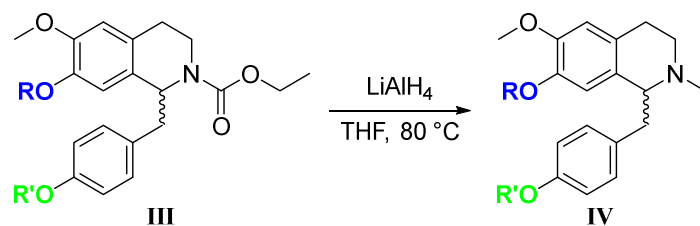
entry	starting material III	reaction time	product IV	name of natural product or derivative	yield
1	R = COOEt R' = COOEt **180**	3 h	SG-132 (**159**)	(±)-*N*-methylcoclaurine	79%
2	R = Me R' = COOEt SG-089 (**181**)	3 h	SG-121 (**185**)	(±)-armepavine	35%
3	R = Ph R' = COOEt **182**	5 h	**186**	-	79%*
4	R = Bn R' = Bn SG-145 (**183**)	18 h	SG-005 (**187**)	(±)-*O,O*-dibenzyl *N*-methylcoclaurine	46%
5	R = Me R' = Ph **184**	20 h	SG-083 (**188**)	-	46%

Synthesis of (±)-armepavine (**185**) had the lowest yield (entry 2, **Table 10**). A reason for this is, that a second tetrahydroisoquinoline (**189**) was isolated (**Scheme 30 A** and **B**). The *N*-acyl Pictet-Spengler reaction as well as the lithium alanate reduction were both performed in large scale (22.1 mmol and 16.9 mmol) and to improve time efficacy purification was reduced to a minimum. Therefore the enol ether **177** also had to be synthesized in large scale and aforementioned side products (aldehyde **175** and enol ether **174**, **Scheme 30 B**) occurred. These two side products were both able to act as starting material for the *N*-acyl Pictet-Spengler reaction to give 1-benzyl-carbamate **190** and 1-phenyl-carbamate **191** (**Scheme 30 B**). Reduction of 1-benzyl-carbamate **190** would also result in SG-121 (**185**) and was therefore not removed. Thus, 1-phenyl-carbamate **191** was carried over as an unrevealed impurity and

following reduction of a mixture of three different carbamates (**181**, **190** and **191**) yielded SG-121 (**185**) and side product SG-121-NP (**189**). The two products were separated by FCC, analyzed and purity was confirmed by analytical HPLC.
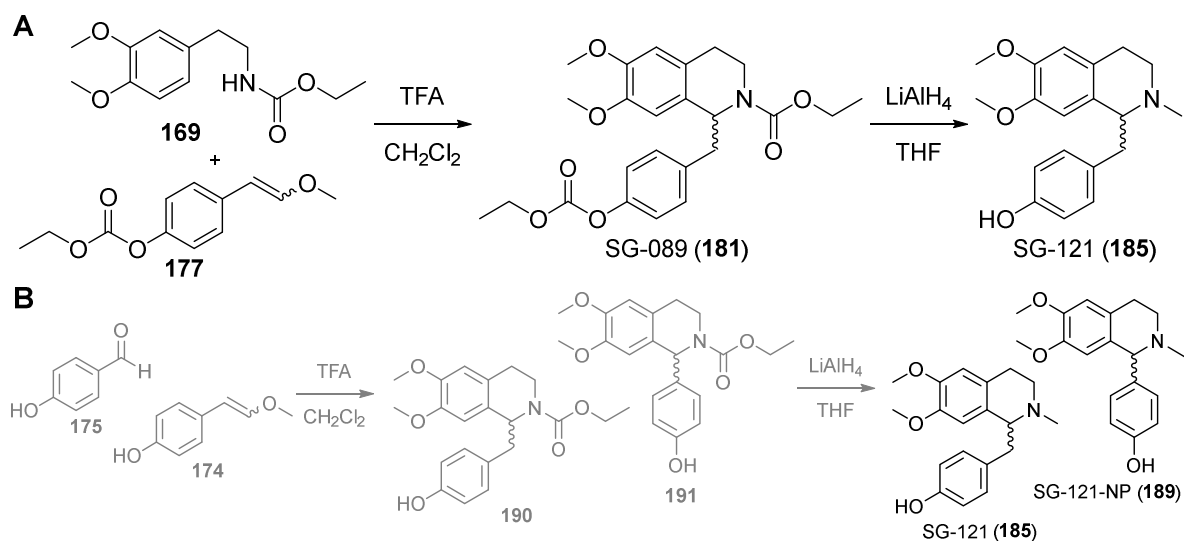
Scheme 30: Synthesis of tetrahydroisoquinolines **185** and **189**. (**A**) Synthesis of (±)-armepavine (**185**), as described above. (**B**) Side products of the Wittig olefination **174** and **175** underwent *N*-acyl Pictet-Spengler reaction to yield carbamates **190** and **191**. Following lithium alanate reduction yielded (±)-armepavine (SG-121, **185**) and side product SG-121-NP (**189**). Shaded products were not isolated within this sequence.
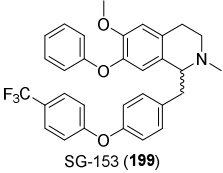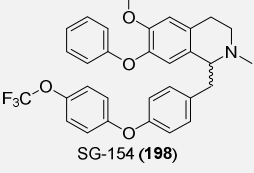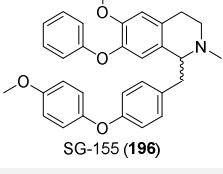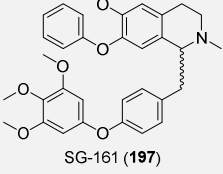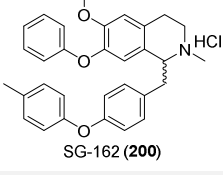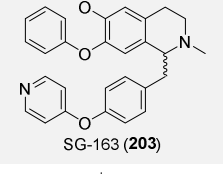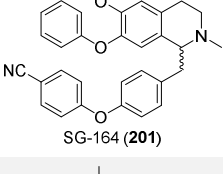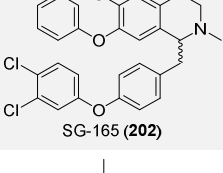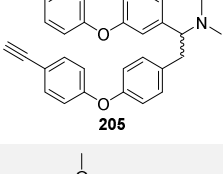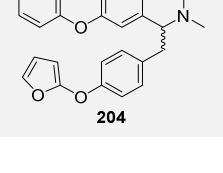
Utilizing the method developed by Chan, Evans and Lam many diaryl ethers (**V**, **Table 11**) were synthesized. Per phenolic group of the amine (**IV**, **Table 11**) 1 equivalent copper acetate, 3 equivalents arylboronic acid (**VI**, **Table 11**) and a mixture of NEt$_3$ and pyridine (1:1, 2.5 eq. each) were used. The resulting oily tertiary amines were characterized and then treated with methanolic HCl solution to give the amorphous hydrochloride salts as solids which were used for biological experiments. Two diaryl ethers were recrystallized as hydrochloride salts (entry 3, 9, **Table 11**) and were also characterized such. The diaryl ether variant of *N*-methylcoclaurine, SG-094 (**192**), was the first to be synthesized using the double amount of equivalents for the two phenolic groups of SG-132 (**159**, entry 1, **Table 11**). Two diaryl ethers with a methoxygroup in C-7 position of the tetrahydroisoquinoline (**193** and **194**, entry 2, 3, **Table 11**) and the 1-phenyl-tetrahydroisoquinoline **195** (entry 4, **Table 11**) were synthesized to study the loss of one phenyl group. Tetrandrine (**1**) has four methoxy moieties, which inspired the synthesis of compounds bearing methoxy residues (**196** and **197**, entry 7, 8, **Table 11**) or replaced them by the metabolically stable bioisosteric trifluoromethoxy group (**198**, entry 6, **Table 11**). Electron releasing groups were also introduced (**199** and **200**, entry 5, 9, **Table 11**). A nitrile residue was also part of the structure of the TPC2 activator TPC2-A1-N (**16**). Hence a nitrile residue was introduced to probably have a better affinity to the ion channel (**201**, entry 11, **Table 11**). A 3,4-dichloro substituted aromatic ring was synthesized to study

the influence of halides (**202**, entry 12, **Table 11**). To analyze the influence of heterocyclic aromatic residues, a pyridine moiety was introduced (**203**, entry 10, **Table 11**), whereas the synthesis of a variant bearing a furan moiety (**204**) was not successful (entry 14, **Table 11**), which is in accordance with one report in literature[166]. Same applied to the tetrahydroisoquinoline **205**, which should have been synthesized to be labeled by click chemistry (entry 13, **Table 11**). Overall 12 tetrahydroisoquinolines bearing a diaryl ether motif were synthesized in moderate to high yield and fully characterized by TLC, NMR, HRMS and IR (melting points only for the hydrochloric acid salts) and purity was affirmed by analytical HPLC.

Table 11: Products of the Chan-Evans-Lam reaction. Using different arylboronic acids (**VI**) and a variety of racemic amines of type **IV** yielded the desired diaryl ethers of type **V**.
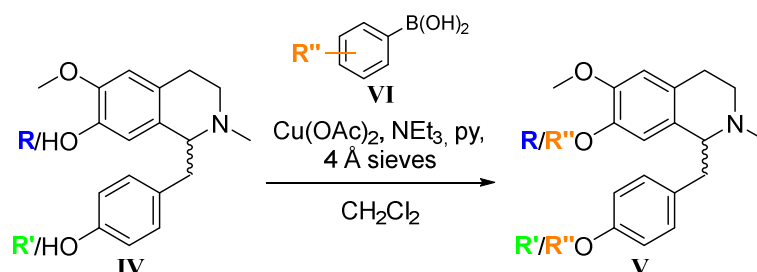
entry	starting material IV	boronic acid VI	reaction time	product V	yield
1	R,R' = H SG-132 (**159**)	R'' = H	18 h	SG-094 (**192**)	70%
2	R = Me R' = H SG-121 (**185**)	R'' = 4-OCH$_3$	18 h	SG-122 (**193**)	88%
3	R = Me R' = H SG-121 (**185**)	R'' = 3,4,5-(OCH$_3$)$_3$	18 h	SG-127 (**194**)	84%
4	R = Me R' = H SG-121-NP (**189**)	R'' = 4-OCH$_3$	18 h	SG-157 (**195**)	95%

5	R = Ph R' = H **186**	R'' = 4-CF$_3$	18 h	 SG-153 (**199**)	24%
6	R = Ph R' = H **186**	R'' = 4-OCF$_3$	13 h	 SG-154 (**198**)	47%
7	R = Ph R' = H **186**	R'' = 4-OCH$_3$	20 h	 SG-155 (**196**)	67%
8	R = Ph R' = H **186**	R'' = 3,4,5- (OCH$_3$)$_3$	20 h	 SG-161 (**197**)	69%
9	R = Ph R' = H **186**	R'' = 4-CH$_3$	20 h	 SG-162 (**200**)	48%
10	R = Ph R' = H **186**	pyridine-4-boronic acid	20 h	 SG-163 (**203**)	25%
11	R = Ph R' = H **186**	R'' = 4-CN	20 h	 SG-164 (**201**)	48%
12	R = Ph R' = H **186**	R'' = 3,4-Cl$_2$	20 h	 SG-165 (**202**)	78%
13	R = Ph R' = H **186**	R'' = 4-C≡C	20 h	 **205**	-
14	R = Ph R' = H **186**	furan-2-ylboronic acid	20 h	 **204**	-

68

The compound collection provided by Prof. Dr. Meinhart Zenk[†] included racemic *O,O*-dibenzylated coclaurine (Z3, **137**, **Scheme 31 A**) and racemic *O,O*-dibenzylated nororientaline (Z6, **145**, **Scheme 31 B**). Utilizing these secondary amines, *N*-methyl amines were obtained by Eschweiler-Clarke reaction[167]. Iminium formation with formaldehyde, followed by reduction with a hydride source yielded tertiary amines. Originally formic acid acted as hydride source, while modified versions used sodium cyanoborohydride. Using the latter yielded SG-005 (**187**) and SG-159 (**206**) in moderate yields, although long reaction times did not lead to complete consumption of the starting material (**Scheme 31 A** and **B**).
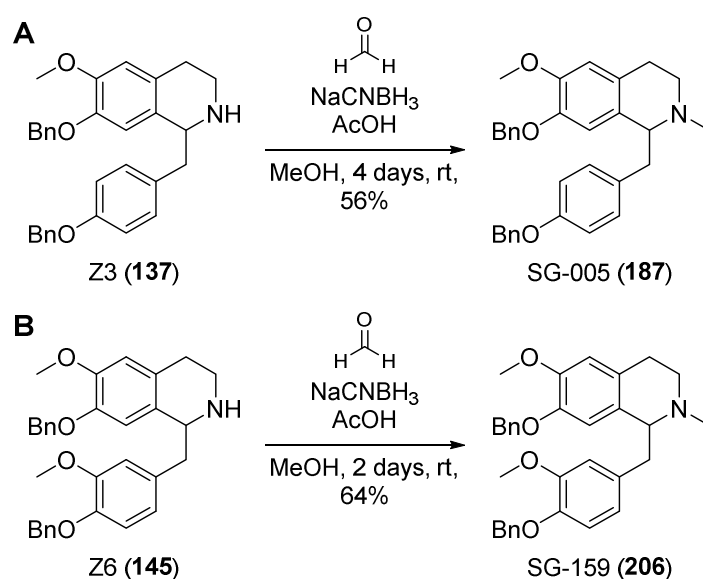
Scheme 31: Eschweiler-Clarke reaction for the synthesis of the *N*-methyl compounds SG-005 (**187**, A) and SG-159 (**206**, B).

Another method for the synthesis of SG-005 (**187**) was the Mitsunobu reaction with SG-132 (**159**) as starting material (**Scheme 32**). Mitsunobu conditions prevented the formation of a quaternary ammonium salt **207**, which was the result of using standard protecting conditions (excess of benzyl chloride and a base) for the phenolic groups (**Scheme 32**). Monitoring *via* TLC indicated the formation of SG-005 (**187**), though after 18 h only the quaternary ammonium salt **207** was found. Mitsunobu reaction, however, gave SG-005 (**187**) in moderate yield and analytical data were in accordance with the analytical data of the two other routes.
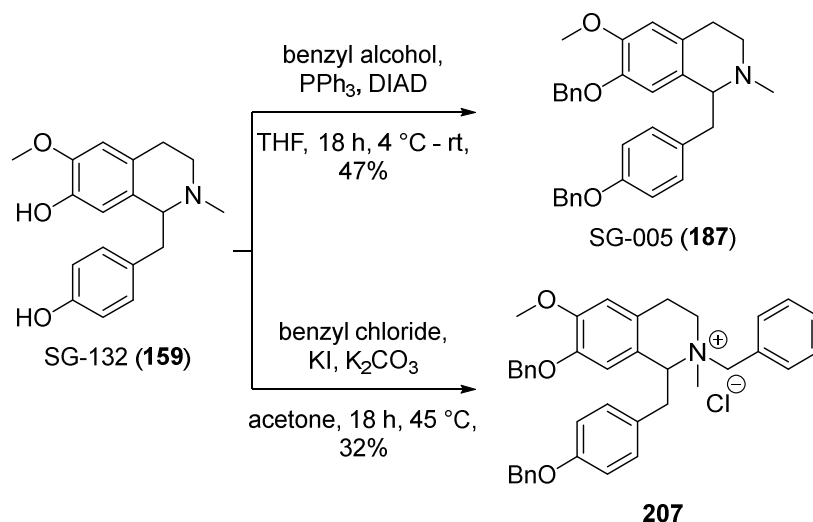
Scheme 32: Mitsunobu reaction of SG-132 (**159**) with benzyl alcohol yielded SG-005 (**187**). Protection of SG-132 (**159**) using benzyl chloride gave quaternary amine **207**.

Synthesis of an *N*-ethyl variant of bis(benzyloxy)-orientaline **208** was performed using bromoethane in alkaline conditions. Potassium iodide was added for an *in situ* Finkelstein reaction to boost the conversion rate. TLC monitoring did not show consumption of the starting material, because product and starting material had the same R_f value. ASAP showed the masses of starting material and product and after 6 days no changes of the conversion rate were observed any more. Purification needed semi-preparative HPLC, because standard FCC did not separate secondary amine **145** from *N*-ethyl amine **208**. This resulted in pure SG-158 (**208**, **Scheme 33**) in moderate yield. A Leuckart-Wallach reaction[168] could be tried to improve the conversion rate. This reaction is related to the Eschweiler-Clarke reaction but is not limited to formaldehyde. Though, the first reaction yielded enough SG-158 (**208**) and repetition was not necessary.
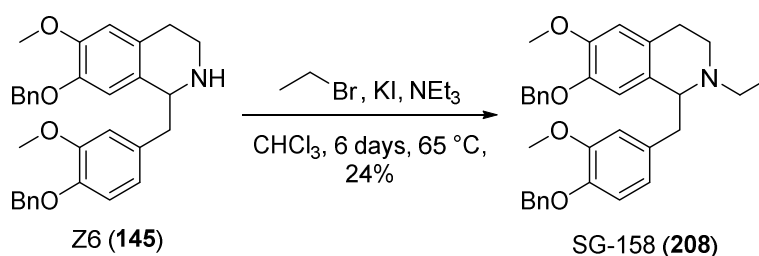
Scheme 33: Synthesis of SG-158 (**208**) with Z6 (**145**) as starting material.

A total amount of 16 *N*-alkyl amines was synthesized, including 3 *O*-benzylated compounds and 13 diaryl ethers. Analysis (TLC, NMR, HRMS, IR and melting points) confirmed the structure and analytical HPLC affirmed the purity of these molecules. All of them resemble one

half of tetrandrine (**1**) plus the two benzenoid rings of the second benzylisoquinoline moiety and were further investigated on their biological activity. The synthetic route furthermore generated intermediates that therefore served as negative controls, as SG-132 (**159**) and SG-145 (**183**).

3.6 Pharmacological investigation of TPC2 antagonists

The effect of the inhibitors of TPC2 was again analyzed by Fura-2 and Fluo-4 based calcium imaging as well as by endo-lysosomal patch clamp experiments. Furthermore, their ability to combat diseases like cancer or virus infections[1] was investigated. Main focus was on tetrandrine (**1**), SG-005 (**187**) and SG-094 (**192**), because these emerged as the most interesting substances. All studies were performed in close cooperation with Prof. Dr. Michael Schaefer's group (Fluo-4 based experiments, performed by Nicole Urban), Prof. Dr. Angelika Vollmar's group (cancer investigation, performed by Martin Müller) and Prof. Dr. Dr. Christian Grimm's as well as Prof. Dr. Martin Biel's groups (Fura-2 based calcium imaging, performed by myself and patch clamp experiments, performed by Dr. Yu-Kai Chao).

3.6.1   First identification of the truncated TPC2 inhibitors

The whole endo-lysosomal patch clamp technique is state-of-the-art to confirm direct effects on the activity of endo-lysosomal ion channels[169]. In brief, endolysosomes are enlarged using vacuolin-1, the membrane is destroyed with a glass pipette and then the enlarged endo-lysosomal organelle is carefully isolated. Having the isolated organelle allows the operator to apply hydrophilic, not membrane permeable compounds like PI(3,5)P$_2$ (**4**) directly to the endolysosome to activate the ion channel. The addition of a potential inhibitor after activation then directly shows the effect of the compound. This unique technique is very accurate but highly complex and requires much time and effort.

Tetrandrine (**1**) has been known to inhibit TPC2 since 2015[2] and was therefore analyzed as a reference. Thus, by applying the endo-lysosomal patch clamp technique, several other bisbenzylisoquinoline alkaloids were also identified as TPC2 inhibitors. Fangchinoline (**9**), cepharanthine (**140**) and the *seco*-analog dauricine (**11**) were virtually equipotent to tetrandrine (**1**, 54% inhibition, **Figure 22 A**). Fangchinoline (**9**) is a nor-derivative of tetrandrine (**1**) and is already known to be a TPC2 inhibitor (**Figure 22 D**)[30]. Cepharanthine (**140**) differs from tetrandrine (**1**) in the absolute stereochemistry and the connection of both benzyl residues and dauricine (**11**) is no macrocyclic compound (**Figure 22 D**). This gave a first hint that

---

[1] Studies for virus infections are still in the early stages and not further discussed.

stereochemistry, the substitutions pattern of lead structure tetrandrine (**1**) and the fact that tetrandrine (**1**) is a macrocyclic ring is not mandatory for TPC2 inhibition. Racemic coclaurine (Z1, **141**) had nearly no effect, whereas racemic *O,O*-bisbenzylcoclaurine (Z3, **137**) was equipotent to tetrandrine (**1**, **Figure 22 A** and **E**). Contrary, Z6 (**145**) showed an (on top)-activating effect (**Figure 22 A** and **E**). Notably, the bis-phenyl ether SG-094 (**192**) significantly increased the percentage of channel inhibition (75%) compared to tetrandrine (**1**, 54%), whereas the corresponding bis-benzyl ether SG-005 (**187**) showed nearly the same inhibition (44%) as tetrandrine (**1**, **Figure 22 B** and **Figure 23 H**). Both compounds are derived from the racemic alkaloid coclaurine (**159**).
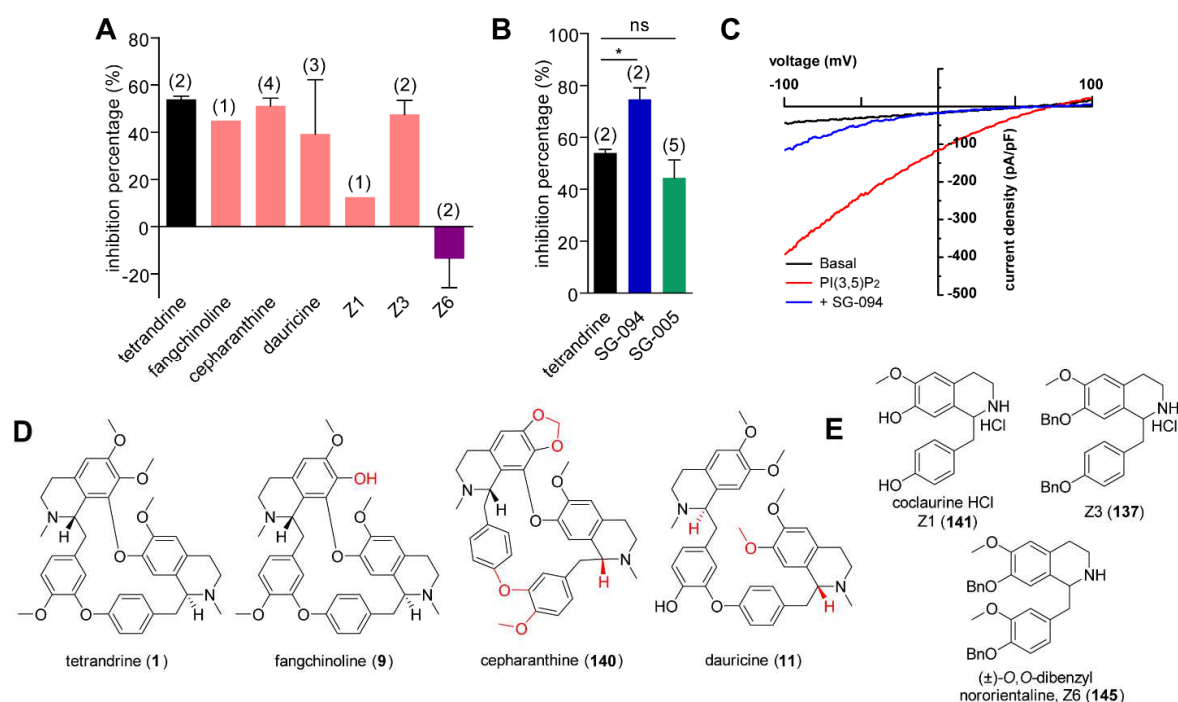
Figure 22: Patch clamp results to identify TPC2 inhibitors, performed by Dr. Yu-Kai Chao. (**A-B**) The inhibition percentage of several TPC2 blockers is displayed. Inhibitors (10 µM) were applied upon activation with PI(3,5)P$_2$ (**4**, 1 µM) on isolated and vacuolin-enlarged endolysosomes from HEK293 cells expressing TPC2-EGFP. The bar graph indicates mean ± SEM of n independent experiments. *p < 0.05, ns = not significant, using unpaired students t-test. (**C**) Representative current density – voltage relation for a recording of the most potent TPC2 inhibitor of this set of compounds, SG-094 (**192**), is shown. (**D**) Structures of tetrandrine (**1**), fangchinoline (**9**), cepharanthine (**140**) and dauricine (**11**). Differences to tetrandrine (**1**) are marked in red. (**E**) Structures of Z1 (**141**), Z3 (**137**) and Z6 (**145**).

The two lipophilic, membrane-permeable TPC2 activators TPC2-A1-N (**16**) and TPC2-A1-P (**17**), developed in the first part of this project, allowed to also test inhibitory activities of the compounds in calcium imaging experiments. Fura-2 based single cell calcium imaging experiments were performed first. The best option to assess inhibitory effects is to first add the inhibitor to the cells and incubate for a defined time, then stimulate the cells with the activator and monitor effects over time in the constant presence of the inhibitor. As control, a subsequent experiment needs to be performed in which vehicle, e.g. DMSO only is added first, followed by

addition of the agonist. The results of these two experiments are then directly compared. If activation levels do not show differences, the substance has no inhibitory activity. At least three independent experiments should be performed for quantification and statistical analysis. Of note, results strongly depend on the transfection levels and these may vary. For more consistent experiments HEK-293 cells stably expressing the plasma membrane variant of hTPC2 were therefore used.

This method was applied for tetrandrine (**1**), two of the synthesized truncated variants, SG-005 (**187**) and SG-094 (**192**), and the controls SG-132 (**159**) and SG-145 (**183**). As expected, tetrandrine (**1**), SG-005 (**187**) and SG-094 (**192**) were able to inhibit TPC2-A1-N (**16**) induced activation significantly (**Figure 23 A-D**). SG-132 (**159**) is lacking the prolonging aromatic groups (benzyl or diaryl ethers) while SG-145 (**183**) has two benzyl ethers but the tetrahydroisoquinoline nitrogen is not basic. Both substances were not able to inhibit TPC2-A1-N (**16**) induced activation (**Figure 23 E-G**) and confirmed that the absent groups were essential for the inhibitory effect on TPC2.
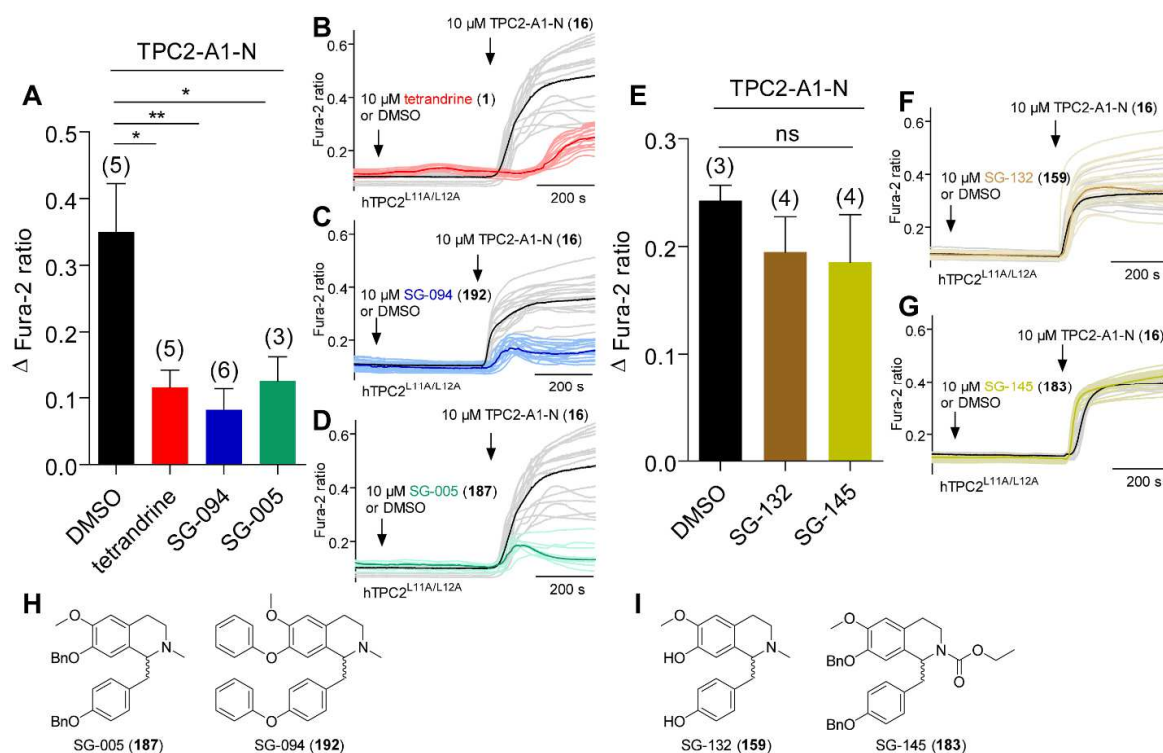
Figure 23: Reversed single cell calcium imaging experiments to identify TPC2 inhibitors. (**A**) Fura-2 based Ca^{2+} imaging results showing the effect of TPC2-A1-N (**16**, 10 µM) after stimulation with tetrandrine (**1**, 10 µM), SG-094 (**192**, 10 µM), SG-005 (**187**, 10 µM) or a DMSO control. HEK293 cells stably expressing hTPC2$^{L11A/L12A}$-RFP were used. Mean values normalized to basal (400 s after activation) ± SEM of at least three independent experiments with 3–10 cells each are shown. (**B-D**) Representative Ca^{2+} signals for experiments as in (**A**). Cells were sequentially stimulated with tetrandrine (**1**, 10 µM, B), SG-094 (**192**, 10 µM, C), SG-005 (**187**, 10 µM, D) or DMSO (0.5% DMSO in HBS) and the activator TPC2-A1-N (**16**, 10 µM, 400 s). (**E**) Experiments as in (**A**) using SG-132 (**159**, 10 µM), SG-145 (**183**, 10 µM) or a DMSO control. (**F-G**) Representative Ca^{2+} signals for experiments as in (**E**). Cells were sequentially stimulated with SG-132 (**159**, 10 µM, C), SG-145 (**183**, 10 µM, D) or DMSO (0.5% DMSO in HBS) and the activator TPC2-A1-N (**16**, 10 µM, 400 s). **$p < 0.01$, *$p < 0.05$, ns = not significant, using one-way ANOVA followed by Tukey's post hoc test. In all experiments highlighted

lines represent the mean response from a population of cells. Shaded traces represent responses of single cells. All experiments were performed on a Leica DMi8 live cell microscope. (**H**) Structures of SG-005 (**187**) and SG-094 (**192**). (**I**) Structures of SG-132 (**159**) and SG-145 (**183**).

This set of experiments proved the accuracy of the method and the previously obtained electrophysiology results. Of the three inhibitors again SG-094 (**192**) had the strongest effect (**) compared to tetrandrine (**1**, *) and SG-005 (**187**, *) when applied at a concentration of 10 µM (**Figure 23 A-D**). In a next step the potencies of the compounds were determined by concentration-effect relationship measurements using the HTS system instead of using only single concentrations.

3.6.2 Analysis of the compound library

All compounds were analyzed by using the Fluo-4 based calcium imaging method (HTS system) described before. The experiments were again performed in the group of Prof. Dr. Michael Schaefer (Leipzig) by sequential application of inhibitors at different concentrations followed by the agonists TPC2-A1-P (**17**) and TPC2-A1-N (**16**).
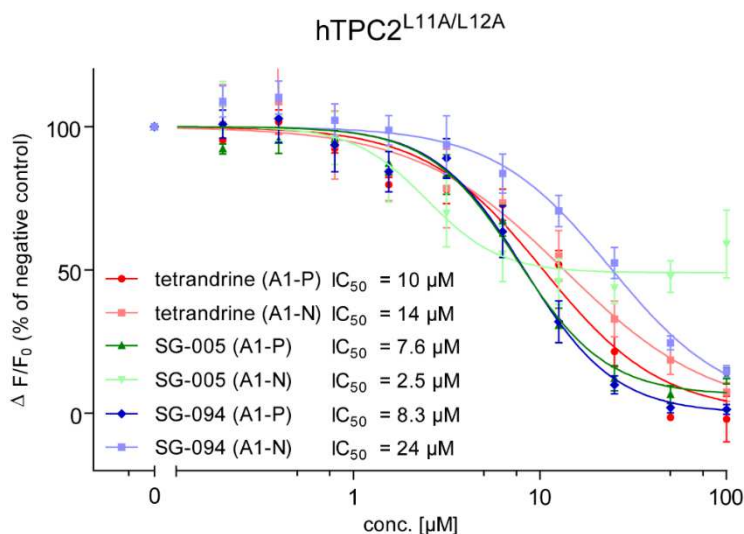
Figure 24: Fluo-4 calcium imaging experiments of the highlighted compounds tetrandrine (**1**), SG-005 (**187**) and SG-094 (**192**). Concentration-effect relationships using HEK293 cells stably expressing hTPC2$^{L11A/L12A}$-RFP are presented. Cells were sequentially stimulated with inhibitor (100 µM → 0.1 µM) and TPC2-A1-N (**16**, 10 µM) or TPC2-A1-P (**17**, 10 µM) as activator. IC$_{50}$ values were calculated out of at least three independent experiments using GraphPad. All experiments were performed by Nicole Urban.

Both activators were used at a concentration of 10 µM. All three inhibitors were found to have IC$_{50}$ values in the range of 2.5 µM – 24 µM (**Figure 24 A**). Significant differences in potencies were not detectable. Surprisingly, SG-005 (**187**) showed a reduced maximum efficacy (only

50%) after activation with TPC2-A1-N (**16**), while tetrandrine (**1**) and SG-094 (**192**) approximated a complete inhibition (nearly 100%, **Figure 24 A**). All three inhibitors had nearly 100% blocking efficacy after activation with TPC2-A1-P (**17**).
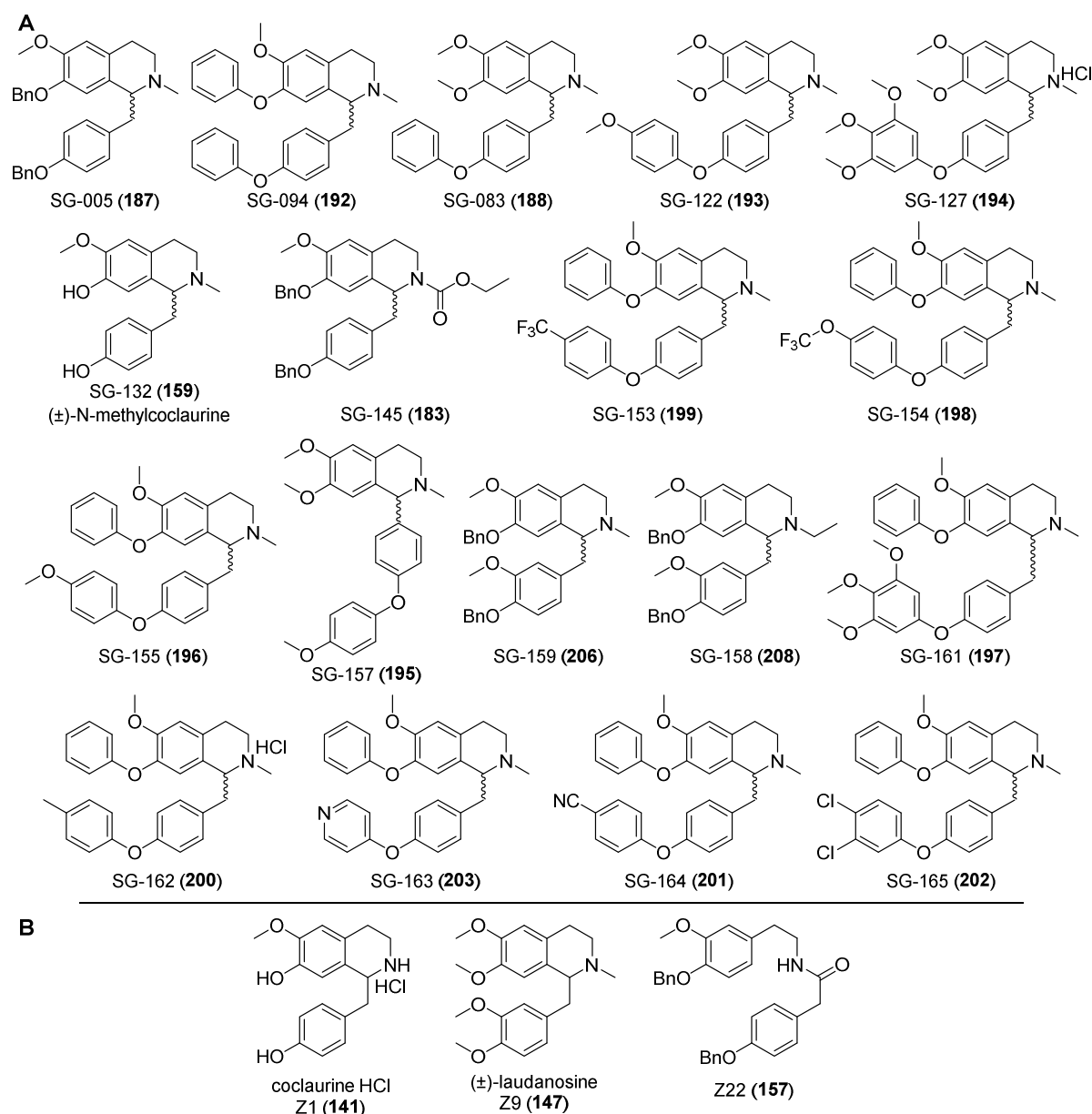
Figure 25: Structures of the truncated tetrandrine analogs, analyzed in SAR. (**A**) Structures of the 1-benzyl-tetrahydroisoquinolines synthesized within this project. (**B**) Structures of the 1-benzyl-tetrahydro-isoquinolines, provided by Prof. Dr. Meinhart Zenk†.

IC_{50} values were obtained for the other compounds as well (**Table 12**). For some Z compounds, unspecific effects were observed at concentrations above 50 µM and concentration-effect relationships were not applicable. Tetrandrine (**1**), fangchinoline (**9**), berbamine (**10**), cepharanthine (**140**), oxyacanthine (**138**) and dauricine (**11**) all showed IC_{50} values in the same range for both activators (entry 1, 4-8, **Table 12**, all depicted in **Figure 19**). These results

confirmed that the substitution pattern of the benzyl residue and the stereochemistry were not determined. SG-005 (**187**), SG-094 (**192**), SG-158 (**208**) and SG-159 (**206**) showed IC_{50} value in the same range for activation with TPC2-A1-P (**17**) while only SG-094 (**192**) had a slightly higher IC_{50} for activation with TPC2-A1-N (**16**, entry 2-3, 17-18, **Table 12**, structures in **Figure 25**). Both compounds selected as controls did either show high IC_{50} values or fitting was not applicable at all (entry 12-13, **Table 12**, structures in **Figure 25**). All analogs of SG-094 (**192**) blocked TPC2 activation with both activators to some extent, while some had differences in potencies (entry 9-11, 14-24, **Table 12**, structures in **Figure 25**). The substances bearing a *para*-methoxy, *para*-methyl or their fluorinated variants (SG-153 (**199**), SG-154 (**198**), SG-155 (**196**), SG-162 (**200**)) showed a lower IC_{50} value after activation with TPC2-A1-P (**17**) compared to activation with TPC2-A1-N (**16**) (entry 14-16, 21, **Table 12**, structures in **Figure 25**). None of the further analogs showed significantly stronger effects on TPC2. The three Z substances that did not show unspecific effects, Z1 (**141**), Z9 (**147**) and Z22 (**157**) were not able to inhibit TPC2 as well, which was verified by high (>50 µM) or not applicable IC_{50} values (entry 25-27, **Table 12**, structures in **Figure 25**). All other compounds, mainly of the Z series, had a slight inhibitory effect on the channel (at 12.5 µM). These compounds were not of further interest because of their already mentioned nonspecific effects on stably transfected HEK293 cells.

Table 12: Screening results of the compound library using Fluo-4 based calcium imaging and toxicity screening using MTT assay. Concentration-effect relationships were generated using HEK293 cells stably expressing hTPC2$^{L11A/L12A}$-RFP and were plotted using GraphPad. Experiments were performed as described in **Figure 24** in duplicates of one replicate for each activator. Calcium imaging experiments were performed by Nicole Urban and MTT assay by Martina Stadler. **was activated with 30 µM TPC2-A1-P (**17**).

entry	compound	IC_{50} (Fluo-4; TPC2-A1-P (17))	IC_{50} (Fluo-4; TPC2-A1-N (16))	IC_{50} (MTT)
1	tetrandrine (**1**)	10 µM	14 µM	43 µM
2	SG-005 (**187**)	7.6 µM	2.5 µM	11 µM
3	SG-094 (**192**)	8.3 µM	24 µM	23 µM
4	fangchinoline (**9**)	11 µM	7.0 µM	38 µM
5	berbamine HCl (**10**)	10 µM	7.0 µM	21 µM
6	cepharanthine (**140**)	8.1 µM	5.1 µM	25 µM
7	oxyacanthine sulfate (**138**)	21 µM	4.5 µM	>50 µM
8	dauricine (**11**)	12 µM	8.6 µM	>50 µM
9	SG-083 (**188**)	11 µM	14 µM	8.2 µM
10	SG-122 (**193**)	14 µM	7.3 µM	22 µM
11	SG-127 (**194**)	n.a.	25 µM	18 µM
12	SG-132 (**159**)	>50 µM**	45 µM	>50 µM
13	SG-145 (**183**)	43 µM	n.a.	>50 µM
14	SG-153 (**199**)	22 µM	>50 µM	15 µM
15	SG-154 (**198**)	12 µM	>50 µM	9.5 µM
16	SG-155 (**196**)	15 µM	37 µM	14 µM
17	SG-157 (**195**)	34 µM	30 µM	29 µM
18	SG-158 (**208**)	9.6 µM	0.33 µM	12 µM

19	SG-159 (**206**)	9.9 µM	0.75 µM	14 µM
20	SG-161 (**197**)	10 µM	24 µM	15 µM
21	SG-162 (**200**)	19 µM	>50 µM	16 µM
22	SG-163 (**203**)	18 µM	21 µM	9.5 µM
23	SG-164 (**201**)	15 µM	43 µM	21 µM
24	SG-165 (**202**)	33 µM	>50 µM	19 µM
25	Z1 (**141**)	>50 µM	>50 µM	>50 µM
26	Z9 (**147**)	>50 µM	>50 µM	>50 µM
27	Z22 (**157**)	n.a.	>50 µM	29 µM

For acute toxicity, MTT assays were again performed by Martina Stadler. For these experiments HL-60 cells were used, which are human leukemia cells. All compounds showed acute toxicity to HL-60 cells. That was to be expected because of the strong correlation between cancer and TPC2[36]. The compounds that were not able to block TPC2 also showed no (entry 12-13, 25-26, **Table 12**) or slight (entry 27, **Table 12**) toxicity on HL-60 cells. Interestingly, the TPC2 inhibitors oxyacanthine (**138**) and dauricine (**11**) were not cytotoxic as well (entry 7-8, **Table 12**).

In house agar diffusion test (Martina Stadler) was used to exclude some side-effects on bacteria (*Escherichia coli*, *Pseudomonas marginalis*, *Staphylococcus equorum*, *Streptococcus entericus*), yeasts (*Yarrowia lipolytica*, *Saccharomyces cerevisiae*) and dermatophytes (*Hyphopichia burtonii*). All compounds of the SG-series (**Figure 25**) did not show an inhibition zone.

A variety of TPC2 inhibitors were identified within this screening. SG-005 (**187**) and SG-094 (**192**) emerged to be the most promising TPC2 inhibitors with low IC$_{50}$ values and high efficacies. Decorations on the aromatic ring impaired the ability to block TPC2. The diaryl or benzyl ethers were necessary for the inhibitory effect as well as a basic nitrogen atom. Tertiary amines were preferred because secondary amines caused unspecific effects in calcium imaging experiments. These results further demonstrated that whole endoysosomal patch clamp experiments are still state-of-the-art for ultimate analysis while calcium imaging experiments can be used for fast ligand identification.

3.6.3 TPC2 and cancer

The influence of TPC2 functions on cancer hallmarks is of high interest[34] which made TPC2 an interesting target for the development of novel anticancer therapeutics. Hence a close cooperation with Martin Müller (group of Prof. Dr. Angelika Vollmar, LMU) was initiated to use small-molecule inhibitors of TPC2 to further study the role of TPC2 in cancer. All experiments discussed in this chapter were performed by Martin Müller and are to be published in a corporate publication.

Thus, after the identification of the novel TPC2 inhibitors, their potential to inhibit cancer cell growth was investigated. More negative controls (SG-089 (**181**), SG-121 (**185**), SG-121-NP (**189**)) and substances of the Z series were also screened for their antiproliferative properties using RIL175 cells in a CTB assay. Numerous molecules with an increased potency in comparison to tetrandrine (**1**, IC_{50}: 9.1 µM, entry 1, **Table 13**) were identified, including truncated variants with IC_{50} values in the low micromolar range. Monomeric benzyltetrahydroisoquinolines bearing additional aromatic residues (phenyl or benzyl ethers) at both benzenoid rings were found to have outstanding properties. When modifying the amino group, antiproliferative activity remained in a similar range. *N*-Alkyl residues of different lengths with a basic nitrogen were equipotent (*N*H (Z3 (**137**)); *N*-methyl (SG-005 (**187**), SG-159 (**206**)); *N*-ethyl (SG-158 (**208**)), IC_{50}: 2.4-4.8 µM, entry 2, 17-18, 28, **Table 13**). *N*-Acyl variants lost their antiproliferative properties as well as their basicity (SG-089 (**181**), SG-145 (**183**), IC_{50}: ≥ 33 µM, entry 12, 25, **Table 13**). Variations at C-6 and C-7 of the isoquinoline unit had a slight effect. In most cases, the loss of the aromatic substituents (aryl- or benzyl ether) in C-7 position slightly decreased antiproliferative activity (SG-083 (**188**), SG-127 (**194**), SG-157 (**195**), IC_{50}: 7.6-11 µM, entry 8, 10, 16, **Table 13**). The same was observed if the 1-benzyl group was replaced by a phenyl group (SG-122 (**193**) vs. SG-157 (**195**), entry 9, 16, **Table 13**), whereas shifting a benzyloxy residue from position C-7 to C-6 had no influence (Z3 (**137**) vs. Z5 (**144**), entry 28-29, **Table 13**). Furthermore, the impact of modifications of the 1-benzyl residue was investigated. Substitution patterns, mostly differing in *meta*- or *para*-position, did not markedly affect antiproliferative activity (SG-005 (**187**), SG-159 (**206**), Z6 (**145**), Z11 (**141**), Z13 (**150**), Z15 (**152**), Z18 (**154**), Z20 (**155**), IC_{50}: 1.2-4.8 µM, entry 2, 18, 30-36, **Table 13**). Miscellaneous diaryl ethers at the 1-benzyl residue were synthesized bearing both electron-donating and -releasing substituents, mainly in *meta*- or *para*-position (SG-153 (**199**), SG-154 (**198**), SG-155 (**196**), SG-161 (**197**), SG-162 (**200**), SG-164 (**201**), SG-165 (**202**)). In most cases, no changes in antiproliferative potencies were observed (IC_{50}: 3.9-5.6 µM, entry 13-15, 19-23, **Table 13**). However, cyano and chlorine substituents slightly (SG-164 (**201**), SG-165 (**202**), IC_{50}: 8.5-9.1 µM, entry 22-23, **Table 13**) and the pyridine moiety strongly reduced the antiproliferative activity (SG-163 (**203**), IC_{50}: 22 µM, entry 21, **Table 13**). The loss of both, benzyl or diaryl ether moieties resulted in significant reduction (SG-132 (**159**), IC_{50}: 11 µM,

entry 11, **Table 13**) or complete loss of activity (SG-089 (**181**), SG-121 (**185**), SG-121-NP (**189**), IC_{50}: > 50 µM, entry 25-27, **Table 13**).

Table 13: Screening of the benzyltetrahydroisoquinoline compound library by cell proliferation assays. Antiproliferative effects of the respective compounds against RIL175 WT cells were assessed by CellTiter-Blue® cell viability assays. Cells were treated for 72 h with the indicated concentrations. IC_{50} values were calculated by nonlinear regression. Experiments were performed by Martin Müller.

entry	compound	IC_{50} (RIL157)	entry	compound	IC_{50} (RIL157)
1	tetrandrine (**1**)	9.1 µM	25	SG-089 (**181**)	>50 µM
2	SG-005 (**187**)	2.4 µM	26	SG-121 (**185**)	>50 µM
3	SG-094 (**192**)	3.7 µM	27	SG-121-NP (**189**)	>50 µM
4	berbamine HCl (**10**)	7.7 µM	28	Z3 (**137**)	2.9 µM
5	cepharanthine (**140**)	6.8 µM	29	Z5 (**144**)	2.7 µM
6	oxyacanthine sulfate (**138**)	11 µM	30	Z6 (**145**)	2.9 µM
7	dauricine (**11**)	9.3 µM	31	Z11 (**148**)	1.2 µM
8	SG-083 (**188**)	7.6 µM	32	Z13 (**150**)	3.5 µM
9	SG-122 (**193**)	4.5 µM	33	Z15 (**152**)	2.7 µM
10	SG-127 (**194**)	8.0 µM	34	Z16 (**153**)	2.6 µM
11	SG-132 (**159**)	11 µM	35	Z18 (**154**)	4.1 µM
12	SG-145 (**183**)	33 µM	36	Z20 (**155**)	4.2 µM
13	SG-153 (**199**)	4.9 µM			
14	SG-154 (**198**)	3.9 µM			
15	SG-155 (**196**)	4.4 µM			
16	SG-157 (**195**)	11 µM			
17	SG-158 (**208**)	4.8 µM			
18	SG-159 (**206**)	4.2 µM			
19	SG-161 (**197**)	4.5 µM			
20	SG-162 (**200**)	5.6 µM			
21	SG-163 (**203**)	32 µM			
22	SG-164 (**201**)	9.1 µM			
23	SG-165 (**202**)	8.5 µM			
24	Z22 (**157**)	18 µM			

All benzyltetrahydroisoquinolines, which carry two aryl or benzyl ether groups and a basic amine, inhibited proliferation of RIL175 cells to a similar extent or stronger than tetrandrine (**1**). The two simplest benzyltetrahydroisoquinolines of this type, SG-005 (**187**) and SG-094 (**192**), were subjected to further investigations. SG-005 (**187**, IC_{50}: 2.4 µM) and SG-094 (**192**, IC_{50}: 3.7 µM) both displayed markedly enhanced antiproliferative effects, compared to tetrandrine (**1**). SG-005 (**187**) and SG-094 (**192**) had similar or increased antiproliferative potencies against various other cancer cell lines, including human hepatocellular carcinoma (HepG2), human colorectal adenocarcinoma (HCT-15) and human vincristine-resistant acute lymphoblastic leukemia (VCR-R CEM) (entry 1-9, **Table 14**). While comparing IC_{50} values of the cell proliferation assay and Fluo-4 based calcium imaging, it was striking that not all compounds that block proliferation were TPC2 inhibitors (SG-132 (**159**), entry 12, **Table 12**, entry 11, **Table 13**) and not all TPC2 inhibitors blocked proliferation (SG-163 (**203**), entry 22,

Table 12, entry 21, **Table 13**). This indicated that these compounds have side effects on further targets in cancer cells.

Table 14: Antiproliferative effects of tetrandrine (**1**), SG-005 (**187**) and SG-094 (**192**) on different cancer cell lines. Antiproliferative effects of the respective compounds on HCT-15, HepG2 and VCR-R CEM cells were assessed by CellTiter-Blue® cell viability assays. HCT-15 and HepG2 cells were treated for 72 h, VCR-R CEM cells were treated for 48 h. IC$_{50}$ values were calculated by nonlinear regression. Experiments were performed by Martin Müller.

entry	compound	cell line	IC$_{50}$ (Ril-175)
1	tetrandrine (**1**)	HCT-15	9.7 µM
2	tetrandrine (**1**)	HepG2	9.4 µM
3	tetrandrine (**1**)	VCR-R CEM	15 µM
4	SG-005 (**187**)	HCT-15	7.8 µM
5	SG-005 (**187**)	HepG2	7.8 µM
6	SG-005 (**187**)	VCR-R CEM	5.5 µM
7	SG-094 (**192**)	HCT-15	7.6 µM
8	SG-094 (**192**)	HepG2	9.9 µM
9	SG-094 (**192**)	VCR-R CEM	10 µM

Cellular uptake, toxicity and the effects on angiogenesis and glucose metabolism of SG-005 (**187**) and SG-094 (**192**) were investigated, all in comparison to tetrandrine (**1**). SG-132 (**159**) and SG-145 (**183**) both identified as non-TPC2 blockers by Ca^{2+} imaging experiments were used as controls. The vascular endothelial growth factor (VEGF) has been demonstrated to be a major contributor to angiogenesis. The role of TPC2-mediated Ca^{2+} release in neoangiogenesis was already described in literature[35, 52] and VEGF inhibitors were used to treat cancer[38]. Western blot analysis revealed that SG-005 (**187**) and SG-094 (**192**) were capable of significantly reducing VEGF-induced phosphorylation levels, while tetrandrine (**1**) had no effect under the chosen treatment conditions. As expected, the analysis of the selected controls, SG-132 (**159**) and SG-145 (**183**), showed no reduced phosphorylation of the investigated VEGFR2 downstream targets.

As the inhibitory effect on TPC2 was similar for tetrandrine (**1**) and SG-005 (**187**), the question arose if they differ in their pharmacokinetic properties. Therefore, together with Dr. Christoph Müller and Anna Niedrig, the cellular uptake was investigated by analytical HPLC. Two different cell lines (HUVECs and RIL175 cells) at two different compound concentrations (2 µM and 10 µM) were tested. Incorporation of SG-005 (**187**) into HUVECs was slightly higher than the uptake of tetrandrine (**1**) and SG-094 (**192**) at 2 µM, while all other settings did not show significant differences. In general, cellular uptake for the cancerous liver cells (RIL175) was preferred compared to the primary endothelial cells (HUVECs). Initial uptake was not a major trigger for the improved on-target activity of SG-005 (**187**) and SG-094 (**192**) on TPC2.

Cancer cells tend to reprogram their energy metabolism in order to boost extensive cell division[38] and according to the Warburg effect, many cancer cells preferentially use glycolysis

for ATP production[170]. Normal cells, however, favor oxidative phosphorylation and conduct glycolysis to generate pyruvate out of glucose for the dismantling of unnecessary biomass. Glucose metabolism was identified as one pathway that is altered as a result of TPC2 deficiency. Upon loss of TPC2 function or pharmacological inhibition of this channel with tetrandrine (**1**), SG-005 (**187**) and SG-094 (**192**), a metabolic shift towards a less glycolytic, and therefore healthier, phenotype was observed.

The toxicity of tetrandrine (**1**) is a serious drawback, especially for *in vivo* studies. It is postulated to be related to metabolic activation by cytochrome P450 (CYP) enzymes[70, 171] or mitochondrial pathways[172]. Both, SG-005 (**187**) and SG-094 (**192**) showed decreased toxicity to non-cancerous hepatic stem cells (HepaRG™) and peripheral blood mononuclear cells (PBMCs), which was not related to CYP3A4 levels. This indicates that metabolic oxidation by CYP enzymes is not responsible for the toxicity of tetrandrine (**1**). Thus, truncation of tetrandrine (**1**) slightly (SG-005 (**187**)) or substantially (SG-094 (**192**)) improved the toxicity prolife.

In vivo studies using tetrandrine (**1**) are limited due to the poor solubility as well as the high toxicity. The simplified, less toxic and good soluble substances SG-005 (**187**) and SG-094 (**192**) were evaluated for their therapeutic potential in an ectopic mouse model using C57Bl/6-Tyr mice and RIL175 HCC cells. SG-005 (**187**) did not show the expected *in vivo* efficacy, while SG-094 (**192**), successfully managed to reduce tumor growth *in vivo* at tolerated doses.

In short, pharmacological inhibition of TPC2 function reduced cancer cell proliferation, altered cellular energy metabolism and prevented tumor growth. The two small-molecule TPC2 inhibitors, SG-005 (**187**) and SG-094 (**192**), showed a great drug-likeness compared to the limited panel of currently available direct TPC2 blockers. The cellular uptake could be improved and the toxicity was lowered in comparison to tetrandrine (**1**). Using these molecules enables to perform *in vivo* experiments which increases their possible applications.

3.6.4 Separation of the enantiomers

The racemic mixtures of SG-005 (**187**) and SG-094 (**192**) were separated by semipreparative chiral HPLC in order to identify the eutomer. The absolute stereochemistry was determined using ECD spectra and was confirmed by computational calculations by Aaron Gerwien (group of Prof. Dr. Henry Dube, LMU) (**Figure 26 C** and **F**). The separated enantiomers were analyzed in Fluo-4 based calcium imaging and compared with the racemic mixtures, respectively. For activation of the ion channel both TPC2 activators, TPC2-A1-N (**16**) and TPC2-A1-P (**17**) were used. (*S*)-SG-005 (**209**) showed a decreased potency (IC$_{50}$: 7.8 µM) compared to its enantiomer (*R*)-SG-005 (**210**, IC$_{50}$: 2.4 µM) after activation with TPC2-A1-N (**16**, **Figure 26 E**), while there was no difference after activation with TPC2-A1-P (**17**, **Figure 26 D**). The same applied to (*S*)-SG-094 (**211**, IC$_{50}$: 31 µM) and (*R*)-SG-094 (**212**, IC$_{50}$: 14 µM) to some extent (**Figure 26 A** and **B**). Thus, all enantiomers showed inhibition of TPC2 after activation with both activators.
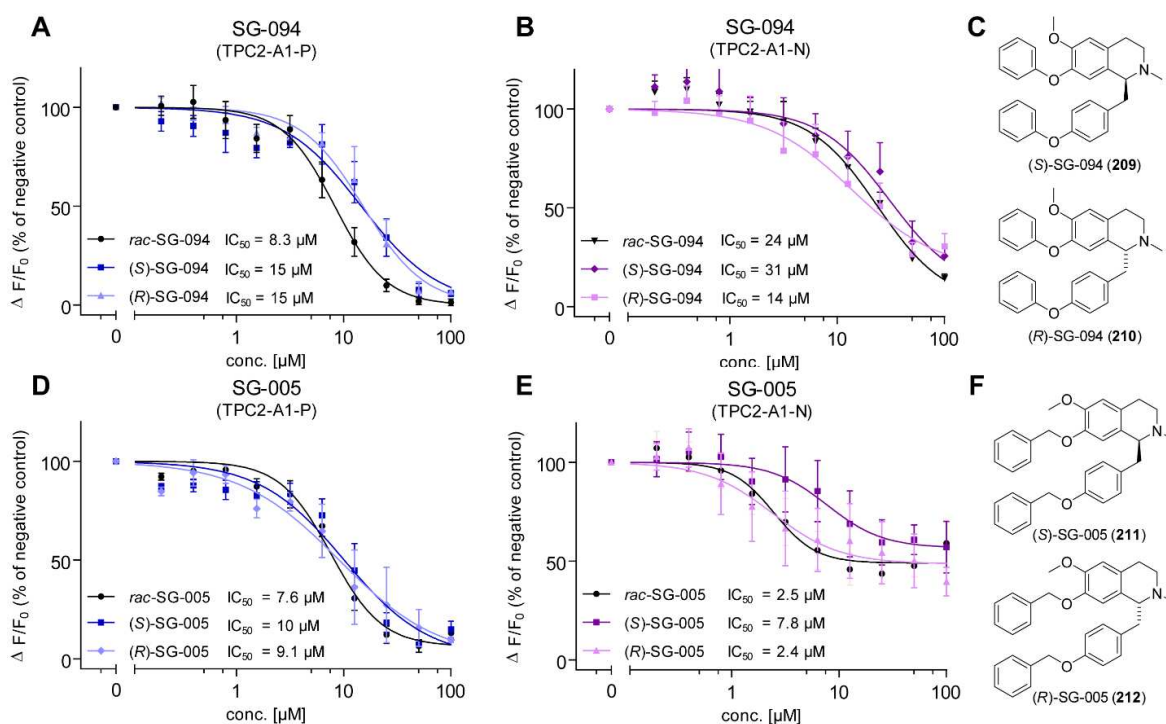
Figure 26: Fluo-4 based calcium imaging of enantiopure SG-005 (**187**) and SG-094 (**192**). (**A-B**) Concentration-effect relationships using HEK293 cells stably expressing hTPC2$^{L11A/L12A}$-RFP. Cells were sequentially stimulated with SG-094 (*rac*: **192**, (*S*): **211**, (*R*): **212**) and TPC2-A1-P (**17**, 10 µM, A) or TPC2-A1-N (**16**, 10 µM, B) as activator. IC$_{50}$ values were calculated out of at least three independent experiments using GraphPad. (**C**) Structures of both enantiomers of SG-094 ((*S*): **211**, (*R*): **212**). (**D-E**) Experiment as in A-B but using SG-005 (*rac*: **187**, (*S*): **209**, (*R*): **210**). (**F**) Structures of both enantiomers of SG-005 ((*S*): **209**, (*R*): **210**). Experiments were performed by Nicole Urban.

The different enantiomers were further analyzed for toxicity and their ability to inhibit proliferation. All compounds were not toxic to non-cancerous HepaRG cells in a CTB assay at

10 µM, while tetrandrine (**1**) already showed toxicity at this concentration (**Figure 27 A**). In particular, SG-094 (**192**) and enantiomers (**211**, **212**) showed a significantly decreased toxicity compared to tetrandrine (**1**). Antiproliferative properties of these compounds were evaluated using RIL175 cells in a CTB assay. Both enantiomers of both compounds did reduce cell proliferation, though both (*R*)-enantiomers (**210**, **212**) were less potent than the corresponding (*S*)-enantiomers (**209**, **211**) and the racemates (**187**, **192**), as depicted in **Figure 27 B** and **C**.
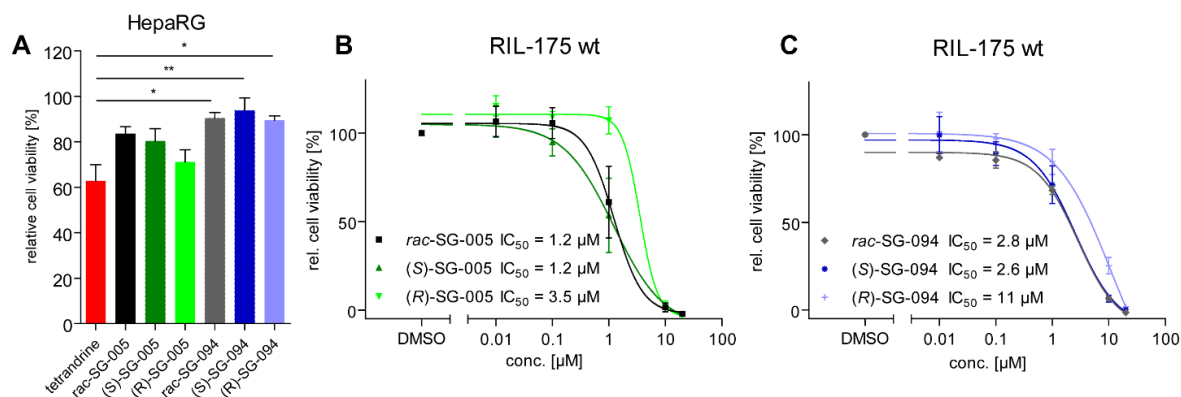
Figure 27: Toxicity and cell proliferation of the enantiopure compounds. (**A**) Toxicity of tetrandrine (**1**), SG-005 (*rac*: **187**, (*S*): **209**, (*R*): **210**) and SG-094 (*rac*: **192**, (*S*): **211**, (*R*): **212**) to non-cancerous cells was probed by treating HepaRG cells with 10 µM of the corresponding compound for 72 h. Cell viability was assessed by CellTiter-Blue® cell viability assay and was normalized to vehicle control. Bar graphs indicate mean ± SEM of three independent experiments. **p < 0.01, *p < 0.05, using one-way ANOVA followed by Tukey's post hoc test. (**B-C**) Antiproliferative effects of the SG-005 (B, *rac*: **187**, (*S*): **209**, (*R*): **210**) and SG-094 (C, *rac*: **192**, (*S*): **211**, (*R*): **212**) were assessed by CellTiter-Blue® cell viability assays. RIL-175 cells were treated for 72 h. IC_{50} values were calculated by nonlinear regression. Fluorescence intensities were normalized to vehicle control and are displayed as mean ± SEM of three independent experiments. Experiments were performed by Martin Müller.

Notably, calcium imaging revealed that both enantiomers of SG-005 (**187**) and SG-094 (**192**) inhibit TPC2 upon activation to a similar extent. Furthermore, the racemates showed virtually the same effects as the more potent compound in cell proliferation assay. Consequently, the racemates were preferred for all subsequent experiments.

3.6.5 Expanding the TPC2 inhibitor panel

The aforementioned panel of TPC2 inhibitors comprises indirect TPC inhibitors like *trans*-Ned-19 (**2**)[36, 60, 173] and direct inhibitors like the flavonoid naringenin (**8**)[52], the listed drugs fluphenazine (**6**) and raloxifene (**7**)[31] and the bisbenzylisoquinoline alkaloid tetrandrine (**1**)[2, 36]. There are other reported compounds which interfere with NAADP-mediated Ca^{2+} signaling like BZ194, an *N*-alkylated nicotinic acid derivative[174], and pyridoxal phosphate 6-azophenyl-2′,4′-disulfonic acid (PPADS)[175, 176]. For both compounds, however, no direct measurements of TPC inhibition are published, questioning the accuracy of these inhibitors.

Naringenin (**8**) and *trans*-Ned-19 (**2**) require high concentrations to inhibit TPCs (500 µM and

125 µM, respectively)[52, 60]. Raloxifene (**7**) and fluphenazine (**6**) both exhibit a low IC_{50} in endo-lysosomal patch clamp experiments (0.63 µM and 8.2 µM) after stimulation with $PI(3,5)P_2$ (**4**)[31]. The application of raloxifene (**7**), however, is limited to postmenopausal women regarding the influence upon hormone levels and fluphenazine (**6**) is known for its broad spectrum of adverse effects. The most prominent and potent TPC inhibitor, tetrandrine (**1**), blocks TPCs at nano-molar concentrations (500 nM) in endo-lysosomal patch clamp experiments[2]. It is used in different studies as exemplary TPC inhibitor, but the poor solubility combined with the reported toxicity make tetrandrine (**1**) not applicable for *in vivo* studies. None of these antagonists of TPCs is selective, neither can they discriminate between the two TPC isoforms.

The new developed TPC2 inhibitors, SG-005 (**187**) and SG-094 (**192**) showed improved efficacy in electrophysiological endo-lysosomal patch clamp experiments for SG-094 (**192**, 74% inhibition) or equipotent efficacy for SG-005 (**187**, 44%), compared to tetrandrine (**1**, 54%) after activation with $PI(3,5)P_2$ (**4**). These results were confirmed by Fura-2 calcium imaging experiments. Again SG-094 (**192**) had the strongest effect (**) compared to tetrandrine (**1**, *) and SG-005 (**187**, *) when applied at a concentration of 10 µM. Furthermore the cellular uptake could be improved and the toxicity was lowered in comparison to tetrandrine (**1**). The great solubility of SG-005 (**187**) and SG-094 (**192**) enabled *in vivo* studies in an ectopic mouse model. Both compounds were well tolerated at given doses and SG-094 (**192**), successfully managed to reduce tumor growth *in vivo*. These results demonstrate that the two small-molecule TPC2 inhibitors, SG-005 (**187**) and SG-094 (**192**), showed a promising drug-likeness and expanded the limited panel of available TPC2 blockers.

3.7 Side Projects

The developed calcium imaging methods were further used in some side projects to confirm inhibitory effects on TPC2 or TRPML channels. Within projects in the group of Prof. Dr. Bracher substances were synthesized or purchased and subsequently tested by me on TPC2 to evaluate their effect on endo-lysosomal ion channels.

3.7.1 The isoquinoline-benzylisoquinoline alkaloid *rac*-muraricine (213)

Ramona Schütz performed the first racemic total synthesis of the isoquinoline-benzylisoquinoline alkaloid *rac*-muraricine (**213**, **Figure 28 A**)[177]. Pharmacological characterization identified *rac*-muraricine (**213**) as a moderate inhibitor of P-glycoprotein, while it showed only low antiproliferative effects. Structural similarities to tetrandrine (**1**) and dauricine (**11**) led to the presumption that *rac*-muraricine (**213**) can block TPC2. Therefore Fura-2 based calcium imaging was performed using TPC2-A1-N (**16**) for activation. The alkaloid *rac*-muraricine (**213**) was not able to inhibit TPC2 activation in comparison to a DMSO control (**Figure 28 B** and **C**).
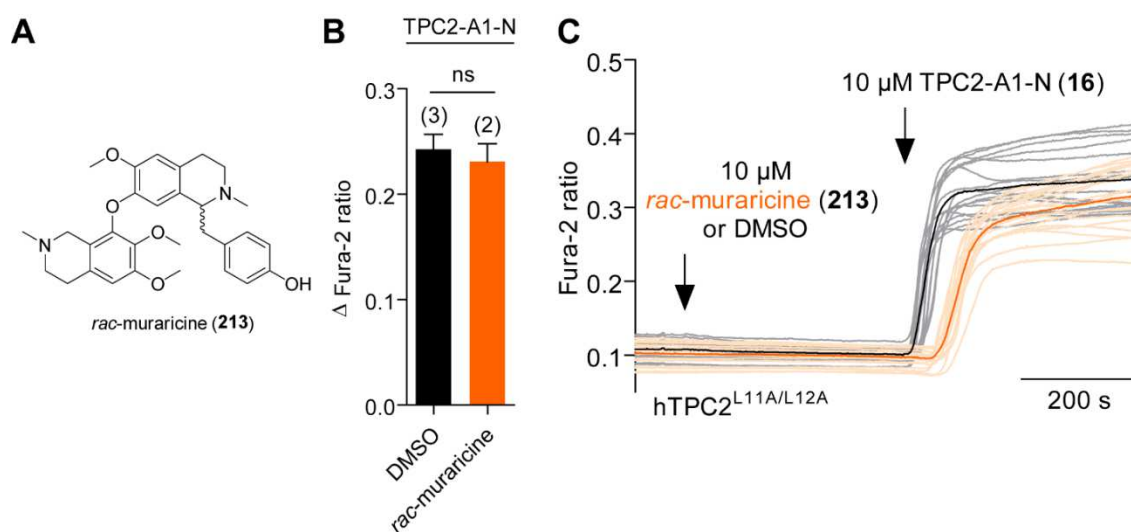
Figure 28: Fura-2 based calcium imaging results of *rac*-muraricine (**213**) and a DMSO control using the TPC2 activator TPC2-A1-N (**16**). (**A**) Structure of *rac*-muraricine (**213**). (**B**) Statistical analysis of the maximal change in the Fura-2 ratio (mean ± SEM) with the number of independent experiments in parentheses. An unpaired t-test was applied. ns = not significant. (**C**) Representative Ca^{2+} signals recorded from HEK293 cells stably expressing TPC2$^{L11A/L12A}$–RFP. After applying *rac*-muraricine (**213**, 10 µM; n = 19 single cells) or DMSO (0.1% in HBS; n = 16 single cells) and monitoring the signal for 400 s, cells were stimulated with TPC2-A1-N (**16**, 10 µM) and further recorded for 400 s. Highlighted lines represent the mean response from a population of cells. Shaded traces represent responses of single cells. All experiments were performed on a Leica DMi8 live cell microscope.

3.7.2 The TRPML inhibitors ML-SI1 (214) and ML-SI3 (215)

In the course of an Erasmus project the TRPML inhibitor ML-SI1 (**214**) was synthesized under the supervision of Dr. Marco Keller (**Figure 29 D**). This compound was one out of two published TRPML inhibitors with undefined stereochemistry[178]. The product was received as a racemic mixture of two diastereomers (4 isomers in total) and was tested on the TRPML channels for its postulated inhibitory effect. Experiments were performed by first activating the ion channel with ML-SA1 or MK6-83 (10 µM, respectively) and subsequent inhibition using ML-SI1 (**214**, 10 µM) or ML-SI3 (**214**, 10 µM). For statistical analysis the median activation was normalized to 1 to compare the percentage inhibitory effect.
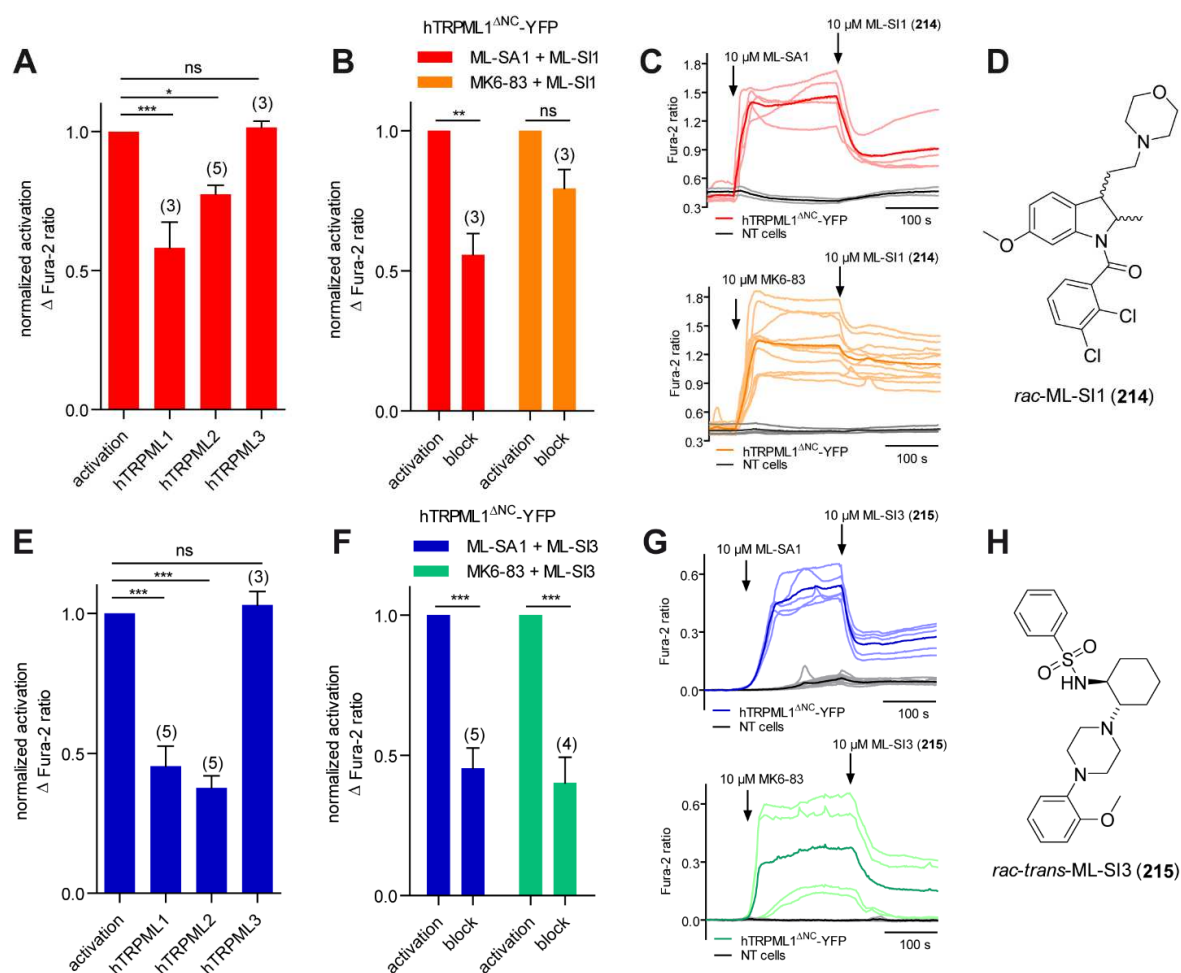
Figure 29: Fura-2 based calcium imaging experiments for TRPML inhibitors. (**A**) Statistical analysis of the inhibitory effect of ML-SI1 (**214**) on TRPMLs in Fura-2 based Ca^{2+} imaging experiments (normalized activation). Experiments were carried out as previously described[115] on a Polychrome IV mono-chromator (for hTRPML1) or a Leica DMi8 live cell microscope (for TRPML2 and 3). After stimulation with ML-SA1 (10 µM) for 200 s, the inhibitor ML-SI1 (**214**, 10 µM) was applied for another 200 s. For measurements HEK293 cells stably expressing hTRPML2-YFP or hTRPML3-YFP, and transiently transfected hTRPML1$^{\Delta NC}$-YFP cells were used[114]. (**B**) Statistical analysis as in (A), using ML-SA1 (10 µM) or MK6-83 (10 µM) for activation of hTRPML1$^{\Delta NC}$-YFP transiently transfected HEK293 cells. (**C**) Representative Ca^{2+} signals recorded from hTRPML1$^{\Delta NC}$-YFP transiently transfected HEK293 cells, loaded with Fura-2/AM (**126**) and sequentially stimulated with ML-SA1 (10 µM, red, n = 5 transfected and 2 NT cells) or MK6-83 (10 µM, orange, n = 11 transfected and 3 NT cells) and ML-SI1 (**214**, 10 µM). Highlighted lines represent the mean response from a population of cells. Shaded traces represent responses of single cells. (**D**) Structure of *rac*-ML-SI1 (**214**), synthesized by Dr. Marco Keller. (**E**)

Statistical analysis of the inhibitory effect of ML-SI3 (**215**) as in (A) using ML-SA1 (10 µM) for activation and ML-SI3 (**215**, 10 µM from Enamine store) for inhibition. All experiments were performed on a Leica DMi8 live cell microscope. (**F**) Statistical analysis as in (B) but inhibition with ML-SI3 (**215**, 10 µM). All experiments were performed on a Leica DMi8 live cell microscope. (**G**) Representative Ca^{2+} signals as in (C) but performed on a Leica DMi8 live cell microscope. Cells were sequentially stimulated with ML-SA1 (10 µM, blue, n = 5 transfected and 8 NT cells) or MK6-83 (10 µM, green, n = 4 transfected and 5 NT cells) and ML-SI3 (**215**, 10 µM). Highlighted lines represent the mean response from a population of cells. Shaded traces represent responses of single cells. In all statistical analyses of Ca^{2+} imaging experiments, mean values of n independent experiments are shown as indicated. ***$p < 0.001$, **$p < 0.01$, *$p < 0.05$, ns = not significant, one-way ANOVA test followed by Tukey's post-hoc test.

Single cell calcium imaging experiments confirmed that the synthesized racemic ML-SI1 (**214**) had an inhibitory effect on TRPML1 (**Figure 29 A**-**C**). Statistical analysis of the three isoforms of the ion channel showed strong inhibitory effect on hTRPML1, a weaker effect on hTRPML2 and no effect on hTRPML3, all after activation with ML-SA1 (**Figure 29 A**). While inhibition after activation with ML-SA1 showed a robust signal, it was not possible to significantly block MK6-83 induced activation (**Figure 29 B** and **C**). This indicates an activator dependent inhibition.

The second published inhibitor, ML-SI3 (**215**)[178], was commercially available at Enamine store (CAS: 891016-02-7) but with undefined stereochemistry. Within a new project, Charlotte Leser identified the commercially available ML-SI3 (**215**) as racemic mixture of *trans*-ML-SI3 (**215**, **Figure 29 H**). The commercially available ML-SI3 (**215**, **Figure 29 H**) was able to block ML-SA1 evoked hTRPML1 and 2 activation around 50% but did not inhibit hTRPML3 activation (**Figure 29 E**). The comparison of the different activators showed that ML-SI3 (**215**) was able to block both ML-SA1 and MK6-83 induced activation in the same manner (**Figure 29 F** and **G**). Thus, ML-SI3 (**215**) seemed the more promising antagonist for further investigations.

4 Summary

The first aim of this thesis was the identification of small-molecule TPC2 activators. This was achieved by performing a high-throughput screening of a compound library, containing 80000 substances. Two TPC2 activators (TPC2-A1-N (**16**), TPC2-A1-P (**17**)) were identified within this screening process. Both compounds were confirmed by fluorescence-based Ca^{2+}-imaging and electrophysiological endo-lysosomal patch clamp measurements. To verify the structures, both substances were synthesized and re-evaluated.

Sjogren et al. published a two-step synthesis for α-cyano-β-hydroxypropenamides, which resulted in the desired TPC2-A1-N (**16**)[91]. Only slight changes in this procedure were necessary for optimization. Different aniline building blocks (**IV**, **Figure 30 A**), 2-cyanoacetic acid (**18**) and DCC as coupling reagent yielded 23 cyanoacetanilides (**II**, **Figure 30 A**), nearly all in high yield. Acylation of these intermediates (**II**, **Figure 30 A**) using different benzoic acid building blocks (**III**, **Figure 30 A**) and NaH as a strong base gave the desired α-cyano-β-hydroxypropenamides (**I**, **Figure 30 A**) as analogs of TPC2-A1-N (**16**, **Figure 30 B**). Only the thio-analog SGA-167 (**91**) was synthesized with another method. Collectively, 47 compounds were synthesized in moderate to high yield, including the hit TPC2-A1-N (**16**), and two drugs (prinomide (**58**), teriflunomide (**76**)).

Fura-2 based calcium imaging experiments were performed to study SAR. Surprisingly, none of the 46 modified versions of TPC2-A1-N (**16**, **Figure 30 B**) did show significantly increased efficacies. Replacing the *p*-trifluoromethyl group on the anilide side of the molecule (R^1; blue) with other electron-withdrawing groups in *para*-position did not lead to significant changes. The introduction of electron-releasing groups in *para*-position was tolerated to some extent (SGA-4 (**47**), SGA-84 (**72**)). *Meta*-disubstitution patterns were most beneficial for the benzoyl ring system (R^2, green), while more drastic changes in this aromatic region caused a complete loss of activity. This was demonstrated for the approved drugs teriflunomide (**76**) and prinomide (**58**) as well as the 4-trifluoromethyl variant of prinomide (SGA-32 (**59**)), all possessing methyl or pyrrole residues instead of the benzoyl ring. In total, 24 analogs were able to activate TPC2 with similar or lower efficacy compared to TPC2-A1-N (**16**)[22, 135]. All results were confirmed by determination of concentration-effect relationships, underlining the very flat SAR of this chemotype on TPC2. The increased potency and efficacy of SGA-85 (**73**) were relativized by non-specific effects on control cells. Selectivity-screening revealed that SGA-108 (**77**) showed an improved selectivity spectrum, which explains the loss of efficacy. All these findings have proven the high efficacy of TPC2-A1-N (**16**) and the fact that it is the most promising candidate to be a great tool compound.
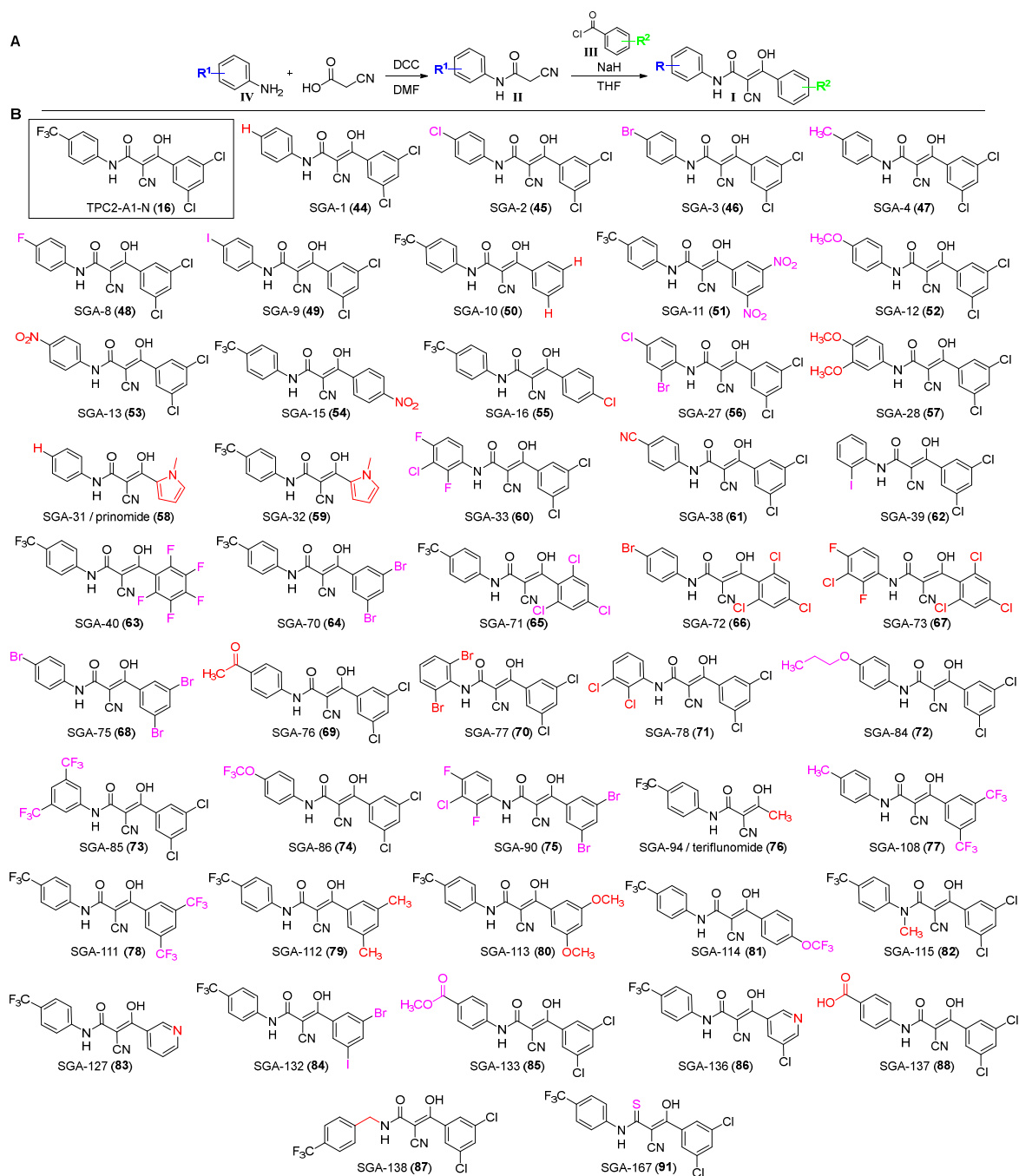
Figure 30: Synthesis and compound overview of TPC2-A1-N (**16**) and analogs. (**A**) Synthesis scheme for the preparation of most *α*-cyano-*β*-hydroxypropenamides. (**B**) Structures of TPC2-A1-N (**16**) and analogs. Differences to the hit compound are marked in magenta (TPC2 activators) or red (no TPC2 activators).

The synthesis of the second activator, TPC2-A1-P (**17**), was more challenging than the synthesis of TPC2-A1-N (**16**), as the required intermediate, an *α*-halogenated acetophenone (**IV**, **Figure 31**) substituted in C-2 position with a trifluoromethoxy and in C-5 position with a bromo group, was not commercially available. Many different synthetic approaches were not successful until the main problem was detected: The desired product was highly volatile.

Hence, a synthesis avoiding these conditions was chosen and the *α*-halogenated acetophenone (**IV**, **Figure 31 A**) was synthesized successfully.

For the synthesis of the highly substituted TPC2-A1-P scaffold a Paal-Knorr pyrrole synthesis was performed. Under alkaline conditions 1,4-diketones (**VIII**, **Figure 31 A**) were synthesized, using the *α*-halogenated acetophenone (**IV**, **Figure 31 A**) and *β*-ketoester (**V**, **Figure 31 A**) building blocks. These 1,4-diketones (**VIII**, **Figure 31 A**) were not isolated and directly condensed with a primary amine building block (**III**, **Figure 31 A**) in acidic medium to give multi-substituted pyrroles (**II**, **Figure 31 A**). In total, 13 esters were synthesized and 8 of them isolated. Hydrolysis of the esters (**II**, **Figure 31 A**) required harsh conditions, utilizing microwave irradiation for several hours to give the hit TPC2-A1-P (**17**) and 12 analogs varying all substituents of the pyrrole moiety (**Figure 31 B**).
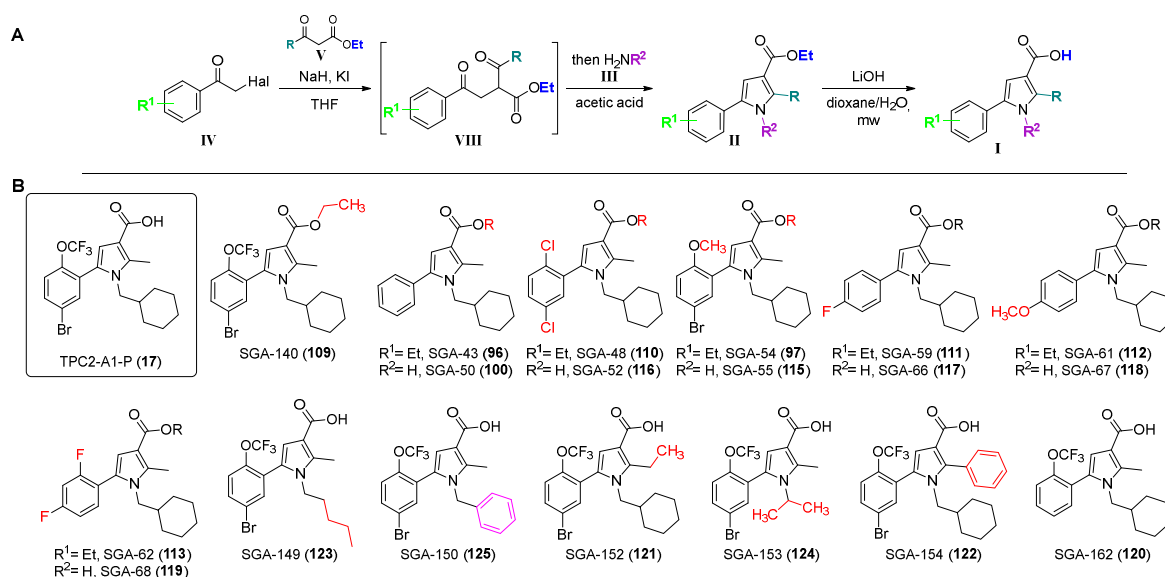
Figure 31: Synthesis and compound overview of TPC2-A1-P (**17**) and analogs. (**A**) Synthesis scheme for the synthesis of TPC2-A1-P (**17**) and analogs. (**B**) Structures of TPC2-A1-P (**17**) and analogs. Differences to the hit compound are marked in magenta (TPC2 activators) or red (no TPC2 activators).

Similar to TPC2-A1-N (**16**), calcium imaging experiments were performed to gain first insights into SAR. Again, all modified versions of TPC2-A1-P (**17**) showed no improvement of efficacy[22]. Every change in structure resulted in a decrease or total loss of activity. SAR revealed that the free carboxylic acid is essential for the activating effect, as the ester SGA-140 (**109**) was not active. It could possibly serves as a prodrug of TPC-A1-P (**17**) in living systems, but this has not been investigated yet. Both substituents at the phenyl ring, the trifluoromethoxy and the bromine group, were essential for activating TPC2, as exemplified by the inactive methoxy (SGA-55, **115**) and des-bromo (SGA-162, **120**) analogs. Moderate expansion of the size of the pyrrole substituent at C-2 position (methyl in TPC2-A1-P (**17**) vs. ethyl in SGA-152 (**121**) and phenyl analog SGA-154 (**122**)), had the same effect. The only fairly tolerated structure modification was replacing the cyclohexylmethyl moiety in 1-positon

of the pyrrole ring by a benzyl residue (SGA-150, **125**), whereas linear or branched alkyl chains (SGA-149 (**123**), SGA-153 (**124**)) caused loss of activity (**Figure 31 B**). All results were further confirmed by full concentration-effect relationships, generated by Fluo-4 calcium imaging experiments. These harsh limitations showed that TPC2-A1-P (**17**) had an unusually steep structure-activity relationship resulting in TPC2-A1-P (**17**) as great chemical tool.

Comparing the results of both activator classes, a considerable number of TPC2-A1-N (**16**) analogs caused remarkable TPC2 activation, but none of them showed significantly increased efficacies. In contrast to TPC2-A1-N (**16**), TPC2-A1-P (**17**) showed an unusually steep structure-activity relationship, and except for one analog (SGA-150, **125**) none of the analogs showed any activity. TPC2-A1-N (**16**) itself and some of its analogs bearing residues in *para*-position at the benzoyl ring were known as anthelmintic agents[91], while TPC2-A1-P (**17**) was only namely mentioned as a precursor in the synthesis of cannabinoid-1 receptor (CB1R) inverse agonists[105]. Two analogs of TPC2-A1-N (**16**) were launched drugs (teriflunomide (**76**), prinomide (**58**)), proving the drug-likeness of the TPC2-A1-N skeleton. There were no drugs comprising the TPC2-A1-P skeleton and furthermore no reports for using the free carboxylic acids. Thus, the two HTS hits TPC2-A1-N (**16**) and TPC2-A1-P (**17**) can be regarded as novel, strong chemical tools.

In a very recent publication we published initial steps for the pharmacological profile of TPC2-A1-N (**16**) and TPC2-A1-P (**17**)[22]. The subtype selectivity to TPC1 and cell permeability were proven. These small-molecules finally helped to resolve the conflict, whether TPC2 is a NAADP-activated Ca^{2+} release channel[5, 12, 14, 127, 128] or a PI(3,5)P_2 gated Na^+ channel[15, 20, 129]: TPC2 is a ligand-dependent, non-selective cation channel with malleable cation selectivity. Depending on the agonist, TPC2 shows higher calcium permeability (activation with TPC2-A1-N (**16**), similar to NAADP (**3**)) or increased sodium permeability (activation with TPC2-A1-P (**17**), similar to PI(3,5)P_2 (**4**)). Additionally the PI(3,5)P_2 (**4**) binding site in TPC2[8] has been identified to be the overlapping with the pore for TPC2-A1-P (**17**). While TPC2-A1-N (**16**) induced an alkalinization of single vesicles in cells expressing wild-type TPC2, as described for NAADP (**3**)[130, 131], TPC2-A1-P (**17**) promoted lysosomal exocytosis.

In comparison with other new TPC2 activators, identified by Zhang et al.[111], our two new activators were more potent and selective, which made them the perfect chemical tools for the identification of TPC2 inhibitors.

Because of their anti-cancer or anti-viral effects TPC2 inhibitors are currently of higher therapeutic significance than activators. Hence, a set of TPC2 inhibitors was synthesized, inspired by the known TPC2 inhibitor tetrandrine (**1**). These molecules mimicked one half of the bisbenzylisoquinoline tetrandrine (**1**) and further decoration, not only in form of *O*-benzyl derivatives but also as diaryl ethers, was supposed to closely imitate tetrandrine (**1**) in shape

and size (**Scheme 34 A**). Iturriaga-Vásquez et al. designed simplified and more accessible congeners of tetrandrine (**1**) bearing extensions as benzyl groups, which were developed as L-type calcium channel blockers[82]. This was a promising hint for the plan to design truncated analogs of tetrandrine (**1**).

Starting materials for the synthesis of the desired tetrahydroisoquinolines were carbamates and enol ethers (**I** and **II**, **Scheme 34 B**). Using ethyl chloroformate (**162**), NEt$_3$ and 3-methoxytyramine (**160**) or its *O*-protected derivatives gave different carbamates (**I**). Enol ethers (**II**) were received *via* Wittig olefination of commercially available *para*-substituted benzaldehydes. These precursors underwent *N*-acyl Pictet-Spengler reaction using TFA and to yield *N*-acethoxycarbonyl-1-benzyltetrahydroisoquinolines (**III**). Tertiary *N*-methyl amines (**IV**) were received by reduction of the carbamate group and, if applicable, *in situ* deprotection of carbonate-protected phenols using lithium alanate. Diverse diaryl ethers (**V**) were introduced at the generated phenolic groups *via* gentle Chan-Evans-Lam coupling with the appropriate arylboronic acids. Furthermore, three routes were established to yield SG-005 (**187**): lithium alanate reduction of the carbamate SG-145 (**183**), Eschweiler-Clarke reaction starting with the secondary amine Z3 (**137**) and Mitsunobu reaction on *N*-methylcoclaurine (SG-132, **159**) to receive benzyl protecting groups. The Eschweiler-Clarke reaction using Z6 (**145**) also yielded SG-159 (**206**) and an alkylation reaction using bromoethane yielded SG-158 (**208**).

The racemates SG-005 (**187**) and SG-094 (**192**) were separated by semi-preparative chiral HPLC for the identification of the potential eutomers. The absolute configuration of the enantiomers was determined using ECD spectra and confirmed by computational calculations performed by Aaron Gerwien. Notably, Ca^{2+} imaging revealed that both enantiomers of SG-005 (**187**) and SG-094 (**192**) inhibit TPC2 upon activation to a similar extent. Consequently, the racemates were used for all further experiments.

A Fura-2 based single cell calcium imaging method was developed and the TPC2-blocking effect of SG-005 (**187**) and SG-094 (**192**) was confirmed. These two substances were highlighted within this project because of their outstanding effects in a variety of experiments. While tetrandrine (**1**) and SG-005 (**187**) were equipotent (54% and 44% inhibition or *, respectively), SG-094 (**192**) was significantly more potent (74%, **) at the tested conditions (10 µM of inhibitor, activated with 1 µM PI(3,5)P$_2$ (**4**)) in endo-lysosomal patch-clamp experiments (performed by Dr. Yu-Kai Chao) and Fura-2 based calcium imaging experiments (10 µM TPC2-A1-N (**16**), followed by 10 µM of the respective inhibitor). Furthermore, two negative controls were identified to assure the accuracy of the experiments. SG-132 (**159**, *N*-methylcoclaurine) is missing the decoration on the phenol groups and SG-145 (**183**) the alkaline nitrogen function of the tetrahydroisoquinoline, which represent the two most important structural moieties.
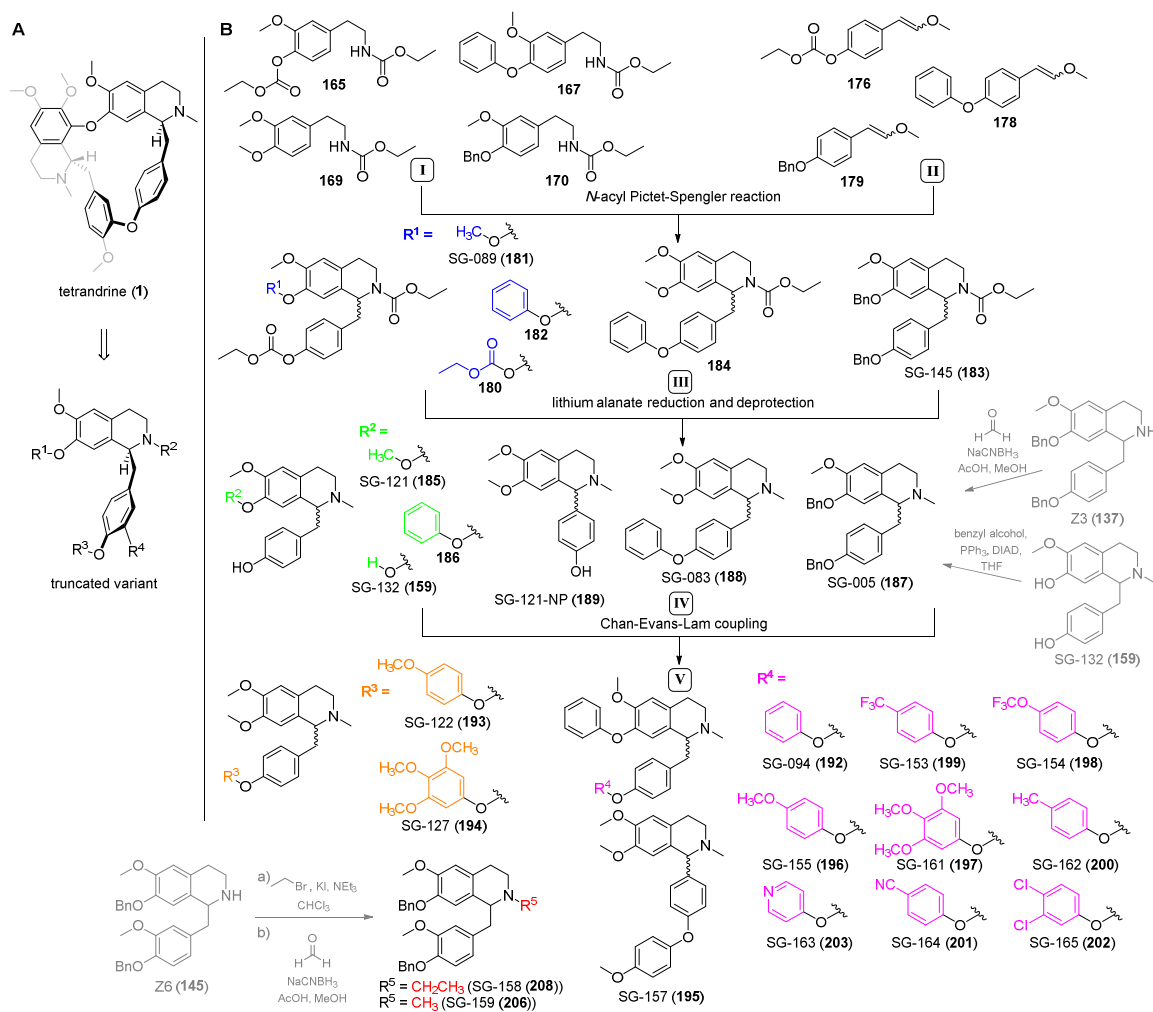
Scheme 34: Summary for the synthesis of truncated tetrandrine analogs. (**A**) Schematic overview for the truncation of tetrandrine (**1**). Decorations on the former phenols (R's) make the molecule resemble tetrandrine (**1**) even more. (**B**) Complete synthesis branches for the synthesis of truncated analogs, starting with carbamate and enol ether building blocks. *N*-acyl Pictet-Spengler reaction resulted in benzyltetrahydroisoquinolines, that were deprotected and reduced using lithium alanate. The resulting tertiary amines received their final decoration using the Chan-Evans-Lam coupling. Shaded reactions are additional reactions to receive different benzylated analogs.

All compounds were analyzed for their ability to inhibit TPC2-A1-N (**16**) and TPC2-A1-P (**17**) induced TPC2 activation in Fluo-4 calcium imaging experiments performed by Nicole Urban. Within this screening IC$_{50}$ values were obtained not only for the synthesized substances, but also for more alkaloids: intermediates of the morphine biosynthesis like racemic coclaurine (Z1, **141**), kindly provided by Prof. Dr. Meinhart Zenk[†], tetrandrine (**1**) and derivatives as fangchinoline (**9**), kindly provided by Prof. Dr. Peter Pachaly[†]. Commercially available benzylisoquinoline alkaloids like dauricine (**11**) and oxyacanthine (**138**) completed the screening library. This screening pointed out that tetrandrine (**1**), fangchinoline (**9**) and the other alkaloids inhibit TPC2 to the same extent (around 50%). SG-005 (**187**), SG-094 (**192**) and the orientaline derivatives SG-158 (**208**) and SG-159 (**206**) were able to inhibit TPC2 activation similarly or even better than tetrandrine (**1**). None of the further analogs showed

significant stronger effects on TPC2. The substances bearing a *para*-methoxy, *para*-methyl or their fluorinated variants (SG-153 (**199**), SG-154 (**198**), SG-155 (**196**), SG-162 (**200**)) showed a lower IC_{50} value after activation with TPC2-A1-P (**17**) compared to activation with TPC2-A1-N (**16**). As mentioned before, SG-005 (**187**) and SG-094 (**192**), derived from the alkaloid coclaurine, were selected as most promising TPC2 inhibitors for further investigation.

After the identification of the novel TPC2 inhibitors, their potential to inhibit cancer cell growth was investigated. All 1-benzyltetrahydroisoquinolines carrying two aryl or benzyl ether groups and a basic amine inhibited proliferation of RIL175 cells to a similar or stronger extent than tetrandrine (**1**). The two simplest 1-benzyltetrahydroisoquinolines, SG-005 (**187**, IC_{50}: 2.4 µM) and SG-094 (**192**, IC_{50}: 3.7 µM), both displayed markedly enhanced antiproliferative effects compared to tetrandrine (**1**) also against various other cancer cell lines including HepG2, HCT-15 and VCR-R CEM. The comparison of IC_{50} values of the cell proliferation assay and Fluo-4 based calcium imaging showed that not all compounds that block proliferation were TPC2 inhibitors (SG-132 (**159**)) and not all TPC2 inhibitors block proliferation (SG-163 (**203**)), indicating additional effects of these compounds on other targets in cancer cells.

In an effort to conclude the correlation between TPC2 inhibition and hallmarks of cancer, cellular uptake, toxicity and the effects on angiogenesis and glucose metabolism of SG-005 (**187**) and SG-094 (**192**) were investigated by Martin Müller (Vollmar group), all in comparison to tetrandrine (**1**). The non TPC2-blockers SG-132 (**159**) and SG-145 (**183**) were used as controls. Pharmacological inhibition of TPC2 function reduced cancer cell proliferation altered cellular energy metabolism and prevented tumor growth *in vivo*. The cellular uptake could be improved and the toxicity was lowered in comparison to tetrandrine (**1**). Thus, the two small-molecule TPC2 inhibitors SG-005 (**187**) and SG-094 (**192**) showed a great potential for drug development especially considering the limited panel of currently available TPC2 blockers.

Summarizing, big steps to boost the basic research of two pore channels have been achieved within this project. The two novel small-molecule activators of TPC2, TPC2-A1-N (**16**) and TPC2-A1-P (**17**), were discovered and analyzed in extensive studies. Now they represent two powerful chemical tools for the analysis of TPC2 function. These activators enable the use of fluorescent based assays on intact cells to study TPC2 inhibitors. Therefore a new generation of TPC2 inhibitors was synthesized, resembling one half of the alkaloid tetrandrine (**1**) plus the two benzenoid rings of the second benzylisoquinoline moiety. The two new TPC2 inhibitors with improved or at least equipotent ability to inhibit TPC2 were developed, SG-005 (**187**) and SG-094 (**192**). Together with our cooperation partners TPC2 was proven to be an exciting target in tumor therapy and these two compounds were identified as promising lead structures for cancer therapy.

5   Experimental part

Synthesis details and analytical data

All chemicals used were of analytical grade and were obtained from abcr (Karlsruhe, Germany), Fischer Scientific (Schwerte, Germany), Sigma-Aldrich (now Merck, Darmstadt, Germany), TCI (Eschborn, Germany) or Th. Geyer (Renningen, Germany). HPLC grade and dry solvents were purchased from VWR (Darmstadt, Germany) or Sigma-Aldrich, all other solvents were purified by distillation. Hydrophobic phase separation filters (MN 617 WA, 125 mm) were purchased from Macherey Nagel (Düren, Germany). All reactions were monitored by thin-layer chromatography (TLC) using pre-coated plastic sheets POLYGRAM® SIL G/UV254 from Macherey-Nagel and detected by irradiation with UV light (254 nm or 366 nm). Furthermore reactions were monitored by atmospheric pressure solids analysis probe (ASAP) via atmospheric-pressure chemical ionization (APCI) on an expression^L CMS device (Advion, Ithaca, USA). Flash column chromatography (FCC) was performed on Merck silica gel Si 60 (0.015 – 0.040 mm). Preparative and semipreparative (chiral) HPLC was performed on a Shimadzu HPLC system consisting of a LC-20AP solvent delivery module, a CTO-20A column oven, a SPD-M20A photodiode array UV/vis detector and a CBM-20A system controller using a semipreparative CHIRALPAK® IC column (particle size 5 µm, Diacel) or a preparative NUCLEODUR® 100-5 column (particle size 5 µm, Macherey-Nagel). Microwave-assisted reactions were carried out in a Discover (S-Class Plus) SP microwave reactor (CEM GmbH, Kamp-Lintfort, Germany). NMR spectra (^{1}H, ^{13}C, DEPT, H-H-COSY, HMQC/HSQC, HMBC) were recorded at 23 °C on an Avance III 400 MHz Bruker BioSpin or Avance III 500 MHz Bruker BioSpin instrument, unless otherwise specified. Chemical shifts $δ$ are stated in parts per million (ppm) and are calibrated using residual protic solvents as an internal reference for proton (CDCl$_3$: $δ$ = 7.26 ppm, (CD$_3$)$_2$SO: $δ$ = 2.50 ppm, C$_2$D$_2$Cl$_4$: $δ$ = 5.91 ppm, CD$_3$OD: $δ$ = 3.31 ppm, C$_3$D$_6$O: $δ$ = 2.05 ppm) and for carbon the central carbon resonance of the solvent (CDCl$_3$: $δ$ = 77.16 ppm, (CD$_3$)$_2$SO: $δ$ = 39.52 ppm, C$_2$D$_2$Cl$_4$: $δ$ = 74.20 ppm, CD$_3$OD: $δ$ = 49.00 ppm, C$_3$D$_6$O: $δ$ = 29.84 ppm). Multiplicity is defined as s = singlet, d = doublet, t = triplet, q = quartet, m = multiplet. NMR spectra were analyzed with NMR software MestReNova, version 12.0.1-20560 (Mestrelab Research S.L.). High resolution mass spectra were performed by the LMU Mass Spectrometry Service applying a Thermo Finnigan MAT 95 or Joel MStation Sektorfeld instrument at a core temperature of 250 °C and 70 eV for EI or a Thermo Finnigan LTQ FT Ultra Fourier Transform Ion Cyclotron Resonance device at 250 °C for ESI. IR spectra were recorded on a Perkin Elmer FT-IR Paragon 1000 instrument as neat materials. Absorption bands were reported in wave number (cm^{-1}) with ATR PRO450-S. Melting points were determined by the open tube capillary method on a Büchi melting point B-540 apparatus and are uncorrected. HPLC purities were determined using an HP Agilent 1100 HPLC with a diode array detector and an Agilent Poroshell column (120 EC-C18; 3.0 × 100

mm; 2.7 micron) with acetonitrile/water as eluent. Electronic circular dichroism (ECD) spectra were measured on a Jasco J-810 Spectropolarimeter. Optical rotations were further measured at the given temperature (T in [°C]) on a Perkin Elmer 241 Polarimeter instrument using a sodium lamp (Na D-line, 589 nm). Measurements were carried out in a cell with path lengths (l) of 1.0 dm. Concentrations are given in g/100 mL.

5.1 Preparation of TPC2 activators

5.1.1   General procedures

General Procedure A – Synthesis of *N*-aryl cyanoacetamides

According to Sjogren, et al.[91] the appropriate aniline (1.0 eq.) and 2-cyanoacetic acid (**18**, 1.0 eq.) were dissolved in DMF and cooled to 0 °C. DCC (1.0 eq.) was added portion wise. The mixture was warmed up to rt over 1 h and subsequently diluted with hexanes/EtOAc (1:1). Precipitates were removed by filtration and the filtrate was extracted once with 1 M aq. HCl and thrice with EtOAc. The combined organic layers were washed with sat. aq. NaCl solution, dried over Na_2SO_4, filtered and concentrated *in vacuo*. Recrystallization from EtOH yielded the desired amides.

General Procedure B – Synthesis of α-cyanoaroylacetanilides

According to Sjogren, et al.[91] the appropriate amides received from general procedure **A** (1.0 eq.) were dissolved in dry THF, the solution was cooled to 0 °C and NaH (dispersion in paraffin, 60%, 2.3 eq.) was added. After stirring for 15 min, the appropriate benzoyl chloride (1.1 eq.) was added. The mixture was stirred at 0 °C for 1 h and then cautiously treated with 1 M HCl. The precipitate was collected by filtration, washed with ice water and cold EtOH and recrystallized from toluene to give the desired cyanoaroylacetanilide.

If the appropriate benzoyl chloride was not commercially available, it was prepared by refluxing the appropriate benzoic acid (1.1 eq.) in $SOCl_2$ (55 eq.) for 1 h and concentrating *in vacuo*. The resulting acid chloride was immediately transferred to the reaction.

General Procedure C – Paal Knorr Pyrrole synthesis

Following a general procedure published by Kang, et al.[103] the appropriate *β*-ketoester (1.1 eq.) was dissolved in dry THF and cooled to 0 °C, before NaH (dispersion in paraffin, 60%, 1.5 eq.) was added portion wise. After the suspension was stirred for 30 min, a solution of appropriate halogenated acetophenone (1.0 eq.) and KI (1.0 eq.) in dry THF was added dropwise. The reaction mixture was allowed to warm up to rt over 2 h, then poured on water and extracted thrice with Et_2O. The combined organic phases were washed with sat. aq. $NaHCO_3$ solution, dried over Na_2SO_4, filtered and concentrated *in vacuo*. The residue was dissolved in acetic acid and the appropriate primary amine (2.0 eq.) was added dropwise. The reaction mixture was stirred at 80 °C for 18 h. The solvent was removed *in vacuo*, the residue dispersed in water and extracted thrice with diethyl ether. The collected organic phases were washed with sat. aq. $NaHCO_3$ solution, dried over Na_2SO_4 and concentrated *in vacuo*.

Purification was accomplished by FCC and recrystallization from EtOH if not otherwise specified.

General Procedure D – Alkaline deprotection of esters

LiOH (10 eq.) was added to a solution of the appropriate ester (1.0 eq.) in dioxane/H_2O (5:1) and the reaction mixture was stirred in a closed vessel under microwave irradiation (p_{max} = 8 bar, P_{max} = 200 W, T_{max} = 180 °C) for 1-18 h. The suspension was diluted with water to thrice original volume and aq. 2 M HCl was added dropwise under vigorous stirring until the mixture was strongly acidic. The formed precipitate was collected by filtration, washed with water and dried. If necessary, the acids were recrystallized from EtOH to yield the pure products.

5.1.2   Synthetic procedures
5.1.2.1 Synthesis of TPC2-A1-N (16) and analogs

2-Cyano-*N*-(4-(trifluoromethyl)phenyl)acetamide – SGA-34 (19)
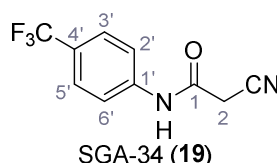
According to general procedure **A**, 4-(trifluoromethyl)aniline (**20**, 812 µL, 6.47 mmol, 1.1 eq.), 2-cyanoacetic acid (**18**, 500 mg, 5.88 mmol, 1.0 eq.) and DCC (1.27 g, 6.17 mmol, 1.1 eq.) in DMF (7.0 mL) were used to yield amide SGA-34 (**19**) as colorless crystals (983 mg, 4.31 mmol, 73%). Analytical data are in accordance with literature[91, 179].

R*f* = 0.14 (4:1 hexanes/acetone).

m.p.: 195 °C. [lit.[91]: 191 – 193 °C]

¹H NMR (400 MHz, (CD₃)₂SO) δ/ppm = 10.65 (s, 1H, NH), 7.75 (d, *J* = 8.8 Hz, 2H, 3'-H, 5'-H), 7.70 (d, *J* = 8.8 Hz, 2H, 2'-H, 6'-H), 3.95 (s, 2H, 2-H).

¹³C NMR (101 MHz, (CD₃)₂SO) δ/ppm = 161.9 (C-1), 141.9 (C-1'), 126.3 (q, J_{CF} = 3.7 Hz, C-3', C-5'), 124.4 (q, J_{CF} = 271.4 Hz, CF₃), 124.0 (q, J_{CF} = 32.0 Hz, C-4'), 119.2 (C-2', C-6'), 115.7 (CN), 27.0 (C-2).

IR (ATR) $\tilde{v}_{max}$/cm⁻¹ = 3287, 3221, 3147, 1681, 1612, 1557, 1319, 1110, 1065, 849, 835.

HRMS (ESI): calcd. for $C_{10}H_6F_3N_2O$ (M-H)⁻ 227.04377; found 227.04371.

Purity (HPLC): > 96% (λ = 210 nm), > 96% (λ = 254 nm).

2-Cyano-*N*-(*p*-tolyl)acetamide (21)
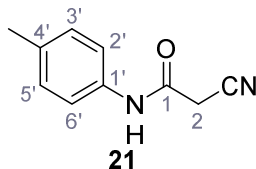
According to general procedure **A**, *p*-toluidine (712 µL, 6.47 mmol, 1.1 eq.), 2-cyanoacetic acid (**18**, 500 mg, 5.88 mmol, 1.0 eq.) and DCC (1.27 g, 6.17 mmol, 1.1 eq.) in DMF (7.0 mL) were used to yield amide **21** as colorless crystals (728 mg, 4.18 mmol, 71%). Analytical data are in accordance with literature[180].

R_f = 0.14 (4:1 hexanes/acetone).

m.p.: 184 °C. [lit.[180]: 186 °C]

^{1}H NMR (400 MHz, (CD$_3$)$_2$SO) δ/ppm = 10.19 (s, 1H, NH), 7.47 – 7.36 (m, 2H, 2'-H, 6'-H), 7.13 (d, J = 8.2 Hz, 2H, 3'-H, 5'-H), 3.86 (s, 2H, 2-H), 2.25 (s, 3H, CH$_3$).

^{13}C NMR (101 MHz, (CD$_3$)$_2$SO) δ/ppm = 160.7 (C-1), 135.9 (C-1'), 132.9 (C-4'), 129.3 (C-3', C-5'), 119.2 (C-2', C-6'), 116.0 (CN), 26.6 (C-2), 20.4 (CH$_3$).

IR (ATR) $\tilde{v}_{max}$/cm^{-1} = 3267, 3207, 3137, 1660, 1613, 1552, 1510, 819.

HRMS (ESI): calcd. for C$_{10}$H$_9$N$_2$O (M-H)$^-$ 173.07204; found 173.07194.

Purity (HPLC): > 96% (λ = 210 nm), > 96% (λ = 254 nm).

2-Cyano-*N*-phenylacetamide (22)
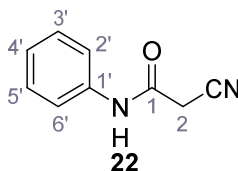
According to general procedure **A**, aniline (1.96 mL, 21.5 mmol, 1.0 eq.), 2-cyanoacetic acid (**18**, 2.01 g, 23.6 mmol, 1.1 eq.) and DCC (4.87 g, 23.6 mmol, 1.1 eq.) in DMF (20 mL) were used to yield amide **22** as colorless crystals (2.60 g, 16.2 mmol, 76%). Analytical data are in accordance with literature[180].

R_f = 0.12 (4:1 hexanes/acetone).

m.p.: 202 °C. [lit.[180]: 172 °C]

^{1}H NMR (500 MHz, (CD$_3$)$_2$SO) δ/ppm = 10.28 (s, 1H, NH), 7.54 (dt, J = 8.7, 1.6 Hz, 2H, 2'-H, 6'-H), 7.39 – 7.29 (m, 2H, 3'-H, 5'-H), 7.15 – 7.04 (m, 1H, 4'-H), 3.89 (s, 2H, 2-H).

^{13}C NMR (126 MHz, (CD$_3$)$_2$SO) δ/ppm = 161.0 (C-1), 138.4 (C-1'), 128.9 (C-3', C-5'), 123.9 (C-4'), 119.2 (C-2', C-6'), 115.9 (CN), 26.7 (C-2).

IR (ATR) $\tilde{v}_{max}$/cm^{-1} = 3265, 3207, 3143, 3099, 3052, 1653, 1620, 1557, 1299, 943, 761, 696.

HRMS (ESI): calcd. for C$_9$H$_7$N$_2$O (M-H)$^-$ 159.05639; found 159.05628.

Purity (HPLC): > 96% (λ = 210 nm), > 96% (λ = 254 nm).

2-Cyano-*N*-(4-methoxyphenyl)acetamide (23)
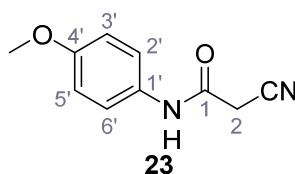
According to general procedure **A**, *p*-anisidine (2.36 mL, 20.3 mmol, 1.0 eq.), 2-cyanoacetic acid (**18**, 19.0 g, 22.3 mmol, 1.1 eq.) and DCC (4.61 g, 22.3 mmol, 1.1 eq.) in DMF (20 mL) were used to yield amide **23** as pale blue crystals (1.58 g, 8.31 mmol, 41%). Analytical data are in accordance with literature[180].

R$_f$ = 0.10 (4:1 hexanes/acetone).

m.p.: 137 °C. [lit.[180]: 176 °C]

^{1}H NMR (400 MHz, (CD$_3$)$_2$SO) δ/ppm = 10.14 (s, 1H, NH), 7.53 – 7.38 (m, 2H, 2'-H, 6'-H), 7.00 – 6.83 (m, 2H, 3'-H, 5'-H), 3.84 (s, 2H, 2-H), 3.72 (s, 3H, OCH$_3$).

^{13}C NMR (101 MHz, (CD$_3$)$_2$SO) δ/ppm = 160.4 (C-1), 155.6 (C-4'), 131.4 (C-1'), 120.8 (C-2', C-6'), 116.0 (CN), 114.0 (C-3', C-5'), 55.2 (OCH$_3$), 26.5 (C-2).

IR (ATR) $\tilde{v}_{max}$/cm^{-1} = 3299.3150, 1655, 1608, 1557, 1511, 1251, 1032, 828.

HRMS (ESI): calcd. for C$_{10}$H$_9$N$_2$O$_2$ (M-H)$^-$ 189.06695; found 189.06688.

Purity (HPLC): > 96% (λ = 210 nm), > 96% (λ = 254 nm).

N-(4-Chlorophenyl)-2-cyanoacetamide (24)
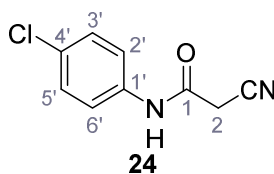
According to general procedure **A**, 4-chloroaniline (682 µL, 23.0 mmol, 1.0 eq.), 2-cyanoacetic acid (**18**, 2.16 g, 25.4 mmol, 1.1 eq.) and DCC (5.23 g, 25.4 mmol, 1.1 eq.) in DMF (20 mL) were used to yield amide **24** as colorless crystals (3.46 g, 17.8 mmol, 77%). Analytical data are in accordance with literature[180].

R$_f$ = 0.14 (3:2 hexanes/acetone).

m.p.: 207 °C. [lit.[180]: 179 °C]

^{1}H NMR (500 MHz, (CD$_3$)$_2$SO) δ/ppm = 10.42 (s, 1H, NH), 7.62 – 7.51 (m, 2H, 2'-H, 6'-H), 7.50 – 7.27 (m, 2H, 3'-H, 5'-H), 3.91 (s, 2H, 2-H).

^{13}C NMR (126 MHz, (CD$_3$)$_2$SO) δ/ppm = 161.2 (C-1), 137.3 (C-1'), 128.8 (C-3', C-5'), 127.5 (C-4'), 120.8 (C-2', C-6'), 115.8 (CN), 26.8 (C-2).

IR (ATR) $\tilde{\nu}_{max}$/cm^{-1} = 3264, 3200, 3132, 3083, 1664, 1610, 1548, 1491, 832.

HRMS (ESI): calcd. for C$_9$H$_6$^{35}ClN$_2$O (M-H)$^-$ 193.01741; found 193.01750.

Purity (HPLC): > 96% (λ = 210 nm), > 96% (λ = 254 nm).

N-(4-Bromophenyl)-2-cyanoacetamide (25)
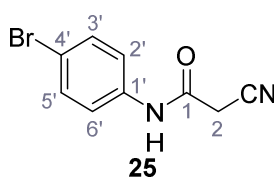
According to general procedure **A**, 4-bromoaniline (2.00 mL, 17.1 mmol, 1.0 eq.), 2-cyanoacetic acid (**18**, 1.60 g, 18.8 mmol, 1.1 eq.) and DCC (3.88 g, 18.8 mmol, 1.1 eq.) in DMF (20 mL) were used to yield amide **25** as colorless crystals (1.62 g, 6.76 mmol, 40%). Analytical data are in accordance with literature[180].

R$_f$ = 0.14 (4:1 hexanes/acetone).

m.p.: 186 °C. [lit.[180]: 185 °C]

¹H NMR (400 MHz, (CD₃)₂SO) δ/ppm = 10.42 (s, 1H, NH), 7.52 (s, 4H, 2'-H, 3'-H, 5'-H, 6'-H), 3.90 (s, 2H, 2-H).

¹³C NMR (101 MHz, (CD₃)₂SO) δ/ppm = 161.2 (C-1), 137.7 (C-1'), 131.7 (C-2', C-6' or C-3', C-5'), 121.2 (C-2', C-6' or C-3', C-5'), 115.8 (C-4'), 115.5 (CN), 26.8 (C-2).

IR (ATR) $\tilde{v}_{max}$/cm⁻¹ = 3322, 2927, 2849, 1608, 1547, 1245, 828.

HRMS (ESI): calcd. for $C_9H_6{}^{79}BrN_2O$ (M-H)⁻ 236.96690; found 236.96692.

Purity (HPLC): > 96% (λ = 210 nm), > 96% (λ = 254 nm).

2-Cyano-*N*-(4-fluorophenyl)acetamide (26)
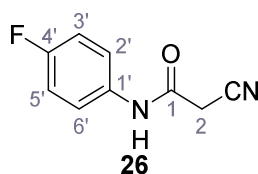
According to general procedure **A**, 4-fluoroaniline (2.16 mL, 22.5 mmol, 1.0 eq.), 2-cyanoacetic acid (**18**, 1.91 g, 22.5 mmol, 1.0 eq.) and DCC (4.64 g, 22.5 mmol, 1.0 eq.) in DMF (20 mL) were used to yield amide **26** as colorless crystals (3.00 g, 16.9 mmol, 75%). Analytical data are in accordance with literature[181].

R$_f$ = 0.11 (4:1 hexanes/acetone).

m.p.: 179 °C. [lit.[181]: 158 – 160 °C]

¹H NMR (400 MHz, (CD₃)₂SO) δ/ppm = 10.34 (s, 1H, NH), 7.66 – 7.46 (m, 2H, 2'-H, 6'-H), 7.27 – 7.09 (m, 2H, 3'-H, 5'-H), 3.89 (s, 2H, 2-H).

¹³C NMR (101 MHz, (CD₃)₂SO) δ/ppm = 161.0 (C-1), 158.3 (d, J_{CF} = 240.5 Hz, C-4'), 134.7 (d, J_{CF} = 2.7 Hz, C-1'), 121.1 (d, J_{CF} = 7.9 Hz, C-2', C-6'), 115.9 (CN), 115.5 (d, J_{CF} = 22.3 Hz, C-3', C-5'), 26.6 (C-2).

IR (ATR) $\tilde{v}_{max}$/cm⁻¹ = 3274, 3166, 3107, 1662, 1623, 1566, 1505, 834.

HRMS (ESI): calcd. for $C_9H_6FN_2O$ (M-H)⁻ 177.04696; found 177.04687.

Purity (HPLC): > 96% (λ = 210 nm), > 96% (λ = 254 nm).

2-Cyano-*N*-(4-iodophenyl)acetamide (27)
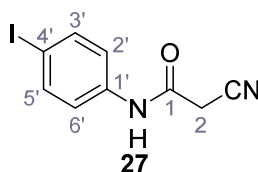
According to general procedure **A**, 4-iodoaniline (4.50 g, 20.5 mmol, 1.0 eq.), 2-cyanoacetic acid (**18**, 17.5 g, 20.5 mmol, 1.0 eq.) and DCC (4.24 g, 20.5 mmol, 1.0 eq.) in DMF (20 mL) were used to yield amide **27** as pale blue crystals (4.50 g, 15.7 mmol, 77%). The compound is literature known, but no analytical data are available[91].

R$_f$ = 0.11 (4:1 hexanes/acetone).

m.p.: 218 °C.

^{1}H NMR (400 MHz, (CD$_3$)$_2$SO) δ/ppm = 10.38 (s, 1H, NH), 7.78 – 7.60 (m, 2H, 3'-H, 5'-H), 7.49 – 7.29 (m, 2H, 2'-H, 6'-H), 3.90 (s, 2H, 2-H).

^{13}C NMR (101 MHz, (CD$_3$)$_2$SO) δ/ppm = 161.2 (C-1), 138.2 (C-1'), 137.6 (C-3', C-5'), 121.4 (C-2', C-6'), 115.8 (CN), 87.6 (C-4'), 26.8 (C-2).

IR (ATR) $\tilde{v}_{max}$/cm^{-1} = 3265, 3188, 3113, 3078, 1666, 1543, 1391, 1299, 823.

HRMS (ESI): calcd. for C$_9$H$_6$IN$_2$O (M-H)$^-$ 284.95303; found 284.95302.

Purity (HPLC): > 96% (λ = 210 nm), > 96% (λ = 254 nm).

2-Cyano-*N*-(4-nitrophenyl)acetamide (28)
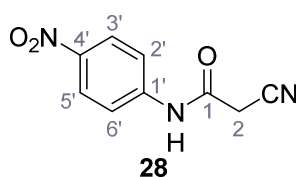
According to general procedure **A**, 4-nitroaniline (696 µL, 7.24 mmol, 1.0 eq.), 2-cyanoacetic acid (**18**, 616 mg, 7.24 mmol, 1.0 eq.) and DCC (1.49 g, 7.24 mmol, 1.0 eq.) in DMF (20 mL) were used to yield amide **28** as yellow solid (918 mg, 4.47 mmol, 62%). Analytical data are in accordance with literature[182].

R$_f$ = 0.11 (4:1 hexanes/acetone).

m.p.: 218 °C. [lit.[182]: 220 °C]

^{1}H NMR (400 MHz, (CD$_3$)$_2$SO) δ/ppm = 10.88 (s, 1H, NH), 8.35 – 8.15 (m, 2H, 3'-H, 5'-H), 7.93 – 7.71 (m, 2H, 2'-H, 6'-H), 4.00 (s, 2H, 2-H).

^{13}C NMR (101 MHz, (CD$_3$)$_2$SO) δ/ppm = 162.2 (C-1), 144.4 (C-1'), 142.7 (C-4'), 125.1 (C-3', C-5'), 119.0 (C-2', C-6'), 115.5 (CN), 27.2 (C-2).

IR (ATR) $\tilde{v}_{max}$/cm^{-1} = 3287, 1673, 1562, 1503, 1336, 1259, 860, 748.

HRMS (ESI): calcd. for C$_9$H$_6$N$_3$O$_3$ (M-H)$^-$ 204.04146; found 204.04146.

Purity (HPLC): > 96% (λ = 210 nm), > 96% (λ = 254 nm).

2-Cyano-*N*-(4-cyanophenyl)acetamide (29)
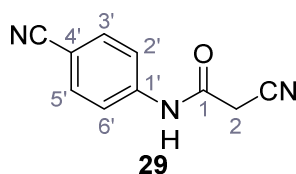
According to general procedure **A**, 4-aminobenzonitrile (1.00 g, 8.46 mmol, 1.0 eq.), 2-cyanoacetic acid (**18**, 7.20 g, 8.46 mmol, 1.0 eq.) and DCC (1.75 g, 8.46 mmol, 1.0 eq.) in DMF (10 mL) were used to yield amide **29** as yellow solid (1.22 g, 6.57 mmol, 78%). The compound is literature known, but no analytical data are available[91].

R$_f$ = 0.08 (4:1 hexanes/acetone).

m.p.: 201 °C.

^{1}H NMR (500 MHz, (CD$_3$)$_2$SO) δ/ppm = 10.72 (s, 1H, NH), 7.82 – 7.78 (m, 2H, 3'-H, 5'-H), 7.74 – 7.70 (m, 2H, 2'-H, 6'-H), 3.97 (s, 2H, 2-H).

^{13}C NMR (126 MHz, (CD$_3$)$_2$SO) δ/ppm = 162.0 (C-1), 142.5 (C-1'), 133.5 (C-3', C-5'), 119.3 (C-2', C-6'), 118.9 (C-4'), 115.6 (CH$_2$$\underline{\text{C}}$N), 105.7 (CN), 27.1 (C-2).

IR (ATR) $\tilde{v}_{max}$/cm^{-1} = 3268, 3194, 3118, 2229, 1599, 1538, 1504, 845.

HRMS (ESI): calcd. for C$_{10}$H$_6$N$_3$O (M-H)$^-$ 184.05164; found 184.05161.

Purity (HPLC): > 96% (λ = 210 nm), > 96% (λ = 254 nm).

N-(4-Acetylphenyl)-2-cyanoacetamide (30)
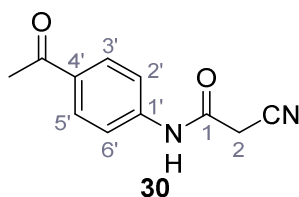
According to general procedure **A**, 4-aminoacetophenone (1.30 mL, 7.40 mmol, 1.0 eq.), 2-cyanoacetic acid (**18**, 629 mg, 7.40 mmol, 1.0 eq.) and DCC (1.53 g, 7.40 mmol, 1.0 eq.) in DMF (10 mL) were used to yield amide **30** as yellow crystals (802 mg, 3.97 mmol, 54%). Analytical data are in accordance with literature[183].

R_f = 0.37 (3:2 hexanes/acetone).

m.p.: 194 °C. [lit.[183]: 225 °C]

^{1}H NMR (500 MHz, (CD$_3$)$_2$SO) δ/ppm = 10.63 (s, 1H, NH), 7.99 – 7.91 (m, 2H, 3'-H, 5'-H), 7.74 – 7.62 (m, 2H, 2'-H, 6'-H), 3.96 (s, 2H, 2-H), 2.53 (s, 3H, CH$_3$).

^{13}C NMR (101 MHz, (CD$_3$)$_2$SO) δ/ppm = 196.5 (COCH$_3$), 161.7 (C-1), 142.6 (C-1'), 132.2 (C-4'), 129.6 (C-3', C-5'), 118.5 (C-2', C-6'), 115.7 (CN), 27.0 (C-2), 26.5 (CH$_3$).

IR (ATR) $\tilde{v}_{max}$/cm^{-1} = 3286, 2250, 1695, 1651, 1599, 1536, 1279, 1249, 833, 720.

HRMS (ESI): calcd. for C$_{11}$H$_9$N$_2$O$_2$ (M-H)$^-$ 201.06695; found 201.06694.

Purity (HPLC): > 96% (λ = 210 nm), > 96% (λ = 254 nm).

2-Cyano-*N*-(4-propoxyphenyl)acetamide (31)
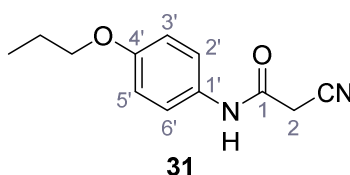
According to general procedure **A**, 4-propoxyaniline (679 µL, 4.49 mmol, 1.0 eq.), 2-cyanoacetic acid (**18**, 382 mg, 4.49 mmol, 1.0 eq.) and DCC (927 mg, 4.49 mmol, 1.0 eq.) in DMF (2.0 mL) were used to yield amide **31** as colorless crystals (604 mg, 2.77 mmol, 62%).

R_f = 0.24 (95:5 CH$_2$Cl$_2$/EtOH).

m.p.: 183 °C.

¹H NMR (400 MHz, (CD₃)₂SO) δ/ppm = 10.13 (s, 1H, NH), 7.51 – 7.38 (m, 2H, 2'-H, 6'-H), 6.98 – 6.83 (m, 2H, 3'-H, 5'-H), 3.88 (t, J = 7.1 Hz, 2H, C$\underline{H}_2$CH₂CH₃), 3.84 (s, 2H, 2-H), 1.70 (sext, J = 7.1 Hz, 2H, CH₂C$\underline{H}_2$CH₃), 0.96 (t, J = 7.1 Hz, 3H, CH₂CH₂C$\underline{H}_3$).

¹³C NMR (101 MHz, (CD₃)₂SO) δ/ppm = 160.4 (C-1), 155.1 (C-4'), 131.4 (C-1'), 120.8 (C-2', C-6'), 116.0 (CN), 114.5 (C-3', C-5'), 69.0 ($\underline{C}$H₂CH₂CH₃), 26.5 (C-2), 22.0 (CH₂$\underline{C}$H₂CH₃), 10.4 (CH₂CH₂$\underline{C}$H₃).

IR (ATR) $\tilde{v}_{max}$/cm⁻¹ = 3283, 3096, 1607, 1559, 1508, 1239, 828, 570.

HRMS (ESI): calcd. for $C_{12}H_{13}N_2O_2$ (M-H)⁻ 217.09825; found 217.09832.

Purity (HPLC): > 96% (λ = 210 nm), > 96% (λ = 254 nm).

2-Cyano-*N*-(4-(trifluoromethoxy)phenyl)acetamide (32)
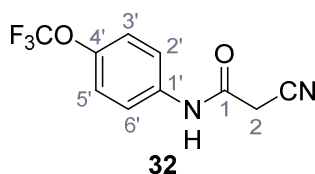
According to general procedure **A**, 4-(trifluoromethoxy)aniline (939 µL, 7.00 mmol, 1.0 eq.), 2-cyanoacetic acid (**18**, 595 mg, 7.00 mmol, 1.0 eq.) and DCC (1.44 g, 7.00 mmol, 1.0 eq.) in DMF (10 mL) were used to yield amide **32** as colorless solid (1.23 g, 5.03 mmol, 72%). The compound is literature known, but no analytical data are available[91].

R$_f$ = 0.39 (95:5 CH₂Cl₂/EtOH).

m.p.: 154 °C.

¹H NMR (400 MHz, (CD₃)₂SO) δ/ppm = 10.49 (s, 1H, NH), 7.74 – 7.55 (m, 2H, 2'-H, 6'-H), 7.47 – 7.26 (m, 2H (3'-H, 5'-H), 3.92 (s, 2H, 2-H).

¹³C NMR (101 MHz, (CD₃)₂SO) δ/ppm = 161.3 (C-1), 144.0 (C-4'), 137.5 (C-1'), 121.8 (C-3', C-5'), 120.7 (C-2', C-6'), 120.1 (q, J_{CF} = 255.7 Hz, OCF₃), 115.8 (CN), 26.8 (C-2).

IR (ATR) $\tilde{v}_{max}$/cm⁻¹ = 3278, 2975, 1667, 1616, 1557, 1508, 1277, 1205, 1171.

HRMS (ESI): calcd. for $C_{10}H_6F_3N_2O_2$ (M-H)⁻ 243.03869; found 243.03869.

Purity (HPLC): > 96% (λ = 210 nm), > 96% (λ = 254 nm).

Methyl 4-(2-cyanoacetamido)benzoate (33)
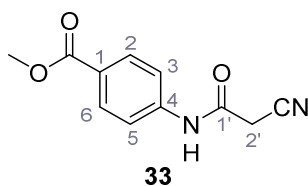
According to general procedure **A**, methyl 4-aminobenzoate (3.00 g, 19.5 mmol, 1.0 eq.), 2-cyanoacetic acid (**18**, 1.66 g, 19.5 mmol, 1.0 eq.) and DCC (4.01 g, 19.5 mmol, 1.0 eq.) in DMF (15 mL) were used to yield amide **33** as colorless solid (2.76 g, 12.6 mmol, 65%). The compound is literature known, but no analytical data are available[91].

**R$_f$** = 0.44 (3:2 hexanes/acetone).

m.p.: 162 °C.

^{1}H NMR (500 MHz, (CD$_3$)$_2$SO) δ/ppm = 10.63 (s, 1H, NH), 8.01 – 7.87 (m, 2H, 2-H, 6-H), 7.76 – 7.61 (m, 2H, 3-H, 5-H), 3.96 (s, 2H, 2-H), 3.82 (s, 3H, CH$_3$).

^{13}C NMR (126 MHz, (CD$_3$)$_2$SO) δ/ppm = 165.7 ($\underline{C}$OOCH$_3$), 161.7 (C-1'), 142.7 (C-4), 130.4 (C-2, C-6), 124.6 (C-1), 118.6 (C-3, C-5), 115.7 (CN), 52.0 (CH$_3$), 27.0 (C-2').

IR (ATR) $\tilde{v}_{max}$/cm^{-1} = 2809, 1722, 1608, 1558, 1507, 1431, 1274, 1110, 757.

HRMS (ESI): calcd. for C$_{11}$H$_9$N$_2$O$_3$ (M-H)$^-$ 217.06187; found 217.06187.

Purity (HPLC): > 96% (λ = 210 nm), > 96% (λ = 254 nm).

N-(2-Bromo-4-chlorophenyl)-2-cyanoacetamide (34)
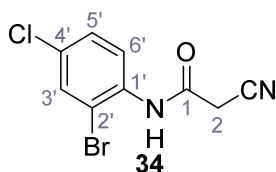
According to general procedure **A**, 2-bromo-4-chloroaniline (1.00 g, 4.84 mmol, 1.0 eq.), 2-cyanoacetic acid (**18**, 412 mg, 4.84 mmol, 1.0 eq.) and DCC (999 mg, 4.84 mmol, 1.0 eq.) in DMF (10 mL) were used to yield amide **34** as colorless crystals (919 mg, 3.36 mmol, 69%).

R$_f$ = 0.22 (3:2 hexanes/acetone).

m.p.: 157 °C.

^{1}H NMR (400 MHz, (CD$_3$)$_2$SO) δ/ppm = 9.97 (s, 1H, NH), 7.83 (d, J = 2.4 Hz, 1H, 3'-H), 7.63 (d, J = 8.7 Hz, 1H, 6'-H), 7.49 (dd, J = 8.7, 2.4 Hz, 1H, 5'-H), 3.98 (s, 2H, 2-H).

^{13}**C NMR (101 MHz, (CD$_3$)$_2$SO)** δ/ppm = 161.8 (C-1), 134.7 (C-1'), 132.0 (C-3'), 130.7 (C-4'), 128.2 (C-5'), 128.0 (C-6'), 118.5 (C-2'), 115.7 (CN), 26.1 (C-2).

IR (ATR) $\tilde{v}_{max}$/cm^{-1} = 3281, 2258, 1666, 1577, 1530, 1470, 1284, 822.

HRMS (ESI): calcd. for C$_9$H$_5$^{79}Br^{35}ClN$_2$O (M-H)$^-$ 270.92793; found 270.92809.

Purity (HPLC): > 93% (λ = 210 nm), > 93% (λ = 254 nm).

2-Cyano-*N*-(2-iodophenyl)acetamide (35)
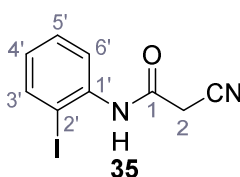
According to general procedure **A**, 2-iodoaniline (1.00 g, 4.57 mmol, 1.0 eq.), 2-cyanoacetic acid (**18**, 388 mg, 4.57 mmol, 1.0 eq.) and DCC (942 mg, 4.57 mmol, 1.0 eq.) in DMF (10 mL) were used to yield amide **35** as brown crystals (913 g, 3.19 mmol, 70%).

R$_f$ = 0.16 (4:1 hexanes/acetone).

m.p.: 161 °C.

^{1}**H NMR (400 MHz, (CD$_3$)$_2$SO)** δ/ppm = 9.88 (s, 1H, NH), 7.90 (d, *J* = 7.6 Hz, 1H, 3'-H), 7.46 – 7.38 (m, 2H, 5'-H, 6'-H), 7.03 (ddd, *J* = 8.6, 5.4, 3.6 Hz, 1H, 4'-H), 3.93 (s, 2H, 2-H).

^{13}**C NMR (101 MHz, (CD$_3$)$_2$SO)** δ/ppm = 161.4 (C-1), 139.1 (C-3'), 138.7 (C-1'), 128.8 (C-5'), 128.3 (C-4'), 127.4 (C-6'), 115.8 (CN), 96.4 (C-2'), 26.0 (C-2).

IR (ATR) $\tilde{v}_{max}$/cm^{-1} = 3252, 2263, 1658, 1577, 1542, 1433, 1015, 758, 768.

HRMS (ESI): calcd. for C$_9$H$_6$IN$_2$O (M-H)$^-$ 284.95303; found 284.95295.

Purity (HPLC): > 96% (λ = 210 nm), > 96% (λ = 254 nm).

N-(3-Chloro-2,4-difluorophenyl)-2-cyanoacetamide (36)
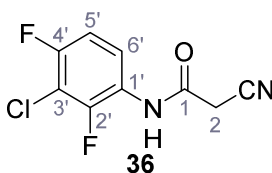
According to general procedure **A**, 3-chloro-2,4-difluoroaniline (1.06 g, 6.48 mmol, 1.0 eq.), 2-cyanoacetic acid (**18**, 551 mg, 6.48 mmol, 1.0 eq.) and DCC (1.34 g, 6.48 mmol, 1.0 eq.) in DMF (10 mL) were used to yield amide **36** as colorless crystals (1.01 g, 4.39 mmol, 68%).

R$_f$ = 0.16 (4:1 hexanes/acetone).

m.p.: 144 °C.

^{1}H NMR (400 MHz, (CD$_3$)$_2$SO) δ/ppm = 10.32 (s, 1H, NH), 7.79 (td, J = 9.0, 5.8 Hz, 1H, 6'-H), 7.33 (td, J = 9.0, 2.1 Hz, 1H, 5'-H), 3.99 (s, 2H, 2-H).

^{13}C NMR (101 MHz, (CD$_3$)$_2$SO) δ/ppm = 162.0 (C-1), 154.8 (dd, J_{CF} = 246.5, 2.0 Hz, C-2' or C-4'), 150.4 (dd, J_{CF} = 250.4, 3.3 Hz, C-2' or C-4'), 123.4 (dd, J_{CF} = 8.8, 2.4 Hz, C-6'), 123.0 (dd, J_{CF} = 11.8, 3.5 Hz, C-1'), 115.7 (CN), 111.9 (dd, J_{CF} = 21.4, 3.8 Hz, C-5'), 108.7 (dd, J_{CF} = 21.9, 19.7 Hz, C-3'), 26.3 (C-2).

IR (ATR) $\tilde{v}_{max}$/cm^{-1} = 3274.2935, 2264, 1681, 1551, 1488, 1443, 1012, 831, 628.

HRMS (ESI): calcd. for C$_9$H$_4$^{35}ClF$_2$N$_2$O (M-H)$^-$ 228.99857; found 228.99850.

Purity (HPLC): > 96% (λ = 210 nm), > 96% (λ = 254 nm).

2-Cyano-*N*-(3,4-dimethoxyphenyl)acetamide (37)
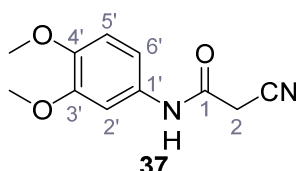
According to general procedure **A**, 3,4-dimethoxyaniline (1.00 g, 6.53 mmol, 1.0 eq.), 2-cyanoacetic acid (**18**, 555 mg, 6.53 mmol, 1.0 eq.) and DCC (1.35 g, 6.53 mmol, 1.0 eq.) in DMF (10 mL) were used to yield amide **37** as violet crystals (1.10 g, 4.99 mmol, 76%). The compound is literature known, but no analytical data are available[184].

R$_f$ = 0.05 (4:1 hexanes/acetone).

m.p.: 174 °C.

^{1}H NMR (500 MHz, (CD$_3$)$_2$SO) δ/ppm = 10.15 (s, 1H, NH), 7.21 (d, J = 2.4 Hz, 1H, 2'-H), 7.04 (dd, J = 8.7, 2.4 Hz, 1H, 6'-H), 6.90 (d, J = 8.7 Hz, 1H, 5'-H), 3.84 (s, 2H, 2-H), 3.79 – 3.66 (m, 6H, 2x OCH$_3$).

^{13}C NMR (126 MHz, (CD$_3$)$_2$SO) δ/ppm = 160.5 (C-1), 148.6 (C-3'), 145.3 (C-4'), 131.9 (C-1'), 116.0 (CN), 112.0 (C-5'), 111.2 (C-6'), 104.3 (C-2'), 55.7 (OCH$_3$), 55.4 (OCH$_3$), 26.6 (C-2).

IR (ATR) $\tilde{v}_{max}$/cm^{-1} = 3273, 2914, 2256, 1660, 1513, 1239, 1132, 1020, 837.

HRMS (ESI): calcd. for $C_{11}H_{11}N_2O_3$ (M-H)$^-$ 219.07752; found 219.07751.

Purity (HPLC): > 96% (λ = 210 nm), > 96% (λ = 254 nm).

2-Cyano-*N*-(2,3-dichlorophenyl)acetamide (38)
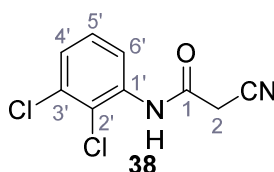
According to general procedure **A**, 2,3-dichloroaniline (745 μL, 6.30 mmol, 1.0 eq.), 2-cyanoacetic acid (**18**, 536 mg, 6.30 mmol, 1.0 eq.) and DCC (1.30 g, 6.30 mmol, 1.0 eq.) in DMF (10 mL) were used to yield amide **38** as colorless crystals (414 mg, 1.81 mmol, 29%).

R$_f$ = 0.21 (4:1 hexanes/acetone).

m.p.: 176 °C.

^{1}H NMR (500 MHz, (CD$_3$)$_2$SO) δ/ppm = 10.11 (s, 1H, NH), 7.69 (dd, *J* = 8.1, 1.3 Hz, 1H, 4'-H or 6'-H), 7.51 (dd, *J* = 8.1, 1.3 Hz, 1H, 4'-H or 6'-H), 7.38 (t, *J* = 8.1 Hz, 1H, 5'-H), 4.02 (s, 2H, 2-H).

^{13}C NMR (126 MHz, (CD$_3$)$_2$SO) δ/ppm = 161.9 (C-1), 136.1 (C-1' or C-3'), 132.0 (C-1' or C-3'), 128.2 (C-5'), 127.3 (C-4' or C-6'), 125.3 (C-2'), 124.8 (C-4' or C-6'), 115.7 (CN), 26.3 (C-2).

IR (ATR) $\tilde{v}_{max}$/cm^{-1} = 3287, 2253, 1666, 1580, 1527, 1415, 1338, 1182, 953, 788.

HRMS (ESI): calcd. for $C_9H_5{}^{35}Cl_2N_2O$ (M-H)$^-$ 226.97844; found 226.97859.

Purity (HPLC): > 96% (λ = 210 nm), > 96% (λ = 254 nm).

2-Cyano-*N*-(2,6-dibromophenyl)acetamide (39)
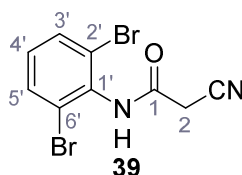
According to general procedure **A**, 2,6-dibromoaniline (1.00 g, 4.00 mmol, 1.0 eq.), 2-cyanoacetic acid (**18**, 340 mg, 4.00 mmol, 1.0 eq.) and DCC (825 mg, 4.00 mmol, 1.0 eq.) in DMF (10 mL) were used to yield amide **39** as colorless crystals (514 mg, 1.62 mmol, 40%).

R$_f$ = 0.48 (3:2 hexanes/acetone).

m.p.: 187 °C.

^{1}H NMR (500 MHz, (CD$_3$)$_2$SO) δ/ppm = 10.37 (s, 1H, NH), 7.74 (d, J = 8.1 Hz, 2H, 3'-H, 5'-H), 7.22 (t, J = 8.1 Hz, 1H, 4'-H), 3.93 (s, 2H, 2-H).

^{13}C NMR (126 MHz, (CD$_3$)$_2$SO) δ/ppm = 161.1 (C-1), 134.7 (C-1'), 132.4 (C-3', C-5'), 130.7 (C-4'), 123.9 (C-2', C-6'), 115.6 (CN), 25.4 (C-2).

IR (ATR) $\tilde{v}_{max}$/cm^{-1} = 3326, 2926, 2851, 1626, 1568, 1539, 1242, 642.

HRMS (ESI): calcd. for C$_9$H$_5$^{79}Br$_2$N$_2$O (M-H)$^-$ 314.87741; found 314.87761.

Purity (HPLC): > 96% (λ = 210 nm), > 96% (λ = 254 nm).

N-(3,5-Bis(trifluoromethyl)phenyl)-2-cyanoacetamide (40)
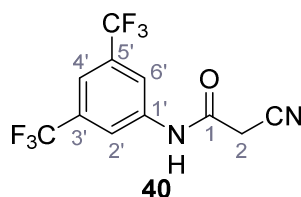
According to general procedure **A**, 3,5-bis(trifluoromethyl)aniline (1.09 mL, 7.00 mmol, 1.0 eq.), 2-cyanoacetic acid (**18**, 595 mg, 7.00 mmol, 1.0 eq.) and DCC (1.44 g, 7.00 mmol, 1.0 eq.) in DMF (10 mL) were used to yield amide **40** as colorless crystals (1.68 g, 5.67 mmol, 81%). The compound is literature known, but no analytical data are available[185].

R$_f$ = 0.43 (95:5 CH$_2$Cl$_2$/EtOH).

m.p.: 141 °C.

^{1}H NMR (500 MHz, (CD$_3$)$_2$SO) δ/ppm = 10.96 (s, 1H, NH), 8.28 – 8.12 (m, 2H, 2'-H, 6'-H), 7.90 – 7.77 (m, 1H, 4'-H), 4.00 (s, 2H, 2-H).

^{13}C NMR (126 MHz, (CD$_3$)$_2$SO) δ/ppm = 162.4 (C-1), 140.2 (C-1'), 130.9 (q, J_{CF} = 32.9 Hz, C-3', C-5'), 123.1 (q, J_{CF} = 272.7 Hz, CF$_3$), 119.2 – 118.7 (m, C-2', C-6'), 116.9 – 116.5 (m, C-4'), 115.4 (CN), 27.1 (C-2).

IR (ATR) $\tilde{v}_{max}$/cm^{-1} = 3313, 1695, 1572, 1471, 1381, 1272, 1132, 889, 703, 681.

HRMS (ESI): calcd. for $C_{11}H_5F_6N_2O$ (M-H)$^-$ 295.03116; found 295.03127.

Purity (HPLC): > 96% (λ = 210 nm), > 96% (λ = 254 nm).

2-Cyano-*N*-methyl-*N*-(4-(trifluoromethyl)phenyl)acetamide (41)
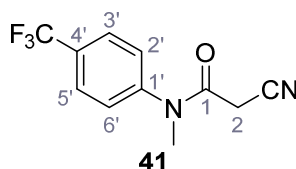
According to general procedure **A**, *N*-methyl-4-(trifluoromethyl)aniline (403 µL, 2.85 mmol, 1.0 eq.), 2-cyanoacetic acid (**18**, 243 mg, 2.85 mmol, 1.0 eq.) and DCC (589 mg, 2.85 mmol, 1.0 eq.) in DMF (10 mL) were used to yield amide **41** as colorless solid (513 mg, 2.12 mmol, 74%). Analytical data are in accordance with literature[186].

R$_f$ = 0.58 (95:5 CH$_2$Cl$_2$/EtOH).

m.p.: 70 °C. [lit.[186]: 66-68 °C]

^{1}H NMR (400 MHz, (CD$_3$)$_2$SO) δ/ppm = 7.77 (d, *J* = 8.6 Hz, 2H, 3'-H, 5'-H), 7.40 (d, *J* = 8.2 Hz, 2H, 2'-H, 6'-H), 3.34 (s, 3H, CH$_3$), 3.23 (s, 2H, 2-H).

^{13}C NMR (101 MHz, (CD$_3$)$_2$SO) δ/ppm = 161.4 (C-1), 145.6 (C-1'), 131.7 (C-4'), 127.9 (C-2', C-6' or C-3', C-5'), 127.8 (C-2', C-6' or C-3', C-5'), 123.5 (q, *J* = 271.4 Hz, CF$_3$), 113.7 (CN), 38.1 (CH$_3$), 25.6 (C-2).

IR (ATR) $\tilde{\nu}_{max}$/cm^{-1} = 3152, 2355, 1657, 1611, 1322, 1122, 1103, 1065, 848.

HRMS (ESI): calcd. for $C_{11}H_8F_3N_2O$ (M-H)$^-$ 241.05942; found 241.05939.

Purity (HPLC): > 96% (λ = 210 nm), > 96% (λ = 254 nm).

2-Cyano-*N*-(4-(trifluoromethyl)benzyl)acetamide (42)
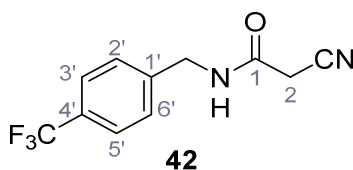
According to general procedure **A**, 4-(trifluoromethyl)benzylamine (2.50 mL, 17.5 mmol, 1.0 eq.), 2-cyanoacetic acid (**18**, 1.49 g, 17.5 mmol, 1.0 eq.) and DCC (3.62 g, 17.5 mmol, 1.0 eq.)

in DMF (15 mL) were used to yield amide **42** as colorless solid (299 mg, 1.23 mmol, 7%). Analytical data are in accordance with literature[187].

R$_f$ = 0.46 (3:2 hexanes/acetone).

m.p.: 113 °C. [lit.[187]: 128 °C]

^{1}H NMR (500 MHz, (CD$_3$)$_2$SO) δ/ppm = 8.83 (t, J = 5.7 Hz, 1H, NH), 7.74 – 7.66 (m, 2H, 3'-H, 5'-H), 7.54 – 7.44 (m, 2H, 2'-H, 6'-H), 4.38 (d, J = 5.7 Hz, 2H, CH$_2$), 3.73 (s, 2H, 2-H).

^{13}C NMR (126 MHz, (CD$_3$)$_2$SO) δ/ppm = 162.5 (C-1), 143.6 (C-1'), 128.0 (C-2', C-6'), 127.7 (q, J_{CF} = 31.7 Hz, C-4'), 125.2 (q, J_{CF} = 3.7 Hz, C-3', C-5'). 124.3 (q, J_{CF} = 272.1 Hz, CF$_3$), 116.1 (CN), 42.2 (CH$_2$), 25.3 (C-2).

IR (ATR) $\tilde{v}_{max}$/cm^{-1} = 3316, 2937, 2364, 1734, 1664, 1547, 1325, 1152, 1107, 1066.

HRMS (ESI): calcd. for C$_{11}$H$_8$F$_3$N$_2$O (M-H)$^-$ 241.05942; found 241.05949.

Purity (HPLC): > 96% (λ = 210 nm), > 96% (λ = 254 nm).

2-Cyano-3-(3,5-dichlorophenyl)-3-hydroxy-*N*-(4-(trifluoromethyl)phenyl)acrylamide – TPC2-A1-N (16)
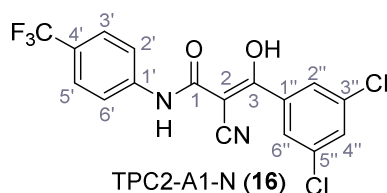
TPC2-A1-N (**16**)

According to general procedure **B**, SGA-34 (**19**, 228 mg, 1.00 mmol, 1.0 eq.) in dry THF (10 mL), NaH (92.0 mg, 2.30 mmol, 2.3 eq.) and 3,5-dichlorobenzoyl chloride (**43**, 230 mg, 1.10 mmol, 1.1 eq.) were used to yield TPC2-A1-N (**16**) as colorless crystals (276 mg, 0.688 mmol, 69%).

R$_f$ = 0.62 (4:1 hexanes/acetone).

m.p.: 202 °C. [lit.[91]: 208 – 210 °C]

^{1}H NMR (500 MHz, (CD$_3$)$_2$SO) δ/ppm = 12.36 (s, 1H, NH), 7.79 – 7.76 (m, 2H, 2'-H, 6'-H), 7.65 (t, J = 1.9 Hz, 1H, 4''-H), 7.62 – 7.60 (m, 2H, 3'-H, 5'-H), 7.59 (d, J = 1.9 Hz, 2H, 2''-H, 6''-H).

^{13}C NMR (126 MHz, (CD$_3$)$_2$SO) δ/ppm = 182.7 (C-3), 166.5 (C-1), 144.9 (C-1''), 143.6 (C-1'), 133.5 (C-3'', C-5''), 128.6 (C-4''), 126.2 – 125.9 (m, C-3', C-5' and C-2'', C-6''), 124.6 (q, J_{CF} = 286.1 Hz, CF$_3$), 123.3 (C-2), 121.8 (q, J_{CF} = 31.8 Hz, C-4'), 118.7 (C-2', C-6'), 77.7 (CN).

IR (ATR) $\tilde{v}_{max}/cm^{-1}$ = 3293, 2213, 1538, 1409, 1320, 1268, 1244, 1167, 1106, 1070, 837, 810, 660, 591.

HRMS (ESI): calcd. for $C_{17}H_8{}^{35}Cl_2F_3N_2O_2$ (M-H)⁻ 398.99204; found 398.99202.

Purity (HPLC): > 96% (λ = 210 nm), > 96% (λ = 254 nm).

2-Cyano-3-(3,5-dichlorophenyl)-3-hydroxy-*N*-phenylacrylamide – SGA-1 (44)
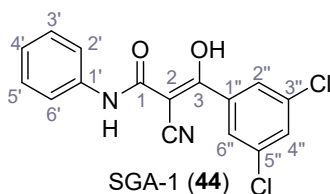
SGA-1 (**44**)

According to general procedure **B**, amide **22** (160 mg, 1.00 mmol, 1.0 eq.) in dry THF (10 mL), NaH (92.0 mg, 2.30 mmol, 2.3 eq.) and 3,5-dichlorobenzoyl chloride (**43**, 230 mg, 1.10 mmol, 1.1 eq.) were used to give SGA-1 (**44**) as yellow solid (227 mg, 0.681 mmol, 68%).

R$_f$ = 0.67 (3:2 hexanes/acetone).

m.p.: 200 °C.

¹H NMR (500 MHz, (CD₃)₂SO) δ/ppm = 11.95 (s, 1H, NH), 7.61 (t, *J* = 1.9 Hz, 1H, 4''-H), 7.56 (d, *J* = 1.9 Hz, 2H, 2''-H, 6''-H), 7.53 (dd, *J* = 8.5, 1.0 Hz, 2H, 2'-H, 6'-H), 7.27 – 7.22 (m, 2H, 3'-H, 5'-H), 6.96 – 6.90 (m, 1H, 4'-H).

¹³C NMR (126 MHz, (CD₃)₂SO) δ/ppm = 182.2 (C-3), 166.1 (C-1), 145.3 (C-1''), 140.1 (C-1'), 133.4 (C-3'', C-5''), 128.7 (C-3', C-5'), 128.3 (C-4''), 126.1 (C-2'', C-6''), 123.6 (C-2), 121.7 (C-4'), 118.8 (C-2', C-6'), 77.4 (CN).

IR (ATR) $\tilde{v}_{max}/cm^{-1}$ = 3294, 2212, 1579, 1445, 810, 748, 683.

HRMS (ESI): calcd. for $C_{16}H_9{}^{35}Cl_2N_2O_2$ (M-H)⁻ 331.00466; found 331.00465.

Purity (HPLC): > 96% (λ = 210 nm), > 96% (λ = 254 nm).

N-(4-Chlorophenyl)-2-cyano-3-(3,5-dichlorophenyl)-3-hydroxyacrylamide – SGA-2 (45)
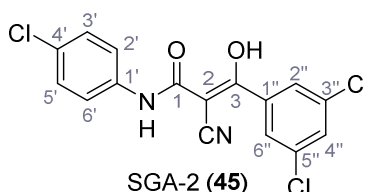
SGA-2 (**45**)

According to general procedure **B**, amide **24** (195 mg, 1.00 mmol, 1.0 eq.) in dry THF (10 mL), NaH (92.0 mg, 2.30 mmol, 2.3 eq.) and 3,5-dichlorobenzoyl chloride (**43**, 230 mg, 1.10 mmol, 1.1 eq.) were used to give SGA-2 (**45**) as yellow solid (256 mg, 0.695 mmol, 70%).

R$_f$ = 0.71 (3:2 hexanes/acetone).

m.p.: 230 °C.

^{1}H NMR (500 MHz, (CD$_3$)$_2$SO) δ/ppm = 12.12 (s, 2H, NH), 7.62 (t, *J* = 1.9 Hz, 1H, 4''-H), 7.60 – 7.57 (m, 2H, 2'-H, 6'-H), 7.55 (d, *J* = 1.9 Hz, 2H, 2''-H, 6''-H), 7.30 – 7.26 (m, 2H, 3'-H, 5'-H).

^{13}C NMR (126 MHz, (CD$_3$)$_2$SO) δ/ppm = 182.5 (C-3), 166.1 (C-1), 145.4 (C-1''), 139.1 (C-1'), 133.4 (C-3'', C-5''), 128.6 (C-3', C-5'), 128.3 (C-4''), 126.0 (C-2'', C-6''), 125.0 (C-4'), 123.6 (C-2), 120.2 (C-2', C-6'), 77.2 (CN).

IR (ATR) $\tilde{v}_{max}$/cm^{-1} = 3305, 2212, 1545, 1495, 1506, 1316, 1098, 809.

HRMS (ESI): calcd. for C$_{16}$H$_8$^{35}Cl$_3$N$_2$O$_2$ (M-H)$^-$ 364.96568; found 364.96593.

Purity (HPLC): > 96% (λ = 210 nm), > 96% (λ = 254 nm).

N-(4-Bromophenyl)-2-cyano-3-(3,5-dichlorophenyl)-3-hydroxyacrylamide – SGA-3 (46)
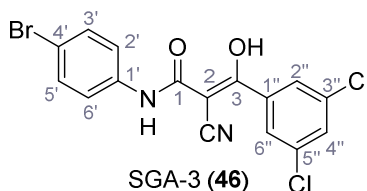
SGA-3 (**46**)

According to general procedure **B**, amide **25** (239 mg, 1.00 mmol, 1.0 eq.) in dry THF (10 mL), NaH (92.0 mg, 2.30 mmol, 2.3 eq.) and 3,5-dichlorobenzoyl chloride (**43**, 230 mg, 1.10 mmol, 1.1 eq.) were used to give SGA-3 (**46**) as yellow crystals (289 mg, 0.702 mmol, 70%).

R$_f$ = 0.73 (3:2 hexanes/acetone).

m.p.: 237 °C.

^{1}H NMR (400 MHz, (CD$_3$)$_2$SO) δ/ppm = 12.09 (s, 1H, NH), 7.62 (t, *J* = 1.9 Hz, 1H, 4''-H), 7.58 – 7.51 (m, 4H, 2'-H, 6'-H, 2''-H, 6''-H), 7.44 – 7.38 (m, 2H, 3'-H, 5'-H).

^{13}C NMR (101 MHz, (CD$_3$)$_2$SO) δ/ppm = 182.4 (C-3), 166.1 (C-1), 145.2 (C-1''), 139.4 (C-1'), 133.4 (C-3'', C-5''), 131.4 (C-3', C-5'), 128.3 (C-4''), 126.0 (C-2'', C-6''), 122.6 (C-2), 120.7 (C-2', C-6'), 112.9 (C-4'), 77.4 (CN).

IR (ATR) $\tilde{v}_{max}$/cm^{-1} = 3309, 2211, 1540, 1493, 1403, 1316, 1290, 1012, 809.

HRMS (ESI): calcd. for $C_{16}H_8{}^{79}Br^{35}Cl_2N_2O_2$ (M-H)$^-$ 408.91517; found 408.91581.

Purity (HPLC): > 96% (λ = 210 nm), > 96% (λ = 254 nm).

2-Cyano-3-(3,5-dichlorophenyl)-3-hydroxy-*N*-(*p*-tolyl)acrylamide – SGA-4 (47)
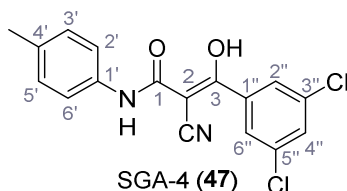
SGA-4 (**47**)

According to general procedure **B**, amide **21** (174 mg, 1.00 mmol, 1.0 eq.) in dry THF (10 mL), NaH (92.0 mg, 2.30 mmol, 2.3 eq.) and 3,5-dichlorobenzoyl chloride (**43**, 230 mg, 1.10 mmol, 1.1 eq.) were used to give SGA-4 (**47**) as yellow crystals (185 mg, 0.534 mmol, 53%).

R$_f$ = 0.28 (3:2 hexanes/acetone).

m.p.: 214 °C.

^{1}H NMR (400 MHz, (CD$_3$)$_2$SO) δ/ppm = 11.82 (s, 1H, NH), 7.63 (t, *J* = 1.9 Hz, 1H, 4''-H), 7.56 (d, *J* = 1.9 Hz, 2H, 2''-H, 6''-H), 7.46 – 7.39 (m, 2H, 2'-H, 6'-H), 7.09 – 7.02 (m, 2H, 3'-H, 5'-H), 2.24 (s, 3H, CH$_3$).

^{13}C NMR (101 MHz, (CD$_3$)$_2$SO) δ/ppm = 182.0 (C-3), 166.0 (C-1), 145.1 (C-1''), 137.4 (C-1'), 133.4 (C-3'', C-5''), 130.6 (C-4'), 129.1 (C-3', C-5'), 128.3 (C-4''), 126.1 (C-2'', C-6''), 123.5 (C-2), 119.0 (C-2', C-6'), 77.5 (CN), 20.4 (CH$_3$).

IR (ATR) $\tilde{v}_{max}$/cm^{-1} = 3299, 2212, 1543, 1518.866, 806, 654.

HRMS (ESI): calcd. for $C_{17}H_{11}{}^{35}Cl_2N_2O_2$ (M-H)$^-$ 345.02031; found 345.02052.

Purity (HPLC): > 96% (λ = 210 nm), > 96% (λ = 254 nm).

2-Cyano-3-(3,5-dichlorophenyl)-*N*-(4-fluorophenyl)-3-hydroxyacrylamide – SGA-8 (48)
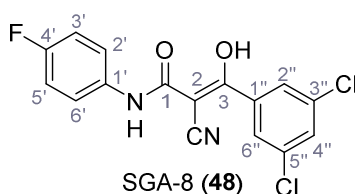
SGA-8 (**48**)

According to general procedure **B**, amide **26** (178 mg, 1.00 mmol, 1.0 eq.) in dry THF (10 mL), NaH (92.0 mg, 2.30 mmol, 2.3 eq.) and 3,5-dichlorobenzoyl chloride (**43**, 230 mg, 1.10 mmol, 1.1 eq.) were used to give SGA-8 (**48**) as white crystals (220 mg, 0.626 mmol, 63%).

R$_f$ = 0.69 (3:2 hexanes/acetone).

m.p.: 225 °C.

^{1}H NMR (400 MHz, (CD$_3$)$_2$SO) δ/ppm = 11.92 (s, 1H, NH), 7.63 (t, J = 1.9 Hz, 1H, 4''-H), 7.60 – 7.53 (m, 4H, 2'-H, 6'-H, 2''-H, 6''-H), 7.12 – 7.03 (m, 2H, 3'-H, 5'-H).

^{13}C NMR (101 MHz, (CD$_3$)$_2$SO) δ/ppm = 182.2 (C-3), 166.1 (C-1), 157.3 (d, J_{CF} = 236.9 Hz, C-4'), 144.9 (C-1''), 136.3 (d, J_{CF} = 2.4 Hz, C-1'), 133.4 (C-3'', C-5''), 128.4 (C-4''), 126.1 (C-2'', C-6''), 123.3 (C-2), 120.5 (d, J_{CF} = 7.6 Hz, C-2', C-6'), 115.2 (d, J_{CF} = 22.0 Hz, C-3', C-5'), 77.4 (CN).

IR (ATR) $\tilde{v}_{max}$/cm^{-1} = 3296, 2212, 1739, 1549, 1506, 1210, 823, 809, 645.

HRMS (ESI): calcd. for C$_{16}$H$_8$^{35}Cl$_2$FN$_2$O$_2$ (M-H)$^-$ 348.99523; found 348.99526.

Purity (HPLC): > 96% (λ = 210 nm), > 96% (λ = 254 nm).

2-Cyano-3-(3,5-dichlorophenyl)-*N*-(4-iodophenyl)-3-hydroxyacrylamide – SGA-9 (49)
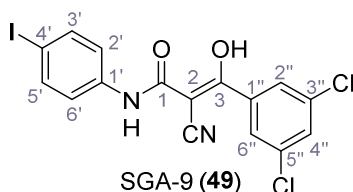
SGA-9 (**49**)

According to general procedure **B**, amide **27** (286 mg, 1.00 mmol, 1.0 eq.) in dry THF (10 mL), NaH (92.0 mg, 2.30 mmol, 2.3 eq.) and 3,5-dichlorobenzoyl chloride (**43**, 230 mg, 1.10 mmol, 1.1 eq.) were used to give SGA-9 (**49**) as yellow crystals (279 mg, 0.608 mmol, 61%).

R$_f$ = 0.71 (3:2 hexanes/acetone).

m.p.: 238 °C.

^{1}H NMR (400 MHz, (CD$_3$)$_2$SO) δ/ppm = 12.04 (s, 1H, NH), 7.63 (t, J = 1.9 Hz, 1H, 4''-H), 7.59 – 7.53 (m, 4H, 3'-H, 5'-H, 2''-H, 6''-H), 7.44 – 7.38 (m, 2H, 2'-H, 6'-H).

^{13}C NMR (101 MHz, (CD$_3$)$_2$SO) δ/ppm = 182.4 (C-3), 166.2 (C-1), 145.1 (C-1''), 139.8 (C-1'), 137.3 (C-3', C-5' or C-2'', C-6''), 133.4 (C-3'', C-5''), 128.4 (C-4''), 126.1 (C-3', C-5' or C-2'', C-6''), 123.3 (C-2), 121.1 (C-2', C-6'), 84.5 (C-4'), 77.5 (CN).

IR (ATR) $\tilde{v}_{max}$/cm^{-1} = 3303, 2217, 1592, 1523, 1485, 1314, 817, 806, 658.

HRMS (ESI): calcd. for $C_{16}H_8{}^{35}Cl_2IN_2O_2$ (M-H)$^-$ 456.90130; found 456.90014.

Purity (HPLC): > 96% (λ = 210 nm), > 96% (λ = 254 nm).

2-Cyano-3-hydroxy-3-phenyl-*N*-(4-(trifluoromethyl)phenyl)acrylamide – SGA-10 (50)
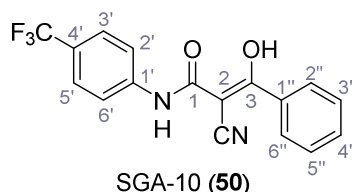
SGA-10 (**50**)

According to general procedure **B**, SGA-34 (**19**, 228 mg, 1.00 mmol, 1.0 eq.) in dry THF (10 mL), NaH (92.0 mg, 2.30 mmol, 2.3 eq.) and benzoyl chloride (128 μL, 1.10 mmol, 1.1 eq.) were used to give SGA-10 (**50**) as colorless crystals (185 mg, 0.557 mmol, 56%). Analytical data are in accordance with literature[179].

R$_f$ = 0.28 (3:2 hexanes/acetone).

m.p.: 242 °C. [lit.[179]: 245 – 247 °C]

^{1}H NMR (400 MHz, (CD$_3$)$_2$SO) δ/ppm = 12.12 (s, 1H, NH), 7.84 – 7.74 (m, 2H, 2'-H, 6'-H), 7.70 – 7.58 (m, 4H, 3'-H, 5'-H, Ph), 7.48 – 7.39 (m, 3H, Ph).

^{13}C NMR (101 MHz, (CD$_3$)$_2$SO) δ/ppm = 185.7 (C-3), 167.3 (C-1), 143.1 (C-1'), 139.7 (qPh), 135.0 (C-2), 130.0 (Ph), 127.8 (Ph), 127.6 (Ph), 126.0 (q, J_{CF} = 3.8 Hz, C-3', C-5'), 125.0 (d, J_{CF} = 270.6 Hz, CF$_3$), 122.3 (d, J_{CF} = 35.2 Hz, C-4'), 119.4 (C-2', C-6'), 77.8 (CN).

IR (ATR) $\tilde{v}_{max}$/cm^{-1} = 3283, 2216, 1592, 1550, 1309, 1109, 1067, 840, 694.

HRMS (ESI): calcd. for $C_{17}H_{10}F_3N_2O_2$ (M-H)$^-$ 331.06999; found 331.06985.

Purity (HPLC): > 96% (λ = 210 nm), > 96% (λ = 254 nm).

2-Cyano-3-(3,5-dinitrophenyl)-3-hydroxy-*N*-(4-(trifluoromethyl)phenyl)acrylamide – SGA-11 (51)
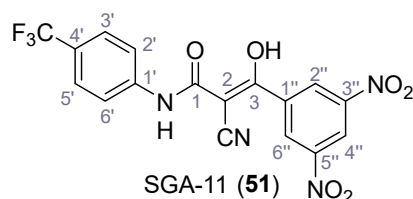
SGA-11 (**51**)

According to general procedure **B**, SGA-34 (**19**, 228 mg, 1.00 mmol, 1.0 eq.) in dry THF (10 mL), NaH (92.0 mg, 2.30 mmol, 2.3 eq.) and 3,5-dinitrobenzoyl chloride (254 mg, 1.10 mmol, 1.1 eq.) were used to give SGA-11 (**51**) as red crystals (124 mg, 0.294 mmol, 29%).

R$_f$ = 0.21 (3:2 hexanes/acetone).

m.p.: 240 °C.

^{1}H NMR (500 MHz, (CD$_3$)$_2$SO) δ/ppm = 12.32 (s, 1H, NH), 10.00 (s, 1H, OH), 8.89 – 8.80 (m, 3H, 2''-H, 4''-H, 6''-H), 7.84 – 7.75 (m, 2H, 2'-H, 6'-H), 7.67 – 7.58 (m, 2H, 3'-H, 5'-H).

^{13}C NMR (126 MHz, (CD$_3$)$_2$SO) δ/ppm = 180.5 (C-3), 166.1 (C-1), 147.6 (C-3'', C-5''), 144.4 (C-1''), 143.5 (C-1'), 127.6 (C-2'', C-6''),126.1 (q, J_{CF} = 3.5 Hz, C-3', C-5'),124.2 (q, J_{CF} = 271.0 Hz, CF$_3$), 123.3 (C-2), 121.8 (q, J_{CF} = 31.7 Hz, C-4'), 119.0 (C-4''), 118.6 (C-2', C-6'), 77.7 (CN).

IR (ATR) $\tilde{v}_{max}$/cm^{-1} = 3262, 3093, 2223, 1539, 1342, 1317, 1115, 1067, 841, 730, 703, 687.

HRMS (ESI): calcd. for C$_{17}$H$_8$F$_3$N$_4$O$_6$ (M-H)$^-$ 421.04014; found 421.04021.

Purity (HPLC): > 96% (λ = 210 nm), > 96% (λ = 254 nm).

2-Cyano-3-(3,5-dichlorophenyl)-*N*-(4-methoxyphenyl)-3-hydroxyacrylamide – SGA-12 (52)
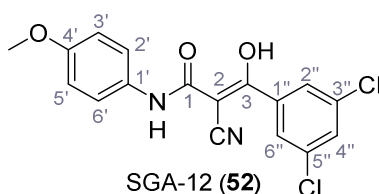
SGA-12 (**52**)

According to general procedure **B**, amide **23** (190 mg, 1.00 mmol, 1.0 eq.) in dry THF (10 mL), NaH (92.0 mg, 2.30 mmol, 2.3 eq.) and 3,5-dichlorobenzoyl chloride (**43**, 230 mg, 1.10 mmol, 1.1 eq.) were used to give SGA-12 (**52**) as yellow solid (220 mg, 0.606 mmol, 61%).

R$_f$ = 0.76 (3:2 hexanes/acetone).

m.p.: 207 °C.

^{1}H NMR (400 MHz, (CD$_3$)$_2$SO) δ/ppm = 11.36 (s, 1H, NH), 9.87 (s, 1H, OH), 7.71 (t, J = 1.8 Hz, 1H, 4'-H), 7.65 (d, J = 1.8 Hz, 2H, 2''-H, 6''-H), 7.49 – 7.41 (m, 2H, 2'-H, 6'-H), 6.90 – 6.85 (m, 2H, 3'-H, 5'-H), 3.72 (s, 3H, OCH$_3$).

¹³C NMR (101 MHz, (CD₃)₂SO) δ/ppm = 181.6 (C-3), 166.4 (C-1), 155.2 (C-4'), 142.6 (C-1''), 133.7 (C-3'', C-5''), 131.9 (C-1'), 129.3 (C-4''), 126.3 (C-2'', C-6''), 121.7 (C-2', C-6'), 121.4 (C-2), 113.9 (C-3', C-5'), 78.1 (CN), 55.2 (OCH₃).

IR (ATR) $\tilde{v}_{max}$/cm⁻¹ = 3296, 2211, 1601, 1467, 1441, 1297, 1251, 1032, 764.

HRMS (ESI): calcd. for $C_{17}H_{11}{}^{35}Cl_2N_2O_3$ (M-H)⁻ 361.01522; found 361.01516.

Purity (HPLC): > 96% (λ = 210 nm), > 96% (λ = 254 nm).

2-Cyano-3-(3,5-dichlorophenyl)-*N*-(4-nitrophenyl)-3-hydroxyacrylamide – SGA-13 (53)
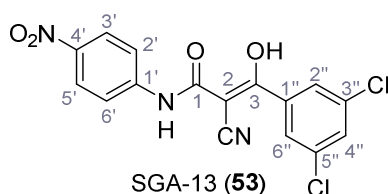
SGA-13 (**53**)

According to general procedure **B**, amide **28** (205 mg, 1.00 mmol, 1.0 eq.) in dry THF (16 mL), NaH (92.0 mg, 2.30 mmol, 2.3 eq.) and 3,5-dichlorobenzoyl chloride (**43**, 230 mg, 1.10 mmol, 1.1 eq.) were used to give SGA-13 (**53**) as yellow solid (208 mg, 0.550 mmol, 55%).

R$_f$ = 0.82 (3:2 hexanes/acetone).

m.p.: 246 °C.

¹H NMR (400 MHz, (CD₃)₂SO) δ/ppm = 12.64 (s, 1H, NH), 8.19 – 8.13 (m, 2H, 3'-H, 5'-H), 7.82 – 7.77 (m, 2H, 2'-H, 6'-H), 7.64 (t, *J* = 1.9 Hz, 1H, 4''-H), 7.57 (d, *J* = 1.9 Hz, 2H, 2''-H, 6''-H).

¹³C NMR (101 MHz, (CD₃)₂SO) δ/ppm = 181.6 (C-3), 166.9 (C-1), 149.4 (C-1''), 147.0 (C-1'), 141.3 (C-4'), 133.9 (C-3'', C-5''), 129.0 (C-4''), 126.5 (C-2'', C-6''), 125.7 (C-3', C-5'), 121.8 (C-2), 118.6 (C-2', C-6'), 77.0 (CN).

IR (ATR) $\tilde{v}_{max}$/cm⁻¹ = 3314, 2209, 1568, 1546, 1514, 1498, 1340, 1309, 847, 813, 656.

HRMS (ESI): calcd. for $C_{16}H_8{}^{35}Cl_2N_3O_4$ (M-H)⁻ 375.98973; found 375.98970.

Purity (HPLC): > 96% (λ = 210 nm), > 96% (λ = 254 nm).

2-Cyano-3-(4-nitrophenyl)-3-hydroxy-*N*-(4-(trifluoromethyl)phenyl)acrylamide – SGA-15 (54)
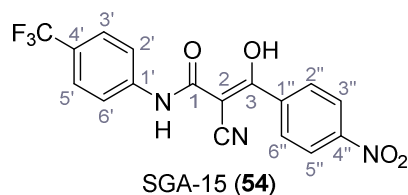
SGA-15 (**54**)

According to general procedure **B**, SGA-34 (**19**, 228 mg, 1.00 mmol, 1.0 eq.) in dry THF (10 mL), NaH (92.0 mg, 2.30 mmol, 2.3 eq.) and 4-nitrobenzoyl chloride (204 mg, 1.10 mmol, 1.1 eq.) were used to give SGA-15 (**54**) as yellow crystals (276 mg, 0.688 mmol, 69%).

R$_f$ = 0.19 (3:2 hexanes/acetone).

m.p.: 217 °C. [lit.[91]: 211 – 214 °C]

^{1}H NMR (500 MHz, (CD$_3$)$_2$SO) δ/ppm = 12.39 (s, 1H, NH), 8.28 – 8.19 (m, 2H, 3''-H, 5''-H), 7.84 – 7.80 (m, 2H, 2''-H, 6''-H), 7.78 (d, J = 8.6 Hz, 2H, 2'-H, 6'-H), 7.60 (d, J = 8.6 Hz, 2H, 3''-H, 5''-H).

^{13}C NMR (126 MHz, (CD$_3$)$_2$SO) δ/ppm = 184.3 (C-3), 166.4 (C-1), 148.1 (C-1''), 147.5 (C-4''), 143.7 (C-1'), 128.6 (C-2'', C-6''), 126.1 (q, J_{CF} = 3.6 Hz, C-3', C-5'), 124.6 (q, J_{CF} = 270.9 Hz, CF$_3$), 123.2 (C-2), 123.1 (C-3'', C-5''), 121.6 (q, J_{CF} = 32.0 Hz, C-4'), 118.6 (C-2', C-6'), 77.9 (CN).

IR (ATR) $\tilde{v}_{max}$/cm^{-1} = 3307, 2219, 1551, 1320, 1111, 1069, 844, 750, 700.

HRMS (ESI): calcd. for C$_{17}$H$_9$F$_3$N$_3$O$_4$ (M-H)$^-$ 376.05506; found 376.05509.

Purity (HPLC): > 96% (λ = 210 nm), > 96% (λ = 254 nm).

3-(4-Chlorophenyl)-2-cyano-3-hydroxy-*N*-(4-(trifluoromethyl)phenyl)acrylamide – SGA-16 (55)
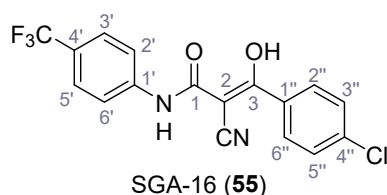
SGA-16 (**55**)

According to general procedure **B**, SGA-34 (**19**, 228 mg, 1.00 mmol, 1.0 eq.) in dry THF (10 mL), NaH (92.0 mg, 2.30 mmol, 2.3 eq.) and 4-chlorobenzoyl chloride (141 µL, 1.10 mmol, 1.1 eq.) were used to give SGA-16 (**55**) as colorless crystals (222 mg, 0.605 mmol, 61%).

R$_f$ = 0.32 (3:2 hexanes/acetone).

m.p.: 220 °C. [lit.[91]: 218 – 220 °C]

^{1}H NMR (500 MHz, (CD$_3$)$_2$SO) δ/ppm = 12.31 (s, 1H, NH), 7.81 – 7.75 (m, 2H, 2'-H, 6'-H), 7.68 – 7.63 (m, 2H, 2''-H, 6''-H), 7.63 – 7.58 (m, 2H, 3'-H, 5'-H), 7.49 – 7.44 (m, 2H, 3''-H, 5''-H).

^{13}C NMR (126 MHz, (CD$_3$)$_2$SO) δ/ppm = 184.8 (C-3), 167.0 (C-1), 143.5 (C-1'), 139.6 (C-1''), 134.1 (C-4''), 129.4 (C-2'', C-6''), 127.8 (C-3'', C-5''), 126.0 (q, J_{CF} = 3.6 Hz, C-3', C-5'), 124.6 (q, J_{CF} = 271.0 Hz, CF$_3$), 123.0 (C-2), 121.8 (q, J_{CF} = 31.0 Hz, C-4'), 118.9 (C-2', C-6'), 77.5 (CN).

IR (ATR) ṽ$_{max}$/cm^{-1} = 3282.2215, 1587, 1240, 1302, 1129, 1113, 1097, 839.

HRMS (ESI): calcd. for C$_{17}$H$_9$^{35}ClF$_3$N$_2$O$_2$ (M-H)$^-$ 365.03101; found 365.03108.

Purity (HPLC): > 96% (λ = 210 nm), > 96% (λ = 254 nm).

N-(2-Bromo-4-chlorophenyl)-2-cyano-3-(3,5-dichlorophenyl)-3-hydroxyacrylamide – SGA-27 (56)
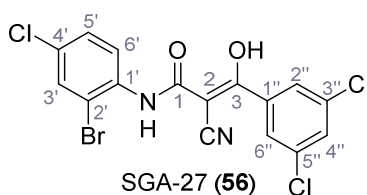
SGA-27 (**56**)

According to general procedure **B**, amide **34** (274 mg, 1.00 mmol, 1.0 eq.) in dry THF (10 mL), NaH (92.0 mg, 2.30 mmol, 2.3 eq.) and 3,5-dichlorobenzoyl chloride (**43**, 230 mg, 1.10 mmol, 1.1 eq.) were used to give SGA-27 (**56**) as colorless solid (330 mg, 0.738 mmol, 74%).

R$_f$ = 0.25 (3:2 hexanes/acetone).

m.p.: 203 °C.

^{1}H NMR (500 MHz, (CD$_3$)$_2$SO) δ/ppm = 12.29 (s, 1H, NH), 8.56 (d, J = 9.0 Hz, 1H, 6'-H), 7.68 (d, J = 2.5 Hz, 1H, 3'-H), 7.63 (t, J = 1.9 Hz, 1H, 4''-H), 7.58 (d, J = 1.9 Hz, 2H, 2''-H, 6''-H), 7.36 (dd, J = 9.0, 2.5 Hz, 1H, 5'-H).

^{13}C NMR (126 MHz, (CD$_3$)$_2$SO) δ/ppm = 182.7 (C-3), 166.4 (C-1), 145.2 (C-1''), 137.8 (C-1'), 133.4 (C-3'', C-5''), 131.4 (C-6'), 128.4 (C-4''), 127.8 (C-5'), 126.1 (C-2'', C-6''), 125.4 (C-4'), 123.5 (C-2), 122.1 (C-3'), 112.1 (C-2'), 77.3 (CN).

IR (ATR) ṽ$_{max}$/cm^{-1} = 3366, 3087, 2208, 1556, 1521, 1469, 1360, 1292, 863, 815.

HRMS (ESI): calcd. for $C_{16}H_7{}^{79}Br^{35}Cl_3N_2O_2$ (M-H)$^-$ 442.87620; found 442.87736.

Purity (HPLC): > 96% (λ = 210 nm), > 96% (λ = 254 nm).

2-Cyano-3-(3,5-dichlorophenyl)-*N*-(3,4-dimethoxyphenyl)-3-hydroxyacrylamide – SGA-28 (57)
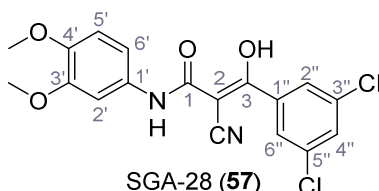
SGA-28 (**57**)

According to general procedure **B**, amide **37** (220 mg, 1.00 mmol, 1.0 eq.) in dry THF (10 mL), NaH (92.0 mg, 2.30 mmol, 2.3 eq.) and 3,5-dichlorobenzoyl chloride (**43**, 230 mg, 1.10 mmol, 1.1 eq.) were used to give SGA-28 (**57**) as yellow solid (200 mg, 0.508 mmol, 51%).

R$_f$ = 0.17 (3:2 hexanes/acetone).

m.p.: 195 °C.

^{1}H NMR (500 MHz, (CD$_3$)$_2$SO) δ/ppm = 11.52 (s, 1H, NH), 7.68 (t, *J* = 1.8 Hz, 1H, 4''-H), 7.62 (d, *J* = 1.8 Hz, 2H, 2''-H, 6''-H), 7.30 (d, *J* = 2.2 Hz, 1H, 2'-H), 7.01 (dd, *J* = 8.7, 2.2 Hz, 1H, 6'-H), 6.86 (d, *J* = 8.7 Hz, 1H, 5'-H), 3.73 (s, 3H, OCH$_3$), 3.71 (s, 3H, OCH$_3$).

^{13}C NMR (126 MHz, (CD$_3$)$_2$SO) δ/ppm = 181.7 (C-3), 166.2 (C-1), 148.6 (C-3'), 144.4 (C-4'), 143.6 (C-1''), 133.6 (C-3'', C-5''), 133.0 (C-1'), 128.9 (C-4''), 126.2 (C-2'', C-6''), 122.2 (C-2), 112.3 (C-5'), 111.5 (C-6'), 104.9 (C-2'), 77.9 (CN), 55.8 (OCH$_3$), 55.4 (OCH$_3$).

IR (ATR) $\tilde{v}_{max}$/cm^{-1} = 3284, 2217, 1608, 1549, 1516, 1238, 1028, 810.

HRMS (ESI): calcd. for $C_{18}H_{13}{}^{35}Cl_2N_2O_4$ (M-H)$^-$ 391.02579; found 391.02608.

Purity (HPLC): > 96% (λ = 210 nm), > 96% (λ = 254 nm).

2-Cyano-3-(1-methyl-1*H*-pyrrol-2-yl)-3-hydroxy-*N*-phenylacrylamide (prinomide) – SGA-31 (58)
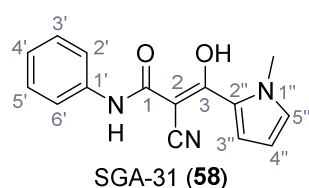
SGA-31 (**58**)

According to general procedure **B**, amide **22** (228 mg, 1.00 mmol, 1.0 eq.) in dry THF (10 mL), NaH (92.0 mg, 2.30 mmol, 2.3 eq.) and 1-methylpyrrole-2-carbonyl chloride (158 mg, 1.10 mmol, 1.1 eq.) were used to give SGA-31 (**58**) as colorless crystals (200 mg, 0.747 mmol, 75%).

R$_f$ = 0.65 (3:2 hexanes/acetone).

m.p.: 171 °C. [lit.[188]: 174 – 175 °C]

^{1}H NMR (400 MHz, CDCl$_3$) δ/ppm = 7.74 (s, 1H, NH), 7.54 (dd, J = 4.3, 1.6 Hz, 1H, 3''-H), 7.50 (d, J = 8.0 Hz, 2H, 2'-H, 6'-H), 7.44 – 7.34 (m, 2H, 3'-H, 5'-H), 7.20 (t, J = 7.4 Hz, 1H, 4'-H), 6.89 (t, J = 1.9 Hz, 1H, 5''-H), 6.25 (dd, J = 4.3, 2.5 Hz, 1H, 4''-H), 3.92 (s, 3H, CH$_3$).

^{13}C NMR (101 MHz, CDCl$_3$) δ/ppm = 175.6 (C-3), 170.0 (C-1), 136.2 (C-1'), 132.0 (C-5''), 129.3 (C-3', C-5'), 125.7 (C-4'), 124.4 (C-2''), 121.3 (C-2', C-6'), 120.7 (C-3''), 119.1 (C-2), 109.7 (C-4''), 72.6 (CN), 38.5 (CH$_3$).

IR (ATR) $\tilde{v}_{max}$/cm^{-1} = 3293, 2210, 1526, 1382, 1231, 751, 736, 687.

HRMS (ESI): calcd. for C$_{15}$H$_{12}$N$_3$O$_2$ (M-H)$^-$ 266.09350; found 266.09370.

Purity (HPLC): > 96% (λ = 210 nm), > 96% (λ = 254 nm).

2-Cyano-3-(1-methyl-1*H*-pyrrol-2-yl)-3-hydroxy-*N*-(4-(trifluoromethyl)phenyl)acrylamide – SGA-32 (59)
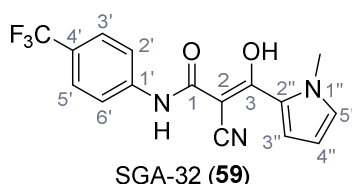
SGA-32 (**59**)

According to general procedure **B**, SGA-34 (**19**, 228 mg, 1.00 mmol, 1.0 eq.) in dry THF (10 mL), NaH (92.0 mg, 2.30 mmol, 2.3 eq.) and 1-methylpyrrole-2-carbonyl chloride (158 mg, 1.10 mmol, 1.1 eq.) were used to give SGA-32 (**59**) as colorless crystals (221 mg, 0.660 mmol, 66%).

R$_f$ = 0.57 (3:2 hexanes/acetone).

m.p.: 203 °C.

^{1}H NMR (400 MHz, CDCl$_3$) δ/ppm = 7.86 (s, 1H, NH), 7.69 – 7.61 (m, 4H, 2'-H, 6'-H, 3'-H, 5'-H), 7.57 (dd, J = 4.3, 1.6 Hz, 1H, 3''-H), 6.93 – 6.90 (m, 1H, 4''-H), 6.27 (dd, J = 4.3, 2.5 Hz, 1H, 5''-H), 3.93 (s, 3H, CH$_3$).

^{13}C NMR (101 MHz, CDCl$_3$) δ/ppm = 175.6 (C-3), 170.2 (C-1), 139.5 (C-1'), 132.6 (C-5''), 127.4 (q, J_{CF} = 31.8 Hz, C-4'), 126.6 (q, J = 3.8 Hz, C-3', C-5'), 124.1 (C-2''), 124.0 (q, J_{CF} = 271.4 Hz, CF$_3$), 121.3 (C-3''), 120.7 (C-2', C-6'), 119.0 (C-2), 110.0 (C-4''), 72.6 (CN), 38.7 (CH$_3$).

IR (ATR) $\tilde{v}_{max}$/cm^{-1} = 3273, 2210, 1518, 1379, 1228, 1111, 996, 837, 745.

HRMS (ESI): calcd. for C$_{16}$H$_{11}$F$_3$N$_3$O$_2$ (M-H)$^-$ 334.08088; found 334.08090.

Purity (HPLC): > 96% (λ = 210 nm), > 96% (λ = 254 nm).

N-(3-Chloro-2,4-difluorophenyl)-2-cyano-3-(3,5-dichlorophenyl)-3-hydroxyacrylamide – SGA-33 (60)
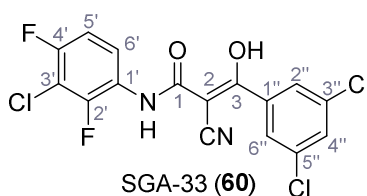
SGA-33 (**60**)

According to general procedure **B**, amide **36** (231 mg, 1.00 mmol, 1.0 eq.) in dry THF (10 mL), NaH (92.0 mg, 2.30 mmol, 2.3 eq.) and 3,5-dichlorobenzoyl chloride (**43**, 230 mg, 1.10 mmol, 1.1 eq.) were used to give SGA-33 (**60**) as colorless crystals (290 mg, 0.719 mmol, 72%).

R$_f$ = 0.15 (3:2 hexanes/acetone).

m.p.: 193 °C.

^{1}H NMR (400 MHz, (CD$_3$)$_2$SO) δ/ppm = 12.34 (s, 1H, NH), 8.43 (td, J = 9.0, 6.0 Hz, 1H, 6'-H), 7.63 (t, J = 1.9 Hz, 1H, 4''-H), 7.58 (d, J = 1.9 Hz, 2H, 2''-H, 6''-H), 7.23 (td, J = 9.2, 2.1 Hz, 1H, 5'-H).

^{13}C NMR (101 MHz, (CD$_3$)$_2$SO) δ/ppm = 182.9 (C-3), 166.3 (C-1), 152.1 (d, J_{CF} = 242.4 Hz, C-4'), 147.7 (d, J_{CF} = 245.4 Hz, C-2'), 145.0 (C-1''), 133.4 (C-3'', C-5''), 128.5 (C-4''), 126.3 (dd, J_{CF} = 10.3, 2.6 Hz, C-1'), 126.1 (C-2'', C-6''), 123.2 (C-2), 119.1 (dd, J_{CF} = 7.8, 3.0 Hz, C-6'), 111.5 (dd, J_{CF} = 20.7, 3.6 Hz, C-5'), 107.8 (dd, J_{CF} = 22.2, 2.9 Hz, C-3'), 77.3 (CN).

IR (ATR) $\tilde{v}_{max}$/cm^{-1} = 3293, 2206, 1539, 1497, 1370, 1289, 1023, 803.

HRMS (ESI): calcd. for C$_{16}$H$_6$^{35}Cl$_3$F$_2$N$_2$O$_2$ (M-H)$^-$ 400.94684; found 400.94724.

Purity (HPLC): > 96% (λ = 210 nm), > 96% (λ = 254 nm).

2-Cyano-*N*-(4-cyanophenyl)-3-(3,5-dichlorophenyl)-3-hydroxyacrylamide – SGA-38 (61)

SGA-38 (**61**)

According to general procedure **B**, amide **29** (185 mg, 1.00 mmol, 1.0 eq.) in dry THF (10 mL), NaH (92.0 mg, 2.30 mmol, 2.3 eq.) and 3,5-dichlorobenzoyl chloride (**43**, 230 mg, 1.10 mmol, 1.1 eq.) were used to give SGA-38 (**61**) as yellow solid (137 mg, 0.382 mmol, 38%).

R$_f$ = 0.12 (3:2 hexanes/acetone).

m.p.: 236 °C.

^{1}H NMR (500 MHz, (CD$_3$)$_2$SO) δ/ppm = 12.42 (s, 1H, NH), 7.75 – 7.72 (m, 2H, 3'-H, 5'-H), 7.71 – 7.67 (m, 2H, 2'-H, 6'-H), 7.64 (t, *J* = 1.9 Hz, 1H, 4''-H), 7.57 (d, *J* = 1.9 Hz, 2H, 2''-H, 6''-H).

^{13}C NMR (126 MHz, (CD$_3$)$_2$SO) δ/ppm = 183.0 (C-3), 166.4 (C-1), 145.1 (C-1''), 144.3 (C-1'), 133.5 (C-3'', C-5''), 133.3 (C-3', C-5'), 128.5 (C-4''), 126.0 (C-2'', C-6''), 123.2 (C-4'), 119.4 (C-2), 118.8 (C-2', C-6'), 103.1 (4'-CN), 77.4 (2-CN).

IR (ATR) $\tilde{v}_{max}$/cm^{-1} = 3321, 2360, 2340, 1533, 839, 655.

HRMS (ESI): calcd. for C$_{17}$H$_8$^{35}Cl$_2$N$_3$O$_2$ (M-H)$^-$ 355.99991; found 356.00057.

Purity (HPLC): > 96% (λ = 210 nm), > 96% (λ = 254 nm).

2-Cyano-3-(3,5-dichlorophenyl)-3-hydroxy-*N*-(2-iodophenyl)acrylamide – SGA-39 (62)
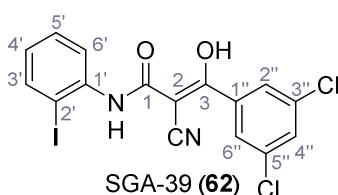
SGA-39 (**62**)

According to general procedure **B**, amide **35** (286 mg, 1.00 mmol, 1.0 eq.) in dry THF (10 mL), NaH (92.0 mg, 2.30 mmol, 2.3 eq.) and 3,5-dichlorobenzoyl chloride (**43**, 230 mg, 1.10 mmol, 1.1 eq.) were used to give SGA-39 (**62**) as yellow solid (237 mg, 0.515 mmol, 52%).

R$_f$ = 0.20 (3:2 hexanes/acetone).

m.p.: 171 °C.

^{1}H NMR (400 MHz, (CD$_3$)$_2$SO) δ/ppm = 11.87 (s, 1H, NH), 8.27 (dd, J = 8.3, 1.5 Hz, 1H, 6'-H), 7.80 (dd, J = 7.9, 1.5 Hz, 1H, 3'-H), 7.63 (t, J = 1.9 Hz, 1H, 4''-H), 7.59 (d, J = 1.9 Hz, 2H, 2''-H, 6''-H), 7.29 (ddd, J = 8.4, 7.3, 1.5 Hz, 1H, 5'-H), 6.80 – 6.67 (m, 1H, 4'-H).

^{13}C NMR (126 MHz, (CD$_3$)$_2$SO) δ/ppm = 182.2 (C-3), 166.4 (C-1), 145.1 (C-1''), 141.5 (C-1'), 139.0 (C-3'), 133.4 (C-3'', C-5''), 128.4 (C-4''), 128.3 (C-5'), 126.1 (C-2'', C-6''), 124.0 (C-4'), 123.6 (C-2), 122.1 (C-6'), 89.2 (C-2'), 77.2 (CN).

IR (ATR) $\tilde{v}_{max}$/cm^{-1} = 3337, 2213, 1579, 1537, 1294, 742.

HRMS (ESI): calcd. for C$_{16}$H$_8{}^{35}$Cl$_2$IN$_2$O$_2$ (M-H)$^-$ 456.90130; found 456.90095.

Purity (HPLC): > 96% (λ = 210 nm), > 96% (λ = 254 nm).

2-Cyano-3-hydroxy-3-(perfluorophenyl)-*N*-(4-(trifluoromethyl)phenyl)acrylamide – SGA-40 (63)
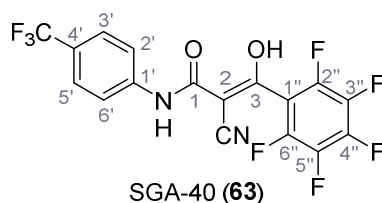
SGA-40 (**63**)

According to general procedure **B**, SGA-34 (**19**, 228 mg, 1.00 mmol, 1.0 eq.) in dry THF (10 mL), NaH (92.0 mg, 2.30 mmol, 2.3 eq.) and 2,3,4,5,6-pentafluorobenzoyl chloride (158 µL, 1.10 mmol, 1.1 eq.) were used to give SGA-40 (**63**) as colorless crystals (236 mg, 0.560 mmol, 56%).

R$_f$ = 0.28 (3:2 hexanes/acetone).

m.p.: 161 °C.

^{1}H NMR (400 MHz, (CD$_3$)$_2$SO) δ/ppm = 11.70 (s, 1H, NH), 7.81 – 7.72 (m, 2H, 2'-H, 6'-H), 7.67 – 7.56 (m, 2H, 3'-H, 5'-H).

^{13}C NMR (101 MHz, (CD$_3$)$_2$SO) δ/ppm = 172.6 (C-3), 164.9 (C-1), 143.9 – 140.9 (m, C-2'', C-6'' or C-3'', C-5''), 143.3 (C-1'), 141.9 – 138.9 (m, C-4''), 138.5 – 135.1 (m, C-2'', C-6'' or C-3'', C-5''), 126.1 (q, J_{CF} = 3.6 Hz, C-3', C-5'), 124.6 (q, J_{CF} = 271.0 Hz, CF$_3$), 122.0 (q, J_{CF} = 31.9 Hz, C-4'), 117.5 – 117.0 (m, C-1''), 121.7 (C-2', C-6'), 118.7 (C-2), 81.8 (CN).

IR (ATR) $\tilde{v}_{max}$/cm^{-1} = 2230, 1590, 1543, 1524, 1497, 1323, 1116, 1000, 839.

HRMS (ESI): calcd. for C$_{17}$H$_5$F$_8$N$_2$O$_2$ (M-H)$^-$ 421.02288; found 421.02337.

Purity (HPLC): > 96% (λ = 210 nm), > 96% (λ = 254 nm).

2-Cyano-3-(3,5-dibromophenyl)-3-hydroxy-*N*-(4-(trifluoromethyl)phenyl)acrylamide – SGA-70 (64)
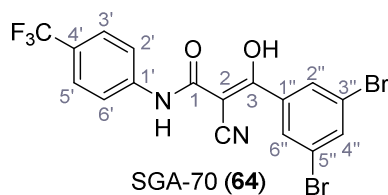
SGA-70 (**64**)

According to general procedure **B**, SGA-34 (**19**, 228 mg, 1.00 mmol, 1.0 eq.) in dry THF (10 mL), NaH (92.0 mg, 2.30 mmol, 2.3 eq.) and 3,5-dibromobenzoic acid (308 mg, 1.10 mmol, 1.1 eq., converted into the corresponding aryl chloride) were used to give SGA-70 (**64**) as light yellow crystals (206 mg, 0.420 mmol, 42%).

R$_f$ = 0.32 (3:2 hexanes/acetone).

m.p.: 211 °C.

^{1}H NMR (400 MHz, (CD$_3$)$_2$SO) δ/ppm = 12.32 (s, 1H, NH), 8.96 (s, 1H, OH), 7.91 – 7.81 (m, 1H, 4''-H), 7.78 – 7.72 (m, 4H, 2'-H, 6'-H, 2''-H, 6''-H), 7.65 – 7.55 (m, 2H, 3'-H, 5'-H).

^{13}C NMR (101 MHz, (CD$_3$)$_2$SO) δ/ppm = 182.5 (C-3), 166.4 (C-1), 145.5 (C-1''), 143.6 (C-1'), 133.7 (C-4''), 129.2 (C-2'', C-6''), 126.0 (q, J_{CF} = 3.5 Hz, C-3', C-5'), 123.9 (q, J_{CF} = 271.2 Hz, CF$_3$), 123.3 (C-2), 121.8 (C-3'', C-5''), 121.6 (q, J_{CF} = 31.9 Hz, C-4'), 118.5 (C-2', C-6'), 77.4 (CN).

IR (ATR) $\tilde{v}_{max}$/cm^{-1} = 2218, 1594, 1538, 1315, 1166, 1109, 1068, 838, 750.

HRMS (ESI): calcd. for C$_{17}$H$_8$^{79}Br$_2$F$_3$N$_2$O$_2$ (M-H)$^-$ 486.89101; found 486.89128.

Purity (HPLC): > 96% (λ = 210 nm), > 96% (λ = 254 nm).

2-Cyano-3-hydroxy-3-(2,4,6-trichlorophenyl)-*N*-(4-(trifluoromethyl)phenyl)acrylamide – SGA-71 (65)
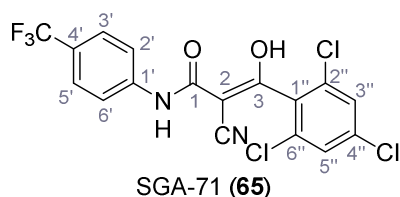
SGA-71 (**65**)

According to general procedure **B**, SGA-34 (**19**, 228 mg, 1.00 mmol, 1.0 eq.) in dry THF (10 mL), NaH (92.0 mg, 2.30 mmol, 2.3 eq.) and 2,4,6-trichlorobenzoyl chloride (172 µL,

1.10 mmol, 1.1 eq.) were used to give SGA-71 (**65**) as colorless crystals (158 mg, 0.363 mmol, 36%).
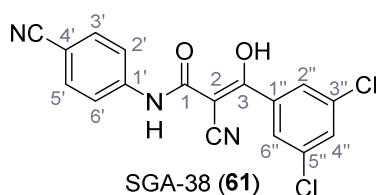
R$_f$ = 0.14 (3:2 hexanes/acetone).

m.p.: 220 °C.

^{1}H NMR (500 MHz, (CD$_3$)$_2$SO) δ/ppm = 11.92 (s, 1H, NH), 7.79 – 7.74 (m, 2H, 2'-H, 6'-H), 7.66 (s, 2H, 3''-H, 5''-H), 7.63 – 7.58 (m, 2H, 3'-H, 5'-H).

^{13}C NMR (126 MHz, (CD$_3$)$_2$SO) δ/ppm = 180.7 (C-3), 165.7 (C-1), 143.6 (C-1'), 139.5 (C-1''), 133.1 (C-4''), 132.0 (C-2'', C-6''), 127.8 (C-3'', C-5''), 126.1 (q, J_{CF} = 3.6 Hz, C-3', C-5'), 124.6 (q, J_{CF} = 271.1 Hz, CF$_3$), 121.9 (C-2), 121.6 (q, J_{CF} = 31.9 Hz, C-4'), 118.4 (C-2', C-6'), 79.5 (CN).

IR (ATR) $\tilde{v}_{max}$/cm^{-1} = 2230, 1598, 1541, 1318, 1116, 841.

HRMS (ESI): calcd. for C$_{17}$H$_7$^{35}Cl$_3$F$_3$N$_2$O$_2$ (M-H)$^-$ 432.95307; found 432.95394.

Purity (HPLC): > 96% (λ = 210 nm), > 96% (λ = 254 nm).

N-(4-Bromophenyl)-2-cyano-3-hydroxy-3-(2,4,6-trichlorophenyl)acrylamide – SGA-72 (66)
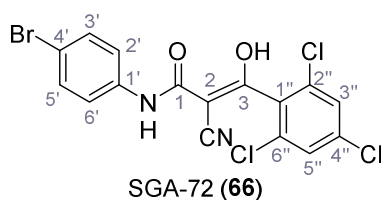
SGA-72 (**66**)

According to general procedure **B**, amide **25** (239 mg, 1.00 mmol, 1.0 eq.) in dry THF (10 mL), NaH (92.0 mg, 2.30 mmol, 2.3 eq.) and 2,4,6-trichlorobenzoyl chloride (172 µL, 1.10 mmol, 1.1 eq.) were used to give SGA-72 (**66**) as colorless solid (227 mg, 0.507 mmol, 51%).

R$_f$ = 0.14 (3:2 hexanes/acetone).

m.p.: 191 °C.

^{1}H NMR (400 MHz, (CD$_3$)$_2$SO) δ/ppm = 11.69 (s, 1H, NH), 7.65 (s, 2H, 3''-H, 5''-H), 7.58 – 7.52 (m, 2H, 2'-H, 6'-H), 7.44 – 7.38 (m, 2H, 3'-H, 5'-H).

^{13}C NMR (101 MHz, (CD$_3$)$_2$SO) δ/ppm = 180.3 (C-3), 165.4 (C-1), 139.6 (C-1' or C-1''), 139.4 (C-1' or C-1''), 133.0 (C-4''), 132.0 (C-2'', C-6''), 131.5 (C-3', C-5'), 127.8 (C-3'', C-5''), 122.1 (C-2), 120.5 (C-2', C-6'), 112.9 (C-4'), 79.5 (CN).

IR (ATR) $\tilde{v}_{max}$/cm^{-1} = 2238, 1588, 1539, 1488, 1307, 856, 818.

HRMS (ESI): calcd. for $C_{16}H_7{}^{79}Br{}^{35}Cl_3N_2O_2$ (M-H)$^-$ 442.87620; found 442.87747.

Purity (HPLC): > 96% (λ = 210 nm), > 96% (λ = 254 nm).

N-(3-Chloro-2,4-difluorophenyl)-2-cyano-3-hydroxy-3-(2,4,6-trichlorophenyl)acrylamide – SGA-73 (67)
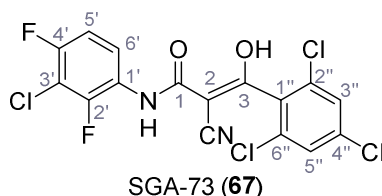
SGA-73 (**67**)

According to general procedure **B**, amide **36** (231 mg, 1.00 mmol, 1.0 eq.) in dry THF (10 mL), NaH (92.0 mg, 2.30 mmol, 2.3 eq.) and 2,4,6-trichlorobenzoyl chloride (172 µL, 1.10 mmol, 1.1 eq.) were used to give SGA-73 (**67**) as colorless solid (217 mg, 0.496 mmol, 50%).

R$_f$ = 0.16 (1:1 hexanes/acetone).

m.p.: 199 °C.

^{1}H NMR (500 MHz, (CD$_3$)$_2$SO) δ/ppm = 11.93 (s, 1H, NH), 8.45 (td, *J* = 9.1, 5.9 Hz, 1H, 6'-H), 7.66 (s, 2H, 3''-H, 5''-H), 7.23 (td, *J* = 9.2, 2.0 Hz, 1H, 5'-H).

^{13}C NMR (126 MHz, (CD$_3$)$_2$SO) δ/ppm = 180.8 (C-3), 165.6 (C-1), 152.1 (d, J_{CF} = 242.6 Hz, C-4'), 147.5 (d, J_{CF} = 245.6 Hz, C-2'), 139.4 (C-1'' or C-4''), 133.1 (C-1'' or C-4''), 132.0 (C-2'', C-6''), 127.8 (C-3'', C-5''), 126.3 (dd, J_{CF} = 10.2, 3.2 Hz, C-1'), 121.8 (C-2), 118.8 (dd, J_{CF} = 7.9, 2.9 Hz, C-6'), 111.5 (dd, J_{CF} = 20.7, 3.5 Hz, C-5'), 107.9 (dd, J_{CF} = 22.0, 19.2 Hz, C-3'), 79.4 (CN).

IR (ATR) $\tilde{v}_{max}$/cm^{-1} = 3279, 2222, 1626, 1590, 1519, 1484, 1445, 1359, 1275, 1017, 816, 631.

HRMS (ESI): calcd. for $C_{16}H_5{}^{35}Cl_4F_2N_2O_2$ (M-H)$^-$ 434.90787; found 434.90791.

Purity (HPLC): > 96% (λ = 210 nm), > 96% (λ = 254 nm).

N-(4-Bromophenyl)-2-cyano-3-(3,5-dibromophenyl)-3-hydroxyacrylamide – SGA-75 (68)
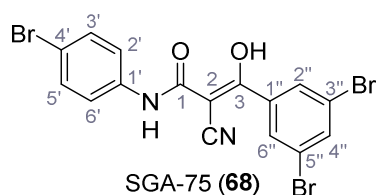
According to general procedure **B**, amide **25** (239 mg, 1.00 mmol, 1.0 eq.) in dry THF (10 mL), NaH (92.0 mg, 2.30 mmol, 2.3 eq.) and 3,5-dibromobenzoic acid (308 mg, 1.10 mmol, 1.1 eq.; converted into the corresponding aryl chloride) were used to give SGA-75 (**68**) as colorless crystals (222 mg, 0.443 mmol, 44%).

R$_f$ = 0.20 (3:2 hexanes/acetone).

m.p.: 233 °C.

^{1}H NMR (400 MHz, (CD$_3$)$_2$SO) δ/ppm = 12.05 (s, 1H, NH), 7.86 (t, J = 1.8 Hz, 1H, 4'-H), 7.73 (d, J = 1.8 Hz, 2H, 2''-H, 6''-H), 7.57 – 7.50 (m, 2H, 2'-H, 6'-H), 7.46 – 7.37 (m, 2H, 3'-H, 5'-H).

^{13}C NMR (101 MHz, (CD$_3$)$_2$SO) δ/ppm = 182.2 (C-3), 166.1 (C-1), 145.5 (C-1''), 139.4 (C-1'), 133.7 (C-4''), 131.5 (C-3', C-5'), 129.2 (C-2'', C-6''), 122.7 (C-2), 121.8 (C-3'', C-5''), 120.8 (C-2', C-6'), 113.0 (C-4'), 77.4 (CN).

IR (ATR) $\tilde{v}_{max}$/cm^{-1} = 3314, 2214, 1596, 1543, 865, 817, 748, 658.

HRMS (ESI): calcd. for C$_{16}$H$_8$^{79}Br$_3$N$_2$O$_2$ (M-H)$^-$ 496.81414; found 496.81449.

Purity (HPLC): > 96% (λ = 210 nm), > 96% (λ = 254 nm).

N-(4-Acetylphenyl)-2-cyano-3-(3,5-dichlorophenyl)-3-hydroxyacrylamide – SGA-76 (69)
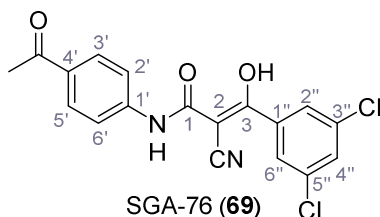
According to general procedure **B**, amide **30** (202 mg, 1.00 mmol, 1.0 eq.) in dry THF (10 mL), NaH (92.0 mg, 2.30 mmol, 2.3 eq.) and 3,5-dichlorobenzoyl chloride (**43**, 230 mg, 1.10 mmol, 1.1 eq.) were used to give SGA-76 (**69**) as off white solid (296 mg, 0.789 mmol, 79%).

R$_f$ = 0.08 (3:2 hexanes/acetone).

m.p.: 209 °C.

¹H NMR (500 MHz, (CD₃)₂SO) δ/ppm = 12.32 (s, 1H, NH), 7.91 – 7.86 (m, 2H, 3'-H, 5'-H), 7.71 – 7.66 (m, 2H, 2'-H, 6'-H), 7.64 (t, J = 1.9 Hz, 1H, 4''-H), 7.58 (d, J = 1.9 Hz, 2H, 2''-H, 6''-H), 2.51 (s, 3H, CH₃, collapses with DMSO).

¹³C NMR (101 MHz, (CD₃)₂SO) δ/ppm = 196.3 (CO), 182.8 (C-3), 166.3 (C-1), 145.1 (C-1''), 144.5 (C-1'), 133.5 (C-3'', C-5''), 130.4 (C-4'), 129.7 (C-3', C-5'), 128.5 (C-4''), 126.1 (C-2'', C-6''), 123.3 (C-2), 117.9 (C-2', C-6'), 77.6 (CN), 26.3 (CH₃).

IR (ATR) $\tilde{v}_{max}$/cm⁻¹ = 3304, 2207, 1682, 1596, 1544, 1355, 1272, 809.

HRMS (ESI): calcd. for $C_{18}H_{11}{}^{35}Cl_2N_2O_3$ (M-H)⁻ 373.01522; found 373.01580.

Purity (HPLC): > 96% (λ = 210 nm), > 96% (λ = 254 nm).

2-Cyano-*N*-(2,6-dibromophenyl)-3-(3,5-dichlorophenyl)-3-hydroxyacrylamide – SGA-77 (70)
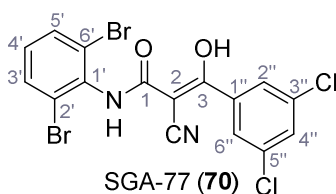
SGA-77 (**70**)

According to general procedure **B**, amide **39** (318 mg, 1.00 mmol, 1.0 eq.) in dry THF (10 mL), NaH (92.0 mg, 2.30 mmol, 2.3 eq.) and 3,5-dichlorobenzoyl chloride (**43**, 230 mg, 1.10 mmol, 1.1 eq.) were used to give SGA-77 (**70**) as colorless crystals (66.0 mg, 0.134 mmol, 13%).

R$_f$ = 0.78 (3:2 hexanes/acetone).

m.p.: 226 °C.

¹H NMR (400 MHz, (CD₃)₂SO) δ/ppm = 10.64 (s, 1H, NH), 8.09 – 7.90 (m, 3H, 2''-H, 6''-H, 4''-H), 7.79 (d, J = 8.0 Hz, 2H, 3'-H, 5'-H), 7.26 (t, J = 8.0 Hz, 1H, 4'-H).

¹³C NMR (101 MHz, (CD₃)₂SO) δ/ppm = 162.4 (C-1, C-3), 136.6 (C-1''), 135.2 (C-1'), 134.6 (C-3'', C-5''), 132.3 (C-3', C-5'), 131.5 (C-4''), 130.7 (C-4'), 126.4 (C-2'', C-6''), 124.4 (C-2', C-6'), 76.4 (CN), C-2 is missing.

IR (ATR) $\tilde{v}_{max}$/cm⁻¹ = 3206, 2215, 1650.1567, 1516, 1283, 779, 750, 723.

HRMS (ESI): calcd. for $C_{16}H_7{}^{79}Br_2{}^{35}Cl_2N_2O_2$ (M-H)⁻ 486.82568; found 486.82870.

Purity (HPLC): > 96% (λ = 210 nm), > 96% (λ = 254 nm).

2-Cyano-*N*-(2,3-dichlorophenyl)-3-(3,5-dichlorophenyl)-3-hydroxyacrylamide – SGA-78 (71)
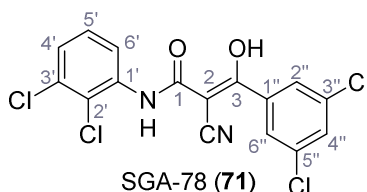
SGA-78 (**71**)

According to general procedure **B**, amide **38** (229 mg, 1.00 mmol, 1.0 eq.) in dry THF (10 mL), NaH (92.0 mg, 2.30 mmol, 2.3 eq.) and 3,5-dichlorobenzoyl chloride (**43**, 230 mg, 1.10 mmol, 1.1 eq.) were used to give SGA-78 (**71**) as colorless crystals (344 mg, 0.856 mmol, 86%).

R$_f$ = 0.17 (3:2 hexanes/acetone).

m.p.: 211 °C.

^{1}H NMR (400 MHz, (CD$_3$)$_2$SO) δ/ppm = 12.49 (s, 1H, NH), 8.58 (dd, *J* = 8.3, 1.5 Hz, 1H, 6'-H), 7.63 (t, *J* = 1.9 Hz, 1H, 4''-H), 7.59 (d, *J* = 1.9 Hz, 2H, 2''-H, 6''-H), 7.27 (t, *J* = 8.2 Hz, 1H, 5'-H), 7.20 (dd, *J* = 8.0, 1.5 Hz, 1H, 4'-H).

^{13}C NMR (126 MHz, (CD$_3$)$_2$SO) δ/ppm = 182.8 (C-3), 166.4 (C-1), 145.1 (C-1''), 139.3 (C-1'), 133.4 (C-3'', C-5''), 131.4 (C-3'), 128.5 (C-4''), 128.0 (C-5'), 126.1 (C-2'', C-6''), 123.4 (C-2), 122.6 (C-4'), 119.3 (C-2'), 119.1 (C-6'), 77.5 (CN).

IR (ATR) $\tilde{v}_{max}$/cm^{-1} = 3355, 2203, 1649, 1584, 1539, 1453, 1415, 872, 812, 777.

HRMS (ESI): calcd. for C$_{16}$H$_7$^{35}Cl$_4$N$_2$O$_2$ (M-H)$^-$ 398.92671; found 398.92789.

Purity (HPLC): > 96% (λ = 210 nm), > 96% (λ = 254 nm).

2-Cyano-3-(3,5-dichlorophenyl)-3-hydroxy-*N*-(4-propoxyphenyl)acrylamide – SGA-84 (72)
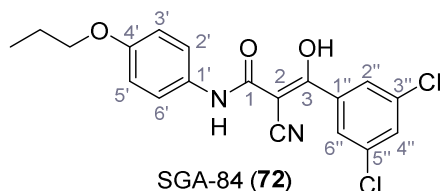
SGA-84 (**72**)

According to general procedure **B**, amide **31** (218 mg, 1.00 mmol, 1.0 eq.) in dry THF (10 mL), NaH (92.0 mg, 2.30 mmol, 2.3 eq.) and 3,5-dichlorobenzoyl chloride (**43**, 230 mg, 1.10 mmol, 1.1 eq.) were used to give SGA-84 (**72**) as yellow solid (245 mg, 0.626 mmol, 63%).

R$_f$ = 0.15 (3:2 hexanes/acetone + 2% TEA).

m.p.: 184 °C.

¹H NMR (500 MHz, (CD₃)₂SO) δ/ppm = 11.36 (s, 1H, NH), 9.30 (s, 1H, OH), 7.71 (t, J = 1.7 Hz, 1H, 4''-H), 7.67 – 7.62 (m, 2H, 2''-H, 6''-H), 7.49 – 7.40 (m, 2H, 3'-H, 5'-H), 6.90 – 6.82 (m, 2H, 2'-H, 6'-H), 3.88 (t, J = 6.5 Hz, 2H, C$\underline{H}_2$CH₂CH₃), 1.71 (sext, J = 7.2 Hz, 2H, CH₂C$\underline{H}_2$CH₃), 0.97 (t, J = 7.4 Hz, 3H, CH₂CH₂C$\underline{H}_3$).

¹³C NMR (126 MHz, (CD₃)₂SO) δ/ppm = 181.6 (C-3), 166.4 (C-1), 154.6 (C-4'), 142.7 (C-1''), 133.7 (C-3'', C-5''), 131.9 (C-1'), 129.3 (C-4''), 126.3 (C-2'', C-6''), 121.6 (C-3', C-5'), 121.5 (C-2), 114.5 (C-2', C-6'), 78.0 (CN), 69.1 ($\underline{C}$H₂CH₂CH₃), 22.1 (CH₂$\underline{C}$H₂CH₃), 10.4 (CH₂CH₂$\underline{C}$H₃).

IR (ATR) $\tilde{v}_{max}$/cm⁻¹ = 3304, 2208, 1601, 1550, 1511, 1249, 1235, 822, 811.

HRMS (ESI): calcd. for C₁₉H₁₅³⁵Cl₂N₂O₃ (M-H)⁻ 389.04652; found 389.04631.

Purity (HPLC): > 96% (λ = 210 nm), > 96% (λ = 254 nm).

N-(3,5-Bis(trifluoromethyl)phenyl)-2-cyano-3-(3,5-dichlorophenyl)-3-hydroxyacrylamide – SGA-85 (73)
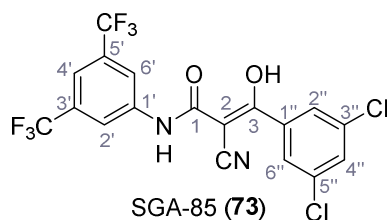
SGA-85 (**73**)

According to general procedure **B**, amide **40** (296 mg, 1.00 mmol, 1.0 eq.) in dry THF (10 mL), NaH (92.0 mg, 2.30 mmol, 2.3 eq.) and 3,5-dichlorobenzoyl chloride (**43**, 230 mg, 1.10 mmol, 1.1 eq.) were used to give SGA-85 (**73**) as colorless solid (320 mg, 0.682 mmol, 68%).

R$_f$ = 0.15 (3:2 hexanes/acetone).

m.p.: 210 °C.

¹H NMR (400 MHz, (CD₃)₂SO) δ/ppm = 12.58 (s, 1H, NH), 8.93 (s, 1H, OH), 8.25 (s, 2H, 2'-H, 6'-H), 7.65 (t, J = 1.9 Hz, 1H, 4''-H), 7.62 – 7.56 (m, 3H, 4'-H, 2''-H, 6''-H).

¹³C NMR (101 MHz, (CD₃)₂SO) δ/ppm = 183.5 (C-3), 167.3 (C-1), 145.4 (C-1''), 142.3 (C-1'), 134.0 (C-3'', C-5''), 131.2 (q, J_{CF} = 32.6 Hz, C-3', C-5'), 129.1 (C-4''), 126.5 (C-2'', C-6''), 123.7 (q, J_{CF} = 270.8 Hz, CF₃), 123.4 (C-2), 119.1 – 118.8 (m, C-2', C-6'), 114.8 – 114.5 (m, C-4'), 77.6 (CN).

IR (ATR) $\tilde{v}_{max}$/cm⁻¹ = 2230, 1637, 1571, 1547, 1375, 1275, 1175, 1128, 810.

Purity (HPLC): > 96% (λ = 210 nm), > 96% (λ = 254 nm).

2-Cyano-3-(3,5-dichlorophenyl)-3-hydroxy-*N*-(4-(trifluoromethoxy)phenyl)acrylamide – SGA-86 (74)
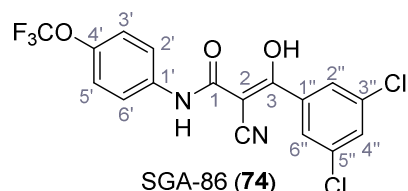
SGA-86 (**74**)

According to general procedure **B**, amide **32** (244 mg, 1.00 mmol, 1.0 eq.) in dry THF (10 mL), NaH (92.0 mg, 2.30 mmol, 2.3 eq.) and 3,5-dichlorobenzoyl chloride (**43**, 230 mg, 1.10 mmol, 1.1 eq.) were used to give SGA-86 (**74**) as colorless solid (344 mg, 0.825 mmol, 83%).

R$_f$ = 0.53 (3:2 hexanes/acetone).

m.p.: 195 °C.

^{1}H NMR (500 MHz, (CD$_3$)$_2$SO) δ/ppm = 12.02 (s, 1H, NH), 9.41 (s, 1H, OH), 7.69 – 7.64 (m, 3H, 2'-H, 6'-H, 4''-H), 7.59 (d, *J* = 1.9 Hz, 2H, 2''-H, 6''-H), 7.28 – 7.23 (m, 2H, 3'-H, 5'-H).

^{13}C NMR (126 MHz, (CD$_3$)$_2$SO) δ/ppm = 182.3 (C-3), 166.3 (C-1), 144.6 (C-1''), 142.7 (C-4'), 139.1 (C-1'), 133.5 (C-3'', C-5''), 128.6 (C-4''), 126.1 (C-2'', C-6''), 123.0 (C-2), 121.6 (C-3', C-5'), 120.3 (q, *J$_{CF}$* = 255.2 Hz, OCF$_3$), 120.2 (C-2', C-6'), 77.6 (CN).

IR (ATR) $\tilde{v}_{max}$/cm^{-1} = 3304, 2218, 1614, 1536, 1506, 1262, 1208, 1164, 661.

Purity (HPLC): > 96% (λ = 210 nm), > 96% (λ = 254 nm).

N-(3-Chloro-2,4-difluorophenyl)-2-cyano-3-(3,5-dibromophenyl)-3-hydroxyacrylamide – SGA-90 (75)
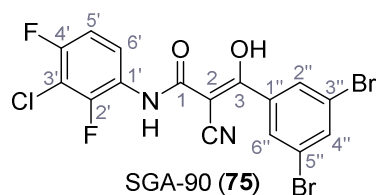
SGA-90 (**75**)

According to general procedure **B**, amide **36** (231 mg, 1.00 mmol, 1.0 eq.) in dry THF (10 mL), NaH (92.0 mg, 2.30 mmol, 2.3 eq.) and 3,5-dibromobenzoic acid (308 mg, 1.10 mmol, 1.1 eq.; converted into the corresponding aryl chloride) were used to give SGA-90 (**75**) as light yellow solid (374 mg, 0.759 mmol, 76%).

R$_f$ = 0.16 (1:1 hexanes/acetone).

m.p.: 192 °C.

¹H NMR (400 MHz, (CD₃)₂SO) δ/ppm = 12.33 (s, 1H, NH), 8.43 (td, J = 8.9, 6.0 Hz, 1H, 6'-H), 7.86 (t, J = 1.7 Hz, 1H, 4''-H), 7.74 (d, J = 1.7 Hz, 2H, 2''-H, 6''-H), 7.23 (td, J = 9.3, 2.0 Hz, 1H, 5'-H).

¹³C NMR (101 MHz, (CD₃)₂SO) δ/ppm = 182.7 (C-3), 166.3 (C-1), 152.1 (d, J_{CF} = 242.4 Hz, C-2'), 147.7 (d, J_{CF} = 242.4 Hz, C-4'), 145.4 (C-1''), 133.7 (C-4''), 129.2 (C-2'', C-6''), 126.3 (dd, J_{CF} = 10.3, 3.2 Hz, C-1'), 123.2 (C-2), 121.8 (C-3'', C-5''), 119.1 (dd, J_{CF} = 7.5, 2.9 Hz, C-6'), 111.5 (dd, J_{CF} = 20.7, 3.6 Hz, C-5'), 108.3 – 107.7 (m, C-3'), 77.3 (CN).

IR (ATR) $\tilde{v}_{max}$/cm⁻¹ = 3297, 2205, 1586, 1531, 1496, 1022, 803, 750.

HRMS (ESI): calcd. for $C_{16}H_6{}^{79}Br_2ClF_2N_2O_2$ (M-H)⁻ 488.84581; found 488.84607.

Purity (HPLC): > 96% (λ = 210 nm), > 96% (λ = 254 nm).

2-Cyano-3-hydroxy-*N*-(4-(trifluoromethyl)phenyl)but-2-enamide (teriflunomide) – SGA-94 (76)
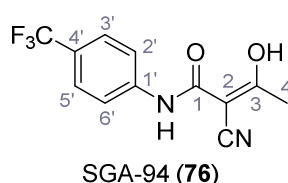
SGA-94 (**76**)

According to general procedure **B**, SGA-34 (**19**, 228 mg, 1.00 mmol, 1.0 eq.) in dry THF (10 mL), NaH (92.0 mg, 2.30 mmol, 2.3 eq.) and acetyl chloride (78.5 μL, 1.10 mmol, 1.1 eq.) were used to give SGA-94 (**76**) as colorless crystals (206 mg, 0.761 mmol, 76%). Analytical data are in accordance with literature.[189]

R$_f$ = 0.65 (3:2 hexanes/acetone).

m.p.: 224 °C. [lit.[189]: 230 – 232 °C]

¹H NMR (400 MHz, (CD₃)₂SO) δ/ppm = 12.28 (s, 1H, OH), 10.91 (s, 1H, NH), 7.81 – 7.72 (m, 2H, 2'-H, 6'-H), 7.70 – 7.61 (m, 2H, 3'-H, 5'-H), 2.25 (s, 3H, 4-H).

^{13}C NMR (101 MHz, (CD$_3$)$_2$SO) δ/ppm = 187.1 (C-3), 166.4 (C-1), 141.9 (C-1'), 125.9 (q, J_{CF} = 3.7 Hz, C-3', C-5'), 124.4 (q, J_{CF} = 271.3 Hz, CF$_3$), 123.5 (q, J_{CF} = 32.1 Hz, C-4'), 120.7 (C-2', C-6'), 118.9 (C-2), 80.5 (CN), 23.5 (C-4).

IR (ATR) $\tilde{v}_{max}$/cm^{-1} = 2335, 2214, 1551, 1319, 1154, 1113, 840, 679.

HRMS (ESI): calcd. for C$_{12}$H$_8$F$_3$N$_2$O$_2$ (M-H)$^-$ 269.05434; found 269.05423.

Purity (HPLC): > 96% (λ = 210 nm), > 96% (λ = 254 nm).

3-(3,5-Bis(trifluoromethyl)phenyl)-2-cyano-3-hydroxy-*N*-(*p*-tolyl)acrylamide – SGA-108 (77)
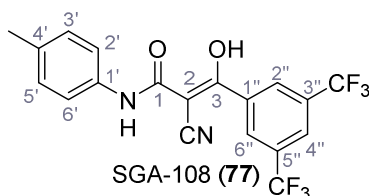
According to general procedure **B**, amide **21** (174 mg, 1.00 mmol, 1.0 eq.) in dry THF (10 mL), NaH (92.0 mg, 2.30 mmol, 2.3 eq.) and 3,5-bis(trifluoromethyl)benzoyl chloride (199 µL, 1.10 mmol, 1.1 eq.) were used to give SGA-108 (**77**) as light yellow crystals (208 mg, 0.502 mmol, 50%).

R$_f$ = 0.28 (3:2 hexanes/acetone).

m.p.: 183 °C.

^{1}H NMR (500 MHz, CDCl$_3$) δ/ppm = 8.45 (s, 2H, 2''-H, 6''-H), 8.10 (s, 1H, 4''-H), 7.86 (s, 1H, NH), 7.43 – 7.37 (m, 2H, 2'-H, 6'-H), 7.25 – 7.20 (m, 2H, 3'-H, 5'-H), 2.37 (s, 3H, CH$_3$).

^{13}C NMR (126 MHz, CDCl$_3$) δ/ppm = 180.4 (C-3), 167.9 (C-1), 136.7 (C-4'), 134.7 (C-1''), 132.7 (C-1'), 132.6 (q, J_{CF} = 34.2 Hz, C-3'', C-5''), 130.1 (C-3', C-5'), 128.6 (q, J_{CF} = 3.1 Hz, C-2'', C-6''), 126.3 (q, J_{CF} = 3.7 Hz, C-4''), 122.8 (q, J_{CF} = 272.9 Hz, CF$_3$), 121.8 (C-2', C-6'), 116.5 (C-2), 79.7 (CN), 21.2 (CH$_3$).

IR (ATR) $\tilde{v}_{max}$/cm^{-1} = 3276, 2213, 1538, 1278, 1129, 811, 681.

HRMS (ESI): calcd. for C$_{19}$H$_{11}$F$_6$N$_2$O$_2$ (M-H)$^-$ 413.07302; found 413.07301.

Purity (HPLC): > 96% (λ = 210 nm), > 96% (λ = 254 nm).

3-(3,5-Bis(trifluoromethyl)phenyl)-2-cyano-3-hydroxy-*N*-(4-(trifluoromethyl)phenyl)-acrylamide – SGA-111 (78)
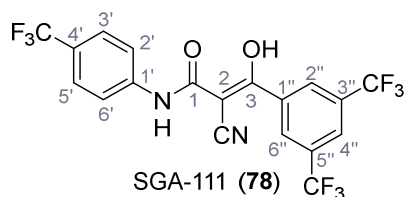
SGA-111 (**78**)

According to general procedure **B**, SGA-34 (**19**, 228 mg, 1.00 mmol, 1.0 eq.) in dry THF (10 mL), NaH (92.0 mg, 2.30 mmol, 2.3 eq.) and 3,5-bis(trifluoromethyl)benzoyl chloride (199 µL, 1.10 mmol, 1.1 eq.) were used to give SGA-111 (**78**) as colorless crystals (357 mg, 0.762 mmol, 76%).

R$_f$ = 0.43 (3:2 hexanes/acetone).

m.p.: 230 °C.

^{1}H NMR (400 MHz, (CD$_3$)$_2$SO) δ/ppm = 12.36 (s, 1H, NH), (m, 3H, 2''-H, 6''-H, 4''-H), 7.87 – 7.71 (m, 2H, 2'-H, 6'-H), 7.69 – 7.51 (m, 2H, 3'-H, 5'-H).

^{13}C NMR (101 MHz, (CD$_3$)$_2$SO) δ/ppm = 182.4 (C-3), 166.3 (C-1), 144.0 (C-1''), 143.6 (C-1'), 129.8 (q, J_{CF} = 32.8 Hz, C-3'', C-5''), 128.1 (q, J_{CF} = 4.7 Hz, C-2'', C-6''), 126.1 (q, J_{CF} = 3.6 Hz, C-3', C-5'), 126.0 (q, J_{CF} = 257.2 Hz, *m*-CF$_3$), 123.4 (C-2), 123.3 (q, J_{CF} = 271.6 Hz, *p*-CF$_3$), 122.7 (q, J_{CF} = 4.0 Hz, C-4''), 121.7 (q, J_{CF} = 31.9 Hz, C-4'), 118.5 (C-2', C-6'), 77.7 (CN).

IR (ATR) $\tilde{v}_{max}$/cm^{-1} = 3289, 2218, 1349, 1323, 1284, 1186, 1139, 1114, 836.

HRMS (ESI): calcd. for C$_{19}$H$_8$F$_9$N$_2$O$_2$ (M-H)$^-$ 467.04475; found 467.04496.

Purity (HPLC): > 96% (λ = 210 nm), > 96% (λ = 254 nm).

2-Cyano-3-(3,5-dimethylphenyl)-3-hydroxy-*N*-(4-(trifluoromethyl)phenyl)acrylamide – SGA-112 (79)
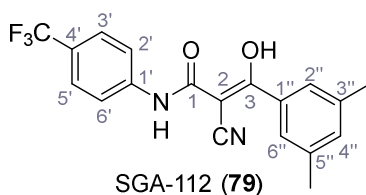
SGA-112 (**79**)

According to general procedure **B**, SGA-34 (**19**, 228 mg, 1.00 mmol, 1.0 eq.) in dry THF (10 mL), NaH (92.0 mg, 2.30 mmol, 2.3 eq.) and 3,5-dimethylbenzoyl chloride (163 µL,

1.10 mmol, 1.1 eq.) were used to give SGA-112 (**79**) as colorless crystals (175 mg, 0.486 mmol, 49%).

R$_f$ = 0.48 (3:2 hexanes/acetone).

m.p.: 187 °C.

^{1}H NMR (500 MHz, (CD$_3$)$_2$SO) δ/ppm = 12.08 (s, 1H, NH), 7.85 – 7.74 (m, 2H, 2'-H, 6'-H), 7.66 – 7.58 (m, 2H, 3'-H, 5'-H), 7.25 (s, 2H, 2''-H, 6''-H), 7.09 (s, 1H,4''-H), 2.30 (s, 6H, CH$_3$).

^{13}C NMR (126 MHz, (CD$_3$)$_2$SO) δ/ppm = 186.5 (C-3), 167.8 (C-1), 143.6 (C-1'), 140.1 (C-1''), 137.2 (C-3'', C-5''), 131.8 (C-4''), 126.4 (q, J_{CF} = 3.8 Hz, C-3', C-5'), 125.8 (C-2'', C-6''), 125.3 (q, J_{CF} = 270.8 Hz, CF$_3$), 122.6 (q, J_{CF} = 31.9 Hz, C-4'), 121.8 (C-2), 119.9 (C-2', C-6'), 78.2 (CN), 21.4 (CH$_3$).

IR (ATR) $\tilde{v}_{max}$/cm^{-1} = 3270, 2218, 1526.1319, 1247, 1157, 1110, 1066, 839.

HRMS (ESI): calcd. for C$_{19}$H$_{14}$F$_3$N$_2$O$_2$ (M-H)$^-$ 359.10129; found 359.10142.

Purity (HPLC): > 96% (λ = 210 nm), > 96% (λ = 254 nm).

2-Cyano-3-(3,5-dimethoxyphenyl)-3-hydroxy-*N*-(4-(trifluoromethyl)phenyl)acrylamide – SGA-113 (80)
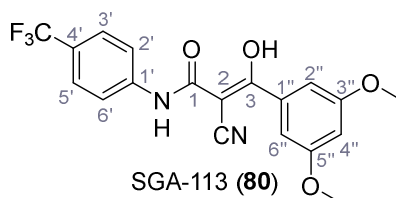
According to general procedure **B**, SGA-34 (**19**, 228 mg, 1.00 mmol, 1.0 eq.) in dry THF (10 mL), NaH (92.0 mg, 2.30 mmol, 2.3 eq.) and 3,5-dimethoxybenzoyl chloride (221 mg, 1.10 mmol, 1.1 eq.) were used to give SGA-113 (**80**) as colorless crystals (309 mg, 0.789 mmol, 79%).

R$_f$ = 0.54 (3:2 hexanes/acetone).

m.p.: 203 °C.

^{1}H NMR (400 MHz, CDCl$_3$) δ/ppm = 7.99 (s, 1H, NH), 7.73 – 7.63 (m, 4H, 2'-H, 6'-H, 3'-H, 5'-H), 7.12 (d, J = 2.3 Hz, 2H, 2''-H, 6''-H), 6.69 (t, J = 2.3 Hz, 1H, 4''-H), 3.85 (s, 6H, OCH$_3$). [1]

^{13}C NMR (101 MHz, CDCl$_3$) δ/ppm = 184.1 (C-3), 168.7 (C-1), 161.0 (C-3'', C-5''), 139.1 (C-1'), 133.9 (C-1''), 127.8 (q, J_{CF} = 33.2 Hz, C-4'), 126.7 (q, J_{CF} = 3.8 Hz, C-3', C-5'), 123.9 (q, J_{CF} =

270.1 Hz, CF$_3$), 121.0 (C-2', C-6'), 117.5 (C-2), 106.4 (C-2'', C-6''), 106.0 (C-4''), 78.5 (CN), 55.8 (OCH$_3$).

IR (ATR) $\tilde{\nu}_{max}$/cm^{-1} = 3297, 2215, 1550, 1324, 1208, 1156, 1095, 1067, 834.

HRMS (ESI): calcd. for C$_{19}$H$_{14}$F$_3$N$_2$O$_4$ (M-H)$^-$ 391.09112; found 391.09140.

Purity (HPLC): > 96% (λ = 210 nm), > 96% (λ = 254 nm).

2-Cyano-3-hydroxy-3-(4-(trifluoromethoxy)phenyl)-*N*-(4-(trifluoromethyl)phenyl)-acrylamide – SGA-114 (81)
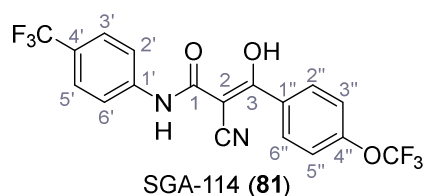
SGA-114 (**81**)

According to general procedure **B**, SGA-34 (**19**, 228 mg, 1.00 mmol, 1.0 eq.) in dry THF (10 mL), NaH (92.0 mg, 2.30 mmol, 2.3 eq.) and 4-(trifluoromethoxy)benzoyl chloride (173 µL, 1.10 mmol, 1.1 eq.) were used to give SGA-114 (**81**) as colorless crystals (200 mg, 0.481 mmol, 48%).

R$_f$ = 0.58 (3:2 hexanes/acetone).

m.p.: 198 °C. [lit.[91]: 188 – 190 °C]

^{1}H NMR (500 MHz, CDCl$_3$) δ/ppm = 8.12 – 8.05 (m, 2H, 2''-H, 6''-H), 7.96 (s, 1H, NH), 7.78 – 7.62 (m, 4H, 2'-H, 6'-H, 3'-H, 5'-H), 7.42 – 7.32 (m, 2H, 3''-H, 5''-H).

^{13}C NMR (126 MHz, CDCl$_3$) δ/ppm = 182.6 (C-3), 168.5 (C-1), 152.8 (C-4''), 139.0 (C-1'), 130.7 (C-2'', C-6''), 130.5 (C-1''), 128.0 (q, J_{CF} = 33.0 Hz, C-4'), 126.7 (q, J_{CF} = 3.7 Hz, C-3', C-5'), 123.9 (q, J_{CF} = 271.7 Hz, CF$_3$), 121.0 (C-2', C-6'), 120.8 (C-3'', C-5''), 120.6 (q, J_{CF} = 259.4 Hz, OCF$_3$), 117.3 (C-2), 78.6 (CN).

IR (ATR) $\tilde{\nu}_{max}$/cm^{-1} = 3285, 2215, 1597, 1551, 1505, 1268, 1168, 1128, 839.

HRMS (ESI): calcd. for C$_{18}$H$_9$F$_6$N$_2$O$_3$ (M-H)$^-$ 415.05228; found 415.05225.

Purity (HPLC): > 96% (λ = 210 nm), > 96% (λ = 254 nm).

2-Cyano-3-(3,5-dichlorophenyl)-3-hydroxy-*N*-methyl-*N*-(4-(trifluoromethyl)phenyl)-acrylamide – SGA-115 (82)
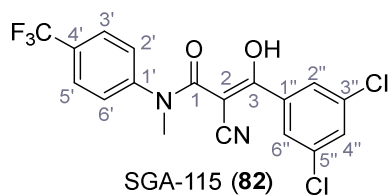
SGA-115 (**82**)

According to general procedure **B**, amide **41** (242 mg, 1.00 mmol, 1.0 eq.) in dry THF (10 mL), NaH (92.0 mg, 2.30 mmol, 2.3 eq.) and 3,5-dichlorobenzoyl chloride (**43**, 230 mg, 1.10 mmol, 1.1 eq.) were used to give SGA-115 (**82**) as colorless solid (198 mg, 0.476 mmol, 48%).

R$_f$ = 0.67 (3:2 hexanes/acetone).

m.p.: 147 °C.

^{1}H NMR (400 MHz, CDCl$_3$) δ/ppm = 7.80 – 7.73 (m, 2H, 3'-H, 5'-H), 7.64 (d, J = 1.9 Hz, 2H, 2''-H, 6''-H), 7.49 (t, J = 1.9 Hz, 1H, 4''-H), 7.47 – 7.41 (m, 2H, 2'-H, 6'-H), 3.48 (s, 3H, CH$_3$).

^{13}C NMR (101 MHz, CDCl$_3$) δ/ppm = 184.2 (C-3), 170.4 (C-1), 145.2 (C-1'), 135.8 (C-1''), 135.5 (C-3'', C-5''), 132.5 (C-4''), 131.4 (q, J_{CF} = 32.9 Hz, C-4'), 127.8 (C-2', C-6'), 127.5 (q, J = 3.6 Hz, C-3', C-5'), 127.2 (C-2'', C-6''), 123.7 (q, J_{CF} = 272.6 Hz, CF$_3$), 115.3 (C-2), 78.6 (CN), 39.9 (CH$_3$).

IR (ATR) $\tilde{v}_{max}$/cm^{-1} = 3074, 2214, 1578, 1540, 1396, 1331, 1165, 1118, 807.

HRMS (ESI): calcd. for C$_{18}$H$_{10}$^{35}Cl$_2$F$_3$N$_2$O$_2$ (M-H)$^-$ 413.00769; found 413.00806.

Purity (HPLC): > 96% (λ = 210 nm), > 96% (λ = 254 nm).

2-Cyano-3-hydroxy-3-(pyridin-3-yl)-*N*-(4-(trifluoromethyl)phenyl)acrylamide – SGA-127 (83)

SGA-127 (**83**)

According to general procedure **B**, SGA-34 (**19**, 228 mg, 1.00 mmol, 1.0 eq.) in dry THF (10 mL), NaH (92.0 mg, 2.30 mmol, 2.3 eq.) and nicotinoyl chloride hydrochloride (196 mg, 1.10 mmol, 1.1 eq.) were used to give SGA-127 (**83**) as orange solid (169 mg, 0.506 mmol, 51%).

R$_f$ = 0.00 (3:2 hexanes/EtOAc).

m.p.: 235 °C.

¹H NMR (400 MHz, (CD₃)₂SO) δ/ppm = 12.22 (s, 1H, NH), 9.12 (s, 1H, 2''-H), 8.88 (d, J = 5.6 Hz, 1H, 6''-H), 8.70 (d, J = 8.0 Hz, 1H, 4''-H), 8.04 (dd, J = 8.0, 5.6 Hz, 1H, 5''-H), 7.83 – 7.72 (m, 2H, 2'-H, 6'-H), 7.67 – 7.56 (m, 2H, 3'-H, 5'-H).

¹³C NMR (101 MHz, (CD₃)₂SO) δ/ppm = 180.0 (C-3), 165.9 (C-1), 143.5 (C-1'), 143.3 (C-6''), 143.0 (C-4''), 141.9 (C-2''), 139.9 (C-3''), 126.2 (C-5''), 126.1 (q, J_{CF} = 3.6 Hz, C-3', C-5'), 124.2 (q, J_{CF} = 270.7 Hz, CF₃), 123.3 (C-2), 121.8 (q, J_{CF} = 32.0 Hz, C-4'), 118.5 (C-2', C-6'), 78.5 (CN).

IR (ATR) $\tilde{v}_{max}$/cm⁻¹ = 2356, 2191, 1533, 1317, 1105, 1060, 849, 698.

HRMS (ESI): calcd. for C₁₆H₉F₃N₃O₂ (M-H)⁻ 332.06523; found 332.06517.

Purity (HPLC): > 96% (λ = 210 nm), > 96% (λ = 254 nm).

3-(3-Bromo-5-iodophenyl)-2-cyano-3-hydroxy-*N*-(4-(trifluoromethyl)phenyl)acrylamide – SGA-132 (84)
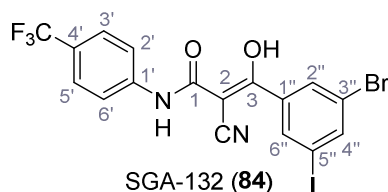
According to general procedure **B**, SGA-34 (**19**, 228 mg, 1.00 mmol, 1.0 eq.) in dry THF (10 mL), NaH (92.0 mg, 2.30 mmol, 2.3 eq.) and 3-bromo-5-iodobenzoic acid (360 mg, 1.10 mmol, 1.1 eq.; converted into the corresponding aryl chloride) were used to give SGA-132 (**84**) as colorless crystals (332 mg, 0.618 mmol, 62%).

R$_f$ = 0.38 (3:2 hexanes/EtOAc).

m.p.: 207 °C.

¹H NMR (400 MHz, (CD₃)₂SO) δ/ppm = 12.31 (s, 1H, NH), 7.97 (s, 1H, 4''-H), 7.89 (s, 1H, 2''-H or 6''-H), 7.78 – 7.72 (m, 3H, 2'-H, 6'-H and 2''-H or 6''-H), 7.63 – 7.55 (m, 2H, 3'-H, 5'-H).

¹³C NMR (101 MHz, (CD₃)₂SO) δ/ppm = 182.6 (C-3), 166.4 (C-1), 145.4 (C-1''), 143.6 (C-1'), 139.1 (C-4''), 135.0 (C-2'' or C-6''), 129.5 (C-2'' or C-6''), 126.0 (q, J_{CF} = 3.8 Hz, C-3', C-5'), 123.9 (q, J_{CF} = 263.8 Hz, CF₃), 123.3 (C-2), 121.7 (q, J_{CF} = 31.6 Hz, C-4'), 121.6 (C-3'' or C-5''), 118.6 (C-2', C-6'), 95.0 (C-3'' or C-5''), 77.4 (CN).

IR (ATR) $\tilde{v}_{max}$/cm^{-1} = 3276, 2213, 1532, 1318, 1163, 1112, 731.

HRMS (ESI): calcd. for $C_{17}H_8{}^{79}BrIF_3N_2O_2$ (M-H)$^-$ 534.87714; found 534.87813.

Purity (HPLC): > 96% (λ = 210 nm), > 96% (λ = 254 nm).

Methyl 4-(2-cyano-3-(3,5-dichlorophenyl)-3-hydroxyacrylamido)benzoate – SGA-133 (85)
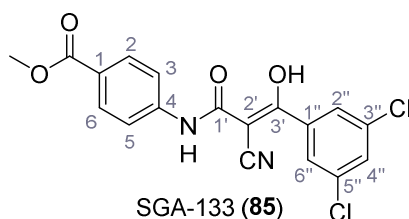
SGA-133 (**85**)

According to general procedure **B**, amide **33** (218 mg, 1.00 mmol, 1.0 eq.) in dry THF (10 mL), NaH (92.0 mg, 2.30 mmol, 2.3 eq.) and 3,5-dichlorobenzoyl chloride (**43**, 230 mg, 1.10 mmol, 1.1 eq.) were used. The resulting solid was washed with hexanes, EtOH and water to give SGA-133 (**85**) as colorless solid (331 mg, 0.846 mmol, 85%).

R$_f$ = 0.15 (3:2 hexanes/acetone).

m.p.: 234 °C.

^{1}H NMR (400 MHz, (CD$_3$)$_2$SO) δ/ppm = 12.33 (s, 1H, NH), 11.41 (s, 1H, OH), 7.90 – 7.83 (m, 2H, 2-H, 6-H), 7.71 – 7.66 (m, 2H, 3-H, 5-H), 7.64 (t, J = 1.9 Hz, 1H, 4''-H), 7.57 (d, J = 1.9 Hz, 2H, 2''-H, 6''-H), 3.81 (s, 3H, CH$_3$).

^{13}C NMR (101 MHz, (CD$_3$)$_2$SO) δ/ppm = 182.8 (C-3'), 166.3 (C-1'), 166.0 (CO), 145.1 (C-1''), 144.6 (C-4), 133.4 (C-3'', C-5''), 130.4 (C-2, C-6), 128.5 (C-4''), 126.1 (C-2'', C-6''), 123.3 (C-2'), 122.3 (C-1), 118.1 (C-3, C-5), 77.6 (CN), 51.7 (CH$_3$).

IR (ATR) $\tilde{v}_{max}$/cm^{-1} = 3304, 3093, 2215, 1727, 1591, 1534, 1415, 1283, 1262, 1112, 810, 766.

HRMS (ESI): calcd. for $C_{18}H_{11}{}^{35}Cl_2N_2O_4$ (M-H)$^-$ 389.01014; found 389.01077.

Purity (NMR): > 96% (λ = 210 nm), > 96% (λ = 254 nm).

3-(5-Chloropyridin-3-yl)-2-cyano-3-hydroxy-*N*-(4-(trifluoromethyl)phenyl)acrylamide – SGA-136 (86)
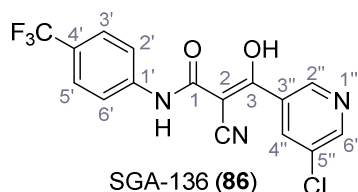
SGA-136 (**86**)

According to general procedure **B**, SGA-34 (**19**, 228 mg, 1.00 mmol, 1.0 eq.) in dry THF (10 mL), NaH (92.0 mg, 2.30 mmol, 2.3 eq.) and 5-chloronicotinic acid (173 mg, 1.10 mmol, 1.1 eq.; converted into the corresponding aryl chloride) were used to give SGA-136 (**86**) as light pink crystals (225 mg, 0.611 mmol, 61%).

R$_f$ = 0.15 (3:2 hexanes/acetone).

m.p.: 221 °C.

^{1}H NMR (500 MHz, (CD$_3$)$_2$SO) δ/ppm = 12.33 (s, 1H, NH), 8.74 (s, 1H, 2''-H or 4''-H), 8.69 – 8.64 (m, 1H, 6''-H), 8.11 – 8.05 (m, 1H, 2''-H or 4''-H), 7.81 – 7.73 (m, 2H, 2'-H, 6'-H), 7.64 – 7.55 (m, 2H, 3'-H, 5'-H).

^{13}C NMR (126 MHz, (CD$_3$)$_2$SO) δ/ppm = 181.7 (C-3), 166.2 (C-1), 147.9 (C-6''), 146.1 (C-2'' or C-4''), 143.6 (C-1'), 138.8 (C-3'' or C-5''), 134.9 (C-2'' or C-4''), 130.5 (C-3'' or C-5''), 126.1 (q, J_{CF} = 3.7 Hz, C-3', C-5'), 124.6 (q, J_{CF} = 271.0 Hz, CF$_3$), 123.5 (C-2), 121.6 (q, J_{CF} = 31.5 Hz, C-4'), 118.5 (C-2', C-6'), 78.2 (CN).

IR (ATR) $\tilde{v}_{max}$/cm^{-1} = 3285, 2225, 1539, 1308, 1113, 951, 838.

HRMS (ESI): calcd. for C$_{16}$H$_8$^{35}ClF$_3$N$_3$O$_2$ (M-H)$^-$ 366.02626; found 366.02652.

Purity (HPLC): > 96% (λ = 210 nm), > 96% (λ = 254 nm).

4-(2-Cyano-3-(3,5-dichlorophenyl)-3-hydroxyacrylamido)benzoic acid – SGA-137 (88)

SGA-137 (**88**)
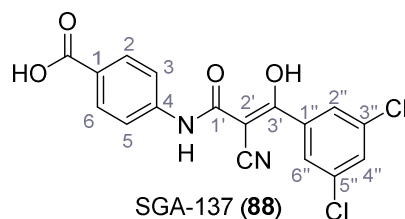
Ester **85** (95.0 mg, 0.243 mmol, 1.0 eq.) was dissolved in dioxane/H$_2$O (3:1; 4.0 mL) and LiOH (61.2 mg, 2.43 mmol, 10 eq.) was added. The mixture was stirred at rt for 3 h, before 1 M aq.

HCl (5.0 mL) was added. The precipitate was filtered off, washed with cold water and dried to give SGA-137 (**88**) as colorless solid (59.6 mg, 0.158 mmol, 65%).

R$_f$ = 0.00 (3:2 hexanes/acetone).

m.p.: 244 °C.

^{1}H NMR (500 MHz, (CD$_3$)$_2$SO) δ/ppm = 12.30 (s, 1H, NH), 7.87 – 7.81 (m, 2H, 2-H, 6-H), 7.68 – 7.64 (m, 2H, 3-H, 5-H), 7.63 (t, J = 1.9 Hz, 1H, 4''-H), 7.57 (d, J = 1.9 Hz, 2H, 2''-H, 6''-H).

^{13}C NMR (126 MHz, (CD$_3$)$_2$SO) δ/ppm = 182.7 (C-3'), 167.1 (CO), 166.3 (C-1'), 145.2 (C-1''), 144.2 (C-4), 133.4 (C-3'', C-5''), 130.5 (C-2, C-6), 128.4 (C-4''), 126.1 (C-2'', C-6''), 123.5 (C-1), 123.4 (C-2'), 118.0 (C-3, C-5), 77.5 (CN).

IR (ATR) $\tilde{v}_{max}$/cm^{-1} = 3311, 2215, 1696, 1595, 1550, 1415, 1294, 855, 770.

HRMS (ESI): calcd. for C$_{17}$H$_9$^{35}Cl$_2$N$_2$O$_4$ (M-H)$^-$ 374.99449; found 374.99480.

Purity (HPLC): > 96% (λ = 210 nm), > 96% (λ = 254 nm).

2-Cyano-3-(3,5-dichlorophenyl)-3-hydroxy-*N*-(4-(trifluoromethyl)benzyl)acrylamide – SGA-138 (87)
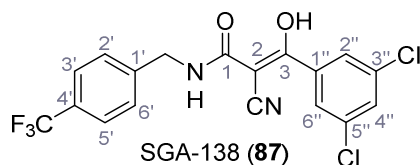
According to general procedure **B**, amide **42** (242 mg, 1.00 mmol, 1.0 eq.) in dry THF (10 mL), NaH (92.0 mg, 2.30 mmol, 2.3 eq.) and 3,5-dichlorobenzoyl chloride (**43**, 230 mg, 1.10 mmol, 1.1 eq.) were used to give SGA-138 (**87**) as colorless solid (228 mg, 0.549 mmol, 55%).

R$_f$ = 0.70 (3:2 hexanes/acetone).

m.p.: 173 °C.

^{1}H NMR (400 MHz, CDCl$_3$) δ/ppm = 7.80 – 7.73 (m, 2H, 3'-H, 5'-H), 7.64 (d, J = 1.9 Hz, 2H, 2''-H, 6''-H), 7.49 (t, J = 1.9 Hz, 1H, 4''-H), 7.47 – 7.41 (m, 2H, 2'-H, 6'-H), 3.48 (s, 3H, CH$_3$).
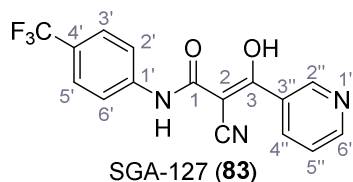
^{13}C NMR (101 MHz, CDCl$_3$) δ/ppm = 184.2 (C-3), 170.4 (C-1), 145.2 (C-1'), 135.8 (C-1''), 135.5 (C-3'', C-5''), 132.5 (C-4''), 131.4 (q, J_{CF} = 32.9 Hz, C-4'), 127.8 (C-2', C-6'), 127.5 (q, J = 3.6 Hz, C-3', C-5'), 127.2 (C-2'', C-6''), 123.7 (q, J_{CF} = 272.6 Hz, CF$_3$), 115.3 (C-2), 78.6 (CN), 39.9 (CH$_3$).

IR (ATR) $\tilde{v}_{max}$/cm^{-1} = 3074, 2214, 1578, 1540, 1396, 1331, 1165, 1118, 807.

HRMS (ESI): calcd. for $C_{18}H_{10}{}^{35}Cl_2F_3N_2O_2$ (M-H)⁻ 413.00769; found 413.00806.

Purity (HPLC): > 96% (λ = 210 nm), > 96% (λ = 254 nm).

2-Cyano-3-(3,5-dichlorophenyl)-3-hydroxy-*N*-(4-(trifluoromethyl)phenyl)prop-2-enethioamide – SGA-167 (91)

SGA-167 (**91**)
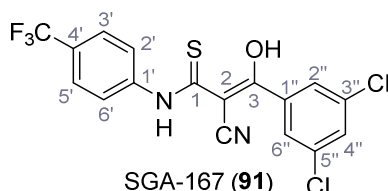
According to a procedure published by Sjogren, et al. [91], a stirred solution of acetonitrile (2.01 mL, 38.2 mmol, 4.0 eq.) in THF (70 mL) was cooled to -78 °C, *n*-BuLi (2.5 M in hexanes, 11.5 mL, 28.6 mmol, 3.0 eq.) was added over 10 minutes and the mixture was stirred for further 15 minutes. A solution of 3,5-dichlorobenzoyl chloride (**43**, 2.00 g, 9.55 mmol, 1.0 eq.) in THF (25 mL) was added over 10 minutes. The mixture was allowed to warm to rt over 40 minutes, followed by addition of sat. aq. NH₄Cl solution (50 mL). The reaction mixture was partitioned between 1 M HCl and hexanes/EtOAc (two times 25 mL/25 mL). The combined organic phases were dried over Na₂SO₄, filtered and concentrated *in vacuo*. The oily residue was redissolved in aq. NH₃ solution (25%, 10 mL), then acidified with 1 M HCl (10 mL) and extracted thrice with EtOAc (15 mL). The combined organic layers were dried over Na₂SO₄, filtered and concentrated *in vacuo* and then recrystallized from hexanes to yield 3-(3,5-dichlorophenyl)-3-oxopropanenitrile (**89**) as orange solid (526 mg, 2.46 mmol, 26%). Analytical data are in accordance with literature.[190] The product was used without further purification or characterization for the next step.

R$_f$ = 0.27 (9:1 hexanes/EtOAc).

HRMS (EI): calcd. for $C_9H_5{}^{35}Cl_2NO$ (M)˙⁺ 212.9743; found 212.9742.

According to general procedure **B**, propanenitrile **89** (526 mg, 2.46 mmol, 1.0 eq, instead of an amide) in dry THF (10 mL), NaH (108 mg, 2.70 mmol, 1.1 eq.) and 4-(trifluoromethyl)phenyl isothiocyanate (**90**, 524 mg, 2.85 mmol, 1.1 eq., instead of the acid chloride) were used to give SGA-167 (**91**) as golden solid (384 mg, 0.92 mmol, 37%).

R$_f$ = 0.33 (9:1 hexanes/EtOAc).

m.p.: 188 °C.

¹H NMR (400 MHz, (CD₃)₂SO) δ/ppm = 14.34 (s, 1H, NH), 8.12 (d, J = 8.5 Hz, 2H, 2'-H, 6'-H), 7.72 – 7.63 (m, 3H, 3'-H, 5'-H, 4''-H), 7.57 (d, J = 1.9 Hz, 2H, 2''-H, 6''-H).

¹³C NMR (101 MHz, (CD₃)₂SO) δ/ppm = 189.4 (C-1), 182.0 (C-3), 144.9 (C-2), 144.1 (C-1'), 133.4 (C-3'', C-5''), 128.6 (C-4''), 126.1 (C-2'', C-6''), 125.5 (q, J_{CF} = 3.7 Hz, C-3', C-5'), 124.4 (q, J_{CF} = 271.3 Hz, CF₃), 123.8 (q, J_{CF} = 31.9 Hz, C-4'), 123.6 (C-1''), 122.2 (C-2', C-6'), 90.9 (CN).

IR (ATR) $\tilde{v}_{max}$/cm⁻¹ = 3267, 2362, 2202, 1550, 1521, 1323, 1106, 1067, 807, 671, 585.

HRMS (ESI): calcd. for C₁₇H₈³⁵Cl₂F₃N₂OS (M-H)⁻ 414.96920; found 414.96915.

Purity (HPLC): > 96% (λ = 210 nm).

5.1.2.2 Synthesis of TPC2-A1-P (17) and analogs

1-(5-Bromo-2-(trifluoromethoxy)phenyl)-2-chloroethan-1-one (102)
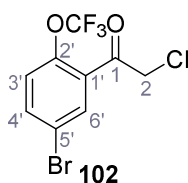
4-Bromo-2-iodo-1-(trifluoromethoxy)benzene (**108**, 610 mg, 1.66 mmol, 1.0 eq.) was dissolved in dry THF (8.0 mL) and cooled to -78 °C, then *n*-BuLi (0.670 mL, 1.66 mmol, 1.0 eq.) was added dropwise. The mixture was stirred for 20 min at -78 °C and a solution of 2-chloro-*N*-methoxy-*N*-methylacetamide (**105**, 700 mg, 4.99 mmol, 3.0 eq.) in dry THF (8.0 mL) was added slowly. The mixture was stirred for 1 h at -78 °C and then poured on sat. aq. NH$_4$Cl solution. The mixture was extracted with pentane, the organic layer was washed with sat. aq. NaCl solution, dried using hydrophobic phase separation filter papers and filtered through a short silica column (eluent: pentane). The product was carefully concentrated under ambient pressure to yield a colorless oil (**102**, 221 mg, 0.696 mmol, 42%).

R$_f$ = 0.65 (9:1 hexanes/EtOAc).

^{1}H NMR (500 MHz, CDCl$_3$) δ/ppm = 7.93 (d, *J* = 2.5 Hz, 1H, 6'-H), 7.71 (dd, *J* = 8.8, 2.5 Hz, 1H, 4'-H), 7.25 – 7.22 (m, 1H, 3'-H), 4.61 (s, 2H, 2-H).

^{13}C NMR (126 MHz, CDCl$_3$) δ/ppm = 190.5 (C-1), 146.2 (C-2'), 137.1 (C-4'), 134.1 (C-6'), 130.8 (C-5'), 122.2 (C-3'), 120.8 (C-1'), 120.3 (q, *J$_{CF}$* = 261 Hz, OCF$_3$), 49.0 (C-2).

IR (ATR) ṽ$_{max}$/cm^{-1} = 1703, 1592, 1480, 1398, 1308, 1252, 1174, 1129, 1088, 822, 664.

HRMS (EI): calcd. for C$_9$H$_5$^{79}Br^{35}ClF$_3$O$_2$ (M)$^{·+}$ 315.9108; found 315.9106.

Purity (HPLC): > 96% (λ = 210 nm), > 96% (λ = 254 nm).

2-Bromo-1-(2-(trifluoromethoxy)phenyl)ethan-1-one (101)
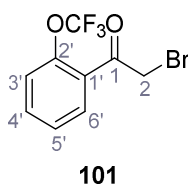
2'-(Trifluoromethoxy)acetophenone (**103**, 779 µL, 4.90 mmol, 1.0 eq.) was dissolved in CH$_2$Cl$_2$ (10 mL), then *p*-toluenesulfonic acid (86.1 mg, 0.490 mmol, 0.10 eq.) and *N*-bromosuccinimide (872 mg, 4.90 mmol, 1.0 eq.) were added. The mixture was stirred for 24 h at rt, then sat. aq.

NaCl solution (10 mL) was added. The aqueous phase was extracted with CH_2Cl_2 (3 x 10 mL), dried using a hydrophobic filter paper and concentrated *in vacuo*. Purification by FCC (pentane/EtOAc 9:1) yielded bromoketone **101** (672 mg, 2.87 mmol, 49%) as light brown liquid. Analytical data are in accordance with literature[106].

R_f = 0.58 (9:1 hexanes/EtOAc).

¹H NMR (400 MHz, CDCl₃) δ/ppm = 7.81 (dd, J = 7.8, 1.8 Hz, 1H, 6'-H), 7.60 (ddd, J = 8.3, 7.6, 1.8 Hz, 1H, 4'-H), 7.41 (td, J = 7.6, 1.0 Hz, 1H, 5'-H), 7.37 – 7.32 (m, 1H, 3'-H), 4.47 (s, 2H, 2-H).

¹³C NMR (101 MHz, CDCl₃) δ/ppm = 191.5 (C-1), 147.1 (q, J = 1.7 Hz, C-2'), 134.3 (C-4'), 131.6 (C-6'), 129.3 (C-1'), 127.3 (C-5'), 120.6 (C-3'), 120.5 (q, J = 260.1 Hz, OCF_3), 35.1 (C-2).

IR (ATR) $\tilde{v}_{max}$/cm⁻¹ = 1698, 1603, 1450, 1295, 1248, 1200, 1160.

HRMS (EI): calcd. for $C_9H_6{}^{79}BrF_3O_2$ (M)·⁺ 281.9498; found 281.9494.

Purity (HPLC): > 96% (λ = 210 nm), > 96% (λ = 254 nm).

Ethyl 5-(5-bromo-2-(trifluoromethoxy)phenyl)-1-(cyclohexylmethyl)-2-methyl-1*H*-pyrrole-3-carboxylate – SGA-140 (109)

SGA-140 (**109**)
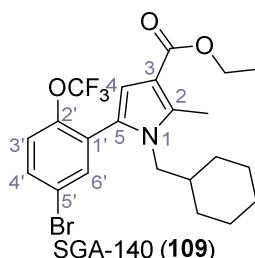
Following general procedure **C**, ethyl acetoacetate (**94**, 88.0 µL, 0.693 mmol, 1.1 eq.) in dry THF (3.0 mL), NaH (37.8 mg, 0.945 mmol, 1.5 eq.) and a solution of ketone **102** (200 mg, 0.630 mmol, 1.0 eq.) and KI (209 mg, 1.26 mmol, 2.0 eq.) in dry THF (3.0 mL) was used. Then, the residue was dissolved in acetic acid (6.0 mL) and cyclohexanemethanamine (**95**, 160 µL, 1.26 mmol, 2.0 eq.) was added. FCC (hexanes/EtOAc 99:1) yielded SGA-140 (**109**) as colorless oil (140 mg, 0.287 mmol, 46%).

R_f = 0.30 (9:1 hexanes/EtOAc).

¹H NMR (400 MHz, CDCl₃) δ/ppm = 7.54 – 7.50 (m, 2H, 4'-H, 6'-H), 7.20 (ddt, J = 7.6, 3.0, 1.5 Hz, 1H, 3'-H), 6.55 (s, 1H, 4-H), 4.27 (q, J = 7.1 Hz, 2H, C<u>H</u>₂CH₃), 3.59 (d, J = 7.1 Hz, 2H, C<u>H</u>₂-

cy), 2.59 (s, 3H, CH₃), 1.60 – 1.54 (m, 3H, cy), 1.38 – 1.32 (m, 6H, CH₂CH₃, cy), 1.07 – 0.99 (m, 3H, cy), 0.68 – 0.59 (m, 2H, cy).

¹³C NMR (121 MHz, CDCl₃) δ/ppm = 165.6 (COOEt), 146.3 (C-2'), 137.6 (C-3), 135.7 (C-6'), 132.4 (C-4'), 129.0 (C-5'), 126.5 (C-5), 122.1 (C-3'), 120.3 (q, J_{CF} = 260.2 Hz, OCF₃), 119.9 (C-1'), 112.6 (C-2), 112.2 (C-4), 59.6 (CH₂CH₃), 50.8 (CH₂-cy), 39.0 (cy), 30.6 (cy), 26.2 (cy), 25.7 (cy), 14.7 (CH₂CH₃), 12.1 (CH₃).

IR (ATR) $\tilde{v}_{max}$/cm⁻¹ = 2976, 2925, 2854, 1699, 1254, 1240, 1206, 1190, 1169, 1080, 1064, 774.

HRMS (ESI): calcd. for C₂₂H₂₆⁷⁹BrF₃NO₃ (M+H)⁺ 488.10427; found 488.10459.

Purity (HPLC): > 96% (λ = 210 nm), > 96% (λ = 254 nm).

5-(5-Bromo-2-(trifluoromethoxy)phenyl)-1-(cyclohexylmethyl)-2-methyl-1*H*-pyrrole-3-carboxylic acid – TPC2-A1-P (17)
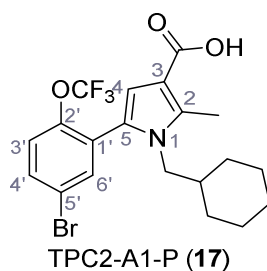
TPC2-A1-P (**17**)

According to general procedure **D**, LiOH (51.6 mg, 2.05 mmol, 10 eq.) and a solution of SGA-140 (**140**, 100 mg, 0.205 mmol, 1.0 eq.) in dioxane/H₂O (3.0 mL) were used. After 2 h the reaction was completed and recrystallization from EtOH gave TPC2-A1-P (**17**) as colorless solid (51.2 mg, 0.111 mmol, 54%).

R*f* = 0.14 (9:1 hexanes/EtOAc).

m.p.: 202 °C.

¹H NMR (500 MHz, CDCl₃) δ/ppm = 11.34 (s, 1H, COOH), 7.56 – 7.51 (m, 2H, 3'-H, 4'-H), 7.23 – 7.19 (m, 1H, 6'-H), 6.61 (s, 1H, 4-H), 3.60 (d, J = 7.1 Hz, 2H, CH₂-cy), 2.60 (s, 3H, CH₃), 1.62 – 1.56 (m, 3H, cy), 1.40 – 1.33 (m, 3H, cy), 1.09 – 1.01 (m, 3H, cy), 0.68 – 0.61 (m, 2H, cy).

¹³C NMR (126 MHz, CDCl₃) δ/ppm = 170.0 (COOH), 146.4 (C-2'), 138.8 (C-2), 135.7 (C-6'), 132.6 (C-4'), 128.8 (C-5'), 126.8 (C-5), 122.2 (C-3'), 120.3 (q, J_{CF} = 259.3 Hz, OCF₃), 119.9 (C-1'), 112.9 (C-4), 111.6 (C-3), 50.9 (CH₂-cy), 39.0 (cy), 30.6 (cy), 26.2 (cy), 25.7 (cy), 12.3 (CH₃).

IR (ATR) $\tilde{v}_{max}$/cm^{-1} = 2961, 2924, 2875, 2853, 2359, 2342, 1667, 1266, 1243, 1212, 1198, 1171, 925, 779, 658.

HRMS (ESI): calcd. for $C_{20}H_{20}{}^{79}BrF_3NO_3$ (M-H)$^-$ 458.05841; found 458.05889.

Purity (HPLC): > 96% (λ = 210 nm), > 96% (λ = 254 nm).

Ethyl 1-(cyclohexylmethyl)-2-methyl-5-phenyl-1*H*-pyrrole-3-carboxylate – SGA-43 (96)

SGA-43 (**96**)
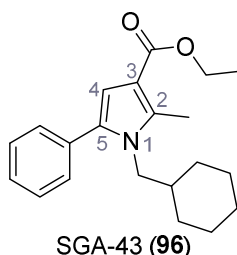
Following general procedure **C**, ethyl acetoacetate (**94**, 42.0 µL, 3.30 mmol, 1.1 eq.) in dry THF (12 mL), NaH (180 mg, 4.50 mmol, 1.5 eq.) and a solution of 2-bromo-1-phenylethan-1-one (**92**, 0.405 mL, 3.00 mmol, 1.0 eq.) and KI (996 mg, 6.00 mmol, 2.0 eq.) in dry THF (10 mL) were used. Then, the residue was dissolved in acetic acid (10 mL) and cyclohexanemethanamine (**95**, 781 µL, 6.00 mmol, 2.0 eq.) was added. FCC (hexanes/EtOAc 9:1) yielded SGA-43 (**96**) as colorless solid (516 mg, 1.58 mmol, 53%). The compound is literature known, but no analytical data are available[103].

R$_f$ = 0.49 (9:1 hexanes/EtOAc).

m.p.: 91 °C.

^{1}H NMR (400 MHz, CDCl$_3$) δ/ppm = 7.42 – 7.36 (m, 2H, Ph), 7.35 – 7.29 (m, 3H, Ph), 6.53 (s, 1H, 4-H), 4.27 (q, J = 7.1 Hz, 2H, C$\underline{H}_2$CH$_3$), 3.78 (d, J = 7.1 Hz, 2H, C$\underline{H}_2$-cy), 2.60 (s, 3H, CH$_3$), 1.58 – 1.49 (m, 3H, cy), 1.41 – 1.31 (m, 6H, cy, CH$_2$C$\underline{H}_3$), 1.06 – 0.95 (m, 3H, cy), 0.69 – 0.57 (m, 2H, cy).

^{13}C NMR (121 MHz, CDCl$_3$) δ/ppm = 165.9 ($\underline{C}$OOEt), 137.0 (C-2), 134.1 (qPh), 133.7 (C-5), 129.6 (Ph), 128.5 (Ph), 127.4 (Ph), 112.0 (C-3), 110.0 (C-4), 59.4 ($\underline{C}$H$_2$CH$_3$), 50.2 ($\underline{C}$H$_2$-cy), 39.0 (cy), 30.6 (cy), 26.2 (cy), 25.8 (cy), 14.7 (CH$_2\underline{C}$H$_3$), 12.1 (CH$_3$).

IR (ATR) $\tilde{v}_{max}$/cm^{-1} = 2975, 2926, 2850, 1738, 1698, 1420, 1242, 1224, 1191, 1062, 772, 702.

HRMS (ESI): calcd. for $C_{21}H_{28}NO_2$ (M+H)$^+$ 326.21146; found 326.21121.

Purity (HPLC): > 96% (λ = 210 nm), > 96% (λ = 254 nm).

1-(Cyclohexylmethyl)-2-methyl-5-phenyl-1*H*-pyrrole-3-carboxylic acid – SGA-50 (100)
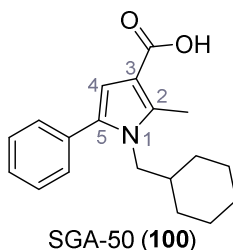
SGA-50 (**100**)

According to general procedure **D**, LiOH (38.7 mg, 1.54 mmol, 10 eq.) and a solution of SGA-43 (**96**, 50.0 mg, 0.154 mmol, 1.0 eq.) in dioxane/H$_2$O (1.3 mL) were used. After 1 h the reaction was completed and gave SGA-50 (**100**) as colorless solid (40.4 mg, 0.136 mmol, 88%). The compound is literature known, but no analytical data are available[103].

R$_f$ = 0.18 (6:1 hexanes/EtOAc).

m.p.: 196 °C.

^{1}H NMR (500 MHz, CDCl$_3$) δ/ppm = 7.42 – 7.38 (m, 2H, Ph), 7.36 – 7.32 (m, 3H, Ph), 6.59 (s, 1H, 4-H), 3.80 (d, J = 7.2 Hz, 2H, CH$_2$), 2.62 (s, 3H, CH$_3$), 1.59 – 1.52 (m, 3H, cy), 1.42 – 1.33 (m, 3H, cy), 1.06 – 0.97 (m, 3H, cy), 0.68 – 0.59 (m, 2H, cy).

^{13}C NMR (101 MHz, CDCl$_3$) δ/ppm = 170.8 (COOH), 138.3 (C-2), 134.5 (C-5), 133.5 (qPh), 129.7 (Ph), 128.5 (Ph), 127.5 (Ph), 111.2 (C-3), 110.7 (C-4), 50.3 (CH$_2$), 39.0 (cy), 30.6 (cy), 26.2 (cy), 25.8 (cy), 12.3 (CH$_3$).

IR (ATR) $\tilde{v}_{max}$/cm^{-1} = 3030, 2971, 2921, 2848, 1738, 1660, 1533, 1435, 1364, 1267, 1227, 1205, 778, 768, 712, 703.

HRMS (ESI): calcd. for C$_{19}$H$_{22}$NO$_2$ (M-H)$^-$ 296.16572; found 296.16560.

Purity (HPLC): > 96% (λ = 210 nm), > 96% (λ = 254 nm).

Ethyl 1-(cyclohexylmethyl)-5-(2,5-dichlorophenyl)-2-methyl-1*H*-pyrrole-3-carboxylate – SGA-48 (110)
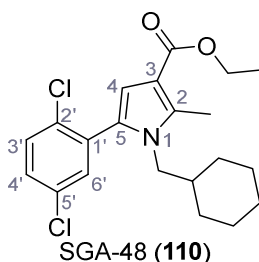
SGA-48 (**110**)

Following general procedure **C**, ethyl acetoacetate (**94**, 208 µL, 1.65 mmol, 1.1 eq.) in dry THF (5.0 mL), NaH (90.0 mg, 2.25 mmol, 1.5 eq.) and a solution of 2-bromo-1-(2,5-dichlorophenyl)ethan-1-one (402 mg, 1.50 mmol, 1.0 eq.) in dry THF (1.0 mL) were used. Then, the residue was dissolved in acetic acid (5.0 mL) and cyclohexanemethanamine (**95**, 390 µL, 3.00 mmol, 2.0 eq.) was added. FCC (hexanes/EtOAc 9:1), followed by recrystallization from EtOH yielded SGA-48 (**100**) as colorless solid (271 mg, 0.686 mmol, 46%).

R$_f$ = 0.48 (9:1 hexanes/EtOAc).

m.p.: 98 °C.

^{1}H NMR (400 MHz, CDCl$_3$) δ/ppm = 7.48 (d, J = 2.0 Hz, 1H, 6'-H), 7.29 (dd, J = 8.2, 2.0 Hz, 1H, 4'-H), 7.25 (d, J = 9.1 Hz, 1H, 3'-H, collapses with chloroform), 6.51 (s, 1H, 4-H), 4.27 (q, J = 7.0 Hz, 2H, C$\underline{H}_2$CH$_3$), 3.55 (d, J = 7.0 Hz, 2H, CH$_2$-cy), 2.59 (s, 3H, CH$_3$), 1.61 – 1.56 (m, 3H, cy), 1.40 – 1.31 (m, 6H, cy, CH$_2$C$\underline{H}_3$), 1.08 – 0.99 (m, 3H, cy), 0.68 – 0.58 (m, 2H, cy).

^{13}C NMR (101 MHz, CDCl$_3$) δ/ppm = 165.6 (COOEt), 137.0 (C-2), 135.9 (C-1' or C-5'), 134.8 (C-1' or C-5'), 134.0 (C-3'), 131.2 (C-2'), 129.6 (C-6'), 129.2 (C-5), 127.2 (C-4'), 112.2 (C-3), 111.1 (C-4), 59.5 ($\underline{C}$H$_2$CH$_3$), 50.8 (CH$_2$-cy), 39.1 (cy), 30.6 (cy), 26.2 (cy), 25.8 (cy), 14.7 (CH$_2$$\underline{C}H_3$), 12.1 (CH$_3$).

IR (ATR) $\tilde{v}_{max}$/cm^{-1} = 2981, 2923, 2845, 1739, 1723, 1695, 1565, 1454, 1262, 1238, 1201, 1159, 1076, 1066, 800, 771.

HRMS (ESI): calcd. for C$_{21}$H$_{26}$^{35}Cl$_2$NO$_2$ (M+H)$^+$ 394.13351; found 394.13343.

Purity (HPLC): > 96% (λ = 210 nm), > 96% (λ = 254 nm).

1-(Cyclohexylmethyl)-5-(2,5-dichlorophenyl)-2-methyl-1*H*-pyrrole-3-carboxylic acid – SGA-52 (116)

SGA-52 (**116**)

According to general procedure **D**, LiOH (63.9 mg, 2.54 mmol, 10 eq.) and a solution of SGA-48 (**110**, 100 mg, 0.254 mmol, 1.0 eq.) in dioxane/H$_2$O (1.3 mL) were used. After 1 h the reaction was completed and gave SGA-52 (**116**) as colorless solid (75.7 mg, 0.207 mmol, 81%).

R$_f$ = 0.18 (6:1 hexanes/EtOAc).

m.p.: 180 °C.

^{1}H NMR (500 MHz, CDCl$_3$) δ/ppm = 7.48 (d, J = 2.0 Hz, 1H, 6'-H), 7.30 (dd, J = 8.2, 2.0 Hz, 1H, 4'-H), 7.26 (d, J = 8.2 Hz, 1H, 3'-H, collapses with chloroform), 6.57 (s, 1H, 4-H), 3.57 (d, J = 6.4 Hz, 2H, C$\underline{H}_2$-cy), 2.60 (s, 3H, CH$_3$), 1.63 – 1.57 (m, 3H, cy), 1.42 – 1.36 (m, 3H, cy), 1.08 – 1.00 (m, 3H, cy), 0.68 – 0.59 (m, 2H, cy).

^{13}C NMR (126 MHz, CDCl$_3$) δ/ppm = 170.7 (COOH), 138.3 (C-2), 136.0 (C-1' or C-5'), 135.0 (C-1' or C-5'), 134.0 (C-3'), 131.0 (C-2'), 129.7 (C-6'), 129.6 (C-5), 127.2 (C-4'), 111.8 (C-4), 111.4 (C-3), 50.9 ($\underline{C}$H$_2$-cy), 39.0 (cy), 30.7 (cy), 26.2 (cy), 25.8 (cy), 12.3 (CH$_3$).

IR (ATR) $\tilde{v}_{max}$/cm^{-1} = 3014, 2970, 2926, 2851, 1739, 1659, 1449, 1365, 1270, 1228, 1217, 1204, 814, 776.

HRMS (ESI): calcd. for C$_{19}$H$_{20}$^{35}Cl$_2$NO$_2$ (M-H)$^-$ 364.08766; found 364.08783.

Purity (HPLC): > 96% (λ = 210 nm), > 96% (λ = 254 nm).

Ethyl 5-(5-bromo-2-methoxyphenyl)-1-(cyclohexylmethyl)-2-methyl-1*H*-pyrrole-3-carboxylate – SGA-54 (97)

SGA-54 (**97**)

Following general procedure **C**, ethyl acetoacetate (**94**, 143 µL, 1.10 mmol, 1.1 eq.) in dry THF (5.0 mL), NaH (60.0 mg, 1.50 mmol, 1.5 eq.) and a solution of 2-bromo-1-(5-bromo-2-methoxyphenyl)ethan-1-one (**93**, 308 mg, 1.00 mmol, 1.0 eq.) in dry THF (1.0 mL) were used. Then, the residue was dissolved in acetic acid (5.0 mL) and cyclohexanemethanamine (**95**, 260 µL, 2.00 mmol, 2.0 eq.) was added. FCC (hexanes/EtOAc 9:1) yielded SGA-54 (**97**) as colorless solid (411 mg, 0.947 mmol, 95%).

R$_f$ = 0.37 (6:1 hexanes/EtOAc).

m.p.: 83 °C.

^{1}H NMR (400 MHz, CDCl$_3$) δ/ppm = 7.45 (dd, J = 8.7, 2.5 Hz, 1H, 4'-H), 7.37 (d, J = 2.5 Hz, 1H, 6'-H), 6.81 (d, J = 8.7 Hz, 1H, 3'-H), 6.48 (s, 1H, 4-H), 4.25 (q, J = 7.1 Hz, 2H, C$\underline{H}_2$CH$_3$),

3.76 (s, 3H, OCH$_3$), 3.56 (d, J = 7.2 Hz, 2H, C$\underline{H}_2$-cy), 2.58 (s, 3H, CH$_3$), 1.60 – 1.54 (m, 3H, cy), 1.41 – 1.29 (m, 6H, cy, CH$_2$C$\underline{H}_3$), 1.08 – 0.97 (m, 3H, cy), 0.68 – 0.57 (m, 2H, cy).

^{13}C NMR (101 MHz, CDCl$_3$) δ/ppm = 165.7 (COOEt), 156.6 (C-2'), 136.9 (C-2), 135.2 (C-6'), 132.3 (C-4'), 128.9 (C-5), 124.8 (C-1'), 112.8 (C-5'), 112.6 (C-3'), 112.1 (C-3), 110.6 (C-4), 59.3 ($\underline{C}$H$_2$CH$_3$), 55.9 (OCH$_3$), 50.9 (CH$_2$-cy), 39.0 (cy), 30.7 (cy), 26.3 (cy), 25.8 (cy), 14.7 (CH$_2\underline{C}$H$_3$), 12.1 (CH$_3$).

IR (ATR) $\tilde{v}_{max}$/cm^{-1} = 2979, 2928, 2849, 1695, 1676, 1473, 1461, 1434, 1253, 1234, 1187, 1176, 1060, 1048, 1027, 774, 619.

HRMS (ESI): calcd. for C$_{22}$H$_{29}$^{79}BrNO$_3$ (M+H)$^+$ 434.13253; found 434.13229.

Purity (HPLC): > 96% (λ = 210 nm), > 96% (λ = 254 nm).

5-(5-Bromo-2-methoxyphenyl)-1-(cyclohexylmethyl)-2-methyl-1H-pyrrole-3-carboxylic acid – SGA-55 (115)

SGA-55 (**115**)

According to general procedure **D**, LiOH (88.4 mg, 3.51 mmol, 10 eq.) and a solution of SGA-54 (**97**, 152 mg, 0.351 mmol, 1.0 eq.) in dioxane/H$_2$O (1.3 mL) were used. After 1 h the reaction was completed and gave SGA-55 (**115**) as colorless solid (90.0 mg, 0.222 mmol, 63%).

R$_f$ = 0.72 (1:1 hexanes/EtOAc).

m.p.: 224 °C.

^{1}H NMR (400 MHz, CDCl$_3$) δ/ppm = 7.46 (dd, J = 8.8, 2.5 Hz, 1H, 4'-H), 7.38 (d, J = 2.5 Hz, 1H, 6'-H), 6.82 (d, J = 8.8 Hz, 1H, 3'-H), 6.54 (s, 1H, 4-H), 3.77 (s, 3H, OCH$_3$), 3.57 (d, J = 7.2 Hz, 2H, CH$_2$-cy), 2.59 (s, 3H, CH$_3$), 1.62 – 1.52 (m, 3H, cy), 1.43 – 1.33 (m, 3H, cy), 1.10 – 0.98 (m, 3H, cy), 0.69 – 0.58 (m, 2H, cy).

^{13}C NMR (101 MHz, CDCl$_3$) δ/ppm = 170.4 (COOH), 156.6 (C-2'), 138.2 (C-2), 135.2 (C-6'), 132.4 (C-4'), 129.3 (C-5), 124.6 (C-1'), 112.8 (C-5'), 112.6 (C-3'), 111.4 (C-4), 111.3 (C-3), 55.9 (OCH$_3$), 51.0 (CH$_2$-cy), 39.0 (cy), 30.7 (cy), 26.3 (cy), 25.8 (cy), 12.3 (CH$_3$).

IR (ATR) $\tilde{v}_{max}$/cm^{-1} = 3027, 2969, 2926, 2850, 1739, 1658, 1476, 1462, 1442, 1362, 1274, 1244, 1205, 1018, 808, 782, 619.

HRMS (ESI): calcd. for $C_{20}H_{23}{}^{79}BrNO_3$ (M-H)$^-$ 404.08668; found 404.08697.

Purity (HPLC): > 96% (λ = 210 nm), > 96% (λ = 254 nm).

Ethyl 1-(cyclohexylmethyl)-5-(4-fluorophenyl)-2-methyl-1*H*-pyrrole-3-carboxylate – SGA-59 (111)

SGA-59 (**111**)

Following general procedure **C**, ethyl acetoacetate (**94**, 208 µL, 1.65 mmol, 1.1 eq.) in dry THF (5.0 mL), NaH (90.0 mg, 2.25 mmol, 1.5 eq.) and a solution of 2-chloro-1-(4-fluorophenyl)ethan-1-one (259 mg, 1.50 mmol, 1.0 eq.) and KI (249 mg, 1.50 mmol, 1.0 eq.) in dry THF (3.0 mL) were used. Then, the residue was dissolved in acetic acid (5.0 mL) and cyclohexanemethanamine (**95**, 390 µL, 3.00 mmol, 2.0 eq.) was added. FCC (hexanes/EtOAc 9:1) yielded SGA-59 (**111**) as yellow oil (499 mg, 1.45 mmol, 97%).

R$_f$ = 0.43 (9:1 hexanes/EtOAc).

^{1}H NMR (500 MHz, CDCl$_3$) δ/ppm = 7.28 – 7.23 (m, 2H, 2'-H, 6'-H), 7.10 – 7.01 (m, 2H, 3'-H, 5'-H), 6.48 (s, 1H, 4-H), 4.25 (q, *J* = 7.1 Hz, 2H, C$\underline{H}_2$CH$_3$), 3.71 (d, *J* = 7.2 Hz, 2H, C$\underline{H}_2$-cy), 2.57 (s, 3H, CH$_3$), 1.58 – 1.48 (m, 3H, cy), 1.38 – 1.28 (m, 6H, cy, CH$_2$C$\underline{H}_3$), 1.06 – 0.89 (m, 3H, cy), 0.68 – 0.53 (m, 2H, cy).

^{13}C NMR (121 MHz, CDCl$_3$) δ/ppm = 165.7 (COOH), 162.2 (d, J_{CF} = 247.0 Hz, C-4'), 136.9 (C-2), 132.8 (C-5), 131.3 (d, J_{CF} = 8.0 Hz, C-2', C-6'), 129.7 (d, J_{CF} = 3.3 Hz, C-1'), 115.4 (d, J_{CF} = 21.3 Hz, C-3', C-5'), 111.9 (C-3), 110.0 (C-4), 59.3 ($\underline{C}$H$_2$CH$_3$), 50.1 ($\underline{C}$H$_2$-cy), 39.0 (cy), 30.5 (cy), 26.1 (cy), 25.7 (cy), 14.6 (CH$_2\underline{C}$H$_3$), 12.0 (CH$_3$).

IR (ATR) $\tilde{v}_{max}$/cm^{-1} = 2977, 2925, 2853, 1693, 1242, 1227, 1218, 1195, 1152, 1062, 844, 811, 774.

HRMS (ESI): calcd. for $C_{21}H_{27}FNO_2$ (M+H)$^+$ 344.20203; found 344.20193.

Purity (HPLC): > 96% (λ = 210 nm), > 96% (λ = 254 nm).

1-(Cyclohexylmethyl)-5-(4-fluorophenyl)-2-methyl-1*H*-pyrrole-3-carboxylic acid – SGA-66 (117)

SGA-66 (**117**)

According to general procedure **D**, LiOH (169 mg, 6.71 mmol, 10 eq.) and a solution of SGA-59 (**111**, 230 mg, 0.671 mmol, 1.0 eq.) in dioxane/H_2O (3.0 mL) were used. After 2 h the reaction was completed and gave SGA-66 (**117**) as colorless solid (186 mg, 0.590 mmol, 88%).

R$_f$ = 0.24 (6:1 hexanes/EtOAc).

m.p.: 171 °C.

^{1}H NMR (400 MHz, CDCl$_3$) δ/ppm = 7.35 – 7.27 (m, 2H, 2'-H, 6'-H), 7.14 – 7.04 (m, 2H, 3'-H, 5'-H), 6.57 (s, 1H, 4-H), 3.75 (d, *J* = 7.1 Hz, 2H, C$\underline{H}_2$-cy), 2.61 (s, 3H, CH$_3$), 1.63 – 1.51 (m, 3H, cy), 1.41 – 1.32 (m, 3H, cy), 1.08 – 0.97 (m, 3H, cy), 0.70 – 0.57 (m, 2H, cy).
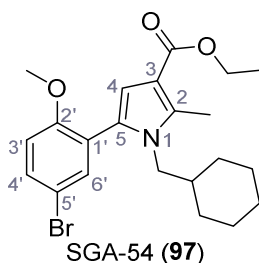
^{13}C NMR (121 MHz, CDCl$_3$) δ/ppm = 171.2 (COOH), 162.37 (d, J_{CF} = 247.1 Hz, C-4'), 138.3 (C-2), 133.3 (C-5), 131.42 (d, J_{CF} = 8.1 Hz, C-2', C-6'), 129.6 (d, J_{CF} = 3.4 Hz, C-1'), 115.57 (d, J_{CF} = 21.5 Hz, C-3', C-5'), 111.2 (C-3), 110.8 (C-4), 50.3 ($\underline{C}$H$_2$-cy), 39.0 (cy), 30.6 (cy), 26.2 (cy), 25.8 (cy), 12.3 (CH$_3$).

IR (ATR) $\tilde{v}_{max}$/cm^{-1} = 2927, 2854, 1739, 1652, 1568, 1494, 1449, 1265, 1223, 1203, 1158, 840, 776, 582.

HRMS (ESI): calcd. for C$_{19}$H$_{21}$FNO$_2$ (M-H)$^-$ 314.15618; found 314.15635.

Purity (HPLC): > 96% (λ = 210 nm), > 96% (λ = 254 nm).

Ethyl 1-(cyclohexylmethyl)-5-(4-methoxyphenyl)-2-methyl-1*H*-pyrrole-3-carboxylate – SGA-61 (112)

SGA-61 (**112**)

Following general procedure **C**, ethyl acetoacetate (**94**, 208 μL, 1.65 mmol, 1.1 eq.) in dry THF (5.0 mL), NaH (90.0 mg, 2.25 mmol, 1.5 eq.) and a solution of 2-bromo-1-(4-

methoxyphenyl)ethan-1-one (344 mg, 1.50 mmol, 1.0 eq.) and KI (249 mg, 1.50 mmol, 1.0 eq.) in dry THF (3.0 mL) were used. Then, the residue was dissolved in acetic acid (5.0 mL) and cyclohexanemethanamine (**95**, 390 µL, 3.00 mmol, 2.0 eq.) was added. FCC (hexanes/EtOAc 9:1), followed by recrystallization from EtOH yielded SGA-61 (**112**) as colorless solid (274 mg, 0.770 mmol, 51%).

R$_f$ = 0.37 (9:1 hexanes/EtOAc).

m.p.: 88 °C.

^{1}H NMR (500 MHz, CDCl$_3$) δ/ppm = 7.25 – 7.21 (m, 2H, 2'-H, 6'-H), 6.95 – 6.89 (m, 2H, 3'-H, 5'-H), 6.47 (s, 1H, 4-H), 4.27 (q, J = 7.1 Hz, 2H, C$\underline{H}_2$CH$_3$), 3.84 (s, 3H, OCH$_3$), 3.73 (d, J = 7.3 Hz, 2H, C$\underline{H}_2$-cy), 2.58 (s, 3H, CH$_3$), 1.60 – 1.51 (m, 3H, cy), 1.42 – 1.31 (m, 6H, cy, CH$_2$C$\underline{H}_3$), 1.07 – 0.96 (m, 3H, cy), 0.70 – 0.59 (m, 2H, cy).

^{13}C NMR (126 MHz, CDCl$_3$) δ/ppm = 165.9 (COOH), 159.0 (C-4'), 136.6 (C-2), 133.8 (C-5), 130.9 (C-2', C-6'), 126.1 (C-1'), 113.9 (C-3', C-5'), 111.7 (C-3), 109.5 (C-4), 59.3 ($\underline{C}$H$_2$CH$_3$), 55.4 (OCH$_3$), 50.1 ($\underline{C}$H$_2$-cy), 39.0 (cy), 30.6 (cy), 26.2 (cy), 25.8 (cy), 14.7 (CH$_2$$\underline{C}H_3$), 12.1 (CH$_3$).

IR (ATR) $\tilde{v}_{max}$/cm^{-1} = 3016, 2970, 2928, 2847, 1739, 1693, 1568, 1532, 1496, 1443, 1424, 1373, 1243, 1226, 1195, 1175, 1064, 1031, 835, 817, 795, 774.

HRMS (ESI): calcd. for C$_{22}$H$_{30}$NO$_3$ (M+H)$^+$ 356.22202; found 356.22192.

Purity (HPLC): > 96% (λ = 210 nm), > 96% (λ = 254 nm).

1-(Cyclohexylmethyl)-5-(4-methoxyphenyl)-2-methyl-1*H*-pyrrole-3-carboxylic acid – SGA-67 (118)
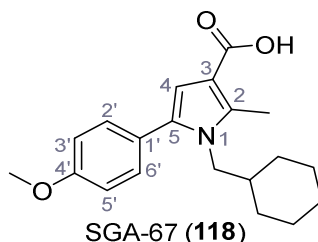
SGA-67 (**118**)

According to general procedure **D**, LiOH (78.7 mg, 3.12 mmol, 10 eq.) and a solution of SGA-61 (**112**, 111 mg, 0.312 mmol, 1.0 eq.) in dioxane/H$_2$O (1.3 mL) were used. After 2 h the reaction was completed and gave SGA-67 (**118**) as colorless solid (95.3 mg, 0.291 mmol, 90%).

R$_f$ = 0.20 (6:1 hexanes/EtOAc).

m.p.: 198 °C.

¹H NMR (400 MHz, CDCl₃) δ/ppm = 7.27 – 7.23 (m, 2H, 2'-H, 6'-H), 6.95 – 6.91 (m, 2H, 3'-H, 5'-H), 6.54 (s, 1H, 4-H), 3.85 (s, 3H, OCH₃), 3.75 (d, J = 7.2 Hz, 2H, CH₂-cy), 2.60 (s, 3H, CH₃), 1.62 – 1.53 (m, 3H, cy), 1.43 – 1.33 (m, 3H, cy), 1.09 – 0.98 (m, 3H, cy), 0.70 – 0.59 (m, 2H, cy).
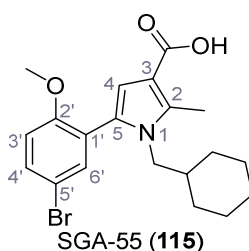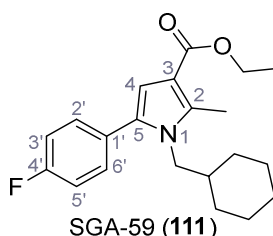
¹³C NMR (101 MHz, CDCl₃) δ/ppm = 171.3 (COOH), 159.0 (C-4'), 137.8 (C-2), 134.1 (C-5), 131.0 (C-2', C-6'), 125.9 (C-1'), 113.9 (C-3', C-5'), 111.0 (C-3), 110.2 (C-4), 55.3 (OCH₃), 50.2 (CH₂-cy), 38.9 (cy), 30.5 (cy), 26.2 (cy), 25.8 (cy), 12.3 (CH₃).

IR (ATR) $\tilde{\nu}_{max}$/cm⁻¹ = 3027, 3002, 2970, 2925, 2849, 1738, 1652, 1569, 1535, 1494, 1435, 1364, 1266, 1247, 1228, 1203, 840, 778.

HRMS (ESI): calcd. for $C_{20}H_{24}NO_3$ (M-H)⁻ 326.17617; found 326.17633.

Purity (HPLC): 93% (λ = 210 nm), > 96% (λ = 254 nm).

Ethyl 1-(cyclohexylmethyl)-5-(2,4-difluorophenyl)-2-methyl-1*H*-pyrrole-3-carboxylate – SGA-62 (113)
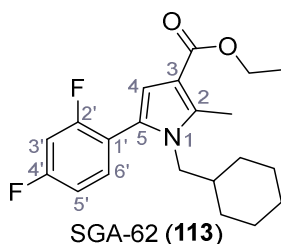
SGA-62 (**113**)

Following general procedure **C**, ethyl acetoacetate (**94**, 208 µL, 1.65 mmol, 1.1 eq.) in dry THF (5.0 mL), NaH (90.0 mg, 2.25 mmol, 1.5 eq.) and a solution of 2-chloro-1-(2,4-difluorophenyl)ethan-1-one (286 mg, 1.50 mmol, 1.0 eq.) and KI (249 mg, 1.50 mmol, 1.0 eq.) in dry THF (3.0 mL) were used. Then, the residue was dissolved in acetic acid (5.0 mL) and cyclohexanemethanamine (**95**, 390 µL, 3.00 mmol, 2.0 eq.) was added. FCC (hexanes/EtOAc 9:1) yielded SGA-62 (**113**) as yellow solid (424 mg, 1.17 mmol, 78%).

R*f* = 0.43 (9:1 hexanes/EtOAc).

m.p.: 94 °C.

¹H NMR (500 MHz, CDCl₃) δ/ppm = 7.27 (td, J = 8.4, 6.5 Hz, 1H, 6'-H), 6.96 – 6.85 (m, 2H, 3'-H, 5'-H), 6.53 (s, 1H, 4-H), 4.26 (q, J = 7.1 Hz, 2H, CH₂CH₃), 3.60 (d, J = 7.1 Hz, 2H, CH₂-cy), 2.58 (s, 3H, CH₃), 1.59 – 1.53 (m, 3H, cy), 1.38 – 1.30 (m, 6H, cy, CH₂CH₃), 1.06 – 0.98 (m, 3H, cy), 0.68 – 0.58 (m, 2H, cy).
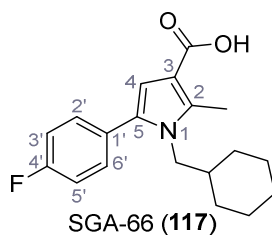
^{13}**C NMR (121 MHz, CDCl$_3$)** δ/ppm = 165.5 (COOEt), 162.9 (dd, J_{CF} = 250.1, 11.6 Hz, C-4'), 160.2 (dd, J_{CF} = 248.9, 12.0 Hz, C-2'), 137.2 (C-2), 133.5 (dd, J_{CF} = 9.4, 4.1 Hz, C-6'), 126.2 (C-5), 117.6 (dd, J_{CF} = 15.7, 3.9 Hz, C-1'), 112.3 (C-3), 111.6 (dd, J_{CF} = 21.1, 3.7 Hz, C-5'), 111.3 (C-4), 104.20 (t, J_{CF} = 25.8 Hz, C-3'), 59.4 (CH$_2$CH$_3$), 50.6 (d, J_{CF} = 3.0 Hz, CH$_2$-cy), 39.0 (cy), 30.5 (cy), 26.1 (cy), 25.7 (cy), 14.6 (CH$_2$CH$_3$), 12.0 (CH$_3$).

IR (ATR) $\tilde{v}_{max}$/cm^{-1} = 2971, 2929, 2848, 1739, 1698, 1571, 1426, 1371, 1235, 1199, 1067, 834.

HRMS (ESI): calcd. for C$_{21}$H$_{26}$F$_2$NO$_2$ (M+H)$^+$ 362.19261; found 362.19247.

Purity (HPLC): > 96% (λ = 210 nm), > 96% (λ = 254 nm).

1-(Cyclohexylmethyl)-5-(2,4-difluorophenyl)-2-methyl-1*H*-pyrrole-3-carboxylic acid - SGA-68 (119)
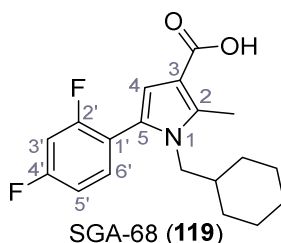
SGA-68 (**119**)

According to general procedure **D**, LiOH (167 mg, 6.61 mmol, 10 eq.) and a solution of SGA-62 (**113**, 239 mg, 0.661 mmol, 1.0 eq.) in dioxane/H$_2$O (1.3 mL) were used. After 1 h the reaction was completed and gave SGA-68 (**119**) as colorless solid (170 mg, 0.511 mmol, 77%).

R$_f$ = 0.29 (6:1 hexanes/EtOAc).

m.p.: 168 °C.

^{1}**H NMR (400 MHz, CDCl$_3$)** δ/ppm = 7.33 – 7.25 (m, 1H, 6'-H, collapses with chloroform), 6.98 – 6.86 (m, 2H, 3'-H, 5'-H), 6.60 (s, 1H, 4-H), 3.62 (d, J = 7.1 Hz, 2H, CH$_2$-cy), 2.61 (s, 3H, CH$_3$), 1.65 – 1.51 (m, 3H, cy), 1.49 – 1.32 (m, 3H, cy), 1.14 – 0.94 (m, 3H, cy), 0.72 – 0.56 (m, 2H, cy).
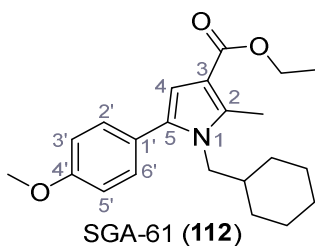
^{13}**C NMR (101 MHz, CDCl$_3$)** δ/ppm = 171.0 (COOH), 163.0 (dd, J_{CF} = 250.3, 11.6 Hz, C-4'), 160.3 (dd, J_{CF} = 249.0, 12.0 Hz, C-2'), 138.5 (C-2), 133.6 (dd, J_{CF} = 9.5, 4.0 Hz, C-6'), 126.7 (C-5), 117.5 (dd, J_{CF} = 15.8, 3.8 Hz, C-1'), 112.0 (C-3), 111.7 (dd, J_{CF} = 21.3, 3.8 Hz, C-5'), 111.6 (C-4), 104.3 (t, J_{CF} = 25.9 Hz, C-3'), 50.72 (d, J_{CF} = 3.0 Hz, CH$_2$-cy), 39.0 (cy), 30.6 (cy), 26.2 (cy), 25.7 (cy), 12.2 (CH$_3$).

IR (ATR) $\tilde{v}_{max}$/cm^{-1} = 2970, 2926, 2854, 1739, 1666, 1573, 1450, 1433, 1364, 1265, 1239, 1200, 1140, 778.

HRMS (ESI): calcd. for $C_{19}H_{20}F_2NO_2$ (M-H)$^-$ 332.14676; found 332.14697.

Purity (HPLC): > 96% (λ = 210 nm), > 96% (λ = 254 nm).

5-(5-Bromo-2-(trifluoromethoxy)phenyl)-2-methyl-1-pentyl-1*H*-pyrrole-3-carboxylic acid – SGA-149 (123)
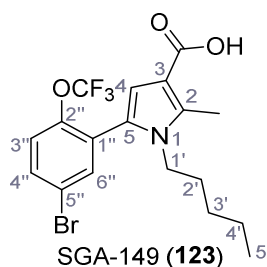
SGA-149 (**123**)

Following general procedure **C**, ethyl acetoacetate (**94**, 87.6 µL, 0.693 mmol, 1.1 eq.) in dry THF (4.0 mL), NaH (37.8 mg, 0.945 mmol, 1.5 eq.) and a solution of ketone **102** (200 mg, 0.630 mmol, 1.0 eq.) and KI (105 mg, 0.630 mmol, 1.0 eq.) in dry THF (2.0 mL) was used. Then, the residue was dissolved in acetic acid (5.0 mL) and *n*-pentylamine (146 µL, 1.26 mmol, 2.0 eq.) was added. FCC (hexanes/EtOAc 99:1) yielded ethyl 5-(5-bromo-2-(trifluoromethoxy)phenyl)-2-methyl-1-pentyl-1*H*-pyrrole-3-carboxylate as colorless oil (81.5 mg, 0.176 mmol). The product was used without further purification or characterization for the next step.

R$_f$ = 0.51 (9:1 hexanes/EtOAc).

According to general procedure **D**, LiOH (44.4 mg, 1.76 mmol, 10 eq.) and a solution of this ester (81.5 mg, 0.176 mmol, 1.0 eq.) in dioxane/H$_2$O (3.0 mL) were used. After 18 h the reaction was completed and gave SGA-149 (**123**) as colorless solid (40.5 mg, 0.0933 mmol, 15% over two steps).

R$_f$ = 0.06 (9:1 hexanes/EtOAc).

m.p.: 121 °C.

^{1}H NMR (400 MHz, CDCl$_3$) δ/ppm = 7.57 – 7.51 (m, 2H, 4''-H, 6''-H), 7.24 – 7.20 (m, 1H, 3''-H), 6.61 (s, 1H, 4-H), 3.74 – 3.68 (m, 2H, 1'-H), 2.61 (s, 3H, CH$_3$), 1.49 – 1.43 (m, 2H, 2'-H), 1.19 – 1.06 (m, 4H, 3'-H, 4'-H), 0.80 (t, *J* = 7.2 Hz, 3H, 5'-H).

^{13}C NMR (101 MHz, CDCl$_3$) δ/ppm = 169.4 (COOH), 146.6 (C-2''), 138.3 (C-2), 135.9 (C-6''), 132.8 (C-4''), 128.7 (C-5''), 126.1 (C-5), 122.5 (q, *J* = 279.8 Hz, OCF$_3$), 122.4 (C-3''), 120.0 (C-1''), 112.7 (C-4), 111.4 (C-3), 44.7 (C-1'), 30.2 (C-2'), 28.8 (C-3'), 22.1 (C-4'), 13.9 (C-5'), 11.9 (CH$_3$).

IR (ATR) $\tilde{v}_{max}$/cm^{-1} = 2929, 1663, 1471, 1436, 1247, 1212, 1194, 1160, 781.

HRMS (ESI): calcd. for $C_{18}H_{20}^{79}BrF_3NO_3$ (M+H)$^+$ 434.05732; found 434.05765.

Purity (HPLC): > 96% (λ = 210 nm), > 96% (λ = 254 nm).

1-Benzyl-5-(5-bromo-2-(trifluoromethoxy)phenyl)-2-methyl-1*H*-pyrrole-3-carboxylic acid – SGA-150 (125)

SGA-150 (**125**)
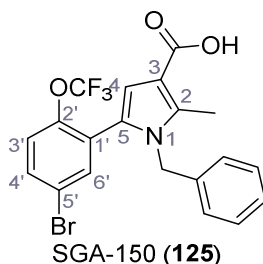
Following general procedure **C**, ethyl acetoacetate (**94**, 104 µL, 0.821 mmol, 1.1 eq.) in dry THF (4.0 mL), NaH (44.8 mg, 1.12 mmol, 1.5 eq.) and a solution of ketone **102** (237 mg, 0.746 mmol, 1.0 eq.) and KI (124 mg, 0.746 mmol, 1.0 eq.) in dry THF (2.0 mL) were used. Then, the residue was dissolved in acetic acid (5.0 mL) and benzylamine (204 µL, 1.87 mmol, 2.5 eq.) was added. FCC (hexanes/EtOAc 97:3) yielded ethyl 5-(5-bromo-2-(trifluoromethoxy)phenyl)-1-isopropyl-2-methyl-1*H*-pyrrole-3-carboxylate as colorless oil (107 mg, 0.222 mmol). The product was used without further purification or characterization for the next step.

R$_f$ = 0.44 (9:1 hexanes/EtOAc).

According to general procedure **D**, LiOH (55.9 mg, 2.22 mmol, 10 eq.) and a solution of this ester (107 mg, 0.222 mmol, 1.0 eq.) in dioxane/H$_2$O (3.0 mL) were used. After 16 h the reaction was completed and gave SGA-150 (**125**) as colorless solid (34.4 mg, 0.0757 mmol, 10% over two steps).

R$_f$ = 0.27 (9:1 hexanes/EtOAc).

m.p.: 185 °C.

^{1}H NMR (400 MHz, CD$_2$Cl$_2$) δ/ppm = 11.12 (s, 1H, COOH), 7.51 (dd, *J* = 8.8, 2.5 Hz, 1H, 4'-H), 7.39 (d, *J* = 2.5 Hz, 1H, 6'-H), 7.30 – 7.18 (m, 4H, 3'-H, Ph), 6.83 – 6.77 (m, 2H, Ph), 6.70 (s, 1H, 4-H), 5.00 (s, 2H, CH$_2$), 2.49 (s, 3H, CH$_3$).

^{13}C NMR (121 MHz, CD$_2$Cl$_2$) δ/ppm = 169.9 (COOH), 147.0 (C-2'), 139.6 (C-2), 137.4 (C-1'), 136.3 (C-6'), 133.4 (C-4'), 129.3 (Ph), 128.5 (qPh), 128.0 (Ph), 127.3 (C-5), 126.2 (Ph), 122.8

(C-3'), 120.8 (q, J_{CF} = 258.7 Hz, OCF$_3$), 120.3 (C-5'), 113.1 (C-4), 112.3 (C-3), 48.7 (CH$_2$), 12.2 (CH$_3$).

IR (ATR) $\tilde{\nu}_{max}$/cm^{-1} = 2925, 2360, 1670, 1249, 1223, 1198, 1171, 733.

HRMS (ESI): calcd. for $C_{20}H_{14}{}^{79}BrF_3NO_3$ (M-H)$^-$ 452.01146; found 452.01168.

Purity (HPLC): > 96% (λ = 210 nm), > 96% (λ = 254 nm).

5-(5-Bromo-2-(trifluoromethoxy)phenyl)-1-(cyclohexylmethyl)-2-ethyl-1*H*-pyrrole-3-carboxylic acid – SGA-152 (121)

SGA-152 (**121**)
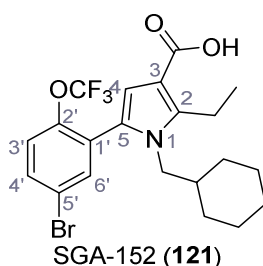
Following general procedure **C**, ethyl propionylacetate (99.9 µL, 0.693 mmol, 1.1 eq.) in dry THF (4.0 mL), NaH (37.8 mg, 0.945 mmol, 1.5 eq.) and a solution of ketone **102** (200 mg, 0.630 mmol, 1.0 eq.) and KI (105 mg, 0.630 mmol, 1.0 eq.) in dry THF (2.0 mL) were used. Then, the residue was dissolved in acetic acid (5.0 mL) and cyclohexanemethanamine (**95**, 164 µL, 1.26 mmol, 2.0 eq.) was added. FCC (hexanes/EtOAc 99:1) yielded ethyl 5-(5-bromo-2-(trifluoromethoxy)phenyl)-1-(cyclohexylmethyl)-2-ethyl-1*H*-pyrrole-3-carboxylate as colorless oil (98.0 mg, 0.195 mmol). The product was used without further purification or characterization for the next step.

R$_f$ = 0.58 (9:1 hexanes/EtOAc).

According to general procedure **D**, LiOH (49.2 mg, 1.95 mmol, 10 eq.) and a solution of this ester (98.0 mg, 0.195 mmol, 1.0 eq.) in dioxane/H$_2$O (3.0 mL) were used. After 18 h the reaction was completed and gave SGA-152 (**121**) as yellow solid (30.8 mg, 0.0649 mmol, 9% over two steps).

R$_f$ = 0.24 (9:1 hexanes/EtOAc).

m.p.: 152 °C.

^{1}H NMR (500 MHz, CDCl$_3$) δ/ppm = 11.35 (s, 1H, COOH), 7.57 – 7.50 (m, 2H, 4'-H, 6'-H), 7.20 (dd, *J* = 8.6, 1.4 Hz, 1H, 3'-H), 6.61 (s, 1H, 4-H), 3.61 (d, *J* = 7.2 Hz, 2H, C$\underline{H}_2$-cy), 3.04 (q, *J* = 7.4 Hz, 2H, C$\underline{H}_2$CH$_3$), 1.64 – 1.54 (m, 3H, cy), 1.39 – 1.31 (m, 3H, cy), 1.23 (t, *J* = 7.4 Hz, 3H, CH$_2$C$\underline{H}_3$), 1.08 – 0.99 (m, 3H, cy), 0.70 – 0.60 (m, 2H, cy).

¹³C NMR (121 MHz, CDCl₃) δ/ppm = 169.8 (COOH), 146.3 (C-2'), 145.1 (C-2), 135.5 (C-4' or C-6'), 132.5 (C-4' or C-6'), 129.1 (C-1'), 126.7 (C-5), 122.3 (C-3'), 120.3 (q, J_{CF} = 259.2 Hz, OCF₃), 120.0 (C-5'), 113.2 (C-4), 110.8 (C-3), 50.9 (CH₂-cy), 39.6 (cy), 30.7 (cy), 26.2 (cy), 25.8 (cy), 19.2 (CH₂CH₃), 14.5 (CH₂CH₃).

IR (ATR) $\tilde{v}_{max}$/cm⁻¹ = 2927, 2359, 1659, 1469, 1441, 1250, 1212, 1192, 1172.

HRMS (ESI): calcd. for C₂₁H₂₂⁷⁹BrF₃NO₃ (M-H)⁻ 472.07406; found 472.07418.

Purity (HPLC): > 96% (λ = 210 nm), > 96% (λ = 254 nm).

5-(5-Bromo-2-(trifluoromethoxy)phenyl)-1-isopropyl-2-methyl-1*H*-pyrrole-3-carboxylic acid – SGA-153 (124)
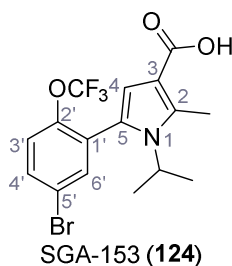
SGA-153 (**124**)

Following general procedure **C**, ethyl acetoacetate (**94**, 87.6 µL, 0.693 mmol, 1.1 eq.) in dry THF (4.0 mL), NaH (37.8 mg, 0.945 mmol, 1.5 eq.) and a solution of ketone **102** (200 mg, 0.630 mmol, 1.0 eq.) and KI (105 mg, 0.630 mmol, 1.0 eq.) in dry THF (2.0 mL) were used. Then, the residue was dissolved in acetic acid (5.0 mL) and isopropylamine (108 µL, 1.26 mmol, 2.0 eq.) was added. FCC (hexanes/EtOAc 99:1) yielded ethyl 5-(5-bromo-2-(trifluoromethoxy)phenyl)-1-isopropyl-2-methyl-1*H*-pyrrole-3-carboxylate as colorless oil (65.9 mg, 0.152 mmol). The product was used without further purification or characterization for the next step.

R_f_ = 0.55 (9:1 hexanes/EtOAc).

According to general procedure **D**, LiOH (38.3 mg, 1.52 mmol, 10 eq.) and a solution of this ester (65.9 mg, 0.152 mmol, 1.0 eq.) in dioxane/H₂O (3.0 mL) were used. After 18 h the reaction was completed and gave SGA-153 (**124**) as colorless solid (32.4 mg, 0.0798 mmol, 12% over two steps).

R_f_ = 0.11 (9:1 hexanes/EtOAc).

m.p.: 192 °C.

¹H NMR (400 MHz, C₃D₆O) δ/ppm = 7.75 (dd, *J* = 8.8, 2.6 Hz, 1H, 4'-H), 7.65 (d, *J* = 2.6 Hz, 1H, 6'-H), 7.44 (dq, *J* = 8.8, 1.5 Hz, 1H, 3'-H), 6.47 (s, 1H, 4-H), 4.27 (p, *J* = 7.0 Hz, 1H, CH), 2.72 (s, 3H, CH₃), 1.45 (d, *J* = 7.0 Hz, 6H, CH(CH₃)₂).

¹³C NMR (101 MHz, C₃D₆O) δ/ppm = 166.4 (COOH), 147.7 (C-2'), 137.5 (C-2), 137.0 (C-6'), 134.0 (C-4'), 130.5 (C-1'), 126.4 (C-5), 123.7 (q, J = 257.6 Hz, OCF₃), 123.5 (C-3'), 120.6 (C-5'), 113.9 (C-3), 113.0 (C-4), 50.2 (CH), 22.0 (CH(CH₃)₂), 13.0 (CH₃).

IR (ATR) $\tilde{\nu}_{max}$/cm⁻¹ = 2936, 2358, 1672, 1248, 1214, 1200, 1166.

HRMS (ESI): calcd. for C₁₆H₁₄⁷⁹BrF₃NO₃ (M-H)⁻ 404.01146; found 404.01164.

Purity (HPLC): > 96% (λ = 210 nm), > 96% (λ = 254 nm).

5-(5-Bromo-2-(trifluoromethoxy)phenyl)-1-(cyclohexylmethyl)-2-phenyl-1*H*-pyrrole-3-carboxylic acid – SGA-154 (122)

SGA-154 (**122**)
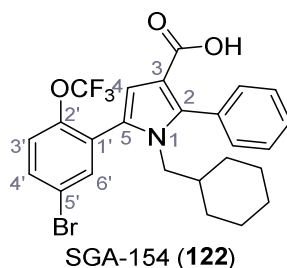
Following general procedure **C**, ethyl benzoylacetate (134 µL, 0.693 mmol, 1.1 eq.) in dry THF (4.0 mL), NaH (37.8 mg, 0.945 mmol, 1.5 eq.) and a solution of ketone **102** (200 mg, 0.630 mmol, 1.0 eq.) and KI (105 mg, 0.630 mmol, 1.0 eq.) in dry THF (2.0 mL) were used. Then, the residue was dissolved in acetic acid (5.0 mL) and cyclohexanemethanamine (**95**, 328 µL, 2.52 mmol, 4.0 eq.) was added. FCC (hexanes/EtOAc 99:1) yielded ethyl 5-(5-bromo-2-(trifluoromethoxy)phenyl)-1-(cyclohexylmethyl)-2-phenyl-1*H*-pyrrole-3-carboxylate as yellow solid (151 mg, 0.274 mmol). The product was used without further purification or characterization for the next step.

R$_f$ = 0.50 (9:1 hexanes/EtOAc).

According to general procedure **D**, LiOH (69.2 mg, 2.74 mmol, 10 eq.) and a solution of this ester (151 mg, 0.274 mmol, 1.0 eq.) in dioxane/H₂O (3.0 mL) were used. After 18 h the reaction was completed and gave SGA-154 (**122**) as yellow solid (91.5 mg, 0.175 mmol, 28% over two steps).

R$_f$ = 0.12 (9:1 hexanes/EtOAc).

m.p.: 170 °C.

¹H NMR (400 MHz, CDCl₃) δ/ppm = 7.61 (d, J = 2.5 Hz, 1H, 6'-H), 7.55 (dd, J = 8.7, 2.5 Hz, 1H, 4'-H), 7.47 – 7.41 (m, 3H, Ph), 7.39 – 7.35 (m, 2H, Ph), 7.23 (dq, J = 8.7, 1.3 Hz, 1H, 3'-

H), 6.74 (s, 1H, 4-H), 3.56 (d, J = 7.4 Hz, 2H, C$\underline{H}_2$-cy), 1.48 – 1.42 (m, 3H, cy), 1.11 – 1.05 (m, 2H, cy), 1.03 – 0.95 (m, 1H, cy), 0.90 – 0.82 (m, 3H, cy), 0.43 – 0.32 (m, 2H, cy).

^{13}C NMR (101 MHz, CDCl$_3$) δ/ppm = 167.7 (COOH), 146.1 (C-2'), 141.7 (C-2), 135.2 (C-6'), 132.7 (C-4'), 131.7 (C-5, C-1', C-5' or qPh), 131.0 (Ph), 128.8 (C-5, C-1', C-5' or qPh), 128.7 (Ph), 128.3 (Ph), 122.4 (C-3'), 120.4 (q, J_{CF} = 266.3 Hz, OCF$_3$), 120.2 (C-5, C-1', C-5' or qPh), 113.8 (C-4), 112.7 (C-3), 52.0 ($\underline{C}H_2$-cy), 38.7 (cy), 30.3 (cy), 26.1 (cy), 25.6 (cy). One quaternary carbon is missing.

IR (ATR) $\tilde{v}_{max}$/cm^{-1} = 2915, 2335, 1667, 1487, 1248, 1208, 1169, 1127, 796, 697.

HRMS (ESI): calcd. for C$_{25}$H$_{22}^{79}$BrF$_3$NO$_3$ (M-H)$^-$ 520.07406; found 520.07418.

Purity (HPLC): > 96% (λ = 210 nm), > 96% (λ = 254 nm).

Ethyl 1-(cyclohexylmethyl)-2-methyl-5-(2-(trifluoromethoxy)phenyl)-1*H*-pyrrole-3-carboxylate (114)

114
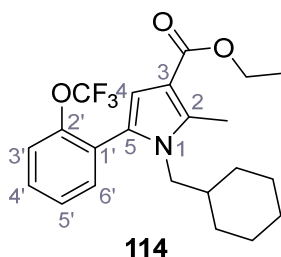
Following general procedure **C**, ethyl acetoacetate (**94**, 123 µL, 0.972 mmol, 1.1 eq.) in dry THF (4.0 mL), NaH (53.0 mg, 1.32 mmol, 1.5 eq.) and a solution of ketone **101** (250 mg, 0.883 mmol, 1.0 eq.) and KI (147 mg, 0.883 mmol, 1.0 eq.) in dry THF (2.0 mL) were used. Then, the residue was dissolved in acetic acid (5.0 mL) and cyclohexanemethanamine (**95**, 230 µL, 1.77 mmol, 2.0 eq.) was added. FCC (hexanes/EtOAc 9:1) yielded ester **114** as colorless solid (345 mg, 0.845 mmol, 95%).

R$_f$ = 0.46 (9:1 hexanes/EtOAc).

m.p.: 66 °C.

^{1}H NMR (100 MHz, CDCl$_3$) δ/ppm = 7.44 – 7.29 (m, 4H, 3'-H, 4'-H, 5'-H, 6'-H), 6.53 (s, 1H, 4-H), 4.27 (q, J = 7.1 Hz, 2H, C$\underline{H}_2$CH$_3$), 3.59 (d, J = 7.1 Hz, 2H, C$\underline{H}_2$-cy), 2.59 (s, 3H, CH$_3$), 1.59 – 1.52 (m, 3H, cy), 1.40 – 1.32 (m, 6H, cy, CH$_2$C$\underline{H}_3$), 1.06 – 0.94 (m, 3H, cy), 0.67 – 0.54 (m, 2H, cy).

^{13}C NMR (101 MHz, CDCl$_3$) δ/ppm = 165.8 (COOEt), 147.4 (C-2'), 137.1 (C-2), 133.4 (C-4', C-5' or C-6'), 129.6 (C-4', C-5' or C-6'), 127.9 (C-5), 126.9 (C-1'), 126.7 (C-4', C-5' or C-6'),

120.5 (q, J_{CF} = 257.4 Hz, OCF$_3$), 120.4 (C-3'), 112.2 (C-3), 111.4 (C-4), 59.5 (CH$_2$CH$_3$), 50.7 (CH$_2$-cy), 39.0 (cy), 30.6 (cy), 26.2 (cy), 25.8 (cy), 14.7 (CH$_2$CH$_3$), 12.1 (CH$_3$).

IR (ATR) $\tilde{v}_{max}$/cm^{-1} = 1934, 1692, 1447, 1422, 1242, 1192, 1155, 1059, 769.

HRMS (ESI): calcd. for C$_{22}$H$_{27}$F$_3$NO$_3$ (M+H)$^+$ 410.19375; found 410.19336.

Purity (HPLC): > 96% (λ = 210 nm), > 96% (λ = 254 nm).

1-(Cyclohexylmethyl)-2-methyl-5-(2-(trifluoromethoxy)phenyl)-1*H*-pyrrole-3-carboxylic acid – SGA-162 (120)
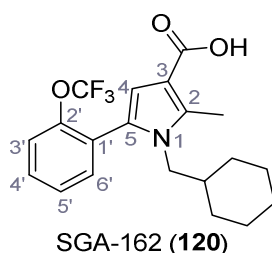
SGA-162 (**120**)

According to general procedure **D**, LiOH (142 mg, 5.62 mmol, 10 eq.) and a solution of ester **114** (230 mg, 0.562 mmol, 1.0 eq.) in dioxane/H$_2$O (3.0 mL) were used. After 2 h the reaction was completed and gave SGA-162 (**120**) as colorless solid (199 mg, 0.523 mmol, 93%).

R$_f$ = 0.11 (9:1 hexanes/EtOAc).

m.p.: 170 °C.

^{1}H NMR (400 MHz, CDCl$_3$) δ/ppm = 11.13 (s, 1H, COOH), 7.46 – 7.30 (m, 4H, 3'-H, 4'-H, 5'-H, 6'-H), 6.59 (s, 1H, 4-H), 3.60 (d, J = 7.1 Hz, 2H, CH$_2$-cy), 2.61 (s, 3H, CH$_3$), 1.61 – 1.52 (m, 3H, cy), 1.41 – 1.31 (m, 3H, cy), 1.09 – 0.96 (m, 3H, cy), 0.67 – 0.55 (m, 2H, cy).

^{13}C NMR (101 MHz, CDCl$_3$) δ/ppm = 169.9 (COOH), 147.4 (C-2'), 138.3 (C-2), 133.4 (C-4', C-5' or C-6'), 129.8 (C-4', C-5' or C-6'), 128.3 (C-5), 126.8 (C-4', C-5' or C-6'), 126.7 (C-1'), 120.5 (q, J_{CF} = 260.2 Hz, OCF$_3$), 120.4 (C-4'), 112.1 (C-4), 111.2 (C-3), 50.8 (CH$_2$-cy), 38.9 (cy), 30.6 (cy), 26.2 (cy), 25.7 (cy), 12.3 (CH$_3$).

IR (ATR) $\tilde{v}_{max}$/cm^{-1} = 2927, 1642, 1473, 1444, 1249, 1199, 1156, 776, 759.

HRMS (ESI): calcd. for C$_{20}$H$_{21}$F$_3$NO$_3$ (M-H)$^-$ 380.14790; found 380.14805.

Purity (HPLC): > 96% (λ = 210 nm).

5.2 Preparation of TPC2 inhibitors

5.2.1   General procedures

General Procedure E – Protection

Following a general procedure published by Schrittwieser et al.[149], the appropriate amines or phenols (1.0 eq.) were dispersed in dry CH_2Cl_2 and cooled to 0 °C, followed by dropwise addition of NEt_3 (1.5-3.5 eq.) and ethyl chloroformate (**162**, 1.3-2.5 eq.). The reaction mixture was stirred at rt or was refluxed for 4-72 h, before water was added. The mixture was extracted thrice with CH_2Cl_2, the combined organic layers were dried over Na_2SO_4 and concentrated *in vacuo.* Purification was accomplished by flash column chromatography (FCC) to yield carbamates and carbonates.

General Procedure F – Wittig reaction

(Methoxymethyl)-triphenylphosphonium chloride (1.2 eq.) was suspended in dry THF and cooled to -4 °C, before LDA (20% in THF/ethylbenzene/heptane, 1.0-1.2 eq.) was added dropwise. The mixture was stirred for 20 min. at -4 °C, followed by slow, dropwise addition of a solution of the appropriate aldehyde (1.0 eq.) in THF. The solution was stirred for 16-50 h, then poured on water and the mixture was extracted thrice with CH_2Cl_2. The combined organic layers were dried over Na_2SO_4, filtered and concentrated *in vacuo*. The crude product was purified by FCC to give the desired *cis/trans*-enol ethers. The products were directly used for the next step without further analysis.

General Procedure G – *N*-acyl Pictet-Spengler reaction

Carbamate (1.0 eq.) and enol ether (1.0-1.2 eq.) were dissolved in dry CH_2Cl_2, 4 Å molecular sieves (1.00 g per 20 mL solvent) was added and the mixture was cooled to 0 °C, before TFA (10-11 eq.) was added dropwise. The mixture was allowed to warm to rt and stirred for 18-90 h, before the molecular sieves was removed by filtration and sat. aq. $NaHCO_3$ solution was added. The mixture was extracted thrice with CH_2Cl_2, the combined organic layers were washed with 2 M aq. HCl solution and brine, dried over Na_2SO_4, filtered and concentrated *in vacuo*. Purification was accomplished by FCC to yield the desired racemic tetrahydroisoquinolines.

General Procedure H – Lithium alanate reductions of nitroolefins, carbamates and carbonates

According to Cava et al.[152], LiAlH$_4$ (7-12 eq.) was suspended in dry THF and a solution of carbamate (1.0 eq.) in dry THF was added dropwise and the suspension was refluxed for 3-20 h. The mixture was allowed to cool to rt and Na$_2$SO$_4$ x 10 H$_2$O was added in small portions under vigorous stirring over 20 minutes. Water was added and the mixture was extracted thrice with EtOAc. The combined organic layers were extracted with 2 M aq. HCl solution, the acidic phase was neutralized with sat. aq. NaHCO$_3$ solution and extracted thrice with EtOAc again. This organic layer was dried over Na$_2$SO$_4$ and concentrated *in vacuo* to give tertiary amines if not otherwise described.

General Procedure I – Chan-Evans-Lam coupling

According to Evans et al.[155], phenols (1.0 eq), Cu(OAc)$_2$ (1.1 eq. per phenolic group), boronic acid (3.0 eq. per phenolic group) and 4 Å molecular sieves (1.00 g per 40 mL solvent) were suspended in dry CH$_2$Cl$_2$ and a mixture of NEt$_3$ and pyridine (1:1, 2.5 eq. each) was added dropwise. The reaction mixture was stirred for 13-22 h at rt under ambient atmosphere, followed by filtration through a celite pad. The organic filtrate was washed with sat. aq. NaHCO$_3$ solution, 10% aq. citric acid solution and brine, dried over Na$_2$SO$_4$, filtered and concentrated *in vacuo*. The crude products were purified by FCC or HPLC to obtain the desired diaryl ethers.

General Procedure J – Formation of hydrochloride-salts

To receive solid and stable compounds for biological experiments, the tertiary amines were dissolved in 1.25 M methanolic HCl solution (3.0 mL per 100 mg amine) and concentrated *in vacuo* to yield the amorphous hydrochloride salts as solids. Melting points were obtained from the hydrochloride salts, remaining analytical data from the free amines, unless stated otherwise.

5.2.2 Synthetic procedures

5.2.2.1 Synthesis of arylethylamine building blocks
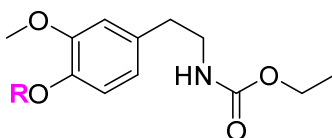
(*E*)-1-(Benzyloxy)-2-methoxy-4-(2-nitrovinyl)benzene (173)
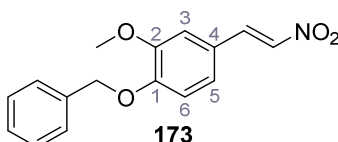
Following a procedure published by Pouysegu et al.[148], 4-benzyloxy-3-methoxybenzaldehyde (**172**, 10.0 g, 41.3 mmol, 1.0 eq.) and ammonium acetate (2.80 g, 36.4 mmol, 0.90 eq.) were dissolved in glacial acetic acid (24 mL) and nitromethane (16.0 mL, 299 mmol, 7.4 eq.) was added under nitrogen atmosphere. The mixture was heated to reflux for 3 h. Water (5.0 mL) was added, the precipitate was collected by filtration and was washed with cold MeOH. The crude product was recrystallized from MeOH to yield nitroolefin **173** (7.08 g, 24.8 mmol, 62%) as yellow crystals. Analytical data are in accordance with literature.

R*f* = 0.46 (4:1 hexanes/acetone).

m.p.: 123 °C. [lit.[148]: 124-125 °C]

^{1}H NMR (400 MHz, CDCl$_3$) δ/ppm = 7.95 (d, *J* = 13.6 Hz, 1H, C$\underline{H}$CHNO$_2$), 7.51 (d, *J* = 13.6 Hz, 1H, CHC$\underline{H}$NO$_2$), 7.44 – 7.32 (m, 5H, $\underline{Ph}$CH$_2$), 7.10 (dd, *J* = 8.4, 2.0 Hz, 1H, 5-H), 7.02 (d, *J* = 2.0 Hz, 1H, 3-H), 6.92 (d, *J* = 8.4 Hz, 1H, 6-H), 5.22 (s, 2H, PhC$\underline{H}_2$), 3.93 (s, 3H, OCH$_3$).

^{13}C NMR (101 MHz, CDCl$_3$) δ/ppm = 152.1 (C-1), 150.2 (C-2), 139.4 ($\underline{C}$HCHNO$_2$), 136.2 (qPh), 135.4 (CH$\underline{C}$HNO$_2$), 128.9 (Ph), 128.4 (Ph), 127.4 (Ph), 124.5 (C-5), 123.2 (C-4), 113.6 (C-3), 111.0 (C-6), 71.0 (Ph$\underline{C}$H$_2$), 56.3 (OCH$_3$).

IR (ATR) $\tilde{v}_{max}$/cm^{-1} = 3112, 3048, 2980, 2358, 1629, 1491, 1258, 1224, 1142, 976, 805, 746, 697.

HRMS (EI): calcd. for C$_{16}$H$_{15}$NO$_4$ (M)$^{•+}$ 285.0996; found 285.0994.

Purity (HPLC): > 96% (λ = 210 nm).

2-(4-(Benzyloxy)-3-methoxyphenyl)ethan-1-amine (171)

171
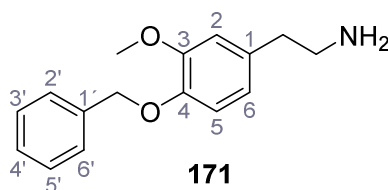
Similar to general procedure **H**, LiAlH$_4$ (1.70 g, 44.8 mmol, 5.1 eq.) in dry THF (10 mL) and nitrovinyl (**173**, 2.53 g, 8.87 mmol, 1.0 eq.) in dry THF (20 mL) were used and the resulting mixture was stirred at 80 °C for 18 h. Amine **171** (1.44 g, 5.60 mmol, 63%) was isolated as yellow oil. Analytical data are in accordance with literature[148].

R$_f$ = 0.30 (9:1 CH$_2$Cl$_2$/MeOH).

¹H NMR (400 MHz, CDCl$_3$) δ/ppm = 7.46 – 7.41 (m, 2H, 2'-H, 6'-H), 7.39 – 7.34 (m, 2H, 3'-H, 5'-H), 7.29 (ddd, J = 7.2, 4.8, 1.4 Hz, 1H, 4'-H), 6.82 (d, J = 8.1 Hz, 1H, 5-H), 6.75 (d, J = 2.0 Hz, 1H, 2-H), 6.67 (dd, J = 8.1, 2.0 Hz, 1H, 6-H), 5.13 (s, 2H, PhCH$_2$), 3.88 (s, 3H, OCH$_3$), 2.94 (t, J = 6.8 Hz, 2H, CH$_2$CH$_2$NH$_2$), 2.68 (t, J = 6.8 Hz, 2H, CH$_2$CH$_2$NH$_2$).

¹³C NMR (101 MHz, CDCl$_3$) δ/ppm = 149.7 (C-3), 146.7 (C-4), 137.4 (C-1'), 133.0 (C-1), 128.5 (C-3', C-5'), 127.8 (C-4'), 127.3 (C-2', C-6'), 120.8 (C-6), 114.3 (C-5), 112.7 (C-2), 71.2 (PhCH$_2$), 56.0 (OCH$_3$), 43.6 (CH$_2$CH$_2$NH$_2$), 39.5 (CH$_2$CH$_2$NH$_2$).

IR (ATR) $\tilde{v}_{max}$/cm^{-1} = 3032, 2938, 2909, 2869, 2838, 1512, 1260, 1227, 1139, 1032, 738, 696.

HRMS (ESI): calcd. for C$_{16}$H$_{20}$NO$_2$ (M+H)$^+$ 258.14886; found 258.14886.

Ethyl (4-(benzyloxy)-3-methoxyphenethyl)carbamate (170)

170
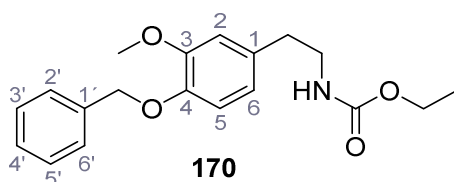
Following general procedure **E**, amine **171** (1.40 g, 5.44 mmol, 1.0 eq.) in CH$_2$Cl$_2$ (20 mL), NEt$_3$ (1.10 mL, 8.16 mmol, 1.5 eq.) and ethyl chloroformate (**162**, 680 µL, 7.07 mmol, 1.3 eq.) were used. The reaction was completed after 72 h and the product was purified by FCC (4:1 hexanes/acetone) to yield carbamate **170** (861 mg, 2.61 mmol, 48%) as light yellow solid. Analytical data are in accordance with literature[149].

R$_f$ = 0.28 (4:1 hexanes/acetone).

m.p.: 76 °C. [lit.[149]: 80-81 °C]

¹H NMR (500 MHz, CDCl₃) δ/ppm = 7.43 (dt, J = 8.1, 1.9 Hz, 2H, 2'-H, 6'-H), 7.36 (ddt, J = 8.1, 6.4, 1.3 Hz, 2H, 3'-H, 5'-H), 7.32 – 7.28 (m, 1H, 4'-H), 6.82 (d, J = 8.1 Hz, 1H, 5-H), 6.76 – 6.70 (m, 1H, 2-H), 6.66 (dd, J = 8.1, 2.0 Hz, 1H, 6-H), 5.13 (s, 2H, PhC$\underline{H}_2$), 4.65 (s, 1H, NH), 4.11 (q, J = 7.0 Hz, 2H, C$\underline{H}_2$CH₃), 3.88 (s, 3H, OCH₃), 3.40 (q, J = 6.8 Hz, 2H, CH₂C$\underline{H}_2$NH), 2.74 (t, J = 6.8 Hz, 2H, C$\underline{H}_2$CH₂NH), 1.23 (t, J = 7.0 Hz, 3H, CH₂C$\underline{H}_3$).

¹³C NMR (126 MHz, CDCl₃) δ/ppm = 156.7 (CO), 149.9 (C-3), 147.0 (C-4), 137.4 (C-1'), 132.1 (C-1), 128.7 (C-3', C-5'), 127.9 (C-4'), 127.4 (C-2', C-6'), 120.8 (C-6), 114.4 (C-5), 112.6 (C-2), 71.3 (Ph$\underline{C}$H₂), 60.9 ($\underline{C}$H₂CH₃), 56.1 (OCH₃), 42.3 (CH₂$\underline{C}$H₂NH), 35.9 ($\underline{C}$H₂CH₂NH), 14.8 (CH₂$\underline{C}$H₃).

IR (ATR) $\tilde{v}_{max}$/cm⁻¹ = 3333, 2980, 2936, 1682, 1515, 1252, 1228, 1138.

HRMS (ESI): calcd. for $C_{19}H_{24}NO_4$ (M+H)⁺ 330.16998; found 330.17056.

Purity (HPLC): > 96% (λ = 210 nm).

Ethyl (4-((ethoxycarbonyl)oxy)-3-methoxyphenethyl)carbamate (165)
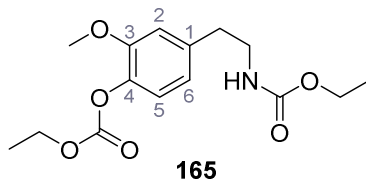
Following general procedure **E**, 3-methoxytyramine hydrochloride (**160**, 5.00 g, 24.5 mmol, 1.0 eq.) in CH₂Cl₂ (25 mL), NEt₃ (12.0 mL, 58.9 mmol, 3.5 eq.) and ethyl chloroformate (**162**, 5.90 mL, 61.4 mmol, 2.5 eq.) were used. The reaction was completed after 16 h and the product was purified by FCC (4:1 hexanes/acetone) to yield carbamate **165** (5.86 g, 18.8 mmol, 77%) as colorless solid.

R$_f$ = 0.10 (CH₂Cl₂).

m.p.: 68 °C.

¹H NMR (500 MHz, CDCl₃) δ/ppm = 7.05 (d, J = 8.0 Hz, 1H, 5-H), 6.81 – 6.74 (m, 2H, 2-H, 6-H), 4.68 (s, 1H, NH), 4.31 (q, J = 7.0 Hz, 2H, OCOOC$\underline{H}_2$CH₃), 4.11 (q, J = 7.0 Hz, 2H, NCOOC$\underline{H}_2$CH₃), 3.84 (s, 3H, OCH₃), 3.43 (q, J = 6.5 Hz, 2H, CH₂C$\underline{H}_2$NH), 2.80 (t, J = 6.5 Hz, 2H, C$\underline{H}_2$CH₂NH), 1.38 (t, J = 7.0 Hz, 3H, OCOOCH₂C$\underline{H}_3$), 1.23 (t, J = 7.0 Hz, 3H, NCOOCH₂C$\underline{H}_3$).

13C NMR (126 MHz, CDCl₃) δ/ppm = 156.7 (N-CO), 153.5 (O-CO), 151.3 (C-3), 138.9 (C-4), 138.1 (C-1), 122.5 (C-5), 120.9 (C-6), 113.2 (C-2), 65.1 (OCOO$\underline{C}$H₂CH₃), 60.9 (NCOO$\underline{C}$H₂CH₃), 56.1 (OCH₃), 42.1 (CH₂$\underline{C}$H₂NH), 36.3 ($\underline{C}$H₂CH₂NH), 14.8 (OCOOCH₂$\underline{C}$H₃), 14.3 (NCOOCH₂$\underline{C}$H₃).

IR (ATR) $\tilde{v}_{max}$/cm⁻¹ = 3336, 2980, 2940, 2872, 1750, 1686, 1541, 1514, 1283, 1251, 1208, 1059, 1032.

HRMS (ESI): calcd. for C₁₅H₂₂NO₆ (M+H)⁺ 312.14416; found 312.14425.

Purity (HPLC): > 96% (λ = 210 nm), > 96% (λ = 254 nm).

Ethyl (4-hydroxy-3-methoxyphenethyl)carbamate (166)

166
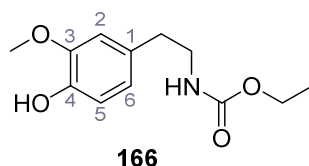
Following general procedure **E**, 3-methoxytyramine hydrochloride (**160**, 10.2 g, 50.0 mmol, 1.0 eq.) in CH₂Cl₂ (50 mL), NEt₃ (24.0 mL, 175 mmol, 3.5 eq.) and ethyl chloroformate (**162**, 12.0 mL, 125 mmol, 2.5 eq.) were used. After 18 h, a 1 M ethanolic NaOH solution (100 mL) was added and the mixture was stirred for 3.5 h. The reaction mixture was neutralized using 2 M aq. HCl solution, followed by extraction with CH₂Cl₂ (4 x 80 mL). The combined organic layers were dried over Na₂SO₄ and concentrated *in vacuo.* Purification was accomplished by FCC (4:1 hexanes/acetone) to yield carbamate **166** (3.49 g, 14.6 mmol, 29%) as colorless solid. Analytical data are in accordance with literature[73].

R_f = 0.18 (4:1 hexanes/acetone).

m.p.: 98 °C. [lit.[73]: 95.0 – 95.5 °C]

1H NMR (400 MHz, CDCl₃) δ/ppm = 6.85 (d, J = 8.4 Hz, 1H, 5-H), 6.74 – 6.63 (m, 2H, 2-H, 6-H), 5.50 (s, 1H, OH), 4.64 (s, 1H, NH), 4.11 (q, J = 7.1 Hz, 2H, C$\underline{H}$₂CH₃), 3.88 (s, 3H, OCH₃), 3.40 (q, J = 7.1 Hz, 2H, CH₂C$\underline{H}$₂NH), 2.74 (t, J = 7.1 Hz, 2H, C$\underline{H}$₂CH₂NH), 1.23 (t, J = 7.1 Hz, 3H, CH₂C$\underline{H}$₃).

13C NMR (101 MHz, CDCl₃) δ/ppm = 156.7 (CO), 146.7 (C-3), 144.4 (C-4), 130.8 (C-1), 121.5 (C-2 or 6), 114.6 (C-5), 111.4 (C-2 or 6), 60.9 ($\underline{C}$H₂CH₃), 56.0 (OCH₃), 42.4 (CH₂$\underline{C}$H₂NH), 36.0 ($\underline{C}$H₂CH₂NH), 14.8 (CH₂$\underline{C}$H₃).

IR (ATR) $\tilde{v}_{max}$/cm⁻¹ = 3276, 2979, 1688, 1516, 1237, 1033.

HRMS (ESI): calcd. for $C_{12}H_{16}NO_4$ (M-H)$^-$ 238.10848; found 238.10860.

Purity (HPLC): > 96% (λ = 210 nm).

Ethyl (3-methoxy-4-phenoxyphenethyl)carbamate (167)
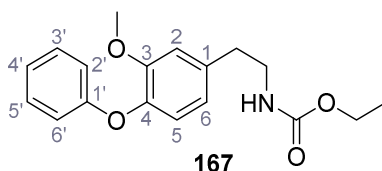
Following general procedure **I**, carbamate **166** (2.00 g, 8.36 mmol, 1.0 eq.), phenylboronic acid (**168**, 3.06 g, 25.1 mmol, 3.0 eq.), copper(II) acetate (1.67 g, 9.20 mmol, 1.1 eq.), NEt$_3$ (2.90 mL, 20.9 mmol, 2.5 eq.) and pyridine (1.70 mL, 20.9 mmol, 2.5 eq.) in CH_2Cl_2 (40 mL) were used. The reaction was completed after 22 h and the product was purified by FCC (4:1 hexanes/acetone) to yield diaryl ether **167** (2.24 g, 8.36 mmol, 85%) as colorless solid.

R$_f$ = 0.35 (4:1 hexanes/acetone).

m.p.: 40 °C.

^{1}H NMR (400 MHz, CDCl$_3$) δ/ppm = 7.32 – 7.26 (m, 2H, 3'-H, 5'-H), 7.07 – 7.01 (m, 1H, 4'-H), 6.96 – 6.92 (m, 2H, 2'-H, 6'-H), 6.90 (d, J = 8.1 Hz, 1H, 5-H), 6.83 (d, J = 1.8 Hz, 1H, 2-H), 6.74 (dd, J = 8.1, 1.8 Hz, 1H, 6-H), 4.69 (s, 1H, NH), 4.12 (q, J = 7.2 Hz, 2H, C$\underline{H}_2$CH$_3$), 3.83 (s, 3H, OCH$_3$), 3.45 (q, J = 7.0 Hz, 2H, CH$_2$C$\underline{H}_2$NH), 2.81 (t, J = 7.0 Hz, 2H, C$\underline{H}_2$CH$_2$NH), 1.24 (t, J = 7.0 Hz, 3H, CH$_2$C$\underline{H}_3$).

^{13}C NMR (101 MHz, CDCl$_3$) δ/ppm = 158.1 (C-1'), 156.7 (CO), 151.6 (C-3), 143.8 (C-4), 135.7 (C-1), 129.6 (C-3', C-5'), 122.6 (C-4'), 121.3 (C-5 or 6), 121.3 (C-5 or 6), 117.3 (C-2', C-6'), 113.5 (C-2), 61.0 ($\underline{C}$H$_2$CH$_3$), 56.2 (OCH$_3$), 42.3 (CH$_2$$\underline{C}H_2$NH), 36.2 ($\underline{C}H_2CH_2$NH), 14.8 (CH$_2$$\underline{C}H_3$).

IR (ATR) $\tilde{v}_{max}$/cm^{-1} = 3303, 2971, 1688, 1490, 1272, 1255, 1222, 1035, 754.

HRMS (ESI): calcd. for $C_{18}H_{22}NO_4$ (M+H)$^+$ 316.15433; found 316.15425.

Purity (HPLC): > 96% (λ = 210 nm).

Ethyl (3,4-dimethoxyphenethyl)carbamate (169)
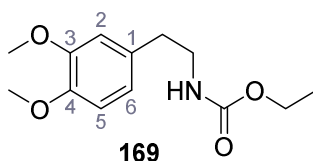
Following general procedure **E**, 3,4-dimethoxyphenylethylamine (**161**, 5.00 mL, 29.6 mmol, 1.0 eq.) in CH_2Cl_2 (30.0 mL), NEt_3 (12.0 mL, 88.9 mmol, 3.0 eq.) and ethyl chloroformate (**162**, 5.70 mL, 59.3 mmol, 2.0 eq.) were used. The mixture was heated to reflux for 4 h and extraction yielded carbamate **169** (7.05 g, 27.8 mmol, 94%) as colorless solid. NMR data are in accordance with literature[160].

R$_f$ = 0.25 (4:1 hexanes/acetone).

m.p.: 63 °C.

¹H NMR (400 MHz, CDCl₃) δ/ppm = 6.81 (d, J = 8.0 Hz, 1H, 5-H), 6.78 – 6.65 (m, 2H, 2-H, 6-H), 4.65 (s, 1H, NH), 4.11 (q, J = 7.1 Hz, 2H, C$\underline{H}_2$CH₃), 3.88 – 3.85 (m, 6H, 2x OCH₃), 3.41 (q, J = 6.8 Hz, 2H, CH₂C$\underline{H}_2$NH), 2.75 (t, J = 6.8 Hz, 2H, C$\underline{H}_2$CH₂NH), 1.23 (t, J = 7.1 Hz, 3H, CH₂C$\underline{H}_3$).

¹³C NMR (101 MHz, CDCl₃) δ/ppm = 156.7 (CO), 149.2 (C-3), 147.8 (C-4), 131.5 (C-1), 120.8 (C-2), 112.1 (C-6), 111.5 (C-5), 60.9 (C$\underline{H}_2$CH₃), 56.1 (OCH₃), 56.0 (OCH₃), 42.3 (CH₂C$\underline{H}_2$NH), 35.9 (C$\underline{H}_2$CH₂NH), 14.8 (CH₂C$\underline{H}_3$).

IR (ATR) $\tilde{v}_{max}$/cm⁻¹ = 3372, 2935, 1697, 1514, 1258, 1234, 1139, 1027.

HRMS (ESI): calcd. for $C_{13}H_{20}NO_4$ (M+H)⁺ 254.13868; found 354.13885.

Purity (HPLC): > 96% (λ = 210 nm).

5.2.2.2 Synthesis of enol ethers
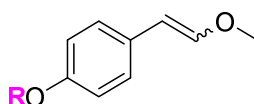
Ethyl (4-formylphenyl) carbonate (176)

176
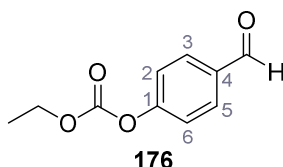
Following general procedure **E**, 4-hydroxybenzaldehyde (**175**, 1.00 g, 8.19 mmol, 1.0 eq.) in CH$_2$Cl$_2$ (10 mL), NEt$_3$ (1.70 mL, 12.3 mmol, 1.5 eq.) and ethyl chloroformate (**162**, 860 µL, 9.01 mmol, 1.1 eq.) were used. The reaction was completed after 14 h and the product was purified by FCC (CH$_2$Cl$_2$) to yield aldehyde **176** (1.53 g, 7.90 mmol, 97%) as colorless solid.

R$_f$ = 0.63 (CH$_2$Cl$_2$).

m.p.: 121 °C.

^{1}H NMR (500 MHz, CDCl$_3$) δ/ppm = 9.99 (s, 1H, CHO), 7.93 – 7.91 (m, 2H, 3-H, 5-H), 7.40 – 7.32 (m, 2H, 2-H, 6-H), 4.36 – 4.32 (m, 2H, C$\underline{H}_2$CH$_3$), 1.41 – 1.38 (m, 3H, CH$_2$C$\underline{H}_3$).

^{13}C NMR (126 MHz, CDCl$_3$) δ/ppm = 190.9 (CHO), 155.7 (C-1), 152.9 (CO), 134.2 (C-4), 131.4 (C-3, C-5), 121.9 (C-2, C-6), 65.4 (CH$_2$), 14.3 (CH$_3$).

IR (ATR) $\tilde{v}_{max}$/cm^{-1} = 1757, 1668, 1602, 1254, 1210, 1159, 1055, 998, 840, 775.

HRMS (EI): calcd. for C$_{10}$H$_9$O$_4$ (M)$^{•+}$ 194.0579; found 194.0579.

Purity (HPLC): > 96% (λ = 210 nm), > 96% (λ = 254 nm).

Ethyl (4-(2-methoxyvinyl)phenyl) carbonate (177)

177
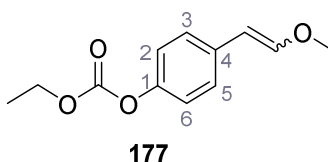
Following general procedure **F**, (methoxymethyl)-triphenylphosphonium chloride (9.53 g, 27.8 mmol, 1.2 eq.) and LDA (20% in THF/ethylbenzene/heptane, 11.6 mL, 23.2 mmol, 1.0 eq.) in dry THF (50 mL) and aldehyde **176** (4.50 g, 23.2 mmol, 1.0 eq.) in dry THF (50 mL) were used. The mixture was stirred for 16 h and the product was purified by FCC (9:1

hexanes/EtOAc) to yield the desired *cis/trans*-enol ether **177** (3.30 g, 14.8 mmol, 64%) as colorless oil.

R$_f$ = 0.28 (4:1 hexanes/EtOAc).

¹H NMR (*cis/trans*, 400 MHz, CDCl₃) δ/ppm = 7.59 – 7.55 (m, 2H, *cis* 3-H, 5-H), 7.24 – 7.20 (m, 2H, *trans* 3-H, 5-H), 7.10 – 7.06 (m, 4H, *cis/trans* 2-H, 6-H), 7.00 (d, *J* = 13.0 Hz, 1H, *trans* CHC<u>H</u>-O), 6.13 (d, *J* = 7.0 Hz, 1H, *cis* C<u>H</u>CH-O), 5.79 (d, *J* = 13.0 Hz, 1H, *trans* CHC<u>H</u>-O), 5.21 (d, *J* = 7.0 Hz, 1H, *cis* CHC<u>H</u>-O), 4.31 (qd, *J* = 7.1, 1.6 Hz, 4H, *cis/trans* C<u>H</u>₂CH₃), 3.78 (s, 3H, *cis* OCH₃), 3.68 (s, 3H, *trans* OCH₃), 1.38 (td, *J* = 7.1, 1.6 Hz, 6H, *cis/trans* CH₂C<u>H</u>₃).

¹³C NMR (*cis/trans*, 126 MHz, CDCl₃) δ/ppm = 153.9 (*trans* CO), 153.8 (*cis* CO), 149.2 (*trans* CH<u>C</u>H-O), 149.2 (*trans* C-1), 148.9 (*cis* C-1), 148.1 (*cis* CH<u>C</u>H-O), 134.5 (*trans* C-4), 134.0 (*cis* C-4), 129.3 (*cis* C-3, C-5), 126.1 (*trans* C-3, C-5), 121.3 (*trans* C-2, C-6), 120.8 (*cis* C-2, C-6), 104.9 (*cis* <u>C</u>HCH-O), 104.3 (*trans* <u>C</u>HCH-O), 64.9 (*trans* <u>C</u>H₂CH₃), 60.8 (*cis* <u>C</u>H₂CH₃), 56.7 (*cis/trans* CH₂CH₃), 14.4 (*cis/trans* CH₂<u>C</u>H₃).

Cis/trans-ratio according to ¹H-NMR is 0.83.

HRMS (EI): calcd. for C₁₂H₁₄O₄ (M)•⁺ 222.0887; found 222.0879.

1-(2-Methoxyvinyl)-4-phenoxybenzene (178)

178
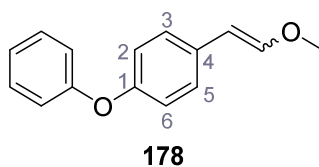
Following general procedure **F**, (methoxymethyl)-triphenylphosphonium chloride (1.18 g, 3.43 mmol, 1.2 eq.) and LDA (20% in THF/ethylbenzene/heptane, 1.90 mL, 2.86 mmol, 1.0 eq.) in dry THF (10 mL) and 4-phenoxybenzaldehyde (500 µL, 2.86 mmol, 1.0 eq.) in dry THF (10 mL) were used. The mixture was stirred for 50 h and the product was purified by FCC (9:1 hexanes/EtOAc) to yield the desired *cis/trans*-enol ether **178** (384 mg, 1.70 mmol, 59%) as colorless oil.

R$_f$ = 0.73 (4:1 hexanes/EtOAc).

¹H NMR (*cis/trans*, 400 MHz, CDCl₃) δ/ppm = 7.60 – 7.53 (m, 2H, *cis* 3-H, 5-H), 7.36 – 7.28 (m, 4H, *cis/trans* Ph), 7.22 – 7.18 (m, 2H, *trans* 2-H, 6-H or 3-H, 5-H), 7.12 – 7.05 (m, 2H, *cis/trans* Ph), 7.02 – 6.91 (m, 9H, 4x *cis/trans* Ph, *trans* C<u>H</u>CH-O, *cis/trans* 2-H, 6-H or/and 3-

H, 5-H), 6.11 (d, J = 7.0 Hz, 1H, *cis* C<u>H</u>CH-O), 5.81 (d, J = 13.0 Hz, 1H, *trans* CHC<u>H</u>-O), 5.22 (d, J = 7.0 Hz, 1H, *cis* CHC<u>H</u>-O), 3.78 (s, 3H, *cis* OCH₃), 3.69 (s, 3H, *trans* OCH₃).

¹³C NMR (*cis*/*trans*, 101 MHz, CDCl₃) δ/ppm = 157.8 (*cis*/*trans* qPh), 157.7 (*cis*/*trans* qPh), 155.2 (*cis*/*trans* C-1), 154.9 (*cis*/*trans* C-1), 148.5 (trans <u>C</u>HCH-O), 147.4 (cis <u>C</u>HCH-O), 131.8 (*cis*/*trans* C-4), 131.5 (*cis*/*trans* C-4), 129.9 (*cis*/*trans* Ph), 129.8 (*cis*/*trans* Ph), 129.7 (cis C-3, C-5), 126.5 (*trans* C-2, C-6 or C-3, C-5), 123.1 (*cis*/*trans* Ph), 123.0 (*cis*/*trans* Ph), 119.6 (*cis*/*trans* Ph or C-2, C-6 or C-3, C-5), 119.1 (*cis*/*trans* Ph or C-2, C-6 or C-3, C-5), 118.7 (*cis*/*trans* Ph or C-2, C-6 or C-3, C-5), 118.6 (*cis*/*trans* Ph or C-2, C-6 or C-3, C-5), 105.1 (*cis* CH<u>C</u>H-O), 104.5 (*trans* CH<u>C</u>H-O), 60.8 (*cis* OCH₃), 56.7 (*trans* OCH₃).

Cis/*trans*-ratio according to ¹H-NMR is 0.75.

IR (ATR) $\tilde{v}_{max}$/cm⁻¹ = 3036, 2935, 2831, 1488, 1234, 1150, 1092, 750, 691.

HRMS (EI): calcd. for $C_{15}H_{14}O_2$ (M)•⁺ 226.0988; found 226.0987.

1-(Benzyloxy)-4-(2-methoxyvinyl)benzene (179)

179
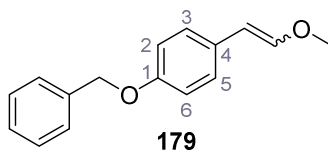
Following general procedure **F**, (methoxymethyl)-triphenylphosphonium chloride (4.11 g, 12.0 mmol, 1.2 eq.) and LDA (20% in THF/ethylbenzene/heptane, 7.90 mL, 12.0 mmol, 1.2 eq.) in dry THF (50 mL) and 4-(benzyloxy)benzaldehyde (2.12 g, 9.99 mmol, 1.0 eq.) in dry THF (50 mL) were used. The mixture was stirred for 16 h and the product was purified by FCC (6:1 hexanes/EtOAc) to yield the desired *cis*/*trans*-enol ether **179** (2.04 g, 8.49 mmol, 85%) as yellow solid.

R$_f$ = 0.68 (4:1 hexanes/EtOAc).

m.p.: 62 °C.

¹H NMR (*cis*/*trans*, 400 MHz, CDCl₃) δ/ppm = 7.53 – 7.49 (m, 2H, *cis* 3-H, 5-H), 7.45 – 7.29 (m, 10H, *cis*/*trans* <u>Ph</u>CH₂), 7.18 – 7.13 (m, 2H, *trans* 3-H, 5-H), 6.95 – 6.88 (m, 5H, *cis*/*trans* 2-H, 6-H, *trans* C<u>H</u>CH-O), 6.06 (d, J = 7.0 Hz, 1H, *cis* C<u>H</u>CH-O), 5.78 (d, J = 13.0 Hz, 1H, *trans* CHC<u>H</u>-O), 5.18 (d, J = 7.0 Hz, 1H, *cis* CHC<u>H</u>-O), 5.09 – 5.03 (m, 4H, *cis*/*trans* PhC<u>H</u>₂), 3.76 (s, 3H, *cis* OCH₃), 3.66 (s, 3H, *trans* OCH₃).

¹³C NMR (*cis*/*trans*, 101 MHz, CDCl₃) δ/ppm = 157.2 (*cis/trans* C-1), 157.0 (*cis/trans* C-1), 147.8 (*trans* <u>C</u>HCH-O), 146.6 (*cis* <u>C</u>HCH-O), 137.3 (*cis/trans* qPh), 137.2 (*cis/trans* qPh),

129.5 (*cis* C-3, C-5), 129.3 (*cis/trans* C-4), 129.2 (*cis/trans* C-4), 128.8 (*cis/trans* Ph), 128.7 (*cis/trans* Ph), 128.1 (*cis/trans* Ph), 128.0 (*cis/trans* Ph), 127.6 (*cis/trans* Ph), 126.3 (*trans* C-3, C-5), 115.3 (*trans* C-2, C-6), 114.8 (*cis* C-2, C-6), 105.4 (*cis* CH<u>C</u>H-O), 104.7 (*trans* CH<u>C</u>H-O), 70.2 (*cis/trans* Ph<u>C</u>H₂), 70.1 (*cis/trans* Ph<u>C</u>H₂), 60.6 (*cis* O<u>C</u>H₃), 56.6 (*trans* O<u>C</u>H₃).

Cis/*trans*-ratio according to ¹H-NMR is 1.1.

HRMS (EI): calcd. for $C_{16}H_{16}O_2$ (M)•⁺ 240.1145; found 240.1146.

5.2.2.3 *N*-Acyl Pictet-Spengler reaction
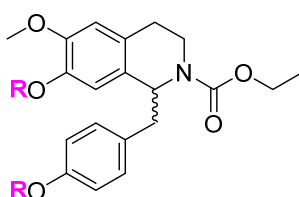
(±)-Ethyl 7-((ethoxycarbonyl)oxy)-1-(4-((ethoxycarbonyl)oxy)benzyl)-6-methoxy-3,4-dihy-droisoquinoline-2(1*H*)-carboxylate (180)

180
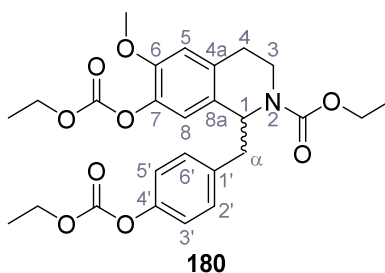
Following general procedure **G**, carbamate **165** (348 mg, 1.12 mmol, 1.0 eq.), enol ether **177** (248 mg, 1.12 mmol, 1.0 eq.) and TFA (840 µL, 11.2 mmol, 10 eq.) were dissolved in CH_2Cl_2 (15 mL). The reaction was completed after 18 h and the product was purified by FCC (5:1 hexanes/acetone) to yield compound **180** (452 mg, 0.901 mmol, 81%) as colorless oil.

R*f* = 0.20 (4:1 hexanes/acetone).

¹H NMR (400 MHz, C₂D₂Cl₄, 100 °C) δ/ppm = 7.03 (s, 4H, 2'-H, 3'-H, 5'-H, 6'-H), 6.69 – 6.63 (m, 2H, 5-H, 8-H), 5.19 (t, *J* = 6.6 Hz, 1H, 1-H), 4.28 – 4.22 (m, 4H, 2 OCOOC<u>H</u>₂CH₃), 4.05 – 3.92 (m, 3H, NCOOC<u>H</u>₂CH₃, 3-H), 3.79 (s, 3H, OCH₃), 3.23 (ddd, *J* = 13.6, 9.7, 4.6 Hz, 1H, 3-H), 3.00 (h, *J* = 6.6 Hz, 2H, α-H), 2.81 (ddd, *J* = 15.8, 9.7, 5.8 Hz, 1H, 4-H), 2.61 – 2.54 (m, 1H, 4-H), 1.35 – 1.31 (m, 6H, 2 OCOOCH₂C<u>H</u>₃), 1.12 (t, *J* = 7.2 Hz, 3H, NCOOCH₂C<u>H</u>₃).

¹³C NMR (101 MHz, C₂D₂Cl₄, 100 °C) δ/ppm = 155.6 (N-CO), 153.6 (O-CO), 153.3 (O-CO), 150.4 (C-4'), 150.3 (C-6), 139.1 (C-7), 136.0 (C-1'), 133.4 (C-4a), 130.7 (C-2', C-6'or C-3', C-5'), 129.3 (C-8a), 121.3 (C-5 or C-8), 120.9 (C-2', C-6' or C-3', C-5'), 113.6 (C-5 or C-8), 65.1

(OCOO$\underline{C}$H$_2$CH$_3$), 64.9 (OCOO$\underline{C}$H$_2$CH$_3$), 61.5 (NCOO$\underline{C}$H$_2$CH$_3$), 56.6 (O$\underline{C}$H$_3$), 56.0 (C-1), 42.5 (C-α), 38.6 (C-3), 28.7 (C-4), 14.8 (NCOOCH$_2$$\underline{C}H_3$), 14.4 (OCOOCH$_2$$\underline{C}H_3$), 14.3 (OCOOCH$_2$$\underline{C}H_3$).

IR (ATR) $\tilde{v}_{max}$/cm^{-1} = 2981, 2940, 1758, 1692, 1248, 1215, 1198.

HRMS (ESI): calcd. for C$_{26}$H$_{35}$N$_2$O$_9$ (M+NH$_4$)$^+$ 519.23371; found 519.23373.

Purity (HPLC): > 96% (λ = 210 nm).

(±)-Ethyl 1-(4-((ethoxycarbonyl)oxy)benzyl)-6,7-dimethoxy-3,4-dihydroisoquinoline-2(1*H*)-carboxylate – SG-089 (181)

SG-089 (**181**)

Following general procedure **G**, carbamate **169** (5.60 g, 22.1 mmol, 1.0 eq.), enol ether **177** (4.92 g, 22.1 mmol, 1.0 eq.) and TFA (18.0 mL, 243 mmol, 11 eq.) were dissolved in CH$_2$Cl$_2$ (50 mL). The reaction was completed after 20 h and the product was purified by FCC (5:1 hexanes/acetone) to give SG-089 **181** (7.50 g, 16.9 mmol, 77%) as colorless solid.

R$_f$ = 0.28 (4:1 hexanes/acetone).

m.p.: 134 °C.

^{1}H NMR (400 MHz, C$_2$D$_2$Cl$_4$, 100 °C) δ/ppm = 7.10 – 6.97 (m, 4H, 2'-H, 3'-H, 5'-H, 6'-H), 6.57 (s, 1H, 5-H), 6.23 (s, 1H, 8-H), 5.15 (t, *J* = 6.6 Hz, 1H, 1-H), 4.26 (q, *J* = 7.1 Hz, 2H, OCOOC$\underline{H}$$_2CH_3$), 4.13 – 3.98 (m, 2H, NCOOC$\underline{H}$$_2CH_3$), 3.98 – 3.82 (m, 1H, 3-H), 3.78 (s, 3H, 6-OCH$_3$), 3.61 (s, 3H, 7-OCH$_3$), 3.30 (ddd, *J* = 13.4, 9.4, 4.7 Hz, 1H, 3-H), 3.09 (dd, *J* = 13.4, 6.8 Hz, 1H, α-H), 2.94 (dd, *J* = 13.4, 6.8 Hz, 1H, α-H), 2.77 (ddd, *J* = 15.6, 9.4, 5.9 Hz, 1H, 4-H), 2.57 (dt, *J* = 15.6, 4.7 Hz, 1H, 4-H), 1.34 (t, *J* = 7.1 Hz, 3H, OCOOCH$_2$C$\underline{H}$$_3$), 1.17 (t, *J* = 7.1 Hz, 3H, NCOOCH$_2$C$\underline{H}$$_3$).

^{13}C NMR (101 MHz, C$_2$D$_2$Cl$_4$, 100 °C) δ/ppm = 155.7 (N-CO), 153.6 (O-CO), 150.3 (C-4'), 148.8 (C-6), 148.1 (C-7), 136.4 (C-1'), 130.8 (C-2', C-6'), 129.0 (C-8a), 127.0 (C-4a), 120.9 (C-3', C-5'), 113.3 (C-5), 112.3 (C-8), 64.9 (OCOO$\underline{C}$H$_2$CH$_3$), 61.5 (NCOO$\underline{C}$H$_2$CH$_3$), 56.7 (OCH$_3$-6), 56.6 (OCH$_3$-7), 56.5 (C-1), 42.6 (C-α), 39.1 (C-3), 28.2 (C-4), 14.8 (OCOOCH$_2$$\underline{C}H_3$), 14.4 (NCOOCH$_2$$\underline{C}H_3$).

IR (ATR) $\tilde{v}_{max}$/cm^{-1} = 3006, 2918, 2849, 1754, 1673, 1281, 1260, 1245, 1206, 1096, 859.

HRMS (ESI): calcd. for $C_{24}H_{30}NO_7$ (M+H)$^+$ 444.20168; found 444.20143.

Purity (HPLC): > 96% (λ = 210 nm), > 96% (λ = 254 nm).

(±)-Ethyl 1-(4-((ethoxycarbonyl)oxy)benzyl)-6-methoxy-7-phenoxy-3,4-dihydroisoquino-line-2(1*H*)-carboxylate (182)

182

Following general procedure **G**, carbamate **167** (1.60 g, 5.06 mmol, 1.0 eq.), enol ether **177** (1.35 g, 6.07 mmol, 1.2 eq.) and TFA (3.80 mL, 50.6 mmol, 10 eq.) were dissolved in CH$_2$Cl$_2$ (50 mL). The reaction was completed after 90 h and the product was purified by FCC (5:1 hexanes/acetone) to yield compound **182** (2.30 g, 4.55 mmol, 90%) as yellow oil.

R$_f$ = 0.31 (4:1 hexanes/acetone).

^{1}H NMR (400 MHz, C$_2$D$_2$Cl$_4$, 100 °C) δ/ppm = 7.25 − 7.21 (m, 2H, Ar), 6.99 (s, 5H, Ph), 6.86 − 6.82 (m, 2H, Ar), 6.69 (s, 1H, 5-H), 6.54 (s, 1H, 8-H), 5.13 (t, J = 6.6 Hz, 1H, 1-H), 4.25 (q, J = 7.1 Hz, 2H, OCOOC$\underline{H}_2$CH$_3$), 4.04 − 3.92 (m, 3H, NCOOC$\underline{H}_2$CH$_3$, 3-H), 3.75 (s, 3H, OCH$_3$), 3.26 (ddd, J = 13.2, 9.6, 4.6 Hz, 1H, 3-H), 3.02 (dd, J = 13.7, 7.0 Hz, 1H, α-H), 2.94 (dd, J = 13.7, 7.0 Hz, 1H, α-H), 2.86 − 2.77 (m, 1H, 4-H), 2.60 (dt, J = 15.8, 4.6 Hz, 1H, 4-H), 1.33 (t, J = 7.0 Hz, 3H, OCOOCH$_2$C$\underline{H}_3$), 1.12 (t, J = 7.2 Hz, 3H, NCOOCH$_2$C$\underline{H}_3$).

^{13}C NMR (101 MHz, C$_2$D$_2$Cl$_4$, 100 °C) δ/ppm = 158.5 (C-4'), 155.7 (N-CO), 153.5 (O-CO), 150.8 (C-6), 150.3 (C-7), 144.1 (C-8a), 136.0 (qPh), 131.2 (C-4a), 130.6 (Ph), 129.8 (C-1'), 129.6 (C-2', C-6' or C-3', C-5'), 122.6 (Ph), 120.8 (Ph), 120.4 (C-8), 117.5 (C-2', C-6' or C-3', C-5'), 114.5 (C-6), 64.9 (OCOO$\underline{C}$H$_2$CH$_3$), 61.5 (NCOO$\underline{C}$H$_2$CH$_3$), 56.8 (OCH$_3$), 56.0 (C-1), 42.5 (C-α), 38.9 (C-3), 28.5 (C-4), 14.8 (NCOOCH$_2$$\underline{C}H_3$), 14.4 (OCOOCH$_2$$\underline{C}H_3$).

IR (ATR) $\tilde{v}_{max}$/cm^{-1} = 2980, 1759, 1688, 1508, 1252, 1215, 1096, 747.

HRMS (ESI): calcd. for $C_{29}H_{32}NO_7$ (M+H)$^+$ 506.21733; found 506.21721.

Purity (HPLC): > 96% (λ = 210 nm), > 96% (λ = 254 nm).

(±)-Ethyl 7-(benzyloxy)-1-(4-(benzyloxy)benzyl)-6-methoxy-3,4-dihydroisoquinoline-2(1*H*)-carboxylate - SG-145 (183)

SG-145 (**183**)

Following general procedure **G**, carbamate **170** (861 mg, 2.61 mmol, 1.0 eq.), enol ether **179** (691 mg, 2.88 mmol, 1.1 eq.) and TFA (2.00 mL, 26.1 mmol, 10 eq.) were dissolved in CH_2Cl_2 (25 mL). The reaction was completed after 18 h and the product was purified by FCC (5:1 hexanes/acetone) to yield SG-145 (**183**, 444 mg, 0.825 mmol, 32%) as yellow solid.

R_f = 0.26 (4:1 hexanes/acetone).

m.p.: 96 °C. [lit.[152]: 115-118 °C]

^{1}H NMR (400 MHz, $C_2D_2Cl_4$, 100 °C) δ/ppm = 7.36 – 7.27 (m, 10H, Ph), 6.95 – 6.92 (m, 2H, 2'-H, 6'-H), 6.85 – 6.83 (m, 2H, 3'-H, 5'-H), 6.59 (s, 1H, 5-H), 6.37 (s, 1H, 8-H), 5.10 (t, J = 6.7 Hz, 1H, 1-H), 4.99 (s, 2H, PhC$\underline{H}_2$), 4.86 (s, 2H, PhC$\underline{H}_2$), 4.10 – 3.90 (m, 3H, C$\underline{H}_2$CH$_3$, 3-H), 3.80 (s, 3H, OCH$_3$), 3.28 – 3.20 (m, 1H, 3-H), 2.98 (dd, J = 13.6, 6.7 Hz, 1H, α-H), 2.86 (dd, J = 13.6, 6.7 Hz, 1H, α-H), 2.80 – 2.71 (m, 1H, 4-H), 2.56 – 2.50 (m, 1H, 4-H), 1.15 (t, J = 7.1 Hz, 3H, CH$_2$C$\underline{H}_3$).

^{13}C NMR (101 MHz, $C_2D_2Cl_4$, 100 °C) δ/ppm = 158.0 (C-4'), 155.7 (CO), 149.5 (C-6), 147.2 (C-7), 137.8 (qPh), 137.7 (qPh), 131.3 (C-1'), 131.0 (C-2', C-6'), 129.5 (C-8a), 128.7 (Ph), 128.6 (Ph), 128.0 (Ph), 127.9 (C-4a), 127.7 (Ph), 127.6 (Ph), 115.4 (C-8 or C-3', C-5'), 115.3 (C-8 or C-3', C-5'), 113.9 (C-5), 72.2 (PhC$\underline{H}_2$), 70.7 (PhC$\underline{H}_2$), 61.4 ($\underline{C}H_2$CH$_3$), 56.9 (OCH$_3$), 56.4 (C-1), 42.3 (C-α), 38.9 (C-3), 28.3 (C-2), 14.8 (CH$_2$$\underline{C}H_3$).
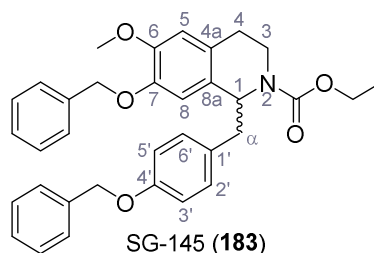
IR (ATR) $\tilde{v}_{max}$/cm^{-1} = 3007, 2940, 1673, 1510, 1254, 1236, 1224, 1200, 1093, 743, 697.

HRMS (ESI): calcd. for $C_{34}H_{36}NO_5$ (M+H)$^+$ 538.25880; found 538.25880.

Purity (HPLC): > 96% (λ = 210 nm), > 96% (λ = 254 nm).

(±)-Ethyl 6,7-dimethoxy-1-(4-phenoxybenzyl)-3,4-dihydroisoquinoline-2(1*H*)-carboxylate (184)

184
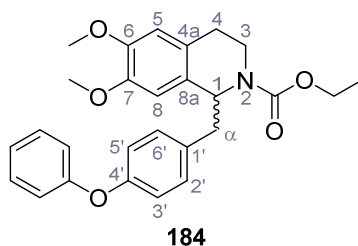
Following general procedure **G**, carbamate **169** (150 mg, 0.663 mmol, 1.0 eq.), enol ether **178** (168 mg, 0.663 mmol, 1.0 eq.) and TFA (500 μL, 6.63 mmol, 10 eq.) were dissolved in CH_2Cl_2 (5.0 mL). The reaction was completed after 6 h and the product was purified by FCC (4:1 hexanes/acetone) to yield compound **184** (181 mg, 0.405 mmol, 92%) as colorless oil that solidifies upon freezing.

R*f* = 0.32 (4:1 hexanes/acetone).

m.p.: 30 °C.

¹H NMR (400 MHz, C₂D₂Cl₄, 100 °C) δ/ppm = 7.30 – 7.25 (m, 2H, Ar), 7.06 – 7.01 (m, 3H, Ph), 6.95 (dd, *J* = 8.7, 1.1 Hz, 2H, Ar), 6.90 – 6.87 (m, 2H, Ph), 6.57 (s, 1H, 5-H), 6.30 (s, 1H, 8-H), 5.17 (t, *J* = 6.9 Hz, 1H, 1-H), 4.05 (q, *J* = 7.1 Hz, 2H, C$\underline{H}_2$CH₃), 4.00 – 3.89 (m, 1H, 3-H), 3.78 (s, 3H, 6-OCH₃), 3.66 (s, 3H, 7-OCH₃), 3.30 (ddd, *J* = 13.5, 9.6, 4.7 Hz, 1H, 3-H), 3.07 (dd, *J* = 13.5, 6.8 Hz, 1H, α-H), 2.94 (dd, *J* = 13.5, 6.8 Hz, 1H, α-H), 2.78 (ddd, *J* = 15.8, 8.9, 6.1 Hz, 1H, 4-H), 2.58 (dt, *J* = 15.0, 4.7 Hz, 1H, 4-H), 1.18 (t, *J* = 7.1 Hz, 3H, CH₂C$\underline{H}_3$).

¹³C NMR (101 MHz, C₂D₂Cl₄, 100 °C) δ/ppm = 157.9 (C-4'), 156.2 (qPh), 155.7 (CO), 148.9 (C-6), 148.1 (C-7), 133.7 (C-1'), 131.2 (Ph), 129.9 (Ar), 129.3 (C-8a), 127.1 (C-4a), 123.3 (Ph), 119.1 (Ar or Ph), 119.0 (Ar or Ph), 113.3 (C-5), 112.5 (C-8), 61.4 ($\underline{C}$H₂CH₃), 56.7 (6-OCH₃ and 7-OCH₃), 56.5 (C-1), 42.6 (C-α), 39.0 (C-3), 28.3 (C-4), 14.9 (CH₂$\underline{C}$H₃).

IR (ATR) $\tilde{v}_{max}$/cm⁻¹ = 2979, 1678, 1506, 1488, 1227, 1098, 694.

HRMS (ESI): calcd. for $C_{27}H_{30}NO_5$ (M+H)⁺ 448.21185; found 448.21224.

Purity (HPLC): > 96% (λ = 210 nm), > 96% (λ = 254 nm).

5.2.2.4 Lithium alanate reductions of carbamates and deprotections of carbonates
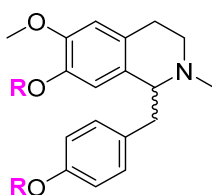
(±)-1-(4-Hydroxybenzyl)-6-methoxy-2-methyl-1,2,3,4-tetrahydroisoquinolin-7-ol ((±)-*N*-methylcoclaurine) – SG-132 (159)

SG-132 (**159**)
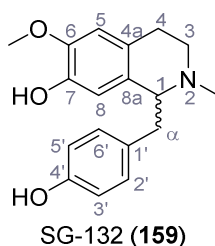
Following general procedure **H**, carbamate **180** (2.58 g, 5.14 mmol, 1.0 eq.) in dry THF (40 mL) and LiAlH$_4$ (1.35 g, 35.6 mmol, 7.0 eq.) in dry THF (40 mL) were used. The mixture was heated to reflux for 3 h to yield (±)-*N*-methylcoclaurine (**159**, 1.21 g, 4.04 mmol, 79%) as off-white solid.

R$_f$ = 0.09 (9:1 CH$_2$Cl$_2$/MeOH).

m.p.: 86 °C. [lit.[191]: 110-112 °C]

^{1}H NMR (500 MHz, CD$_3$OD) δ/ppm = 6.92 – 6.87 (m, 2H, Ar), 6.70 – 6.65 (m, 2H, Ar), 6.63 (s, 1H, 5-H), 6.09 (s, 1H, 8-H), 3.80 (s, 3H, OCH$_3$), 3.66 (dd, *J* = 7.5, 4.9 Hz, 1H, 1-H), 3.15 (ddd, *J* = 12.5, 9.4, 5.5 Hz, 1H, 3-H), 3.06 (dd, *J* = 13.8, 4.9 Hz, 1H, α-H), 2.85 (ddd, *J* = 15.8, 9.4, 6.2 Hz, 1H, 4-H), 2.75 – 2.69 (m, 2H, α-H and 3-H), 2.63 (dt, *J* = 16.3, 4.9 Hz, 1H, 4-H), 2.45 (s, 3H, NCH$_3$).

^{13}C NMR (126 MHz, CD$_3$OD) δ/ppm = 156.8 (C-4'), 147.8 (C-6), 145.0 (C-7), 131.7 (C-1'), 131.6 (Ar), 130.7 (C-8a), 125.5 (C-4a), 116.0 (Ar), 115.8 (C-8), 112.6 (C-5), 66.0 (C-1), 56.3 (OCH$_3$), 47.5 (C-α), 42.6 (NCH$_3$), 40.7 (C-3), 26.1 (C-4).

IR (ATR) $\tilde{v}_{max}$/cm^{-1} = 2929, 1609, 1513, 1445, 1251, 1112, 1022, 830.

HRMS (ESI): calcd. for C$_{18}$H$_{22}$NO$_3$ (M+H)$^+$ 300.15942; found 300.15932.

Purity (HPLC): > 96% (λ = 210 nm).

(±)-4-((6,7-Dimethoxy-2-methyl-1,2,3,4-tetrahydroisoquinolin-1-yl)methyl)phenol ((±)-armepavine) – SG-121 (185) and (±)-4-(6,7-dimethoxy-2-methyl-1,2,3,4-tetrahydroisoquinolin-1-yl)phenol – SG-121-NP (189)

SG-121 (**185**) SG-121-NP (**189**)
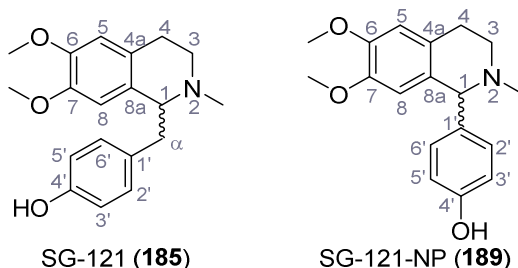
Following general procedure **H**, SG-089 (**181**, 7.50 g, 16.9 mmol, 1.0 eq.) in dry THF (90 mL) and LiAlH$_4$ (7.06 g, 186 mmol, 11 eq.) in dry THF (40 mL) were used. The mixture was heated to reflux for 3 h and the product was purified by FCC (9:1 CH$_2$Cl$_2$/MeOH) to yield (±)-armepavine (**185**, 1.83 g, 5.86 mmol, 35%) as off-white solid. NMR data are in accordance with literature[192].

R$_f$ = 0.34 (9:1 CH$_2$Cl$_2$/MeOH).

m.p.: 76 °C.

^{1}H NMR (400 MHz, CD$_3$OD) δ/ppm = 6.90 – 6.86 (m, 2H, 2'-H, 6'-H), 6.72 – 6.68 (m, 2H, 3'-H, 5'-H), 6.66 (s, 1H, 5-H or 8-H), 5.84 (s, 1H, 5-H or 8-H), 3.77 (s, 3H, OCH$_3$), 3.72 (dd, J = 9.5, 4.3 Hz, 1H, 1-H), 3.42 (s, 3H, OCH$_3$), 3.24 – 3.14 (m, 2H, α-H, 3-H), 2.95 – 2.87 (m, 1H, 4-H), 2.78 (ddd, J = 12.5, 6.3, 3.1 Hz, 1H, 3-H), 2.70 – 2.63 (m, 2H, α-H, 4-H), 2.52 (s, 3H, NCH$_3$).

^{13}C NMR (101 MHz, CD$_3$OD) δ/ppm = 157.0 (C-4'), 149.1 (C-6 or C-7), 147.5 (C-6 or C-7), 132.0 (C-2', C-6'), 131.3 (C-1'), 129.8 (C-4a or C-8a), 126.4 (C-4a or C-8a), 116.1 (C-3', C-5'), 113.0 (C-5 or C-8), 112.9 (C-5 or C-8), 66.0 (C-1), 56.3 (OCH$_3$), 55.9 (OCH$_3$), 47.0 (C-3), 42.4 (NCH$_3$), 40.0 (C-α), 26.0 (C-4).

IR (ATR) $\tilde{v}_{max}$/cm^{-1} = 2979, 2901, 2834, 1509, 1251, 1226, 1100, 828.

HRMS (ESI): calcd. for C$_{19}$H$_{24}$NO$_3$ (M+H)$^+$ 314.17507; found 314.17502.

Purity (HPLC): > 96% (λ = 210 nm), > 96% (λ = 254 nm).

Column chromatography furthermore yielded SG-121-NP (**189**, 1.03 g, 3.44 mmol, 20%) as light yellow solid. Due to the instability of the enol ether (**177**) and for the sake of time, purification was reduced to a minimum during up-scale reactions. This resulted in impurities in form of 4-hydroxybenzaldehyde (**175**) after the Wittig reaction. During the following *N*-acyl Pictet-Spengler reaction, a side product was formed that was carried over as impurity to the next step. Reduction with LiAlH$_4$ then yielded SG-121-NP (**189**).

R$_f$ = 0.21 (9:1 CH$_2$Cl$_2$/MeOH).

m.p.: 85 °C.

^{1}H NMR (400 MHz, CD$_3$OD) δ/ppm = 7.23 – 7.13 (m, 2H, 2',6'-H), 6.98 – 6.84 (m, 3H, 5,3'.5'-H), 6.30 (s, 1H, 8-H), 5.49 (s, 1H, 1-H), 3.85 (s, 3H, OCH$_3$), 3.74 – 3.62 (m, 1H, 3 or 4-H), 3.59 (s, 3H, OCH$_3$), 3.50 – 3.43 (m, 1H, 3 or 4-H), 3.30 – 3.26 (m, 1H, 3 or 4-H), 3.23 – 3.13 (m, 1H, 3 or 4-H), 2.83 (s, 3H, NCH$_3$).

^{13}C NMR (101 MHz, CD$_3$OD) δ/ppm = 160.6 (C-4'), 150.9 (C-6 or C-7), 149.9 (C-6 or C-7), 133.3 (C-1', C-2' and/or C-6'), 133.2 (C-1', C-2' and/or C-6'), 133.0 (C-1', C-2' and/or C-6'), 124.8 (C-4a or C-8a), 124.7 (C-4a or C-8a), 117.0 (C-3', C-5'), 112.2 (C-5 and C-8), 69.6 (C-1), 56.4 (OCH$_3$), 56.3 (OCH$_3$), 41.2 (NCH$_3$), 25.7 (C-3 or C-4), 25.6 (C-3 or C-4).

IR (ATR) $\tilde{v}_{max}$/cm^{-1} = 3132, 2980, 2725, 1615, 1516, 1270, 1229, 1105, 838.

HRMS (ESI): calcd. for C$_{18}$H$_{22}$NO$_3$ (M+H)$^+$ 300.15942; found 300.15964.

Purity (HPLC): > 96% (λ = 210 nm), > 96% (λ = 254 nm).

(±)-4-((6-Methoxy-2-methyl-7-phenoxy-1,2,3,4-tetrahydroisoquinolin-1-yl)methyl)phenol (186)

186
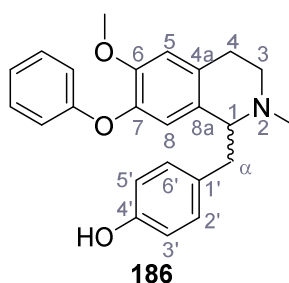
Following general procedure **H**, carbamate **182** (1.80 g, 3.56 mmol, 1.0 eq.) in dry THF (20 mL) and LiAlH$_4$ (1.62 g, 42.7 mmol, 12 eq.) in dry THF (20 mL) were used. The mixture was heated to reflux for 5 h to yield racemic compound **186** (1.21 g, 4.04 mmol, 79%) as off-white solid.

R$_f$ = 0.38 (9:1 CH$_2$Cl$_2$/MeOH).

m.p.: 85 °C.

^{1}H NMR (500 MHz, CD$_3$OD) δ/ppm = 7.26 – 7.20 (m, 2H, Ph), 6.99 – 6.96 (m, 1H, Ph), 6.84 – 6.80 (m, 3H, 5-H, 2'-H, 6'-H), 6.72 – 6.68 (m, 2H, Ph), 6.61 – 6.56 (m, 2H, 3'-H, 5'-H), 6.10 (s, 1H, 8-H), 3.73 (s, 3H, OCH$_3$), 3.67 (dd, J = 8.6, 4.3 Hz, 1H, 1-H), 3.21 (ddd, J = 13.7, 9.3, 6.1 Hz, 1H, 3-H), 3.08 (dd, J = 13.5, 4.3 Hz, 1H, α-H), 2.98 – 2.91 (m, 1H, 4-H), 2.79 – 2.73 (m, 2H, 3-H and 4-H), 2.69 (dd, J = 13.5, 8.6 Hz, 1H, α-H), 2.50 (s, 3H, NCH$_3$).

^{13}C NMR (126 MHz, CD$_3$OD) δ/ppm = 158.0 (qPh), 155.3 (C-4'), 149.9 (C-6), 142.0 (C-7), 130.3 (C-2', C-6'), 129.9 (C-4a, C-8a or C-1'), 129.6 (C-4a, C-8a or C-1'), 129.4 (C-4a, C-8a or C-1'), 129.0 (Ph), 121.8 (Ph), 120.5 (C-8), 116.5 (Ph), 114.7 (C-3', C-5'), 112.6 (C-5), 64.4 (C-1), 54.9 (OCH$_3$), 45.9 (C-3), 41.2 (NCH$_3$), 38.6 (C-α), 25.1 (C-4). **IR (ATR)** $\tilde{v}_{max}$/cm^{-1} = 2980, 2889, 1590, 1508, 1489, 1261, 1215, 749, 690.

IR (ATR) $\tilde{v}_{max}$/cm^{-1} = 2980, 2889, 1590, 1508, 1489, 1261, 1215, 749, 690.

HRMS (ESI): calcd. for C$_{24}$H$_{26}$NO$_3$ (M+H)$^+$ 376.19072; found 376.19069.

Purity (HPLC): > 96% (λ = 210 nm).

(±)-7-(Benzyloxy)-1-(4-(benzyloxy)benzyl)-6-methoxy-2-methyl-1,2,3,4-tetrahydro-isoquinoline – SG-005 (187)

SG-005 (**187**)
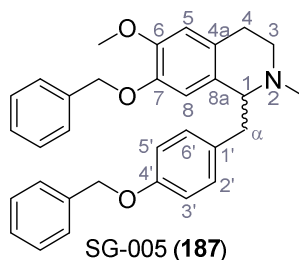
Following general procedure **H**, carbamate **183** (310 mg, 0.557 mmol, 1.0 eq.) in dry THF (10 mL) and LiAlH$_4$ (157 mg, 4.14 mmol, 7.2 eq.) in dry THF (20 mL) were used. The mixture was heated to reflux for 18 h and the product was purified by FCC (9:1 CH$_2$Cl$_2$/MeOH) to yield racemic amine SG-005 (**187**, 126 mg, 0.263 mmol, 46%) as colorless oil. The hydrochloride salt was formed according to general procedure **J** to yield a colorless solid. Analytical data are in accordance with literature[82].

R$_f$ = 0.39 (9:1 CH$_2$Cl$_2$/MeOH).

m.p.: 68 °C (HCl salt).

^{1}H NMR (500 MHz, CD$_3$OD) δ/ppm = 7.37 – 7.22 (m, 10H, PhCH$_2$), 6.96 – 6.93 (m, 2H, 2'-H, 6'-H), 6.93 – 6.90 (m, 2H, 3'-H, 5'-H), 6.68 (s, 1H, 5-H), 5.85 (s, 1H, 8-H), 4.99 (d, J = 2.3 Hz, 2H, 4'-OCH$_2$), 4.60 – 4.54 (m, 2H, 7-OCH$_2$), 3.78 (s, 3H, OCH$_3$), 3.72 (dd, J = 9.4, 4.2 Hz, 1H, 1-H), 3.23 – 3.15 (m, 2H, 4-H, α-H), 2.91 (ddd, J = 16.3, 9.9, 6.3 Hz, 1H, 3-H), 2.78 (ddd, J = 12.5, 6.3, 3.2 Hz, 1H, 4-H), 2.71 – 2.65 (m, 2H, 3-H, α-H), 2.53 (s, 3H, NCH$_3$).

^{13}C NMR (126 MHz, CD$_3$OD) δ/ppm = 158.9 (C-4'), 149.7 (C-6), 146.7 (C-7), 138.7 (qPh), 138.6 (qPh), 132.9 (C-1'), 132.2 (C-2', C-6'), 129.6 (C-8a), 129.5 (Ph), 129.4 (Ph), 128.9 (Ph), 128.8 (Ph), 128.6 (Ph), 127.1 (C-4a), 115.8 (C-3', C-5'), 115.4 (C-8), 113.2 (C-5), 71.8

(PhC̲H₂), 71.0 (PhC̲H₂), 65.9 (C-1), 56.4 (OCH₃), 47.1 (C-4), 42.4 (NCH₃), 39.7 (C-α), 26.2 (C-3).

IR (ATR) $\tilde{v}_{max}$/cm⁻¹ = 2932, 2850, 1608, 1509, 1454, 1222, 1099, 1013, 767, 696.

HRMS (ESI): calcd. for $C_{32}H_{34}NO_3$ (M+H)⁺ 480.25332; found 480.25476.

Purity (HPLC): > 96% (λ = 210 nm), > 96% (λ = 254 nm).

Separation of racemic SG-005 (**187**) *via* chiral HPLC (9:1 *n*-heptane/isopropanol + 0.45% diethylamine) yielded the two enantiomers (*S*)-SG-005 (**209**, colorless oil, retention time: ~ 10 min) and (*R*)-SG-005 (**210**, colorless oil, retention time: ~ 20 min).

(*S*)-SG-005 (**209**)   (*R*)-SG-005 (**210**)
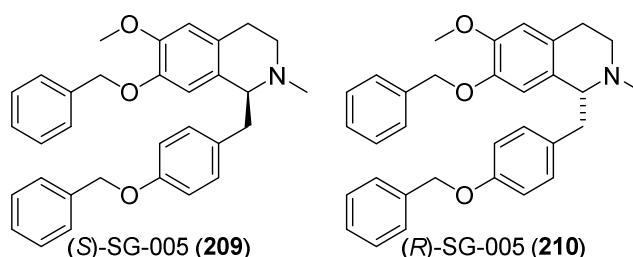
(*S*)-SG-005 (**209**): $[\alpha]_D^{22}$ = + 54.3 (c = 0.078, CHCl₃).

(*R*)-SG-005 (**210**): $[\alpha]_D^{22}$ = - 65.4 (c = 0.052, CHCl₃). (lit.[193]: -37.6 (c = 0.9, CHCl₃).

(±)-6,7-Dimethoxy-2-methyl-1-(4-phenoxybenzyl)-1,2,3,4-tetrahydroisoquinoline – SG-083 (188)

SG-083 (**188**)
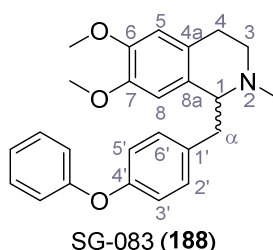
Following general procedure **H**, carbamate **184** (110 mg, 0.246 mmol, 1.0 eq.) in dry THF (15 mL) and LiAlH₄ (37.3 mg, 0.983 mmol, 4.0 eq.) in dry THF (10 mL) were used. The mixture was heated to reflux for 20 h and the product was purified by FCC (9.5:0.5 CH₂Cl₂/MeOH) to yield racemic amine SG-083 (**188**, 44.0 mg, 0.113 mmol, 46%) as light yellow oil.

R$_f$ = 0.55 (9:1 CH₂Cl₂/MeOH).

¹H NMR (500 MHz, CD₃OD) δ/ppm = 7.35 – 7.31 (m, 2H, Ph), 7.10 – 7.05 (m, 3H, Ph, 2'-H, 6'-H), 6.96 – 6.93 (m, 2H, Ph), 6.91 – 6.87 (m, 2H, 3'-H, 5'-H), 6.67 (s, 1H, 5-H), 5.97 (s, 1H, 8-

H), 3.81 – 3.77 (m, 4H, 1-H, OCH$_3$), 3.50 (s, 3H, OCH$_3$), 3.25 – 3.18 (m, 2H, 3-H, α-H), 2.94 – 2.86 (m, 1H, 4-H), 2.81 – 2.75 (m, 2H, 3-H, α-H), 2.67 (ddd, J = 16.6, 5.4, 3.3 Hz, 1H, 4-H), 2.53 (s, 3H, NCH$_3$).

^{13}C NMR (126 MHz, CD$_3$OD) δ/ppm = 159.0 (qPh), 157.1 (C-4'), 149.2 (C-6), 147.7 (C-7), 135.9 (C-1'), 132.4 (C-2', C-6'), 130.8 (Ph), 129.9 (C-8a), 126.9 (C-4a), 124.2 (Ph), 119.8 (C-3', C-5'), 119.6 (Ph), 113.1 (C-5 or C-8), 113.0 (C-5 or C-8), 65.9 (C-1), 56.4 (OCH$_3$), 56.1 (OCH$_3$), 47.1 (C-3), 42.5 (NCH$_3$), 40.2 (C-α), 26.1 (C-4).

IR (ATR) $\tilde{v}_{max}$/cm^{-1} = 2938, 2833, 1589, 1505, 1488, 1228.

HRMS (ESI): calcd. for C$_{25}$H$_{28}$NO$_3$ (M+H)$^+$ 390.20637; found 390.20640.

Purity (HPLC): > 96% (λ = 210 nm), > 96% (λ = 254 nm).

5.2.2.5 Chan-Evans-Lam couplings
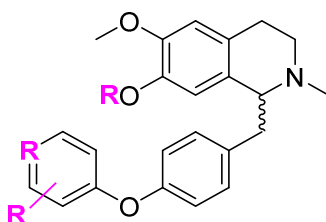
(±)-6-Methoxy-2-methyl-7-phenoxy-1-(4-phenoxybenzyl)-1,2,3,4-tetrahydroisoquinoline – SG-094 (192)

SG-094 (**192**)
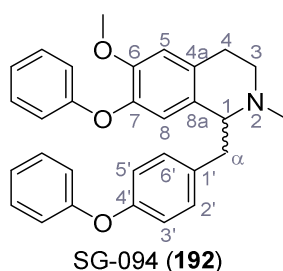
Following general procedure **I**, SG-132 (**159**, 150 mg, 0.500 mmol, 1.0 eq.), phenylboronic acid (**168**, 366 mg, 3.00 mmol, 6.0 eq.), Cu(OAc)$_2$ (200 mg, 1.10 mmol, 2.2 eq.), NEt$_3$ (348 µL, 2.50 mmol, 5.0 eq.), pyridine (202 µL, 2.50 mmol, 5.0 eq.) and CH$_2$Cl$_2$ (50 mL) were used. The reaction was completed after 18 h and FCC (9.9:0.1 CH$_2$Cl$_2$/MeOH) yielded racemic diaryl ether SG-094 (**192**, 158 mg, 0.350 mmol, 70%) as colorless oil. The hydrochloride salt was formed according to general procedure **J** to yield a colorless solid.

R$_f$ = 0.61 (9:1 CH$_2$Cl$_2$/MeOH).

m.p.: 75 °C (HCl salt).

^{1}H NMR (400 MHz, CD$_3$OD) δ/ppm = 7.29 – 7.18 (m, 4H, Ph), 7.07 – 7.00 (m, 3H, 2'-H, 6'-H, Ph), 6.96 – 6.92 (m, 1H, Ph), 6.86 – 6.82 (m, 3H, 5-H, Ph), 6.79 – 6.75 (m, 2H, 3'-H, 5'-H), 6.72 – 6.68 (m, 2H, Ph), 6.10 (s, 1H, 8-H), 3.75 (dd, J = 8.7, 4.4 Hz, 1H, 1-H), 3.72 (s, 3H, OCH$_3$), 3.28 – 3.14 (m, 2H, α-H, 3-H), 2.96 (ddd, J = 15.5, 9.1, 6.6 Hz, 1H, 4-H), 2.83 – 2.74 (m, 3H, α-H, 3-H, 4-H), 2.53 (s, 3H, NCH$_3$).

^{13}C NMR (101 MHz, CD$_3$OD) δ/ppm = 159.8 (qPh), 159.0 (qPh), 156.9 (C-4'), 151.7 (C-6), 143.0 (C-7), 135.5 (C-1'), 132.2 (C-2', C-6'), 131.9 (C-4a or C-8a), 130.8 (Ph), 130.6 (C-4a or C-8a), 130.4 (Ph), 124.0 (Ph), 123.0 (Ph), 122.6 (C-8), 119.9 (C-3', C-5'), 119.5 (Ph), 117.3 (Ph), 114.1 (C-5), 65.7 (C-1), 56.3 (OCH$_3$), 47.3 (C-3), 42.6 (NCH$_3$), 39.9 (C-α), 26.6 (C-4).

IR (ATR) $\tilde{v}_{max}$/cm^{-1} = 3038, 2937, 2838, 2793, 1588, 1505, 1487, 1218, 749, 690.

HRMS (ESI): calcd. for C$_{30}$H$_{30}$NO$_3$ (M+H)$^+$ 452.22202; found 452.22163.

Purity (HPLC): > 96% (λ = 210 nm).

Separation of racemic SG-094 (**192**) *via* chiral HPLC (9.5:0.5 *n*-heptane/isopropanol + 0.45% diethylamine) yielded the two enantiomers (*S*)-SG-094 (**211**, colorless oil, retention time: ~ 8 min) and (*R*)-SG-094 (**212**, colorless oil, retention time: ~ 11 min).

(*S*)-SG-094 (**211**)　　　　　(*R*)-SG-094 (**212**)
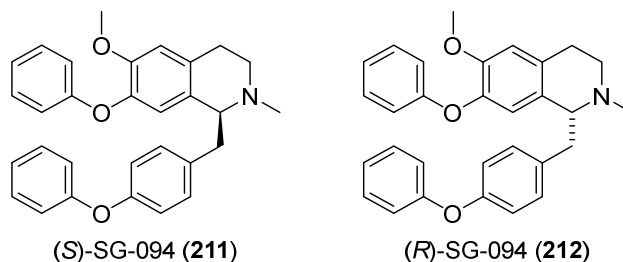
(*S*)-SG-094 (**211**): $[\alpha]_D^{22}$ = + 74.5 (c = 0.043, CHCl₃).

(*R*)-SG-094 (**212**): $[\alpha]_D^{22}$ = - 52.5 (c = 0.057, CHCl₃).

(±)-6,7-Dimethoxy-1-(4-(4-methoxyphenoxy)benzyl)-2-methyl-1,2,3,4-tetrahydro-isoquinoline – SG-122 (193)

SG-122 (**193**)
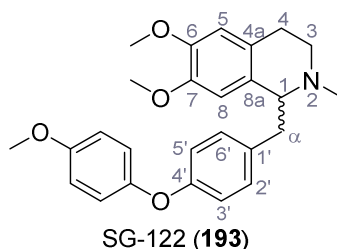
Following general procedure **I**, SG-121 (**185**, 157 mg, 0.500 mmol, 1.0 eq.), 4-methoxyphenyl-boronic acid (228 mg, 1.50 mmol, 3.0 eq.), Cu(OAc)₂ (100 mg, 0.550 mmol, 1.1 eq.), NEt₃ (174 µL, 1.25 mmol, 2.5 eq.), pyridine (101 µL, 1.25 mmol, 2.5 eq.) and CH₂Cl₂ (50 mL) were used. After 18 h the reaction was completed and the product was purified by FCC (9.5:0.5 CH₂Cl₂/MeOH) to yield racemic diaryl ether SG-122 (**193**, 185 mg, 0.441 mmol, 88%) as colorless oil. The hydrochloride salt was formed according to general procedure **J** to yield a colorless solid.

R*f* = 0.45 (9:1 CH₂Cl₂/MeOH).

m.p.: 204 °C (HCl salt).

¹H NMR (500 MHz, CDCl₃) δ/ppm = 7.04 – 7.01 (m, 2H, 2'-H, 6'-H), 6.96 – 6.92 (m, 2H, Ar), 6.88 – 6.83 (m, 4H, 2'-H, 6'-H, Ar), 6.56 (s, 1H, 5-H), 6.05 (s, 1H, 8-H), 3.84 (s, 3H, OCH₃),

3.80 (s, 3H, OCH$_3$), 3.69 (dd, J = 7.5, 5.2 Hz, 1H, 1-H), 3.60 (s, 3H, OCH$_3$), 3.23 – 3.12 (m, 2H, α-H, 3-H), 2.86 – 2.74 (m, 3H, α-H, 3-H, 4-H), 2.58 (dt, J = 15.6, 4.5 Hz, 1H, 4-H), 2.53 (s, 3H, NCH$_3$).

^{13}C NMR (126 MHz, CDCl$_3$) δ/ppm = 156.9 (C-4'), 155.9 (qAr), 150.6 (qAr), 147.4 (C-6), 146.4 (C-7), 134.3 (C-1'), 131.0 (C-2', C-6'), 129.4 (C-8a), 126.1 (C-4a), 120.7 (Ar), 117.6 (C-3', C-5' or Ar), 115.0 (C-3', C-5' or Ar), 111.3 (C-5), 111.2 (C-8), 65.0 (C-1), 55.9 (OCH$_3$), 55.8 (OCH$_3$), 55.7 (OCH$_3$), 47.0 (C-3), 42.8 (NCH$_3$), 40.6 (C-α), 25.6 (C-4).

IR (ATR) $\tilde{v}_{max}$/cm^{-1} = 2971, 2629, 1504, 1265, 1227, 1111, 1006, 845.

HRMS (ESI): calcd. for C$_{26}$H$_{30}$NO$_4$ (M+H)$^+$ 420.21693; found 420.21657.

Purity (HPLC): > 96% (λ = 210 nm), > 96% (λ = 254 nm).

(±)-6,7-Dimethoxy-2-methyl-1-(4-(3,4,5-trimethoxyphenoxy)benzyl)-1,2,3,4-tetrahydro-isoquinoline hydrochloride – SG-127 (194)

SG-127 (**194**)
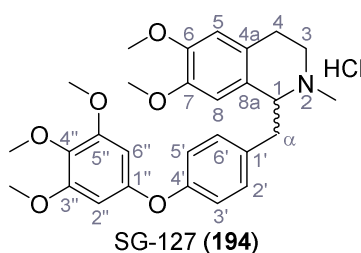
Following general procedure **I**, SG-121 (**185**, 157 mg, 0.500 mmol, 1.0 eq.), 3,4,5-trimethoxy-phenylboronic acid (318 mg, 1.50 mmol, 3.0 eq.), Cu(OAc)$_2$ (100 mg, 0.550 mmol, 1.1 eq.), NEt$_3$ (174 µL, 1.25 mmol, 2.5 eq.), pyridine (101 µL, 1.25 mmol, 2.5 eq.) and CH$_2$Cl$_2$ (50 mL) were used. After 18 h the reaction was completed and the product was purified by FCC (CH$_2$Cl$_2$ + 1% NEt$_3$), followed by recrystallization in EtOH as hydrochloride salt to yield diaryl ether SG-127 (**194**, 216 mg, 0.418 mmol, 84%) as colorless solid. Analytical data are related to the hydrochloride salt.

R$_f$ = 0.47 (9:1 CH$_2$Cl$_2$/MeOH).

m.p.: 183 °C (HCl salt).

^{1}H NMR (500 MHz, CDCl$_3$) δ/ppm = 13.13 (s, 1H, NH), 7.11 – 7.05 (m, 2H, 2'-H, 6'-H), 6.94 – 6.90 (m, 2H, 3'-H, 5'-H), 6.64 (s, 1H, 5-H), 6.22 (s, 2H, 2''-H, 6''-H), 5.71 (s, 1H, 8-H), 4.21 – 4.11 (m, 2H, 1-H, α-H), 3.86 (s, 3H, OCH$_3$), 3.82 (s, 3H, OCH$_3$), 3.78 (s, 6H, 2 OCH$_3$), 3.76 – 3.70 (m, 1H, 3-H), 3.50 (s, 3H, OCH$_3$), 3.40 – 3.33 (m, 1H, 3-H), 3.12 – 3.04 (m, 2H, 4-H), 2.94 – 2.91 (m, 1H, α-H), 2.89 (s, 3H, NCH$_3$).

^{13}C NMR (126 MHz, CDCl$_3$) δ/ppm = 157.2 (C-4'), 154.1 (C-3'', C-5''), 152.9 (C-1''), 149.5 (C-6), 147.5 (C-7), 134.6 (C-4''), 131.8 (C-2', C-6'), 130.2 (C-1'), 120.9 (C-4a or C-8a), 120.6 (C-4a or C-8a), 118.5 (C-3', C-5'), 111.3 (C-5 or C-8), 111.2 (C-5 or C-8), 97.1 (C-2'', C-6''), 65.8 (C-1), 61.2 (OCH$_3$), 56.3 (2 OCH$_3$), 56.1 (OCH$_3$), 55.7 (OCH$_3$), 44.5 (C-3), 41.0 (C-α), 40.1 (NCH$_3$), 21.5 (C-4).

IR (ATR) $\tilde{v}_{max}$/cm^{-1} = 2970, 2834, 2441, 1496, 1221, 1126, 1110, 1009, 989, 857.

HRMS (ESI): calcd. for C$_{28}$H$_{34}$NO$_6$ (M+H)$^+$ 480.23806; found 480.23789.

Purity (HPLC): > 96% (λ = 210 nm), > 96% (λ = 254 nm).

(±)-6,7-Dimethoxy-1-(4-(4-methoxyphenoxy)phenyl)-2-methyl-1,2,3,4-tetrahydro-isoquinoline – SG-157 (195)

SG-157 (**195**)
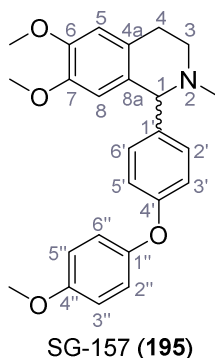
Following general procedure **I**, SG-121-NP (**189**, 150 mg, 0.500 mmol, 1.0 eq.), 4-methoxy-phenylboronic acid (228 mg, 1.50 mmol, 3.0 eq.), Cu(OAc)$_2$ (100 mg, 0.550 mmol, 1.1 eq.), NEt$_3$ (174 µL, 1.25 mmol, 2.5 eq.), pyridine (101 µL, 1.25 mmol, 2.5 eq.) and CH$_2$Cl$_2$ (50 mL) were used. After 18 h the reaction was completed and the product was purified by FCC (CH$_2$Cl$_2$ → 9.8:0.2 CH$_2$Cl$_2$/MeOH) to yield diaryl ether SG-157 (**195**, 192 mg, 0.473 mmol, 95%) as colorless oil. The hydrochloride salt was formed according to general procedure **J** to yield a beige solid.

R$_f$ = 0.49 (9:1 CH$_2$Cl$_2$/MeOH).

m.p.: 97 °C (HCl salt).

^{1}H NMR (500 MHz, (CD$_3$)$_2$SO) δ/ppm = 7.22 – 7.16 (m, 2H, 2'-H, 6'-H), 7.03 – 6.92 (m, 4H, 2''-H, 3''-H, 5''-H, 6''-H), 6.90 – 6.84 (m, 2H, 3'-H, 5'-H), 6.69 (s, 1H, 5-H), 6.08 (s, 1H, 8-H), 4.15 (s, 1H, 1-H), 3.74 (s, 3H, OCH$_3$), 3.71 (s, 3H, OCH$_3$), 3.46 (s, 3H, OCH$_3$), 3.02 – 2.95 (m, 2H, 3-H, 4-H), 2.71 – 2.63 (m, 1H, 4-H), 2.49 – 2.44 (m, 1H, 3-H), 2.12 (s, 3H, NCH$_3$).

^{13}C NMR (126 MHz, (CD$_3$)$_2$SO) δ/ppm = 156.9 (C-4'), 155.5 (C-4''), 149.5 (C-1''), 147.2 (C-6), 146.7 (C-7), 138.2 (C-1'), 130.4 (C-2', C-6'), 130.1 (C-8a), 126.4 (C-4a), 120.6 (C-2'', C-6'' or C-3'', C-5''), 116.9 (C-3', C-5'), 115.0 (C-2'', C-6'' or C-3'', C-5''), 111.8 (C-8), 111.4 (C-5), 69.0 (C-1), 55.5 (OCH$_3$), 55.4 (2 OCH$_3$), 51.2 (C-3), 43.8 (NCH$_3$), 28.4 (C-4).

IR (ATR) $\tilde{v}_{max}$/cm^{-1} = 2970, 2903, 2837, 1514, 1263, 1225, 1025, 820, 744.

HRMS (ESI): calcd. for C$_{25}$H$_{28}$NO$_4$ (M+H)$^+$ 406.20128; found 406.20099.

Purity (HPLC): > 96% (λ = 210 nm), > 96% (λ = 254 nm).

(±)-6-Methoxy-2-methyl-7-phenoxy-1-(4-(4-(trifluoromethyl)phenoxy)benzyl)-1,2,3,4-tetrahydroisoquinoline – SG-153 (199)

SG-153 (**199**)
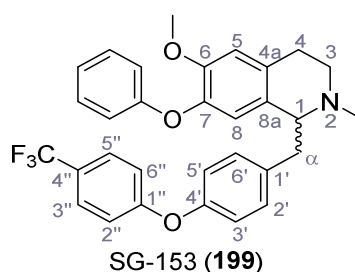
Following general procedure **I**, phenol **186** (150 mg, 0.400 mmol, 1.0 eq.), 4-(trifluoromethyl)-phenylboronic acid (228 mg, 1.20 mmol, 3.0 eq.), Cu(OAc)$_2$ (79.8 mg, 0.440 mmol, 1.1 eq.), NEt$_3$ (139 µL, 1.00 mmol, 2.5 eq.), pyridine (080.8 µL, 1.00 mmol, 2.5 eq.) and CH$_2$Cl$_2$ (50 mL) were used. After 18 h the reaction was completed and the product was purified by FCC (CH$_2$Cl$_2$ → 9.5:0.5 CH$_2$Cl$_2$/MeOH) to yield diaryl ether SG-153 (**199**, 50.7 mg, 0.0976 mmol, 24%) as brown oil. The hydrochloride salt was formed according to general procedure **J** to yield a yellow solid.

R$_f$ = 0.50 (9:1 CH$_2$Cl$_2$/MeOH).

m.p.: 92 °C (HCl salt).

^{1}H NMR (400 MHz, CDCl$_3$) δ/ppm = 7.54 − 7.48 (m, 2H, 3''-H, 5''-H), 7.26 − 7.22 (m, 2H, Ph), 7.08 − 7.04 (m, 2H, 2'-H, 6'-H), 7.01 − 6.92 (m, 3H, 2''-H, 6''-H, Ph), 6.87 − 6.79 (m, 4H, 3'-H, 5'-H, Ph), 6.68 (s, 1H, 5-H), 6.36 (s, 1H, 8-H), 3.77 (s, 3H, OCH$_3$), 3.69 (t, J = 6.0 Hz, 1H, 1-H), 3.18 (ddd, J = 13.0, 7.8, 5.2 Hz, 1H, 3-H), 3.09 (dd, J = 13.3, 5.2 Hz, 1H, α-H), 2.90 − 2.82 (m, 2H, α-H, 4-H), 2.80 − 2.74 (m, 1H, 3-H), 2.66 (dt, J = 15.7, 5.2 Hz, 1H, 4-H), 2.53 (s, 3H, NCH$_3$).

^{13}C NMR (101 MHz, CDCl$_3$) δ/ppm = 160.9 (C-1''), 158.4 (qPh), 153.8 (C-4'), 150.0 (C-6), 142.2 (C-7), 136.0 (C-1'), 131.4 (C-2', C-6'), 130.1 (C-8a), 129.6 (Ph), 128.7 (q, J_{CF} = 277.9

Hz, CF$_3$), 127.2 (q, J_{CF} = 3.6 Hz, C-4''), 124.6 (q, J_{CF} = 32.9 Hz, C-3'', C-5''), 124.4 (C-4a), 122.3 (Ph), 121.0 (C-8), 119.8 (C-3', C-5'), 117.6 (C-2'', C-6''), 116.7 (Ph), 112.8 (C-5), 64.6 (C-1), 56.1 (OCH$_3$), 47.4 (C-3), 43.0 (NCH$_3$), 40.0 (C-α), 26.4 (C-4).

IR (ATR) $\tilde{v}_{max}$/cm^{-1} = 2980, 2907, 1602, 1506, 1325, 1243, 1221, 1103, 1064, 749.

HRMS (ESI): calcd. for C$_{31}$H$_{29}$F$_3$NO$_3$ (M+H)$^+$ 520.20940; found 520.20907.

Purity (HPLC): > 96% (λ = 210 nm), > 96% (λ = 254 nm).

(±)-6-Methoxy-2-methyl-7-phenoxy-1-(4-(4-(trifluoromethoxy)phenoxy)benzyl)-1,2,3,4-tetrahydroisoquinoline – SG-154 (198)

SG-154 (**198**)
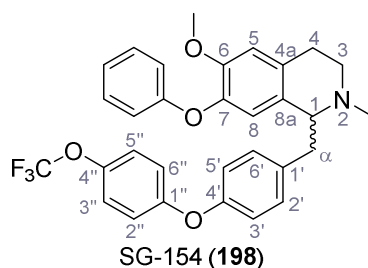
Following general procedure **I**, phenol **186** (150 mg, 0.400 mmol, 1.0 eq.), 4-(trifluoromethoxy)-phenylboronic acid (247 mg, 1.20 mmol, 3.0 eq.), Cu(OAc)$_2$ (79.8 mg, 0.440 mmol, 1.1 eq.), NEt$_3$ (139 µL, 1.00 mmol, 2.5 eq.), pyridine (80.8 µL, 1.00 mmol, 2.5 eq.) and CH$_2$Cl$_2$ (20 mL) were used. After 13 h the reaction was completed and purification of the product *via* preparative HPLC (7:3 *n*-heptane/isopropanol + 0.45% diethylamine, 15 mL flow) yielded diaryl ether SG-154 (**198**, 99.6 mg, 0.186 mmol, 47%) as light yellow oil. The hydrochloride salt was formed according to general procedure **J** to yield a light yellow solid.

R$_f$ = 0.51 (9:1 CH$_2$Cl$_2$/MeOH).

m.p.: 90 °C (HCl salt).

^{1}H NMR (400 MHz, CDCl$_3$) δ/ppm = 7.28 – 7.21 (m, 2H, Ph, collapses with chloroform), 7.15 – 7.10 (m, 2H, 3''-H, 5''-H), 7.05 – 6.97 (m, 3H, 2'-H, 6'-H, Ph), 6.93 – 6.87 (m, 2H, 2''-H, 6''-H), 6.85 – 6.79 (m, 4H, 3'-H, 5'-H, Ph), 6.67 (s, 1H, 5-H), 6.36 (s, 1H, 8-H), 3.77 (s, 3H, OCH$_3$), 3.67 (t, J = 5.8 Hz, 1H, 1-H), 3.18 (ddd, J = 12.4, 8.0, 5.0 Hz, 1H, 3-H), 3.07 (dd, J = 13.8, 5.8 Hz, 1H, α-H), 2.90 – 2.81 (m, 2H, 4-H, α-H), 2.76 (dt, J = 12.4, 5.2 Hz, 1H, 3-H), 2.65 (dt, J = 15.9, 4.9 Hz, 1H, 4-H), 2.53 (s, 3H, NCH$_3$).

^{13}C NMR (101 MHz, CDCl$_3$) δ/ppm = 158.4 (qPh), 156.4 (C-1''), 154.8 (C-4'), 150.0 (C-6), 144.3 (q, J_{CF} = 4.1 Hz, C-4''), 142.2 (C-7), 135.3 (C-1'), 131.3 (C-8a), 131.2 (C-2', C-6'), 130.2 (C-4a), 129.5 (Ph), 122.6 (C-3'', C-5''), 122.2 (Ph), 121.0 (C-8), 120.7 (q, J_{CF} = 256.5 Hz, CF$_3$),

119.2 (C-3', C-5' or C-2'', C-6''), 119.1 (C-3', C-5' or C-2'', C-6''), 116.7 (Ph), 112.8 (C-5), 64.6 (C-1), 56.1 (OCH$_3$), 47.4 (C-3), 43.0 (NCH$_3$), 40.0 (C-α), 26.4 (C-4).

IR (ATR) $\tilde{v}_{max}$/cm^{-1} = 2980, 2889, 2440, 1510, 1497, 1239, 1218, 1187, 1163, 1106, 853, 751.

HRMS (ESI): calcd. for C$_{31}$H$_{29}$F$_3$NO$_4$ (M+H)$^+$ 536.20432; found 536.20393.

Purity (HPLC): > 96% (λ = 210 nm), > 96% (λ = 254 nm).

(±)-6-Methoxy-1-(4-(4-methoxyphenoxy)benzyl)-2-methyl-7-phenoxy-1,2,3,4-tetrahydro-isoquinoline – SG-155 (196)

SG-155 (**196**)
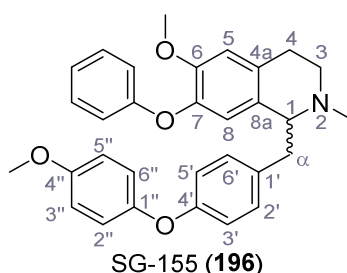
Following general procedure **I**, phenol **186** (188 mg, 0.500 mmol, 1.0 eq.), 4-methoxy-phenylboronic acid (228 mg, 1.50 mmol, 3.0 eq.), Cu(OAc)$_2$ (100 mg, 0.550 mmol, 1.1 eq.), NEt$_3$ (174 µL, 1.25 mmol, 2.5 eq.), pyridine (101 µL, 1.25 mmol, 2.5 eq.) and CH$_2$Cl$_2$ (20 mL) were used. After 20 h the reaction was completed and the product was purified by FCC (CH$_2$Cl$_2$ → 9.9:0.1 CH$_2$Cl$_2$/MeOH) to give diaryl ether SG-155 (**196**, 162 mg, 0.336 mmol, 67%) as colorless oil. The hydrochloride salt was formed according to general procedure **J** to yield a light yellow solid.

R$_f$ = 0.49 (9:1 CH$_2$Cl$_2$/MeOH).

m.p.: 81 °C (HCl salt).

^{1}H NMR (500 MHz, CD$_3$OD) δ/ppm = 7.23 – 7.20 (m, 2H, Ph), 6.98 – 6.94 (m, 3H, 3'-H, 5'-H, Ph), 6.85 – 6.79 (m, 5H, 5-H, 2''-H, 6''-H, 3''-H, 5''-H), 6.72 – 6.68 (m, 4H, 2'-H, 6'-H, 3'-H, 5'-H), 6.07 (s, 1H, 8-H), 3.77 (s, 3H, OCH$_3$), 3.71 (s, 4H, 1-H, OCH$_3$), 3.23 (ddd, J = 13.7, 9.4, 6.1 Hz, 1H, 3-H), 3.15 (dd, J = 13.3, 4.4 Hz, 1H, α-H), 2.97 (ddd, J = 15.9, 9.4, 6.8 Hz, 1H, 4-H), 2.82 – 2.73 (m, 3H, 3-H, 4-H, α-H), 2.53 (s, 3H, NCH$_3$).

^{13}C NMR (126 MHz, CD$_3$OD) δ/ppm = 159.8 (qPh), 158.2 (C-4'), 157.2 (C-4''), 151.9 (C-6 or C-1''), 151.7 (C-6 or C-1''), 142.9 (C-7), 134.6 (C-1'), 132.0 (C-3', C-5'), 131.8 (C-8a), 130.6 (C-4a), 130.4 (Ph), 123.0 (Ph), 122.6 (C-8), 121.4 (C-2'', C-6'' or C-3'', C-5''), 118.7 (C-2', C-6'), 117.3 (Ph), 115.9 (C-2'', C-6'' or C-3'', C-5''), 114.1 (C-5), 65.7 (C-1), 56.3 (OCH$_3$), 56.1 (OCH$_3$), 47.3 (C-3), 42.6 (NCH$_3$), 39.8 (C-α), 26.6 (C-4).

IR (ATR) $\tilde{v}_{max}$/cm^{-1} = 2940, 2907, 2523, 2360, 1496, 1264, 1218, 750, 690.

HRMS (ESI): calcd. for $C_{31}H_{32}NO_4$ (M+H)$^+$ 482.23258; found 482.23255.

Purity (HPLC): > 96% (λ = 210 nm), > 96% (λ = 254 nm).

(±)-6-Methoxy-2-methyl-7-phenoxy-1-(4-(3,4,5-trimethoxyphenoxy)benzyl)-1,2,3,4-tetra-hydroisoquinoline – SG-161 (197)

SG-161 (**197**)
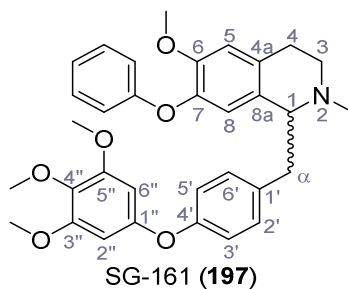
Following general procedure **I**, phenol **186** (100 mg, 0.266 mmol, 1.0 eq.), 3,4,5-trimethoxy-phenylboronic acid (169 mg, 0.799 mmol, 3.0 eq.), Cu(OAc)$_2$ (53.2 mg, 0.293 mmol, 1.1 eq.), NEt$_3$ (92.8 µL, 0.666 mmol, 2.5 eq.), pyridine (53.9 µL, 0.666 mmol, 2.5 eq.) and CH$_2$Cl$_2$ (50 mL) were used. After 20 h the reaction was completed and the product was purified by FCC (CH$_2$Cl$_2$ → 9.7:0.3 CH$_2$Cl$_2$/MeOH) to yield diaryl ether SG-161 (**197**, 100 mg, 0.185 mmol, 69%) as colorless oil. The hydrochloride salt was formed according to general procedure **J** to yield a colorless solid.

R$_f$ = 0.65 (9:1 CH$_2$Cl$_2$/MeOH).

m.p.: 82 °C (HCl salt).

^{1}H NMR (500 MHz, CD$_3$OD) δ/ppm = 7.23 – 7.18 (m, 2H, Ph), 7.04 – 7.00 (m, 2H, 2'-H, 6'-H), 6.96 – 6.92 (m, 1H, Ph), 6.83 (s, 1H, 5-H), 6.80 – 6.76 (m, 2H, 3'-H, 5'-H), 6.71 – 6.66 (m, 2H, Ph), 6.20 (s, 2H, 2''-H, 6''-H), 6.14 (s, 1H, 8-H), 3.76 – 3.74 (m, 1H, 1-H), 3.73 (s, 3H, OCH$_3$), 3.71 (s, 3H, OCH$_3$), 3.70 (s, 6H, 2 OCH$_3$), 3.24 (ddd, J = 13.7, 9.1, 6.1 Hz, 1H, 3-H), 3.16 (dd, J = 13.4, 4.4 Hz, 1H, α-H), 2.99 – 2.92 (m, 1H, 4-H), 2.83 – 2.75 (m, 3H, 3-H, 4-H, α-H), 2.54 (s, 3H, NCH$_3$).

^{13}C NMR (126 MHz, CD$_3$OD) δ/ppm = 159.8 (qPh), 157.1 (C-4'), 155.4 (C-1''), 155.2 (C-3'', C-5''), 151.7 (C-6), 143.0 (C-7), 135.4 (C-1'), 135.0 (C-4''), 132.2 (C-2', C-6'), 132.0 (C-8a), 130.6 (C-4a), 130.4 (Ph), 123.0 (Ph), 122.6 (C-8), 119.6 (C-3', C-5'), 117.3 (Ph), 114.1 (C-5), 97.6 (C-2'', C-6''), 65.7 (C-1), 61.2 (OCH$_3$), 56.5 (2 OCH$_3$), 56.3 (OCH$_3$), 47.5 (C-3), 42.7 (NCH$_3$), 39.9 (C-α), 26.7 (C-4).

IR (ATR) $\tilde{v}_{max}$/cm^{-1} = 3725, 2940, 2360, 2341, 1496, 1216, 1124, 993, 690.

HRMS (ESI): calcd. for $C_{33}H_{36}NO_6$ (M+H)$^+$ 542.25371; found 542.25327.

Purity (HPLC): > 96% (λ = 210 nm), > 96% (λ = 254 nm).

(±)-6-Methoxy-2-methyl-7-phenoxy-1-(4-(*p*-tolyloxy)benzyl)-1,2,3,4-tetrahydroisoquinoline hydrochloride – SG-162 (200)

SG-162 (**200**)
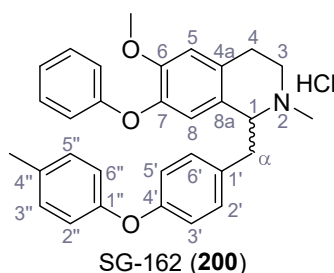
Following general procedure **I**, phenol **186** (100 mg, 0.266 mmol, 1.0 eq.), 4-methylbenzene-boronic acid (109 mg, 0.799 mmol, 3.0 eq.), Cu(OAc)$_2$ (53.2 mg, 0.293 mmol, 1.1 eq.), NEt$_3$ (92.8 µL, 0.666 mmol, 2.5 eq.), pyridine (53.9 µL, 0.666 mmol, 2.5 eq.) and CH$_2$Cl$_2$ (20 mL) were used. After 20 h the reaction was completed and the product was purified by FCC (CH$_2$Cl$_2$ → 9.7:0.3 CH$_2$Cl$_2$/MeOH) to yield diaryl ether SG-162 (**200**, 59.0 mg, 0.127 mmol, 48%) as light brown oil, which was, according to general procedure **J**, directly transferred into its hydrochloride salt to yield a beige solid. Analytical data are related to the hydrochloride salt.

R$_f$ = 0.61 (9:1 CH$_2$Cl$_2$/MeOH).

m.p.: 79 °C (HCl salt).

^{1}H NMR (500 MHz, CD$_3$OD) δ/ppm = 7.27 – 7.23 (m, 2H, Ph), 7.12 – 7.06 (m, 4H, 2'-H, 6'-H, 2''-H, 6''-H), 7.03 – 6.98 (m, 2H, 5-H, Ph), 6.84 – 6.81 (m, 2H, 3'-H, 5'-H), 6.79 – 6.74 (m, 2H, 3''-H, 5''-H), 6.72 – 6.68 (m, 2H, Ph), 6.07 (s, 1H, 8-H), 4.56 (dd, *J* = 10.0, 4.7 Hz, 1H, 1-H), 3.90 – 3.83 (m, 1H, 3-H), 3.78 (s, 3H, OCH$_3$), 3.54 – 3.48 (m, 1H, 3-H), 3.39 (dd, *J* = 13.2, 4.7 Hz, 1H, α-H), 3.28 – 3.20 (m, 2H, 4-H), 3.11 – 2.99 (m, 4H, α-H, NCH$_3$), 2.32 (s, 3H, CH$_3$).

^{13}C NMR (126 MHz, CD$_3$OD) δ/ppm = 159.0 (qPh), 158.8 (C-4'), 155.8 (C-4''), 153.3 (C-6), 144.4 (C-7), 134.4 (C-1''), 132.3 (C-2'', C-6''), 131.3 (C-2', C-6'), 130.6 (Ph), 130.4 (C-1'), 127.7 (C-4a), 123.6 (C-8), 122.3 (C-8a), 120.2 (C-3'', C-5''), 119.6 (C-3', C-5'), 117.8 (Ph), 114.2 (C-5), 65.7 (C-1), 57.5 (C-α), 56.4 (OCH$_3$), 46.5 (C-3), 40.7 (NCH$_3$), 24.7 (C-4), 20.7 (CH$_3$).

IR (ATR) $\tilde{v}_{max}$/cm^{-1} = 3406, 2971, 2443, 1499, 1230, 1107, 749.

HRMS (ESI): calcd. for $C_{31}H_{32}NO_3$ (M+H)$^+$ 466.23767; found 466.23751.

Purity (HPLC): > 96% (λ = 210 nm), > 96% (λ = 254 nm).

(±)-6-Methoxy-2-methyl-7-phenoxy-1-(4-(pyridin-4-yloxy)benzyl)-1,2,3,4-tetrahydro-isoquinoline – SG-163 (203)

SG-163 (**203**)
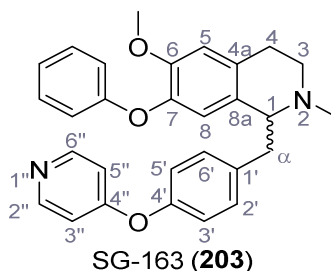
Following general procedure **I**, phenol **186** (100 mg, 0.266 mmol, 1.0 eq.), pyridine-4-boronic acid (98.2 mg, 0.799 mmol, 3.0 eq.), Cu(OAc)$_2$ (53.2 mg, 0.293 mmol, 1.1 eq.), NEt$_3$ (92.8 µL, 0.666 mmol, 2.5 eq.), pyridine (53.9 µL, 0.666 mmol, 2.5 eq.) and CH$_2$Cl$_2$ (20 mL) were used. After 20 h the reaction was completed and the product was purified *via* preparative HPLC (6:4 *n*-heptane/isopropanol + 0.45% diethylamine, 15 mL flow) to yield diaryl ether SG-163 (**203**, 30.6 mg, 0.0676 mmol, 25%) as colorless oil. The hydrochloride salt was formed according to general procedure **J** to yield a colorless solid.

R$_f$ = 0.54 (9:1 CH$_2$Cl$_2$/MeOH).

m.p.: 233 °C (HCl salt).

¹H NMR (400 MHz, CDCl$_3$) δ/ppm = 8.41 (dd, J = 4.8, 1.5 Hz, 2H, 2''-H, 6''-H), 7.27 − 7.22 (m, 2H, Ph, collapses with chloroform), 7.11 − 7.07 (m, 2H, 2'-H, 6'-H), 7.01 − 6.96 (m, 1H, Ph), 6.90 − 6.86 (m, 2H, 3'-H, 5'-H), 6.85 − 6.82 (m, 2H, Ph), 6.76 − 6.72 (m, 2H, 3''-H, 5''-H), 6.68 (s, 1H, 5-H), 6.37 (s, 1H, 8-H), 3.77 (s, 3H, OCH$_3$), 3.70 (t, J = 6.2 Hz, 1H, 1-H), 3.22 − 3.15 (m, 1H, 3-H), 3.10 (dd, J = 14.0, 5.4 Hz, 1H, α-H), 2.90 − 2.75 (m, 3H, 3-H, 4-H, α-H), 2.65 (dt, J = 16.6, 5.1 Hz, 1H, 4-H), 2.54 (s, 3H, NCH$_3$).

¹³C NMR (101 MHz, CDCl$_3$) δ/ppm = 165.1 (C-1''), 158.4 (qPh), 152.2 (C-4'), 151.5 (C-3'', C-5''), 150.0 (C-6), 142.2 (C-7), 136.9 (C-1'), 131.5 (C-2', C-6'), 131.4 (C-4a), 130.0 (C-8a), 129.6 (Ph), 122.3 (Ph), 121.0 (C-8), 120.5 (C-3', C-5'), 116.7 (Ph), 112.8 (C-5), 112.1 (C-2'', C-6''), 64.6 (C-1), 56.1 (OCH$_3$), 47.5 (C-3), 43.0 (NCH$_3$), 40.0 (C-α), 26.5 (C-4).

IR (ATR) $\tilde{v}_{max}$/cm^{-1} = 3406, 2979, 2451, 1636, 1509, 1490, 1273, 1219, 747.

HRMS (ESI): calcd. for C$_{29}$H$_{29}$N$_2$O$_3$ (M+H)$^+$ 453.21727; found 453.21781.

Purity (HPLC): > 96% (λ = 210 nm), > 96% (λ = 254 nm).

(±)-4-(4-((6-Methoxy-2-methyl-7-phenoxy-1,2,3,4-tetrahydroisoquinolin-1-yl)methyl)-phenoxy)benzonitrile – SG-164 (201)

SG-164 (**201**)
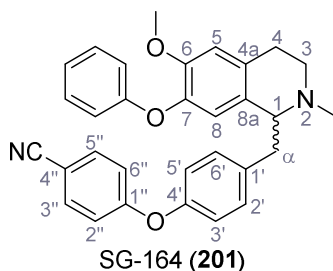
Following general procedure **I**, phenol **186** (100 mg, 0.266 mmol, 1.0 eq.), 4-cyanophenyl-boronic acid (117 mg, 0.799 mmol, 3.0 eq.), $Cu(OAc)_2$ (53.2 mg, 0.293 mmol, 1.1 eq.), NEt_3 (92.8 µL, 0.666 mmol, 2.5 eq.), pyridine (53.9 µL, 0.666 mmol, 2.5 eq.) and CH_2Cl_2 (50 mL) were used. After 20 h the reaction was completed and the product was purified by FCC (CH_2Cl_2 → 9.7:0.3 CH_2Cl_2/MeOH) to yield diaryl ether SG-164 (**201**, 61.1 mg, 0.128 mmol, 48%) as colorless oil. The hydrochloride salt was formed according to general procedure **J** to yield a colorless solid.

R$_f$ = 0.65 (9:1 CH_2Cl_2/MeOH).

m.p.: 124 °C (HCl salt).

^{1}H NMR (400 MHz, CDCl$_3$) δ/ppm = 7.56 – 7.51 (m, 2H, 2''-H, 6''-H), 7.27 – 7.22 (m, 2H, Ph, collapses with chloroform), 7.10 – 7.06 (m, 2H, 2'-H, 6'-H), 7.01 – 6.96 (m, 1H, Ph), 6.92 – 6.88 (m, 2H, 3''-H, 5''-H), 6.88 – 6.81 (m, 4H, 3'-H, 5'-H, Ph), 6.68 (s, 1H, 5-H), 6.37 (s, 1H, 8-H), 3.77 (s, 3H, OCH$_3$), 3.69 (t, J = 6.1 Hz, 1H, 1-H), 3.18 (ddd, J = 12.8, 7.9, 5.1 Hz, 1H, 3-H), 3.09 (dd, J = 13.8, 5.4 Hz, 1H, α-H), 2.90 – 2.74 (m, 3H, 3-H, 4-H, α-H), 2.65 (dt, J = 16.0, 5.0 Hz, 1H, 4-H), 2.53 (s, 3H, NCH$_3$).

^{13}C NMR (101 MHz, CDCl$_3$) δ/ppm = 162.0 (C-1''), 158.4 (qPh), 152.9 (C-4'), 150.0 (C-6), 142.1 (C-7), 136.7 (C-1'), 134.2 (C-2'', C-6''), 131.5 (C-2', C-6'), 131.4 (C-4a), 130.0 (C-8a), 129.6 (Ph), 122.2 (Ph), 121.1 (C-8), 120.2 (C-3', C-5'), 119.1 (C-4''), 117.8 (C-3'', C-5''), 116.6 (Ph), 112.8 (C-5), 105.6 (CN), 64.6 (C-1), 56.1 (OCH$_3$), 47.4 (C-3), 43.0 (NCH$_3$), 40.0 (C-α), 26.4 (C-4).

IR (ATR) ṽ$_{max}$/cm^{-1} = 2940, 2225, 1596, 1495, 1245, 1218, 1166, 836, 750, 736, 690.

HRMS (ESI): calcd. for $C_{31}H_{29}N_2O_3$ (M+H)$^+$ 477.21727; found 477.21773.

Purity (HPLC): > 96% (λ = 210 nm), > 96% (λ = 254 nm).

(±)-1-(4-(3,4-Dichlorophenoxy)benzyl)-6-methoxy-2-methyl-7-phenoxy-1,2,3,4-tetrahydroisoquinoline – SG-165 (202)

SG-165 (**202**)
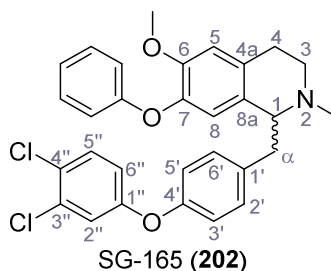
Following general procedure **I**, phenol **186** (100 mg, 0.266 mmol, 1.0 eq.), 3,4-dichlorophenylboronic acid (152 mg, 0.799 mmol, 3.0 eq.), $Cu(OAc)_2$ (53.2 mg, 0.293 mmol, 1.1 eq.), NEt_3 (92.8 µL, 0.666 mmol, 2.5 eq.), pyridine (53.9 µL, 0.666 mmol, 2.5 eq.) and CH_2Cl_2 (20 mL) were used. After 20 h the reaction was completed and the product was purified by FCC (CH_2Cl_2 → 9.7:0.3 CH_2Cl_2/MeOH) to yield diaryl ether SG-165 (**202**, 109 mg, 0.208 mmol, 78%) as brown oil. The hydrochloride salt was formed according to general procedure **J** to yield a beige solid.

R_f = 0.58 (9:1 CH_2Cl_2/MeOH).

m.p.: 92 °C (HCl salt).

^{1}H NMR (400 MHz, CDCl$_3$) δ/ppm = 7.31 (d, J = 8.8 Hz, 1H, 5''-H), 7.28 – 7.22 (m, 2H, Ph, collapses with chloroform), 7.06 – 6.97 (m, 4H, 2'-H, 6'-H, 2''-H, Ph), 6.87 – 6.83 (m, 2H, Ph), 6.82 – 6.78 (m, 2H, 3'-H, 5'-H), 6.75 (dd, J = 8.8, 2.8 Hz, 1H, 6''-H), 6.67 (s, 1H, 5-H), 6.40 (s, 1H, 8-H), 3.78 (s, 3H, OCH$_3$), 3.68 (t, J = 5.6 Hz, 1H, 1-H), 3.17 (ddd, J = 12.6, 7.8, 5.1 Hz, 1H, 3-H), 3.06 (dd, J = 13.9, 5.6 Hz, 1H, α-H), 2.89 – 2.73 (m, 3H, 3-H, 4-H, α-H), 2.64 (dt, J = 15.6, 5.1 Hz, 1H, 4-H), 2.52 (s, 3H, NCH$_3$).

^{13}C NMR (101 MHz, CDCl$_3$) δ/ppm = 158.3 (qPh), 157.1 (C-1'' or C-3''), 154.2 (C-4'), 149.9 (C-6), 142.3 (C-7), 135.8 (C-1'), 133.2 (C-1'' or C-3''), 131.3 (C-2', C-6'), 131.2 (C-4a), 131.0 (C-5''), 130.1 (C-8a), 129.5 (Ph), 126.1 (C-4''), 122.3 (Ph), 120.9 (C-8), 120.1 (C-2''), 119.2 (C-3', C-5'), 117.7 (C-6''), 116.8 (Ph), 112.7 (C-5), 64.6 (C-1), 56.1 (OCH$_3$), 47.6 (C-4), 43.0 (NCH$_3$), 40.1 (C-α), 26.4 (C-4).

IR (ATR) $\tilde{v}_{max}$/cm^{-1} = 2979, 1585, 1505, 1489, 1466, 1261, 1223, 1119, 750.

HRMS (ESI): calcd. for $C_{30}H_{28}^{35}Cl_2NO_3$ (M+H)$^+$ 520.14408; found 520.14478.

Purity (HPLC): > 96% (λ = 210 nm), > 96% (λ = 254 nm).

5.2.2.6 Further reactions

(±)-7-(benzyloxy)-1-(4-(benzyloxy)-3-methoxybenzyl)-2-ethyl-6-methoxy-1,2,3,4-tetrahydroisoquinoline – SG-158 (208)
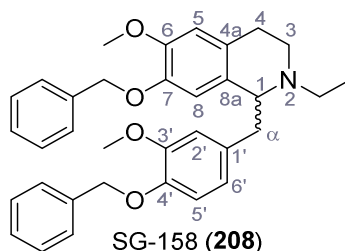
SG-158 (**208**)

(±)-7-(Benzyloxy)-1-(4-(benzyloxy)-3-methoxybenzyl)-6-methoxy-1,2,3,4-tetrahydroisoquinoline (Z6 (**145**), 100 mg, 0.188 mmol, 1.0 eq.), NEt$_3$ (65.5 µL, 0.470 mmol, 2.5 eq.) and KI (31.2 mg, 0.188 mmol, 1.0 eq.) were dispersed in CHCl$_3$ (20 mL) and bromoethane (30.8 µL, 0.282 mmol, 1.5 eq.) was added. The reaction mixture was stirred at 65 °C for 6 days and subsequently concentrated *in vacuo*. The residue was dissolved in CH$_2$Cl$_2$ (30 mL) and washed with sat. aq. NaHCO$_3$ solution (10 mL), 10% aq. citric acid solution (10 mL) and sat. aq. NaCl solution (10 mL). The organic layer was dried over Na$_2$SO$_4$, filtered and concentrated *in vacuo*. Purification by FCC (CH$_2$Cl$_2$ → 9.7:0.3 CH$_2$Cl$_2$/MeOH), followed by purification *via* preparative HPLC (6:4 *n*-heptane/isopropanol + 0.45% diethylamine, 15 mL flow) yielded racemic amine SG-158 (**208**, 23.2 mg, 0.0443 mmol, 24%) as colorless oil. The hydrochloride salt was formed according to general procedure **J** to yield a colorless solid.

R$_f$ = 0.54 (9:1 CH$_2$Cl$_2$/MeOH).

m.p.: 211 °C (HCl salt).

^{1}H NMR (500 MHz, CDCl$_3$) δ/ppm = 7.45 – 7.27 (m, 10H, P̲hCH$_2$, collapses with chloroform), 6.80 (d, *J* = 8.2 Hz, 1H, 5'-H), 6.62 (d, *J* = 1.9 Hz, 1H, 2'-H), 6.59 (s, 1H, 5-H), 6.55 (dd, *J* = 8.3, 2.0 Hz, 1H, 6'-H), 6.05 (s, 1H, 8-H), 5.13 (s, 2H, PhCH̲$_2$), 4.85 (d, *J* = 12.3 Hz, 1H, PhCH̲$_2$), 4.74 (d, *J* = 12.3 Hz, 1H, PhCH̲$_2$), 3.86 (s, 3H, OCH$_3$), 3.82 (s, 3H, OCH$_3$), 3.75 (dd, *J* = 7.4, 6.0 Hz, 1H, 1-H), 3.21 – 3.13 (m, 1H, 4-H), 3.04 (dd, *J* = 13.5, 5.2 Hz, 1H, α-H), 2.91 – 2.81 (m, 2H, 3-H, 4-H), 2.72 – 2.66 (m, 3H, α-H, CH̲$_2$CH$_3$), 2.55 – 2.47 (m, 1H, 3-H), 1.12 (t, *J* = 7.1 Hz, 3H, CH$_2$CH̲$_3$).

^{13}C NMR (126 MHz, CDCl$_3$) δ/ppm = 149.4 (C-3'), 148.0 (C-6), 146.6 (C-4'), 145.6 (C-7), 137.5 (q̲PhCH$_2$), 137.5 (q̲PhCH$_2$), 133.6 (C-1'), 129.8 (C-8a), 128.6 (P̲hCH$_2$), 128.5 (P̲hCH$_2$), 127.9 (P̲hCH$_2$), 127.8 (P̲hCH$_2$), 127.4 (P̲hCH$_2$), 127.3 (P̲hCH$_2$), 127.1 (C-4a), 122.1 (C-6'), 114.2 (C-2'), 113.9 (C-8 or C-5'), 113.8 (C-8 or C-5'), 111.9 (C-5), 71.3 (PhC̲H$_2$), 71.0 (PhC̲H$_2$), 62.6 (C-1), 56.1 (2 OCH$_3$), 47.8 (C̲H$_2$CH$_3$), 43.6 (C-3), 40.8 (C-α), 25.5 (C-4), 13.4 (CH$_2$C̲H$_3$).

IR (ATR) ṽ$_{max}$/cm^{-1} = 2998, 2359, 1589, 1514, 1264, 1226, 1021, 737, 696.

HRMS (ESI): calcd. for $C_{34}H_{38}NO_4$ (M+H)$^+$ 524.27954; found 524.28026.

Purity (HPLC): > 96% (λ = 210 nm), > 96% (λ = 254 nm).

(±)-7-(Benzyloxy)-1-(4-(benzyloxy)-3-methoxybenzyl)-6-methoxy-2-methyl-1,2,3,4-tetrahydroisoquinoline – SG-159 (206)

SG-159 (**206**)
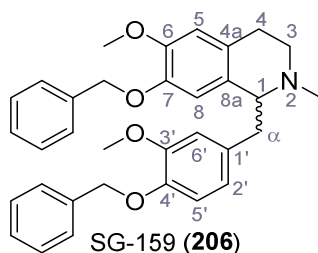
A solution of (±)-7-(benzyloxy)-1-(4-(benzyloxy)-3-methoxybenzyl)-6-methoxy-1,2,3,4-tetrahydro-isoquinoline (Z6 (**145**),100 mg, 0.188 mmol, 1.0 eq.) and 37% aqueous formaldehyde (70.0 μL, 0.940 mmol, 5.0 eq.) in HPLC grade MeOH (5.0 mL) was acidified with glacial acetic acid (0.50 mL, final pH ~ 5), before NaCNBH$_3$ (24.9 mg, 0.376 mmol, 2.0 eq.) was added. The reaction mixture was stirred for 2 days at rt and concentrated *in vacuo* to give a light yellow solid. The residue was dissolved in EtOAc (40 mL) and was washed with sat. aq. NaHCO$_3$ solution (15 mL), 10% aq. citric acid solution (15 mL) and sat. aq. NaCl solution (15 mL). The organic layer was dried over Na$_2$SO$_4$ and concentrated *in vacuo*. The crude product was purified by FCC (CH$_2$Cl$_2$ → 9.7:0.3 CH$_2$Cl$_2$/MeOH) to yield racemic amine SG-159 (**206**, 61.2 mg, 0.120 mmol, 64%) as colorless oil. The hydrochloride salt was formed according to general procedure **J** to yield a colorless solid.

R$_f$ = 0.57 (9:1 CH$_2$Cl$_2$/MeOH).

m.p.: 87 °C (HCl salt).

¹H NMR (400 MHz, CDCl₃) δ/ppm = 7.42 – 7.23 (m, 13H, PhCH$_2$, collapses with chloroform), 6.76 (d, *J* = 8.1 Hz, 1H, 5'-H), 6.61 – 6.54 (m, 2H, 5-H, 2'-H), 6.51 (dd, *J* = 8.1, 1.9 Hz, 1H, 6'-H), 6.08 (s, 1H, 8-H), 5.11 (s, 2H, PhCH$_2$), 4.84 (d, *J* = 12.3 Hz, 1H, PhCH$_2$), 4.72 (d, *J* = 12.3 Hz, 1H, PhCH$_2$), 3.84 (s, 3H, OCH$_3$), 3.78 (s, 3H, OCH$_3$), 3.61 (dd, *J* = 7.2, 5.0 Hz, 1H, 1-H), 3.17 – 3.02 (m, 2H, 3-H, α-H), 2.84 – 2.67 (m, 3H, 3-H, 4-H, α-H), 2.60 – 2.53 (m, 1H, 4-H), 2.51 (s, 3H, NCH$_3$).

¹³C NMR (101 MHz, CDCl₃) δ/ppm = 149.3 (C-3'), 147.9 (C-6), 146.6 (C-4'), 145.6 (C-7), 137.5 (qPhCH$_2$), 137.4 (qPhCH$_2$), 133.2 (C-1'), 129.3 (C-8a), 128.7 (PhCH$_2$), 128.6 (PhCH$_2$), 127.9 (PhCH$_2$), 127.8 (PhCH$_2$), 127.4 (PhCH$_2$), 127.3 (PhCH$_2$), 126.8 (C-4a), 122.0 (C-6'), 113.8 (C-

8 or C-5'), 113.7 (C-8 or C-5'), 113.5 (C-2'), 111.7 (C-5), 71.2 (Ph$\underline{C}H_2$), 70.9 (Ph$\underline{C}H_2$), 64.8 (C-1), 56.1 (2 OCH_3), 47.2 (C-3), 42.9 (NCH_3), 40.8 (C-α), 25.9 (C-4).

IR (ATR) $\tilde{\nu}_{max}$/cm^{-1} = 2980, 2889, 2359, 1513, 1263, 1225, 1012, 696.

HRMS (ESI): calcd. for $C_{33}H_{36}NO_4$ (M+H)$^+$ 510.26389; found 510.26339.

Purity (HPLC): > 96% (λ = 210 nm), > 96% (λ = 254 nm).

(±)-7-(Benzyloxy)-1-(4-(benzyloxy)benzyl)-6-methoxy-2-methyl-1,2,3,4-tetrahydro-isoquinoline – SG-005 (187)

An alternative route to receive SG-005 (**187**): A solution of Z3 (**137**, 251 mg, 0.500 mmol, 1.0 eq.) and 37% aq. formaldehyde solution (68.9 µL, 2.50 mmol, 5.0 eq.) in HPLC grade MeOH (5.0 mL) was acidified with two drops of glacial acetic acid (0.50 mL, final pH ~ 5) and sodium cyanoborohydride (66.1 mg, 1.00 mmol, 2.0 eq.) was added. The reaction mixture was stirred for 4 days at rt and concentrated *in vacuo* to give a white solid. The residue was dissolved in EtOAc (40 mL) and was washed with sat. aq. NaHCO$_3$ solution (15 mL), 10% aq. citric acid solution (15 mL) and sat. aq. NaCl solution (15 mL). The organic layer was dried over Na$_2$SO$_4$ and concentrated *in vacuo*. The crude product was purified by FCC (9.5:0.5 CHCl$_3$/MeOH) to yield SG-005 (**187**, 133 mg, 0.278 mmol, 56%) as off white solid. Analytical data are stated above.

(±)-7-(Benzyloxy)-1-(4-(benzyloxy)benzyl)-6-methoxy-2-methyl-1,2,3,4-tetrahydro-isoquinoline – SG-005 (187)

An alternative route to receive SG-005 (**187**) *via* Mitsunobu reaction: SG-132 (**159**, 150 mg, 0.500 mmol, 1.0 eq.) is dissolved in dry THF (5.0 mL), before PPh$_3$ (629 mg, 2.40 mmol, 4.8 eq.) and benzyl alcohol (145 µL, 1.40 mmol, 2.8 eq.) were added. The reaction mixture was cooled to 4 °C and DIAD (315 µL, 1.60 mmol, 3.2 eq.) was added dropwise. The mixture was allowed to warm to rt for 18 h and was then concentrated *in vacuo*. The residue was purified by FCC (9.9:0.1 → 9.7:0.3 CH$_2$Cl$_2$/MeOH) to yield SG-005 (**187**, 113 mg, 0.236 mmol, 47%) as light yellow oil. Analytical data are stated above.

5.2.2.7 Substances received from other sources

Prof. Dr. Peter Pachaly[†] kindly provided tetrandrine (**1**) and fangchinoline (**9**) from natural sources and semi synthetic *N*,*N*-dimethyl-tetrandrine dichloride (**139**, **Table 15**). Prof. Dr.

Meinhart Zenk[†] kindly provided a compound library of 1-benzyl-1,2,3,4-tetrahydroisoquinolines (Z compounds, **Table 15**).

Table 15: Substances received from other sources. *Analytical data are stated below.

entry	name	abbreviation	literature
1	tetrandrine (**1**)	-	[143]
2	fangchinoline (**9**)	-	[144]
3	*N,N*- dimethyltetrandrine dichloride (**139**)	-	[145]
4	(±)-coclaurine hydrochloride (**141**)	Z1	[194, 195]
5	*R*-coclaurine hydrochloride (**142**)	Z2	[194, 195]
6	(±)-7-(benzyloxy)-1-(4-(benzyloxy)benzyl)-6-methoxy-1,2,3,4-tetrahydroisoquinoline hydrochloride (**137**)	Z3	[82, 195]*
7	(+)-*O,O*-dibenzyl coclaurine / (+)-7-(benzyloxy)-1-(4-(benzyloxy)benzyl)-6-methoxy-1,2,3,4-tetrahydroisoquinoline (**143**)	Z4	[193]
8	(±)-6-(benzyloxy)-1-(4-(benzyloxy)benzyl)-7-methoxy-1,2,3,4-tetrahydroisoquinoline hydrochloride (**144**)	Z5	[196]
9	(±)-*O,O*-dibenzyl nororientaline / (±)-7-(benzyloxy)-1-(4-(benzyloxy)-3-methoxy-benzyl)-6-methoxy-1,2,3,4-tetrahydroisoquinoline (**145**)	Z6	[197]
10	*R*-norreticuline (**146**)	Z7/Z8	[198, 199]
11	(±)-laudanosine (**147**)	Z9	[200]
12	(±)-6-(benzyloxy)-1-(3-(benzyloxy)-4-methoxybenzyl)-7-methoxy-1,2,3,4-tetrahydroisoquinoline hydrochloride (**148**)	Z11	[201]
13	(±)-6,7-bis(benzyloxy)-1-(4-(benzyloxy)-3-methoxybenzyl)-2-methyl-1,2,3,4-tetrahydroisoquinoline hydrochloride (**149**)	Z12	[202]
14	(±)-5-(3,4-bis(benzyloxy)benzyl)-5,6,7,8-tetrahydro-[1,3]dioxolo[4,5-g]isoquinoline hydrochloride (**150**)	Z13	*
15	(±)-1-(benzo[*d*][1,3]dioxol-5-ylmethyl)-6,7-dimethoxy-1,2,3,4-tetrahydroisoquinoline (**151**)	Z14	[203, 204]
16	(±)-1-(benzo[d][1,3]dioxol-5-ylmethyl)-6-(benzyloxy)-7-methoxy-1,2,3,4-tetrahydroisoquinoline (**152**)	Z15	[205]
17	(±)-1-(benzo[d][1,3]dioxol-5-ylmethyl)-6,7-bis(benzyloxy)-1,2,3,4-tetrahydroisoquin-oline (**153**)	Z16/Z17	[206]

18	(±)-1-(benzo[d][1,3]dioxol-5-ylmethyl)-6,7-bis(benzyloxy)-3,4-dihydroisoquinoline (**154**)	Z18	[206]
19	(±)-6,7-bis(benzyloxy)-1-((6-bromobenzo[d][1,3]dioxol-5-yl)methyl)-1,2,3,4-tetrahydro-isoquinoline hydrochloride (**155**)	Z20	*
20	(±)-1-((6-bromobenzo[d][1,3]dioxol-5-yl)methyl)-3,4-dihydroisoquinoline-6,7-diol (**156**)	Z21	[207]
21	*N*-(4-(benzyloxy)-3-methoxyphenethyl)-2-(4-(benzyloxy)-phenyl)acetamide (**157**)	Z22	[208]
22	Epiberberine chloride / 8,9-dimethoxy-11,12-dihydro-[1,3]dioxolo-[4,5-h]isoquinolino[2,1-b]isoquinolin-13-ium chloride (**158**)	Z23	[209]

(±)-7-(benzyloxy)-1-(4-(benzyloxy)benzyl)-6-methoxy-1,2,3,4-tetrahydroisoquinoline hydrochloride – Z3 (137)

1H NMR (500 MHz, CD₃OD) δ/ppm = 7.51 – 7.25 (m, 10H), 7.21 – 7.12 (m, 2H), 7.08 – 6.99 (m, 2H), 6.84 (s, 1H), 6.45 (s, 1H), 5.09 (s, 2H), 4.84 (d, J = 2.7 Hz, 2H), 4.64 (t, J = 7.3 Hz, 1H), 3.85 (s, 3H), 3.61 – 3.47 (m, 1H), 3.42 – 3.34 (m, 1H), 3.31 – 3.24 (m, 1H), 3.17 – 3.00 (m, 3H).

13C NMR (126 MHz, CD₃OD) δ/ppm = 159.8, 151.2, 148.0, 138.6, 138.3, 132.0, 129.5, 129.5, 129.0, 128.9, 128.9, 128.7, 128.6, 125.5, 124.3, 116.5, 114.0, 113.2, 72.0, 71.0, 57.4, 56.5, 49.5, 49.3, 49.2, 49.0, 48.8, 48.7, 48.5, 40.3, 40.1, 25.8.

HRMS (ESI): calcd. for $C_{31}H_{32}NO_3$ (M+H)⁺ 466.23767; found 466.23798.

Purity (HPLC): > 96% (λ = 210 nm), > 96% (λ = 254 nm).

(±)-*O,O*-dibenzyl nororientaline / (±)-7-(benzyloxy)-1-(4-(benzyloxy)-3-methoxy-benzyl)-6-methoxy-1,2,3,4-tetrahydroisoquinoline – Z6 (145)

1H NMR (500 MHz, CDCl₃) δ/ppm = 9.27 (s, 1H), 7.51 – 7.23 (m, 10H), 7.04 – 6.99 (m, 2H), 6.81 (s, 1H), 6.79 (dd, J = 8.2, 1.9 Hz, 1H), 6.63 (s, 1H), 5.05 (s, 2H), 4.90 – 4.76 (m, 2H), 4.59 (t, J = 7.0 Hz, 1H), 3.75 (s, 6H), 3.32 – 3.29 (m, 1H), 3.27 – 3.09 (m, 3H), 3.03 – 2.87 (m, 2H).

13C NMR (126 MHz, CDCl₃) δ/ppm = 159.8, 151.2, 148.0, 138.6, 138.3, 132.0, 129.6, 129.5, 129.0, 128.9, 128.8, 128.7, 128.6, 125.5, 124.3, 116.5, 114.0, 113.2, 72.0, 71.0, 57.4, 56.5, 40.3, 40.1, 25.8.

HRMS (ESI): calcd. for $C_{32}H_{34}NO_4$ (M+H)$^+$ 496.24824; found 496.24827.

Purity (HPLC): > 96% (λ = 210 nm), > 96% (λ = 254 nm).

(±)-5-(3,4-bis(benzyloxy)benzyl)-5,6,7,8-tetrahydro-[1,3]dioxolo[4,5-g]isoquinoline hydrochloride – Z13 (150)

^{1}H NMR (500 MHz, CDCl$_3$) δ/ppm = 10.22 (d, J = 7.6 Hz, 1H), 9.66 (d, J = 8.9 Hz, 1H), 7.42 – 7.24 (m, 10H), 6.88 – 6.84 (m, 1H), 6.82 (s, 1H), 6.73 (dd, J = 8.2, 1.9 Hz, 1H), 6.51 (s, 1H), 6.26 (s, 1H), 5.92 (d, J = 1.3 Hz, 1H), 5.89 (d, J = 1.2 Hz, 1H), 5.16 – 5.00 (m, 4H), 4.68 – 4.57 (m, 1H), 3.44 – 3.34 (m, 1H), 3.27 – 3.16 (m, 2H), 3.08 – 2.95 (m, 2H), 2.83 – 2.71 (m, 1H).

^{13}C NMR (126 MHz, CDCl$_3$) δ/ppm = 149.1, 148.4, 147.6, 146.8, 137.4, 128.7, 128.6, 128.4, 127.9, 127.6, 127.5, 125.5, 124.2, 123.1, 121.5, 116.8, 115.6, 108.8, 107.0, 101.4, 77.4, 76.9, 71.4, 55.3, 40.5, 38.9, 25.6.

HRMS (ESI): calcd. for $C_{31}H_{30}NO_4$ (M+H)$^+$ 480.21693; found 480.21719.

Purity (HPLC): > 96% (λ = 210 nm), > 96% (λ = 254 nm).

(±)-6,7-bis(benzyloxy)-1-((6-bromobenzo[d][1,3]dioxol-5-yl)methyl)-1,2,3,4-tetrahydro-isoquinoline hydrochloride – Z20 (155)

^{1}H NMR (500 MHz, (CD$_3$)$_2$SO) δ/ppm = 9.30 (s, 1H), 7.51 – 7.24 (m, 10H), 7.18 (s, 1H), 6.96 (s, 1H), 6.60 (s, 1H), 6.08 (d, J = 7.7 Hz, 2H), 5.13 (s, 2H), 5.07 – 4.92 (m, 2H), 4.61 – 4.41 (m, 1H), 3.47 – 3.37 (m, 1H), 3.37 – 3.25 (m, 3H), 3.25 – 3.14 (m, 2H), 3.12 – 3.00 (m, 1H), 2.91 – 2.77 (m, 1H).

^{13}C NMR (126 MHz, (CD$_3$)$_2$SO) δ/ppm = 147.8, 147.7, 147.3, 146.5, 137.0, 128.4, 128.4, 128.2, 127.8, 127.8, 127.6, 127.3, 125.0, 123.8, 115.0, 114.1, 112.7, 112.5, 111.9, 102.1, 70.2, 70.0, 53.6, 38.8, 24.5.

HRMS (ESI): calcd. for $C_{31}H_{29}{}^{79}BrNO_4$ (M+H)$^+$ 558.12745; found 558.12829.

Purity (HPLC): > 96% (λ = 210 nm), > 96% (λ = 254 nm).

Berbamine dihydrochloride (**10**) was purchased from Sigma-Aldrich (now Merck, Darmstadt, Germany), cepharanthine (**140**) and dauricine (**11**) from Carbosynth (Compton, Berkshire, United Kingdom) and oxyacanthine sulfate (**138**) from abcr (Karlsruhe, Germany).

5.3 Biological methods

5.3.1 High-throughput screening (HTS)

The high-throughput screening was performed by Dr. Phuong Nguyen and myself in collaboration with the group of Prof. Dr. Michael Schaefer at the *Rudolf-Böhm-Institut für Pharmakologie und Toxikologie*, University of Leipzig. The experiments were run using a custom-made fluorescence imaging plate reader built into a robotic liquid handling station (Freedom Evo 150, Tecan, Männedorf, Switzerland) as previously described[22, 88].

In brief, HEK-293 cells stably expressing human TPC2$^{L11A/L12A}$-RFP and stably expressing human CLN3$^{L253A/I254A}$ -RFP were cultured at 37 °C with 5% of CO_2 in Dulbecco's modified Eagle medium (Thermo Fisher), supplemented with 10% fetal calf serum (Biochrom, Berlin, Germany), 2.00 mM L-glutamine, 100 U/mL penicillin, 0.100 mg/mL streptomycin, and 400-800 µg/mL G418. Cells were incubated with Fluo-4/AM (**15**, 4.00 µM; Life Technologies, Eugene, Oregon, USA) for 30 min at 37 °C, washed and resuspended in a HEPES-buffered solution 1 (HBS1) comprising 132 mM NaCl, 6.00 mM KCl, 1.00 mM $MgCl_2$, 1.00 mM $CaCl_2$, 10.0 mM HEPES, and 5.50 mM D-glucose (pH was adjusted to 7.4 with NaOH). Then, the cells were seeded on black walled, clear bottom 384-well plates (Greiner, Frickenhausen, Germany) and the plates were placed in the imaging reader. Experiments were performed with cell suspensions.

For primary screening, individual compounds from Roche libraries (Xplore libraries X30 and X50, Roche, Basel, Switzerland) were diluted in HBS1 to a working concentration of 100 µM. After recording the baseline for 30 s, compounds were injected to a final concentration of 10 µM. Recording continued for 180 s per quadrant (total 750 s for four quadrants). If high intensities were measured in both cell lines, the compounds were deemed false positives and excluded. From single hits with high intensities concentration effect experiments were performed. In case of a low IC_{50}, hits were confirmed by single cell Ca-imaging. Concentration effect relationships were plotted using GraphPad Prism 5 and fitted to the Hill equation.

Concentration-effect experiments were performed by Nicole Urban (Schäfer group) as described above.

5.3.2 Single cell calcium imaging

Single cell Ca^{2+} imaging experiments were performed as previously described[22, 115]. In more detail, HEK293 cells were cultured at 37 °C with 5% of CO_2 in Dulbecco's modified Eagle medium (Gibco), supplemented with 10% fetal bovine serum, 100 U/mL penicillin, and 0.100 mg/mL streptomycin. Cells were plated onto poly-L-lysine (sigma)-coated glass coverslips, grown over two days and transiently transfected for 18-24 h with plasmids using TurboFect

(Thermo Fisher Scientific, Waltham, USA) according to the manufacturer's instructions. Plasmids used for transfection were generated in the group of Prof. Christian Grimm and are literature known. Experiments for blockers were performed using HEK293 cells stably expressing TPC2$^{L11A/L12A}$ –RFP[14, 22, 28, 114, 115].

Transfected cells were loaded for 1 h at 37 °C with 10% of CO_2 with Fura-2/AM (**126**, 4.0 µM) and 0.005% (v/v) Pluronic® F-127 (both from Thermo Fisher) in HEPES-buffered solution 2 (HBS2) comprising 138 mM NaCl, 6.00 mM KCl, 1.00 mM $MgCl_2$, 2.00 mM $CaCl_2$, 10.0 mM HEPES, and 5.50 mM D-glucose (pH was adjusted to 7.4 with NaOH). After loading, cells were washed in HBS2, and mounted in an imaging chamber. All recordings were performed in HBS2. Images were acquired every 2 s at 40X magnification using a monochromator-based imaging system (Polychrome IV mono-chromator, TILL photonics or a Leica DMi8 live cell microscope). Fura-2 (**13**) was excited at 340 nm/380 nm and emitted fluorescence was captured using 515 nm long-pass filters.

Compound stock solutions (10 mM in DMSO) were pre diluted with HBS2 to a working concentration of 100 µM (1% DMSO). Chambers were filled with 450 µL HBS2 and the baseline was recorded for 50 s. Then, 50 µL of the compound solution to be tested were added to reach a final concentration of 10 µM. After 400 s the experiments were stopped. If no activation was observed or an inhibitor should be tested, a known activator was added to confirm the correctness of the experiment or if the substance is a blocker. Activation/inhibition was illustrated using GraphPad Prism 5.

5.3.3   MTT

The MTT (3-(4,5-di**m**ethyl**t**hiazol-2-yl)-2,5-diphenyl**t**etrazolium bromide) assay was performed by Martina Stadler (Bracher group) and conducted with HL-60 cells. First the number of cells per mL was determined with a hepatocyte cell counter (Fuchs-Rosenthal). Then the cell suspension was diluted with medium to 9 x 10^5 cells mL^{-1}.

Compounds to be tested were dissolved in DMSO to give 10 mM stock solutions and used for a dilution series (10 mM, 5 mM, 2.5 mM, 1.25 mM, 0.625 mM, 0.3125 mM). For negative control 1% DMSO was used and for positive control Triton® X-100 solution with a final concentration of 1 µg/mL was added.

Cell suspensions (99 µL each) were seeded on 96-well plates and incubated at 37 °C with 5% CO_2 for 24 h. Then, compound solutions (1 µL) were added and again incubated at 37 °C with 5% CO_2 for 24 h. After that, 10 µL MTT solution (5.0 mg MTT in 1.0 mL PBS) was added to each well and further incubated for two hours, followed by addition of 190 µL DMSO. After one hour shaking continuously, photometric quantification was conducted at a wavelength of 570

nm with an MRX microplate reader (DYNEX Technologies, Chentilly, USA). Concentration-effect relationships were plotted using GraphPad Prism 5.

5.3.4   Agar diffusion test

Agar diffusion tests were performed by Martina Stadler (Bracher group). Microorganisms were obtained from *Deutsche Sammlung von Mikroorganismen und Zellkulturen GmbH* (DSMZ, Braunschweig) and cultivated according to recommendations in liquid culture using different agars. For *Saccharomyces cerevisiae* (DSM number: 1333), *Hyphopichia burtonii* (DSM number: 70663), *Yarrowia lipolytica* (DSM number: 1345), *Escherichia coli* (DSM number: 426) and *Pseudomonas marginalis* (DSM number: 7527) all-culture agar (AC-agar, Sigma Aldrich) was used. Therefore 35.2 g AC-agar and 20 g agar were suspended in 1.0 L water and treated by autoclave. For *Staphylococcus equorum* (DSM number: 20675) and *Streptococcus entericus* (DSM number: 14446) an agar is likewise prepared from 10.0 g caseinpeptone, 5.0 g yeast extract, 5.0 g glucose and 5.0 g sodium chloride in 1.0 L water. After treatment in the autoclave 15 mL of the warm, liquid agar was filled into Petri dishes and cooled to 8 °C for one hour.

Solutions with 1% (m/V) compound in DMSO were prepared. Then, 3.0 µL of each solution was plated onto small filter plates (diameter 6 mm, Macherey-Nagel), equivalent to 30 µg substance. As positive control clotrimazole and tetracycline were used. Blind control was conducted with mere DMSO. The small filter plates were then dried for 24 hours at room temperature.

For final experiments the germs were brought onto the different agars using cotton swabs. The platelets containing the substances, the reference, and the blind control were put onto the agar, too. The agar plates were incubated for 36 h at 32 °C (bacteria) or 28 °C (yeasts). Then, the diameters of growth inhibition (inhibition zones) were measured manually.

6 Appendices

6.1 Abbreviations

5-HT	5-hydroxytryptamine receptors
Å	Angstrom
ALS	amyotrophic lateral sclerosis
AM	acetoxymethyl
APCI	atmospheric-pressure chemical ionization
aq.	aqueous
ASAP	atmospheric pressure solids analysis probe
BK	large conductance calcium-activated potassium channels/big potassium
Bn	benzyl
calcd.	calculated
Cav	voltage gated calcium channel
CB1R	cannabinoid-1 receptor
CLN3	battenin
CTB	cell titer blue
cy	cyclohexyl
CYP	cytochrome P
DCC	*N*,*N'*-dicyclohexylcarbodiimide
DIPA	diisopropylamine
DMF	dimethylformamide
DMSO	dimethyl sulfoxide
ECD	Electronic circular dichroism spectra
EDC	ethylene dichloride
EGF	epidermal growth factor
EI	electron ionization
eq.	equivalents
ESI	electron spray ionization
FCC	flash column chromatography
h	hour
HCT-15	human colorectal adenocarcinoma cells
HEK293	human embryonic kidney cells
HepaRG	hepatic stem cells
HepG2	human hepatocellular carcinoma cells
HERG	human Ether-à-go-go-Related Gene
HIV	human immunodeficiency virus
HPLC	high-performance liquid chromatography
HRMS	high-resolution mass spectrometry
HSQC	heteronuclear single quantum correlation
HTS	high-throughput screening
HUVEC	human umbilical vein endothelial cells

Hz	hertz
IR	infrared spectroscopy
JNCL	juvenile neuronal ceroid lipofuscinosis
KATP	ATP-sensitive potassium channel
LDA	lithium diisopropylamide
LHMDS	lithium bis(trimethylsilyl)amide
LOPAC	Library of Pharmacologically Active Compounds
LRRK2	leucine-rich repeat kinase 2
LSD	Lysosomal storage disease
m	*meta*
m	multiplet (NMR)
M	molar
m.p.	melting point
Me	methyl
MERS-CoV	Middle East respiratory syndrome coronavirus
min	minutes
mmol	millimole
mol	mole
MS	multiple sclerosis
mTOR	mechanistic target of rapamycin
MTT	3-(4,5-dimethylthiazol-2-yl)-2,5-diphenyltetrazoliumbromid
mw	microwave
n.a.	not applicable
NAADP	nicotinic acid adenine dinucleotide phosphate
Nav	voltage gated sodium channel
NBS	*N*-bromosuccinimide
n-BuLi	*n*-butyllithium
NMDA	*N*-methyl-D-aspartate receptor
NMR	nuclear magnetic resonance
ns	not significant
NT	non-transfected
o	*ortho*
p	*para*
PBMC	peripheral blood mononuclear cells
PG	protecting group
P-gp	P-glycoprotein
ph	phenyl
$PI(3,5)P_2$	phosphatidylinositol 3,5-bisphosphate
PIKfyve	FYVE finger-containing phosphoinositide kinase
ppm	parts per million
q	quartet (NMR)
R_f	retardation factor

RFP	red fluorescent protein
rt	room temperature
s	singlet (NMR)
SAR	structure-activity relationships
SARS-CoV-2	severe acute respiratory syndrome coronavirus 2
sat.	saturated
SEM	standard error of the mean
SERM	selective estrogen receptor modulators
SSRI	selective serotonin reuptake inhibitors
TCA	tricyclic antidepressants
TFA	trifluoroacetic acid
TFEB	transcription factor EB
THF	tetrahydrofuran
TLC	thin-layer chromatography
TPC	two pore channel
TRPA	transient receptor potential channel ankyrin
TRPC	transient receptor potential channel canonical
TRPM	transient receptor potential channel melastatin
TRPML	transient receptor potential cation channel
TRPV	transient receptor potential channel vanilloid
TTX	tetrodotoxin
VCR-R CEM	vincristine-resistant acute lymphoblastic leukemia cells
VEGF	vascular endothelial growth factors
WHO	world health organization
YFP	yellow fluorescent protein

6.2 References

[1]   H. Chen, J. Wu, Y. Gao, H. Chen, J. Zhou, *Curr Top Med Chem* **2016**, *16*, 2107-2114.

[2]   Y. Sakurai, A. A. Kolokoltsov, C. C. Chen, M. W. Tidwell, W. E. Bauta, N. Klugbauer, C. Grimm, C. Wahl-Schott, M. Biel, R. A. Davey, *Science* **2015**, *347*, 995-998.

[3]   S. Patel, *Sci Signal* **2015**, *8*, re7.

[4]   J. Castonguay, J. H. C. Orth, T. Muller, F. Sleman, C. Grimm, C. Wahl-Schott, M. Biel, R. T. Mallmann, W. Bildl, U. Schulte, N. Klugbauer, *Sci Rep* **2017**, *7*, 10038.

[5]   C. Grimm, L. M. Holdt, C. C. Chen, S. Hassan, C. Muller, S. Jors, H. Cuny, S. Kissing, B. Schroder, E. Butz, B. Northoff, J. Castonguay, C. A. Luber, M. Moser, S. Spahn, R. Lullmann-Rauch, C. Fendel, N. Klugbauer, O. Griesbeck, A. Haas, M. Mann, F. Bracher, D. Teupser, P. Saftig, M. Biel, C. Wahl-Schott, *Nat Commun* **2014**, *5*, 4699.

[6]   M. Ruas, K. T. Chuang, L. C. Davis, A. Al-Douri, P. W. Tynan, R. Tunn, L. Teboul, A. Galione, J. Parrington, *Mol Cell Biol* **2014**, *34*, 3981-3992.

[7]   A. F. Kintzer, R. M. Stroud, *Nature* **2016**, *531*, 258-262.

[8]   J. She, W. Zeng, J. Guo, Q. Chen, X. C. Bai, Y. Jiang, *Elife* **2019**, *8*, e45222.

[9]   C. Grimm, K. Bartel, A. M. Vollmar, M. Biel, *Pharmaceuticals (Basel)* **2018**, *11*, 4.

[10]   P. J. Calcraft, M. Ruas, Z. Pan, X. Cheng, A. Arredouani, X. Hao, J. Tang, K. Rietdorf, L. Teboul, K. T. Chuang, P. Lin, R. Xiao, C. Wang, Y. Zhu, Y. Lin, C. N. Wyatt, J. Parrington, J. Ma, A. M. Evans, A. Galione, M. X. Zhu, *Nature* **2009**, *459*, 596-600.

[11]   S. J. Pitt, T. Funnell, M. Sitsapesan, E. Venturi, K. Rietdorf, M. Ruas, A. Ganesan, R. Gosain, G. C. Churchill, M. X. Zhu, J. Parrington, A. Galione, R. Sitsapesan, *J. Biol. Chem* **2010**, *285*, 24925-24932.

[12]   M. Schieder, K. Rotzer, A. Bruggemann, M. Biel, C. A. Wahl-Schott, *J Biol Chem* **2010**, *285*, 21219-21222.

[13]   E. Brailoiu, D. Churamani, X. Cai, M. G. Schrlau, G. C. Brailoiu, X. Gao, R. Hooper, M. J. Boulware, N. J. Dun, J. S. Marchant, S. Patel, *J Cell Biol* **2009**, *186*, 201-209.

[14]   E. Brailoiu, T. Rahman, D. Churamani, D. L. Prole, G. C. Brailoiu, R. Hooper, C. W. Taylor, S. Patel, *J Biol Chem* **2010**, *285*, 38511-38516.

[15]   X. Wang, X. Zhang, X. P. Dong, M. Samie, X. Li, X. Cheng, A. Goschka, D. Shen, Y. Zhou, J. Harlow, M. X. Zhu, D. E. Clapham, D. Ren, H. Xu, *Cell* **2012**, *151*, 372-383.

[16]   C. Cang, Y. Zhou, B. Navarro, Y. J. Seo, K. Aranda, L. Shi, S. Battaglia-Hsu, I. Nissim, D. E. Clapham, D. Ren, *Cell* **2013**, *152*, 778-790.

[17]   V. Rybalchenko, M. Ahuja, J. Coblentz, D. Churamani, S. Patel, K. Kiselyov, S. Muallem, *J Biol Chem* **2012**, *287*, 20407-20416.

[18]   A. Jha, M. Ahuja, S. Patel, E. Brailoiu, S. Muallem, *EMBO J* **2014**, *33*, 501-511.

[19]   M. Ruas, L. C. Davis, C. C. Chen, A. J. Morgan, K. T. Chuang, T. F. Walseth, C. Grimm, C. Garnham, T. Powell, N. Platt, F. M. Platt, M. Biel, C. Wahl-Schott, J. Parrington, A. Galione, *EMBO J* **2015**, *34*, 1743-1758.

[20]   J. Guo, W. Zeng, Y. Jiang, *PNAS* **2017**, *114*, 1009-1014.

[21]   O. A. Ogunbayo, J. Duan, J. Xiong, Q. Wang, X. Feng, J. Ma, M. X. Zhu, A. M. Evans, *Sci Signal* **2018**, *11*, eaao5775.

[22]   S. Gerndt, C. C. Chen, Y. K. Chao, Y. Yuan, S. Burgstaller, A. Scotto Rosato, E. Krogsaeter, N. Urban, K. Jacob, O. N. P. Nguyen, M. T. Miller, M. Keller, A. M. Vollmar, T. Gudermann, S. Zierler, J. Schredelseker, M. Schaefer, M. Biel, R. Malli, C. Wahl-Schott, F. Bracher, S. Patel, C. Grimm, *Elife* **2020**, *9*, e54712.

[23] S. Patel, B. S. Kilpatrick, *Biochim Biophys Acta Mol Cell Res* **2018**, *1865*, 1678-1686.

[24] A. Hamilton, Q. Zhang, A. Salehi, M. Willems, J. G. Knudsen, A. K. Ringgaard, C. E. Chapman, A. Gonzalez-Alvarez, N. C. Surdo, M. Zaccolo, D. Basco, P. R. V. Johnson, R. Ramracheya, G. A. Rutter, A. Galione, P. Rorsman, A. I. Tarasov, *Diabetes* **2018**, *67*, 1128-1139.

[25] R. A. Capel, E. L. Bolton, W. K. Lin, D. Aston, Y. Wang, W. Liu, X. Wang, R. A. Burton, D. Bloor-Young, K. T. Shade, M. Ruas, J. Parrington, G. C. Churchill, M. Lei, A. Galione, D. A. Terrar, *J Biol Chem* **2015**, *290*, 30087-30098.

[26] A. L. Ambrosio, J. A. Boyle, A. E. Aradi, K. A. Christian, S. M. Di Pietro, *PNAS* **2016**, *113*, 5622-5627.

[27] N. W. Bellono, I. E. Escobar, E. Oancea, *Sci Rep* **2016**, *6*, 26570.

[28] Y. K. Chao, V. Schludi, C. C. Chen, E. Butz, O. N. P. Nguyen, M. Muller, J. Kruger, C. Kammerbauer, M. Ben-Johny, A. M. Vollmar, C. Berking, M. Biel, C. A. Wahl-Schott, C. Grimm, *PNAS* **2017**, *114*, E8595-E8602.

[29] L. N. Hockey, B. S. Kilpatrick, E. R. Eden, Y. Lin-Moshier, G. C. Brailoiu, E. Brailoiu, C. E. Futter, A. H. Schapira, J. S. Marchant, S. Patel, *J Cell Sci* **2015**, *128*, 232-238.

[30] G. S. Gunaratne, Y. Yang, F. Li, T. F. Walseth, J. S. Marchant, *Cell Calcium* **2018**, *75*, 30-41.

[31] C. J. Penny, K. Vassileva, A. Jha, Y. Yuan, X. Chee, E. Yates, M. Mazzon, B. S. Kilpatrick, S. Muallem, M. Marsh, T. Rahman, S. Patel, *Biochim Biophys Acta Mol Cell Res* **2019**, *1866*, 1151-1161.

[32] N. Khan, K. L. Lakpa, P. W. Halcrow, Z. Afghah, N. M. Miller, J. D. Geiger, X. Chen, *Sci Rep* **2019**, *9*, 12285.

[33] X. Ou, Y. Liu, X. Lei, P. Li, D. Mi, L. Ren, L. Guo, R. Guo, T. Chen, J. Hu, Z. Xiang, Z. Mu, X. Chen, J. Chen, K. Hu, Q. Jin, J. Wang, Z. Qian, *Nat Commun* **2020**, *11*, 1620.

[34] P. Faris, M. Shekha, D. Montagna, G. Guerra, F. Moccia, *Cancers (Basel)* **2018**, *11*, 27.

[35] A. Favia, M. Desideri, G. Gambara, A. D'Alessio, M. Ruas, B. Esposito, D. Del Bufalo, J. Parrington, E. Ziparo, F. Palombi, A. Galione, A. Filippini, *PNAS* **2014**, *111*, E4706-4715.

[36] O. N. Nguyen, C. Grimm, L. S. Schneider, Y. K. Chao, C. Atzberger, K. Bartel, A. Watermann, M. Ulrich, D. Mayr, C. Wahl-Schott, M. Biel, A. M. Vollmar, *Cancer Res* **2017**, *77*, 1427-1438.

[37] F. Li, J. P. Ji, Y. Xu, R. L. Liu, *Clin Transl Oncol* **2019**, *411*, 5555-5561.

[38] D. Hanahan, R. A. Weinberg, *Cell* **2011**, *144*, 646-674.

[39] K. Kupferschmidt, J. Cohen, *Science* **2020**, *367*, 1412-1413.

[40] R. M. Mingo, J. A. Simmons, C. J. Shoemaker, E. A. Nelson, K. L. Schornberg, R. S. D'Souza, J. E. Casanova, J. M. White, *J Virol* **2015**, *89*, 2931-2943.

[41] X. P. Dong, D. Shen, X. Wang, T. Dawson, X. Li, Q. Zhang, X. Cheng, Y. Zhang, L. S. Weisman, M. Delling, H. Xu, *Nat Commun* **2010**, *1*, 38.

[42] R. Parkesh, A. M. Lewis, P. K. Aley, A. Arredouani, S. Rossi, R. Tavares, S. R. Vasudevan, D. Rosen, A. Galione, J. Dowden, G. C. Churchill, *Cell Calcium* **2008**, *43*, 531-538.

[43] A. Galione, K. T. Chuang, T. M. Funnell, L. C. Davis, A. J. Morgan, M. Ruas, J. Parrington, G. C. Churchill, *Cold Spring Harb Protoc* **2014**, *2014*, pdb prot076927.

[44]   C. Dinkel, M. Moody, A. Traynor-Kaplan, C. Schultz, *Angew Chem Int Ed Engl* **2001**, *40*, 3004-3008.

[45]   N. Provinciali, C. Suen, B. K. Dunn, A. DeCensi, *Expert Rev Clin Pharmacol* **2016**, *9*, 1263-1272.

[46]   S. Y. Tsang, X. Yao, K. Essin, C. M. Wong, F. L. Chan, M. Gollasch, Y. Huang, *Stroke* **2004**, *35*, 1709-1714.

[47]   Q. Wang, L. Lu, X. Gao, C. Wang, J. Wang, J. Cheng, R. Gao, H. Xiao, *Pharmacology* **2011**, *87*, 70-80.

[48]   Y. J. Chae, D. H. Kim, H. J. Lee, K. W. Sung, O. J. Kwon, S. J. Hahn, *Pflugers Arch* **2015**, *467*, 1663-1676.

[49]   N. Divac, M. Prostran, I. Jakovcevski, N. Cerovac, *Biomed Res Int* **2014**, *2014*, 1-6.

[50]   X. Zhou, X. W. Dong, T. Priestley, *Brain Res* **2006**, *1106*, 72-81.

[51]   M. Müller, J. R. De Weille, M. Lazdunski, *Eur J Pharmacol* **1991**, *198*, 101-104.

[52]   I. Pafumi, M. Festa, F. Papacci, L. Lagostena, C. Giunta, V. Gutla, L. Cornara, A. Favia, F. Palombi, F. Gambale, A. Filippini, A. Carpaneto, *Sci Rep* **2017**, *7*, 5121.

[53]   Z. Zhao, G. Jin, Y. Ge, Z. Guo, *Inflammopharmacology* **2019**, *27*, 1021-1036.

[54]   I. Straub, U. Krugel, F. Mohr, J. Teichert, O. Rizun, M. Konrad, J. Oberwinkler, M. Schaefer, *Mol Pharmacol* **2013**, *84*, 736-750.

[55]   H. Gumushan Aktas, T. Akgun, *Biomed Pharmacother* **2018**, *106*, 770-775.

[56]   E. P. Scholz, E. Zitron, C. Kiesecker, S. Luck, D. Thomas, S. Kathofer, V. A. Kreye, H. A. Katus, J. Kiehn, W. Schoels, C. A. Karle, *Naunyn Schmiedebergs Arch Pharmacol* **2005**, *371*, 516-525.

[57]   H. T. Hsu, Y. T. Tseng, Y. C. Lo, S. N. Wu, *BMC Neurosci* **2014**, *15*, 135.

[58]   U. Fuhr, K. Klittich, A. H. Staib, *Br J Clin Pharmacol* **1993**, *35*, 431-436.

[59]   F. P. Guengerich, D. H. Kim, *Carcinogenesis* **1990**, *11*, 2275-2279.

[60]   E. Naylor, A. Arredouani, S. R. Vasudevan, A. M. Lewis, R. Parkesh, A. Mizote, D. Rosen, J. M. Thomas, M. Izumi, A. Ganesan, A. Galione, G. C. Churchill, *Nat Chem Biol* **2009**, *5*, 220-226.

[61]   G. Wang, J. R. Lemos, C. Iadecola, *Trends Pharmacol Sci* **2004**, *25*, 120-123.

[62]   N. Bhagya, K. R. Chandrashekar, *Phytochemistry* **2016**, *125*, 5-13.

[63]   Y. S. Lee, S. H. Han, S. H. Lee, Y. G. Kim, C. B. Park, O. H. Kang, J. H. Keum, S. B. Kim, S. H. Mun, Y. S. Seo, N. Y. Myung, D. Y. Kwon, *Foodborne Pathog Dis* **2012**, *9*, 686-691.

[64]   L. X. Zhao, D. D. Li, D. D. Hu, G. H. Hu, L. Yan, Y. Wang, Y. Y. Jiang, *PLoS One* **2013**, *8*, e79671.

[65]   I. Lieberman, D. P. Lentz, G. A. Trucco, W. K. Seow, Y. H. Thong, *Diabetes* **1992**, *41*, 616-619.

[66]   P. Joshi, R. A. Vishwakarma, S. B. Bharate, *Eur J Med Chem* **2017**, *138*, 273-292.

[67]   S. Dewanjee, T. Dua, N. Bhattacharjee, A. Das, M. Gangopadhyay, R. Khanra, S. Joardar, M. Riaz, V. Feo, M. Zia-Ul-Haq, *Molecules* **2017**, *22*, 871.

[68]   L. W. Fu, Y. M. Zhang, Y. J. Liang, X. P. Yang, Q. C. Pan, *Eur J Cancer* **2002**, *38*, 418-426.

[69]   L. Fu, Y. Liang, L. Deng, Y. Ding, L. Chen, Y. Ye, X. Yang, Q. Pan, *Cancer Chemother Pharmacol* **2004**, *53*, 349-356.

[70] H. Jin, L. Li, D. Zhong, J. Liu, X. Chen, J. Zheng, *Chem Res Toxicol* **2011**, *24*, 2142-2152.

[71] L. Tainlin, H. Tingyi, Z. Changqi, Y. Peipei, Z. Qiong, *Ecotoxicol Environ Saf* **1982**, *6*, 528-534.

[72] Y. Inubushi, Y. Masaki, S. Matsumoto, F. Takami, *Tetrahedron Lett* **1968**, 3399-3402.

[73] R. Schuetz, M. Meixner, I. Antes, F. Bracher, *Org Biomol Chem* **2020**, *18*, 3047-3068.

[74] X. Wei, T. L. Qu, Y. F. Yang, J. F. Xu, X. W. Li, Z. B. Zhao, Y. W. Guo, *J Asian Nat Prod Res* **2016**, *18*, 966-975.

[75] J. Tao, Y. Qian-Hao, G. Wei-Feng, X. Jin-Fang, Q. Ting-Li, J. Graham, Z. Zheng-Bao, *ChemXpress* **2018**.

[76] J. Lan, L. Huang, H. Lou, C. Chen, T. Liu, S. Hu, Y. Yao, J. Song, J. Luo, Y. Liu, B. Xia, L. Xia, X. Zeng, Y. Ben-David, W. Pan, *Eur J Med Chem* **2018**, *143*, 1968-1980.

[77] J. Song, J. Lan, C. Chen, S. Hu, J. Song, W. Liu, X. Zeng, H. Lou, Y. Ben-David, W. Pan, *Med Chem Comm* **2018**, *9*, 1131-1141.

[78] M. Merarchi, G. Sethi, L. Fan, S. Mishra, F. Arfuso, K. S. Ahn, *Molecules* **2018**, *23*, 2538.

[79] Y. Cui, M. Xu, J. Mao, J. Ouyang, R. Xu, Y. Yu, *Eur J Med Chem* **2012**, *54*, 867-872.

[80] Z. Yang, C. Li, X. Wang, C. Zhai, Z. Yi, L. Wang, B. Liu, B. Du, H. Wu, X. Guo, M. Liu, D. Li, J. Luo, *J Cell Physiol* **2010**, *225*, 266-275.

[81] G. Deng, S. Zeng, J. Ma, Y. Zhang, Y. Qu, Y. Han, L. Yin, C. Cai, C. Guo, H. Shen, *Sci Rep* **2017**, *7*, 41616.

[82] P. Iturriaga-Vasquez, R. Miquel, M. D. Ivorra, M. P. D'Ocon, B. K. Cassels, *J Nat Prod* **2003**, *66*, 954-957.

[83] A. F. Kintzer, R. M. Stroud, *FEBS J* **2018**, *285*, 233-243.

[84] R. E. Haskell, C. J. Carr, D. A. Pearce, M. J. Bennett, B. L. Davidson, *Hum Mol Genet* **2000**, *9*, 735-744.

[85] T. J. Lerner, R.-M. N. Boustany, J. W. Anderson, K. L. D'Arigo, K. Schlumpf, A. J. Buckler, J. F. Gusella, J. L. Haines, *Cell* **1995**, *82*, 949-957.

[86] M. Haltia, *Biochim Biophys Acta* **2006**, *1762*, 850-856.

[87] A. Jalanko, T. Braulke, *Biochim Biophys Acta* **2009**, *1793*, 697-709.

[88] N. Urban, L. Wang, S. Kwiek, J. Rademann, W. M. Kuebler, M. Schaefer, *Mol Pharmacol* **2016**, *89*, 197-213.

[89] K. R. Gee, K. A. Brown, W. N. Chen, J. Bishop-Stewart, D. Gray, I. Johnson, *Cell Calcium* **2000**, *27*, 97-106.

[90] F. Di Virgilio, L. H. Jiang, S. Roger, S. Falzoni, A. C. Sarti, V. Vultaggio-Poma, P. Chiozzi, E. Adinolfi, *Methods Enzymol* **2019**, *629*, 115-150.

[91] E. B. Sjogren, M. A. Rider, P. H. Nelson, S. Bingham, Jr., A. L. Poulton, M. A. Emanuel, R. Komuniecki, *J Med Chem* **1991**, *34*, 3295-3301.

[92] M. M. Shoukry, A. El Said Mahgoub, M. H. Elnagdi, *Ann. Chim. (Rome)* **1980**, *70*, 319-321.

[93] M. M. Shoukry, M. H. Elnagdi, A. E.-S. Mahgoub, *Ann. Chim. (Rome)* **1979**, *69*, 211-217.

[94] M. Hesse, H. Meier, B. Zeeh, *Spektroskopische Methoden in der organischen Chemie*, 8 ed., Georg Thieme Verlag, Stuttgart, **2012**.

[95]   S. L. Laurella, C. Latorre, R. Dietrich, J. J. P. Furlong, P. E. Allegretti, *J Phys Org Chem* **2012**, *25*, 1365-1373.

[96]   A. Hantzsch, *Ber Dtsch Chem Ges* **1890**, *23*, 1474-1476.

[97]   F. Feist, *Ber Dtsch Chem Ges* **1902**, *35*, 1537-1544.

[98]   J. Menéndez, M. Leonardi, V. Estévez, M. Villacampa, *Synthesis* **2018**, *51*, 816-828.

[99]   B. Zhao, W. Kan, T. Jing, X.-h. Zhang, Y.-j. Zheng, L. Chen, *Heterocycles* **2015**, *91*, 2367.

[100]   C. Paal, *Ber Dtsch Chem Ges* **1884**, *17*, 2756-2767.

[101]   L. Knorr, *Ber Dtsch Chem Ges* **1884**, *17*, 2863-2870.

[102]   V. Amarnath, D. C. Anthony, K. Amarnath, W. M. Valentine, L. A. Wetterau, D. G. Graham, *J Org Chem* **1991**, *56*, 6924-6931.

[103]   S. Y. Kang, E. J. Park, W. K. Park, H. J. Kim, D. Jeong, M. E. Jung, K. S. Song, S. H. Lee, H. J. Seo, M. J. Kim, M. Lee, H. K. Han, E. J. Son, A. N. Pae, J. Kim, J. Lee, *Bioorg Med Chem Lett* **2010**, *20*, 1705-1711.

[104]   G. Tarzia, A. Duranti, A. Tontini, G. Spadoni, M. Mor, S. Rivara, P. Vincenzo Plazzi, S. Kathuria, D. Piomelli, *Bioorg Med Chem* **2003**, *11*, 3965-3973.

[105]   A. Mayweg, H.P. Marty, W. Mueller, R. Narquizian, W. Neidhardt, P. Pflieger, S. Roever, *WO 2004/060870 A1*, **2003**.

[106]   K. Saruta, N. Hayashi, O. Sakurai, H. Sawamoto, E. Oboki, *EP 2 862 856 A1*, **2015**.

[107]   M. Schlosser, E. Castagnetti, *Eur J Org Chem* **2001**, *2001*, 3991-3997.

[108]   J. B. Liu, C. Chen, L. Chu, Z. H. Chen, X. H. Xu, F. L. Qing, *Angew Chem Int Ed Engl* **2015**, *54*, 11839-11842.

[109]   W. Frick, *US 2011/0059910 A1*, **2011**.

[110]   S. Nahm, S. M. Weinreb, *Tetrahedron Lett* **1981**, *22*, 3815-3818.

[111]   X. Zhang, W. Chen, P. Li, R. Calvo, N. Southall, X. Hu, M. Bryant-Genevier, X. Feng, Q. Geng, C. Gao, M. Yang, K. Tang, M. Ferrer, J. J. Marugan, H. Xu, *Elife* **2019**, *8*, e51423.

[112]   G. Grynkiewicz, M. Poenie, R. Y. Tsien, *J Biol Chem* **1985**, *260*, 3440-3450.

[113]   S. Yamaguchi, A. Jha, Q. Li, A. A. Soyombo, G. D. Dickinson, D. Churamani, E. Brailoiu, S. Patel, S. Muallem, *J Biol Chem* **2011**, *286*, 22934-22942.

[114]   C. Grimm, S. Jors, S. A. Saldanha, A. G. Obukhov, B. Pan, K. Oshima, M. P. Cuajungco, P. Chase, P. Hodder, S. Heller, *Chem Biol* **2010**, *17*, 135-148.

[115]   E. Plesch, C. C. Chen, E. Butz, A. Scotto Rosato, E. K. Krogsaeter, H. Yinan, K. Bartel, M. Keller, D. Robaa, D. Teupser, L. M. Holdt, A. M. Vollmar, W. Sippl, R. Puertollano, D. Medina, M. Biel, C. Wahl-Schott, F. Bracher, C. Grimm, *Elife* **2018**, *7*, e39720.

[116]   B. K. Toeplitz, A. I. Cohen, P. T. Funke, W. L. Parker, J. Z. Gougoutas, *J Am Chem Soc* **1979**, *101*, 3344-3353.

[117]   C.-M. Lui, T. E. Hermann, *J Biol Chem* **1978**, *17*, 5892-5894.

[118]   M. C. Claussen, T. Korn, *Clin Immunol* **2012**, *142*, 49-56.

[119]   H. A. Bird, J. Hill, J. S. Dixon, R. Bojar, A. Traficante, M. A. Catalano, S. F. Adair, L. Liauw, H. Sussman, H. Rotman, et al., *J Rheumatol* **1989**, *16*, 448-454.

[120]   M. Enders, T. Heider, A. Ludwig, S. Kuerten, *Int J Mol Sci* **2020**, *21*, 1663.

[121]   J. C. Stockert, R. W. Horobin, L. L. Colombo, A. Blazquez-Castro, *Acta Histochem* **2018**, *120*, 159-167.

[122] R. L. Williamson, R. L. Metcalf, *Science* **1967**, *158*, 1694-1695.

[123] K. Talavera, M. Gees, Y. Karashima, V. M. Meseguer, J. A. Vanoirbeek, N. Damann, W. Everaerts, M. Benoit, A. Janssens, R. Vennekens, F. Viana, B. Nemery, B. Nilius, T. Voets, *Nat Neurosci* **2009**, *12*, 1293-1299.

[124] J. Garcia-Anoveros, K. Nagata, *Handb Exp Pharmacol* **2007**, 347-362.

[125] K. Shibasaki, *J Physiol Sci* **2016**, *66*, 359-365.

[126] D. E. Clapham, D. Julius, C. Montell, G. Schultz, *Pharmacol Rev* **2005**, *57*, 427-450.

[127] S. J. Pitt, T. M. Funnell, M. Sitsapesan, E. Venturi, K. Rietdorf, M. Ruas, A. Ganesan, R. Gosain, G. C. Churchill, M. X. Zhu, J. Parrington, A. Galione, R. Sitsapesan, *J Biol Chem* **2010**, *285*, 35039-35046.

[128] M. Ruas, L. C. Davis, C. C. Chen, A. J. Morgan, K. T. Chuang, T. F. Walseth, C. Grimm, C. Garnham, T. Powell, N. Platt, F. M. Platt, M. Biel, C. Wahl-Schott, J. Parrington, A. Galione, *EMBO J* **2015**, *34*, 1743-1758.

[129] A. Boccaccio, J. Scholz-Starke, S. Hamamoto, N. Larisch, M. Festa, P. V. Gutla, A. Costa, P. Dietrich, N. Uozumi, A. Carpaneto, *Cell Mol Life Sci* **2014**, *71*, 4275-4283.

[130] A. J. Morgan, A. Galione, *Biochem J* **2007**, *402*, 301-310.

[131] F. Cosker, N. Cheviron, M. Yamasaki, A. Menteyne, F. E. Lund, M. J. Moutin, A. Galione, J. M. Cancela, *J Biol Chem* **2010**, *285*, 38251-38259.

[132] E. Machado, S. White-Gilbertson, D. van de Vlekkert, L. Janke, S. Moshiach, Y. Campos, D. Finkelstein, E. Gomero, R. Mosca, X. Qiu, C. L. Morton, I. Annunziata, A. d'Azzo, *Sci Adv* **2015**, *1*, e1500603.

[133] Y. Miao, G. Li, X. Zhang, H. Xu, S. N. Abraham, *Cell* **2015**, *161*, 1306-1319.

[134] M. A. Samie, H. Xu, *J Lipid Res* **2014**, *55*, 995-1009.

[135] S. Gerndt, E. Krogsaeter, S. Patel, F. Bracher, C. Grimm, *FEBS J* **2020**, ahead of print.

[136] E. Trindade, D. Menon, L. A. Topfer, C. Coloma, *CMAJ* **1998**, *159*, 1245-1252.

[137] P. K. Gillman, *Br J Pharmacol* **2007**, *151*, 737-748.

[138] J. P. Hubert, J. C. Delumeau, J. Glowinski, J. Premont, A. Doble, *Br J Pharmacol* **1994**, *113*, 261-267.

[139] M.-W. Debono, J. Le Guern, T. Canton, A. Doble, L. Pradier, *Eur J Pharmacol* **1993**, *235*, 283-289.

[140] C. Malgouris, M. Daniel, A. Doble, *Neurosci Lett* **1994**, *177*, 95-99.

[141] J. H. Song, C. S. Huang, K. Nagata, J. Z. Yeh, T. Narahashi, *J Pharmacol Exp Ther* **1997**, *282*, 707-714.

[142] M. Bissaro, S. Moro, *Neural Regen Res* **2019**, *14*, 2083-2085.

[143] A. Thevand, I. Stanculescu, C. Mandravel, P. Woisel, G. Surpateanu, *Spectrochim Acta A Mol Biomol Spectrosc* **2004**, *60*, 1825-1830.

[144] Z. Xie, X. Xu, C. Xie, Z. Liang, M. Yang, J. Huang, D. Yang, *J Liq Chromatogr Relat Technol* **2013**, *37*, 343-352.

[145] P. L. Schiff, *J Nat Prod* **1997**, *60*, 934-953.

[146] J. J. Lv, M. Xu, D. Wang, H. T. Zhu, C. R. Yang, Y. F. Wang, Y. Li, Y. J. Zhang, *J Nat Prod* **2013**, *76*, 926-932.

[147] D. L. Comins, P. M. Thakker, M. F. Baevsky, M. M. Badawi, *Tetrahedron* **1997**, *53*, 16327-16340.

[148] L. Pouysegu, A. V. Avellan, S. Quideau, *J Org Chem* **2002**, *67*, 3425-3436.

[149] J. H. Schrittwieser, V. Resch, S. Wallner, W. D. Lienhart, J. H. Sattler, J. Resch, P. Macheroux, W. Kroutil, *J Org Chem* **2011**, *76*, 6703-6714.

[150] W. N. Speckamp, H. Hiemstra, *Tetrahedron* **1985**, *41*, 4367-4416.

[151] B. E. Maryanoff, H. C. Zhang, J. H. Cohen, I. J. Turchi, C. A. Maryanoff, *Chem Rev* **2004**, *104*, 1431-1628.

[152] M. P. Cava, K. T. Buck, *Tetrahedron* **1969**, *25*, 2795-2805.

[153] F. Ullmann, P. Sponagel, *Ber Dtsch Chem Ges* **1905**, *38*, 2211-2212.

[154] D. M. T. Chan, K. L. Monaco, R.-P. Wang, M. P. Winters, *Tetrahedron Lett* **1998**, *39*, 2933-2936.

[155] D. A. Evans, J. L. Katz, T. R. West, *Tetrahedron Lett* **1998**, *39*, 2937-2940.

[156] P. Y. S. Lam, C. G. Clark, S. Saubern, J. Adams, M. P. Winters, D. M. T. Chan, A. Combs, *Tetrahedron Lett* **1998**, *39*, 2941-2944.

[157] G. Evano, J. Wang, A. Nitelet, *Org Chem Front* **2017**, *4*, 2480-2499.

[158] A. E. King, T. C. Brunold, S. S. Stahl, *J Am Chem Soc* **2009**, *131*, 5044-5045.

[159] J. C. Vantourout, H. N. Miras, A. Isidro-Llobet, S. Sproules, A. J. Watson, *J Am Chem Soc* **2017**, *139*, 4769-4779.

[160] E. Awuah, A. Capretta, *J Org Chem* **2010**, *75*, 5627-5634.

[161] M. Eckert, G. Fleischmann, R. Jira, H. M. Bolt, K. Golka, in *Ullmann's Encyclopedia of Industrial Chemistry*, Wiley-VCH Verlag, **2006**.

[162] B. J. Lidster, J. M. Behrendt, M. L. Turner, *Chem Commun (Camb)* **2014**, *50*, 11867-11870.

[163] C. E. Brown, J. McNulty, C. Bordon, R. Yolken, L. Jones-Brando, *Org Biomol Chem* **2016**, *14*, 5951-5955.

[164] G. S. Basarab, P. Hill, B. Sherer, F. Zhou, *WO2010067123A1*, **2009**.

[165] K. Tachibana, H. Sato, M. Ohta, M. Nakamura, T. Shiraishi, H. Yoshino, T. Emura, A. Honma, E. Onuma, H. Kawata, K. Taniguchi, *EP1790640A1*, **2004**.

[166] M. El Khatib, G. A. Molander, *Org Lett* **2014**, *16*, 4944-4947.

[167] W. Eschweiler, *Ber Dtsch Chem Ges* **1905**, *38*, 880-882.

[168] R. Leuckart, *Ber Dtsch Chem Ges* **1885**, *18*, 2341-2344.

[169] C. C. Chen, C. Cang, S. Fenske, E. Butz, Y. K. Chao, M. Biel, D. Ren, C. Wahl-Schott, C. Grimm, *Nat Protoc* **2017**, *12*, 1639-1658.

[170] R. A. Gatenby, R. J. Gillies, *Nat Rev Cancer* **2004**, *4*, 891-899.

[171] Y. Tian, S. Shen, Y. Jiang, Q. Shen, S. Zeng, J. Zheng, *Arch Toxicol* **2016**, *90*, 1737-1748.

[172] C. Yan, Q. Xin-Ming, G. Li-Kun, L. Lin-Lin, C. Fang-Ping, X. Ying, W. Xiong-Fei, L. Xiang-Hong, R. Jin, *Toxicology* **2006**, *218*, 1-12.

[173] J. J. Kelu, H. L. Chan, S. E. Webb, A. H. Cheng, M. Ruas, J. Parrington, A. Galione, A. L. Miller, *Int J Dev Biol* **2015**, *59*, 313-325.

[174] W. Dammermann, B. Zhang, M. Nebel, C. Cordiglieri, F. Odoardi, T. Kirchberger, N. Kawakami, J. Dowden, F. Schmid, K. Dornmair, M. Hohenegger, A. Flugel, A. H. Guse, B. V. Potter, *PNAS* **2009**, *106*, 10678-10683.

[175] K. Singaravelu, J. W. Deitmer, *Cell Calcium* **2006**, *39*, 143-153.

[176] R. A. Billington, A. A. Genazzani, *Cell Calcium* **2007**, *41*, 505-511.

[177] R. Schuetz, M. Mueller, S. Gerndt, K. Bartel, F. Bracher, *Arch Pharm (Weinheim)* **2020**, *353*, e2000106.

[178] W. Wang, Q. Gao, M. Yang, X. Zhang, L. Yu, M. Lawas, X. Li, M. Bryant-Genevier, N. T. Southall, J. Marugan, M. Ferrer, H. Xu, *PNAS* **2015**, *112*, E1373-1381.

[179] M. Davies, T. Heikkila, G. A. McConkey, C. W. Fishwick, M. R. Parsons, A. P. Johnson, *J Med Chem* **2009**, *52*, 2683-2693.

[180] W. Y. Yuan, X. Chen, N. N. Liu, Y. N. Wen, B. Yang, G. Andrei, R. Snoeck, Y. H. Xiang, Y. W. Wu, Z. Jiang, D. Schols, Z. Y. Zhang, Q. P. Wu, *Med Chem* **2019**, *15*, 801-812.

[181] Y. A. Ammar, M. M. Ismail, H. M. El-Sehrawi, E. Noaman, A. H. Bayomi, T. Z. Shawer, *Arch Pharm (Weinheim)* **2006**, *339*, 429-436.

[182] D. H. Sohn, J. I. Park, S. J. Cho, J. Kang, *Tetrahedron* **2017**, *73*, 212-221.

[183] N. H. Metwally, F. M. Abdelrazek, S. M. Eldaly, P. Metz, *J Heterocycl Chem* **2017**, *54*, 289-294.

[184] N. Edraki, A. Iraji, O. Firuzi, Y. Fattahi, M. Mahdavi, A. Foroumadi, M. Khoshneviszadeh, A. Shafiee, R. Miri, *J Iran Chem Soc* **2016**, *13*, 2163-2171.

[185] N. Shah, P. N. Patel, D. C. Karia, *Asian J Chem* **2018**, *30*, 2647-2651.

[186] Y. Kobayashi, T. Harayama, *Tetrahedron Lett* **2009**, *50*, 6665-6667.

[187] D. Guo, T. Chen, D. Ye, J. Xu, H. Jiang, K. Chen, H. Wang, H. Liu, *Org Lett* **2011**, *13*, 2884-2887.

[188] G. N. Walker, *US4256759*, **1981**.

[189] T. X. Metro, J. Bonnamour, T. Reidon, J. Sarpoulet, J. Martinez, F. Lamaty, *Chem Commun (Camb)* **2012**, *48*, 11781-11783.

[190] S. Lee, A. Pyo, A. Park, H. Jung, *Synthesis* **2012**, *44*, 2885-2888.

[191] S.-T. Lu, Y.-C. Wu, S.-P. Leou, *J Chin Chem Soc-Taip* **1987**, *34*, 33-42.

[192] Y. Kawabata, Y. Naito, T. Saitoh, K. Kawa, T. Fuchigami, S. Nishiyama, *Eur J Org Chem* **2014**, *2014*, 99-104.

[193] B. Gawley, R. E. Gawley, G. A. Smith, *ARKIVOC* **2011**, *2011*, 167-179.

[194] Y. Kashiwada, A. Aoshima, Y. Ikeshiro, Y. P. Chen, H. Furukawa, M. Itoigawa, T. Fujioka, K. Mihashi, L. M. Cosentino, S. L. Morris-Natschke, K. H. Lee, *Bioorg Med Chem* **2005**, *13*, 443-448.

[195] R. Stadler, S. Loeffler, B. K. Cassels, M. H. Zenk, *Phytochemistry* **1988**, *27*, 2557-2565.

[196] M. Tomita, H. Yamaguchi, *Yakugaku Zasshi* **1952**, *72*, 1219-1222.

[197] T. Kametani, H. Yagi, *Chem Pharm Bull (Tokyo)* **1967**, *15*, 1283-1286.

[198] P. Steffens, N. Nagakura, M. H. Zenk, *Phytochemistry* **1985**, *24*, 2577-2583.

[199] R. Stadler, M. H. Zenk, *Liebigs Ann* **1990**, *1990*, 555-562.

[200] P. Z.-T. Iturriaga-Vasquez, Gerald; Rezende, Marcos Caroli; Cassels, Bruce K., *J Chil Chem Soc* **2004**, *49*, 17-23.

[201] A. Jossang, M. Lebœuf, A. Cavé, J. Pusset, *J Nat Prod* **1991**, *54*, 466-472.

[202] A. Brossi, K. C. Rice, C. P. Mak, J. Reden, A. E. Jacobson, Y. Nimitkitpaisan, P. Skolnick, J. Daly, *J Med Chem* **1980**, *23*, 648-652.

[203] M. Tomita, J. Niimi, *Yakugaku Zasshi* **1959**, *79*, 1023-1027.

[204] N. Blank, T. Opatz, *J Org Chem* **2011**, *76*, 9777-9784.

[205] C. H. C. Chen, Tzer Ming *J Taiw Pharm Assoc* **1983**, *35*, 1-16.

[206]   C. Schoepf, W. Salzer, *Liebigs Ann* **1940**, *544*, 1.

[207]   M. Lafrance, N. Blaquiere, K. Fagnou, *Eur J Org Chem* **2007**, *2007*, 811-825.

[208]   M. Tomita, K. Nakaguchi, S. Takagi, *Yakugaku Zasshi* **1951**, *71*, 1046-1049.

[209]   Y. Tang, S. Li, S. Li, X. Yang, Y. Qin, C. Liu, Y. Zhang, *Med Chem Res* **2017**, *26*, 3384-3394.